Pincer-Ruthenium and Pincer-Cobalt Catalyzed Value-Addition of Alcohols

A Dissertation

Submitted in Partial Fulfillment for the Degree of

Doctor of Philosophy

by

PRAN GOBINDA NANDI
(Roll No: 186122024)

Thesis Supervisor: Dr. Akshai Kumar A. S.

Department of Chemistry
Indian Institute of Technology Guwahati
Guwahati – 781039, Assam, INDIA

October 2024

Dedicated

To

Grandmother Monmothirani Nandi

कर्मण्येवाधिकारस्ते मा फलेषु कदाचन । मा कर्मफलहेतुर्भुर्मा ते संगोऽस्त्वकर्मणि ॥

कर्मण्येवाधिकारस्ते मा फलेषु कदाचन । मा कर्मफलहेतुर्भुर्मा ते संगोऽस्त्वकर्मणि ॥

Sri Krishna, Shrimad Bhagavad Gita

Acknowledgments

I would like to express my deepest gratitude from the core of my heart to all the imparts with the association of the scientific elite of the Indian Institute of Technology Guwahati, India. I would like to extend my heartfelt gratitude to all who have put an endless support and assistance directly or indirectly during my research journey and made it possible to submit this thesis.

First and foremost, I would like to express my special thanks and gratitude to **Dr. Akshai Kumar A. S.**, my Ph.D supervisor who gave me a wonderful opportunity to carry out my thesis work under his supervision. Thank you for introducing me to the field of pincer-metal catalysed organometallic chemistry and inspiring me to explore challenges in the research work and his continuous motivation, support, effective advice and suggestion helped me in achieving this feat of submitting my research work in the form of this thesis. I am continually motivated by his commitment to research, discipline and hard effort to get through challenging times and to complete my research work. I am also thankful to his family for loving, caring and support during my research journey.

- I am extremely thankful to the collaborator Prof. Biman B. Mondal and his precious suggestions during the research work.
- I am highly obliged to my doctoral committee chairman Prof. Biplab Mondal, along with the doctoral committee members Dr. Chandan K. Jana, and Dr. Chandan Mukherjee for their valuable time, inspiration, suggestions, and evaluation during my entire research period. I would like to thank Prof. Biplab Mondal, Prof. Jubaraj B. Bharua, Prof. Subhas C. Pan and Prof. Ashish Kumar Gupta for the interesting and informative courses they taught me as a part of my coursework. I also extend my thanks to all other faculty members of the Department of Chemistry, IIT Guwahati for their help and support.
- I am thankful to Dr. Babulal Das, Dr. Siriyara Jagannatha Prathapa and my friends Sandeep Kumar for helping me analyze the single crystal XRD data for publication. I also thank my friend Shankhadeep Saha, Mrinmoy Roy for EPR and TGA analysis whenever I made an urgent request. My sincere thanks to Mr. Imdadul Islam and all the NMR operators of Department of chemistry, all the non-teaching staff our chemistry department, for their cooperation and help during my research progress. I am grateful to all the staff and operators of Central Instrument Facility (CIF), Nano Centre, North East

Centre for Biological Sciences and Healthcare Engineering (NECBH), IIT Guwahati. I sincerely admit IIT Guwahati for the financial support during my PhD work.

I am extremely blessed to have talented, passionate and friendly lab mates during my PhD tenure. I am very grateful to my senior Dr. Moumita Dutta, Dr. Kanu Das and Dr. Khadimul Islam for their mentorship during my initial days of research. I have learned everything from Kanu Das who helped me to set basement in organometallic chemistry. I have learned column chromatography from Khadimul Islam and Kanu Das. I extent my special thanks to Kanu Das who guided me to each point of my research work. I am very greatly to my colleague, my friend Vinay Arora, without him I can't imagine research because his assistance, support made my bad day to productive and fruitful. I am also taking the opportunity to thank my lab mates Dr. Lakshay Kathuria, Dr. Harsh Sharma, Ms. Himani Narjinari, Ms. Eileen Yasmin, Ms. Akshara Bisarya, Ms. Niharika Tanwar, Mr. Vikas, Mr. Bedabara Nag, Mr. Rounak Ranjit, Mr. Lalit Kumar Pandey, Mr. Babu Venkatesh, Ms. Susmita Das, Mr. Pabitra Maity, Mr. Soumen Maity, Bidhan Kar, Mr. Sudhanva, Mr. Dhiraj Mr. Kailas Mahipal Mr. Prasad Thombare, Mr. Jatin Gupta, Ms. Poonam Kumari, Mr. Pradhuman Kumar, Ms. Snata Deka, Ms. Tanima Pal for their valuable time and support during my research work.

- I highly obliged to MHRD and IIT Guwahati for providing me with the doctoral fellowship during my research work.
- I am grateful to all my respected teachers for their contributions to my education at different stages, without their education, I would not have been able to reach this stage of life. I would like to thank all of my respected teachers of Bidytirtha vidlaya, Gunananda Bati H.A.K.M High school, Jemo N.N High School, Kandi Raj College and Jadavpur university for their contributions to my passion for Chemistry. From the core of my heart I want to acknowledge my respected teacher Mr. Pallab Sinha who taught me physical science and from there I have started learning science. During My College days I used to go to stay their home due to my weak financial conditions. I also thankful to his family due to their unconditional love and motivated me all times. Specially, I am highly obliged to my chemistry teachers Mr. Palash Maitra, Mr. Tipurari Ghosh, Mr. Banshi Thakur, Dr. Nitty Gopal Mondal, Dr. Debaprasad Panda, Dr. Shouvik Chattyapadhya, Dr. Kajal Krishna Rajak, Dr. Tanurima Bhattyacharjee, Dr. Jnan Prakash Naskar. I have learned chemistry and loved chemistry from them. I want to extent my gratitude to my respected teachers Mr. Animesh Choudhury, Mr. Atanu

Bhattacharjee, Mr. Lakshman Kumar Ghosh, Mr. Kanak Joyti Roy, Mr. Debadittya Das, Mr. Anupam Roy, Mr Sukhen Das, Sukumar Ghosh, Jaydev Sarkar, Supravat Chattopadhyay for their motivation and financial support.

- I am grateful to Srijan Sujan (NGO) and Prerana The Inspiration (NGO) and all the members of Srijan Sujan specially Mr. Abhijit Sengupta for their financial support and motivation.

- I want to express my gratitude to my childhood, school and college friends. Especially I want to acknowledge my friends Palash Nandi, Rajarshi Pal, Niladri Sekhar Mondal, Souvic Mishra, Gopal Ghosh, Suhas Kundu, Budhadeb Konai, Anirban Ghosh, Amit Garai, Taraknathnath Mondal, Nanda Gopal Bar, Paramita Saha, Sanu Saha, Priyanka Halder, Partha Pratim Kayal, Parinita Singhamahapatra, Anushree Medda, Roumi Patra, Anup Kumar Ghosh, Arnab Bisuei, Monimala De, Indrajeet Giri, Shubhajit Mondal, Bitan Sardar, Achena saha, Payel Mukherjee, Ahsish Ghosh, Rajesh Das, Rounak Jahan, Pallabi Thakur, Subhasish Malakar, Sanghamitra Sarkar, Saikat Mondal, Pintu Nusipuri, Kamal Hossen, Nadeem Khan, Udita Mishra, Anirudra Mishra, Rahul mondal, Bikash Mondal, Shubhajit Mondal for their time, valuable suggestions and mentally support during my Ph.D period.

- I want to acknowledge all my PhD batchmates; Dr. Pallab Karjee, Dr. Jitendra Nath, Tanumoy Sarkar, Bapan Samanta, Bikoshita Parashar, Priyanka Adhikari, Bittu Lama, Dr. Rinki Brahma, Dr. Sabina Yashmin, Rahul Sharma, Debjoyti Pal, Indraneel Debnath, Tirupati Roy, Sagnik dey, Samir Roy, Dr. Chan, Dr. Hrishikesh Kalita, Dr. Priyanka Sarkar, Dr. Riya Sinha, Dr. Arin Bhagat, Rajdikshit Gogoi, Sourav Mondal, Somnath Paik, Partha Pratim Nath for making my days memorable in IITG.

- I have some special friends in my life who have always supported me at difficult times, and words cannot explain how much I appreciate them. I extremely show my gratitude to Vinay Arora, Mrinmoy Roy, Monoranjan Konwar, Shankhadeep Saha, Sujay Pal Nanda Gopal Bar, Anirban Ghosh, Amit Garai, Roumi patra from the inner core of my heart. There are ups and down in life, but some friend is always special in life. I express my gratitude to Dimpy Dey and her family.

- Words cannot express my gratefulness to my colleagues, juniors and s seniors pecially Dr. Debasish Barman, Dr. Mihir Manna, Dr. Ashesh Das, Dr. Payel Dewari, Dr. Chandan Gharui, Dr. Gobinda Doloi, Dr. Sandeep Mondal, Dr. Basab Kanti Das, Dr. Abhijeet Mondal, Dr. Nirmallya Bandhyapadhya, Dr. Bharghav Guhathakurtha, Dr. Sandeep Choudhury, Dr. Ipsita Mondal for their time, valuable suggestions during my Ph.D period.
- I could not have started this journey without the help of Academic Section, Student Affairs and R&D Section of IIT Guwahati.
- My sincerest thanks to Doctors and staffs of IIT Guwahati hospital for their caring
- This endeavor would not have been possible without my Ph.D. batchmates, seniors and juniors who helped directly or indirectly during my research.
- My heartfelt gratitude goes to my parents (Abharani Naandi, Rabindranath Nandi), sister (Krishna Mondal), brother (Gautam Nandi, Uttam Nandi, Budhdeb Nandi), and brother-in-law (Debasish Mondal), Sister-in-law (Debashri Das, Soumitra Nandi), Uncles (Abhimannu Nandi, late Chinmoy Nandi), aunts (Vanumati Nandi, Parvati Nandi), cousin (Radharani Nandi) who have always supported and motivated me through all of my ups and downs days. Without their immense patience, good wishes, and great sacrifice, I would have not been able to complete my doctoral studies. Thank all for all the unconditional love, care, and sacrifices that have shaped my life. Without their well wishes and blessings, I would not have been able to reach this stage and complete my doctoral studies. I would like to express my greetings to all my family members and relatives.
- It's very tough to fit all the names into a single paper; any absence in this brief acknowledgment does not imply a lack of gratefulness. I acknowledge all of them from whom I was being helped.
- Finally, I bow down to the almighty God for blessing, protecting, and guiding me throughout this period. I could never have accomplished this without the faith I have in the almighty. Thank you Kanha. Thank you Gopu. Thank you, Om Nama Shivai, Har Har Mahadev. Radhe Radhe. "Hare Krishna Hare Krishna Krishna Krishna Hare Hare Hare Rama Hare Rama Rama Rama Hare Hare".

Indian Institute of Technology Guwahati

Department of Chemistry

Declaration

I do hereby declare that the research work embodied in this thesis entitled "***Pincer-Ruthenium and Pincer-Cobalt Catalyzed Value-Addition of Alcohols***" has been carried out by me in the Department of Chemistry, Indian Institute of Technology Guwahati, Assam-781039, India, under the supervision of **Dr. Akshai Kumar A. S.** for the award of the degree of doctor of philosophy and it has not been submitted elsewhere for the award of any degree or diploma.

In keeping with the general practice of reporting scientific observation, due acknowledgments have been made wherever the work described is based on the findings of other investigators.

Guwahati

October 2024

Pran Gobinda Nandi
Roll No– 186122024
Department of Chemistry
IIT Guwahati, Guwahati
Assam, INDIA-781039

भारतीय प्रौद्योगिकी संस्थान गुवाहाटी
Indian Institute of Technology Guwahati

Dr. Akshai Kumar Alape Seetharam
Associate Professor, Department of Chemistry, Guwahati – 781039, Assam, INDIA
Tel: +91-3612583479 (O), Mobile: +91-8133036890, Fax: +91-3612582349
Email: akshaikumar@iitg.ac.in, akshaikumara@gmail.com

@iit-g
Centre for Nanotechnology

CERTIFICATE

I hereby certify that the entire work embodied in the thesis entitled "***Pincer-Ruthenium and Pincer-Cobalt Catalyzed Value-Addition of Alcohols***" is the result of investigations carried out by **Mr. Pran Gobinda Nandi** (Roll No: 186122024) at the Department of Chemistry, Indian Institute of Technology Guwahati, India under my guidance and the same has not been submitted elsewhere for the award of any degree or diploma.

17/10/2024

Dr. Akshai Kumar A. S.

Supervisor

Guwahati

October 17, 2024

Abbreviation

T	Temperature	IR	Infrared
°C	Degree Celsius	*e.g.*	For example
δ	Chemical shifts	ca.	around
g	Grams	*i.e.*	namely
mg	milligram	*Vs.*	versus
mmol	millimole	*via*	through
μM	micromole	^{i}Pr	*iso*-propyl
mL	milliliter	^{t}Bu	*tert*-butyl
ppm	parts per million	Cy	Cyclohexyl
r.t.	Room temperature	Ar	Aromatic
h	Hours	Ph	Phenyl
EPR	Electron Paramagnetic Resonance	Bim	*bis*-imidazole
MS	Mass spectrometry	MeBim	Methyl-*bis*-imidazole
HRMS	High-resolution mass spectrometry	ACN	acetonitrile
Hz	Hertz	THF	Tetrahydrofuran
MHz	Megahertz	RDS	rate determining step
NMR	Nuclear Magnetic Resonance	TON	Turnover number
J	Spin – spin coupling constant	TOF	Turnover frequency
s	Singlet	TOh^{-1}	Turnover over per hour
d	Doublet	TOs/h	Turnover over per hour
dd	Doublet of Doublet	RDS	Rate determining step
ddd	Doublet of Doublet of Doublet	TS	Transition state
t	Triplet	DFT	Density Functional Theory
q	Quartet	NPs	Nano particles
m	Multiplate	LOHC	Liquid organic hydrogen carrier
bs	Broad singlet	SCXRD	Singe crystal X-ray diffraction
rt	Room temperature	EWG	Electron withdrawing group
Equiv.	Equivalents	KIE	Kinetic isotope effect
m/z	Mass to charge ratio	SEM	Scanning electron microscopy
ORTEP	Oak Ridge Thermal Ellipsoid Plot	TEM	Tunneling electron microscopy
CCDC	Cambridge Crystallographic Data Center	GC	Gas chromatography

Abstract

The contents of the present thesis entitled "**Pincer-Ruthenium and Pincer-Cobalt Catalyzed Value-Addition of Alcohols**" have been divided into five chapters based on the results achieved from the experimental and computational work carried out during the entire course of the PhD research program.

Chapter I discusses a brief description on catalytic organic transformations reported in literature utilizing pincer-metal complexes. A large library of pincer-complexes that have been studied for various reactions such as alkane dehydrogenation, C-C or C-N bond formation and reduction of carbon dioxide, have been briefly reviewed in the chapter. The chapter ends with the identification and scope of the current thesis.

Chapter-II discusses the synthesis and characterization of three novel NNN pincer-Ru complexes based on *bis*(imino)pyridine ligands. These complexes along with other previously reported pincer-Ru complexes based on *bis*(imino)pyridine and 2,6-*bis*(benzimidazol-2-yl)pyridine ligands have been studied for the *β*-methylation of 2-phenylethanol and the selective *β*-dimethylation of 1-phenylethanol utilizing methanol as an alkylating agent. The optimization studies revealed that the pincer-ruthenium complex [(^{MeBim2}NNN)RuCl(PPh_3)$_2$]Cl is the most efficient among the considered catalysts. In the presence of 0.5 mol % of [(^{MeBim2}NNN)RuCl(PPh_3)$_2$]Cl, 0.75 equivalents of KOH and 7.5 equivalents of methanol, up to 92% yield of *β*-methylated 2-phenylethanol was observed at 140 °C after 24 h. Under similar conditions, the *β*-dimethylation of 1-phenylethanol was achieved using 2 equivalents of Na and 24.8 equivalents of methanol. The synthetic protocol was further extended towards the *β*-methylation and selective *β*-dimethylation of about 35 substrates. The evidence for the homogeneous nature of the reaction was revealed from mercury drop experiments and kinetic studies. From the kinetic studies, it was observed that the rate of product formation has a linear dependence on the concentrations of both the pincer-ruthenium catalyst and 2-phenylethanol. DFT studies are in line with the observed secondary kinetic isotope effect (KIE) of 1.56 and suggest that dehydrogenolysis involving σ-bond metathesis of methanol with the Ru-H species leading to the evolution of hydrogen is the RDS with a barrier of 24.06 kcal/mol. The NMR and HRMS analysis have shown the presence of pincer-Ru-H and pincer Ru-OMe species, which are the lowest-energy intermediates of the catalytic cycle and are likely to be the resting states of the catalytic cycle.

Chapter-III formulates the decarboxylative coupling of alcohols to alkanes employing a plethora of new and known NNN pincer-Ru complexes of the type (^{R2}NNN)RuCl$_2$L (R = ^{i}Pr, ^{t}Bu, Cy, Ph, *p*-F-C$_6$H$_4$, *p*-OMe-C$_6$H$_4$ and L = PPh$_3$, CO and CH$_3$CN) based on *bis*(imino)pyridine ligands and [(^{RBim2}NNN)RuClL$_2$]Cl (R = H and Me, L = PPh$_3$ and CO) based on 2,6-*bis*(benzimidazole-2- yl)pyridine ligands. Notably, among the considered pincer-Ru complexes and their Ru precursors, a majority were either not very active or were unselective giving alkene/alkane mixtures. However, in the presence of 0.5 equivalents of NaOH in toluene at 140 °C, the complex (^{MeBim2}NNN)RuCl$_2$(PPh$_3$)$_2$ based on 2,6-*bis*(benzimidazole-2-yl)pyridine ligand gave excellent activity affording up to 91% yield of alkane (1,3-diphenyl propane) with 100% selectivity within 5 h of reaction. Experimental mechanistic studies point to the generation of hydrogen (detected by GC) and formic acid (detected by ^{1}H NMR) during the reaction along with involvement of organic intermediates such as *α*,*β*-unsaturated aldehydes. The [(^{MeBim2}NNN)RuCl(PPh$_3$)$_2$]Cl catalyzed transformation of 2-phenyl ethanol to 1,3-diphenyl propane demonstrated a first-order dependence of initial rate on both the catalyst concentration and the concentration of base. While catalyst poisoning experiments using mercury revealed the homogeneous nature of the catalyst, a few of these molecular species including the resting state [(^{MeBim2}NNN)RuH(PPh$_3$)$_2$]Cl have been detected by HRMS analysis and NMR studies. The experimental studies are nicely complemented by the DFT studies, that indicate the dehydrogenolysis step leading to the formation of 2-phenyl acetaldehyde and the resting state (^{MeBim2}NNN)RuHCl (experimentally trapped as PPh$_3$ adduct) to be the rate-determining step with a barrier of 22.81 kcal/mole at 140 °C. Furthermore, the corresponding cycle with the least active catalyst (^{iPr2}NNN)RuCl$_2$(PPh$_3$) that gave 14% yield of 1,3-diphenyl propane at 25% selectivity, involved insertion of 1,3-diphenyl propene into the Ru-H bond as the RDS that was kinetically unfavorable by 5 kcal/mole in comparison to the rate-determining dehydrogenolysis step of the cycle involving most active catalyst [(^{MeBim2}NNN)RuCl(PPh$_3$)$_2$]Cl. This work elaborates the direct access to jet-fuel-grade 1,3-diphenyl propane starting from 2-phenyl ethanol in a single-step one-pot reaction and offers great promise to open up exciting opportunities in this very important field of study.

Chapter-IV deals with the catalytic *β*-alkylation of alcohols using inexpensive and readily available cobaltous chloride under aerobic conditions at 140 °C. At higher loadings of cobaltous chloride (1 mol%) in the presence of 2.5 mol% NaO^{t}Bu, there is an instant formation of heterogeneous Co nanoparticles (NPs) which are apparently air-sensitive and lead to poor yields (*ca.* 25%) of *β*-alkylated products. On the other hand, performing the reaction in an inert

atmosphere under otherwise identical conditions resulted in higher yields (*ca.* 44%). The heterogenization and gradual loss of activity in air could be mitigated by operating at a lower (0.01 mol%) $CoCl_2$ loading in the presence of 2.5 mol% NaO^tBu at 140 °C. Under these conditions, the catalytic *β*-alkylation of alcohols afforded high yields (up to 89%) and unprecedented turnovers (ca. 8900) of the desired product. Mechanistic studies are indicative of the involvement of catalysts based on *in-situ* generated molecular Co complexes of alcohols. The involvement of C–H activation is confirmed by the deuterium labelling experiments, where a KIE of 1.61 was obtained. Kinetic studies indicate linear dependence of the rate on the concentration (in the regime of homogeneity) of cobaltous chloride and sodium *tert*-butoxide along with a non-linear dependence on the concentration of both the substrates.

Chapter-V describes the synthesis of pincer complexes of the type $(^{R2}NNN)CoCl_2$ (R = ^{i}Pr, ^{t}Bu, Cy, Ph, *p*-F-C_6H_4) derived from the inexpensive base metal cobalt. Among these complexes, $(^{iPr2}NNN)CoCl_2$ was found to be highly active for the catalytic *β* alkylation of alcohols in air at 140 °C. While the pincer-Co (0.0025 mol %) catalyzed *β*- alkylation in the presence of NaO^tBu (2.5 mol %) took 24 h (85%, 34000 TON at 1417 TO/h) under conventional heating (140 °C), the corresponding reaction under microwave conditions (140 °C at 75 W) was complete in only 2 h with comparable yields (83%, 33200 TON), but with a better TOF (16600 TO/h). In contrast, $CoCl_2$ (0.0025 mol %) under similar conditions results in lower yields under both conventional (66%, 26400 TON at 1100 TO/h) and microwave heating (61%, 24400 TON at 12200 TO/h). The catalytic system has been successfully implemented (39 examples) to accomplish the *β*-alkylation of various secondary alcohols with several primary alcohols. EPR studies and magnetic moment measurements using the Evans method demonstrate that Co remains in its +2 oxidation state and in an octahedral geometry throughout the reaction. Significant evidence for the involvement of *β*- hydride elimination leading to acetophenone in the RDS of the pincer-Co catalyzed *β*-alkylation is obtained from competitive deuterium labelling experiments, which are indicative of a KIE of 6.14. The current report on base-metal catalysis in air under microwave conditions that leads to high yields of *β*-alkylation with unprecedented turnovers (33200 TON at 16600 TO/h) in a very short time (2 h) offers exciting atom-economical and greener possibilities for these class of synthetically valuable Guerbet-type reactions.

Contents

Chapter- I

Pincer-Metal Complexes and Their Applications

1.1. Pincer complexes

The term "pincer" represents one of a pair of curved claws of an animal such as a crab. In organometallic chemistry, the pincer complex represents a tridentate ligand coordinated to the metal. The tridentate (pincer) ligand behaves as a chelating ligand where the three binding atoms are coplanar in a meridional fashion (as shown in Figure 1.1).[1] The three binding atoms typically are N/P/C/S/O and the combination of ligating atoms are PCP, NCN, NNN, PNP, PCN, PNO and SCS. The unique chelating properties of pincer ligands imparts rigidity to the metal-ligand complex and the steric and electronic environments of the pincer framework results in the high selectivity in the catalytic reactions. Also, in certain cases the metal-ligand co-operation imparts stability to the metal complex. Tridentate pincer ligand frameworks strike an optimal balance between stability and reactivity.[2-6]

Shaw and Moulton were the first ones who developed meridional tridentate systems with central anionic carbon attached by two *tert*-butyl phosphine units which is now famously abbreviated as $^{t\text{Bu4}}$PCP.[3] In 1989, van Koten coined the term "pincer" to refer to such tridentate systems.

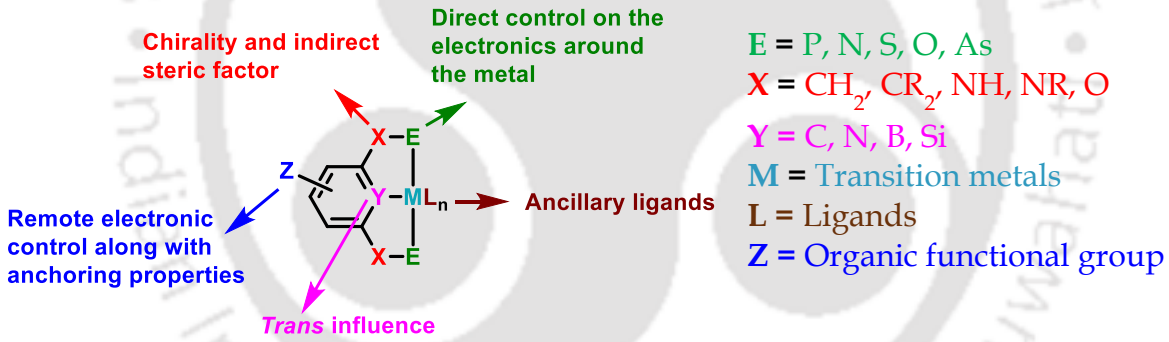

Figure 1.1. Schematic representation of a pincer metal complex representing the variable parameters.

The treatment of $^{t\text{Bu4}}$PCP ligand (**1.1**) with metal salt resulted in C-H activation at the *ipso* position of the $^{t\text{Bu4}}$PCP ligand (Scheme 1.1).[12, 13] The reaction of group **IX** and **X** metal salts with the $^{t\text{Bu4}}$PCP resulted in the formation of hydrido-chloride complexes (**1.Rh1** and **1.Ir1**) and chloride complexes (**1.Ni1**, **1.Pd1**, **1.Pt1**) respectively (scheme 1.1). The synthesis of the pincer-metal complex depends on the nature of the donor atoms, nature of the ligand backbone, the solvent's polarity and hybridization of the *ipso*-atom.

Pincer complexes has been modified by varying the ligating group or the linkers atoms depending on the various reaction requirements.[6, 16, 17] The electronic properties can be tuned

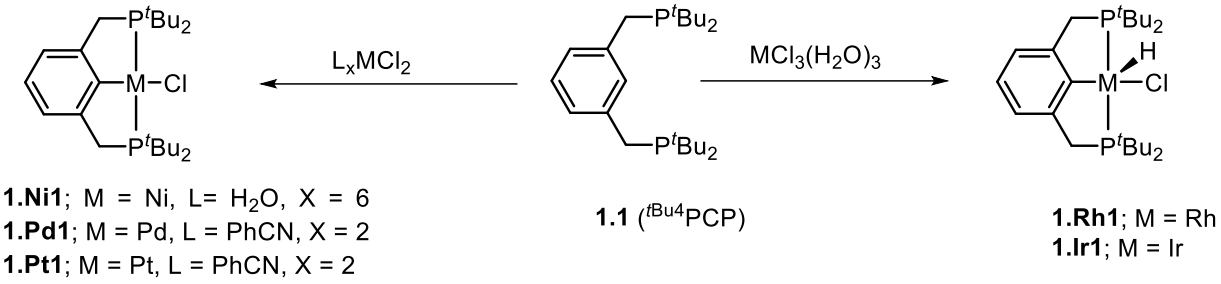

1.Ni1; M = Ni, L= H_2O, X = 6
1.Pd1; M = Pd, L = PhCN, X = 2
1.Pt1; M = Pt, L = PhCN, X = 2

1.1 (^{t}Bu4PCP)

1.Rh1; M = Rh
1.Ir1; M = Ir

Scheme 1.1. Initial report on PCP pincer-metal complexes.[14, 15]

by controlling the carbon *para* to the *ipso* carbon. Several polar functional groups could be placed on the *p*-carbon which provide an option to heterogenize the catalytic system on any solid support.[18] The application of pincer complexes are vast, which has been studied and applied using various pincer frameworks.[19, 20] Depending on the co-ordinating ligand framework the pincer complexes has been generalized as PCP,[21] PNP,[22-24] PCN,[25] PNN,[24, 26, 27] NCN,[21, 28] NNN,[29-31] CNC.[32, 33] Some of the selected examples of different types of pincer complexes are shown in Figure 1.2.

Pincer-metal catalyst plays a pivotal role in obtaining access to several synthetically challenging organic products, commodity chemicals,[7] fine chemicals,[7] fuels,[7] pharmaceuticals, and agrochemicals. Pincer complexes have been widely used as catalysts for hydrogenation,[8] dehydrogenation,[8] hydrofunctionalization[8] and activation of CO_2[9] to CH_3OH as well as N_2[10] to NH_3. The transformation of alcohols which are readily available from bio-mass to several value-added chemicals and fuels are also accomplished using pincer-metal catalysts.[7] Alcohols prove to be versatile feedstock materials for numerous organic transformations in chemical enterprises. Of particular interest are their utility in new C-C bond formations where they can be employed as a substitute of carbon source in hydrocarbon-based chemical industries and petrochemical industries. The traditional methods of synthesizing C-C bonds involve alkyl halide as alkylating agent with alcohols,[9] but these methods produce lot of waste products and it requires expensive reagents which are toxic in nature. Among the various protocols, the one where *β*-alkylation of alcohols have been employed to form C–C bond, catalyzed by transition metals have gathered huge attention.[11] Formation of higher *β*-alkylated alcohols *via* acceptorless dehydrogenative coupling of alcohols proves to be an environmentally benign process. Pincer-based metal complexes have been majorly employed for such transformations and the reports are crowded with precious metals having phosphine-based ligand systems.[10]

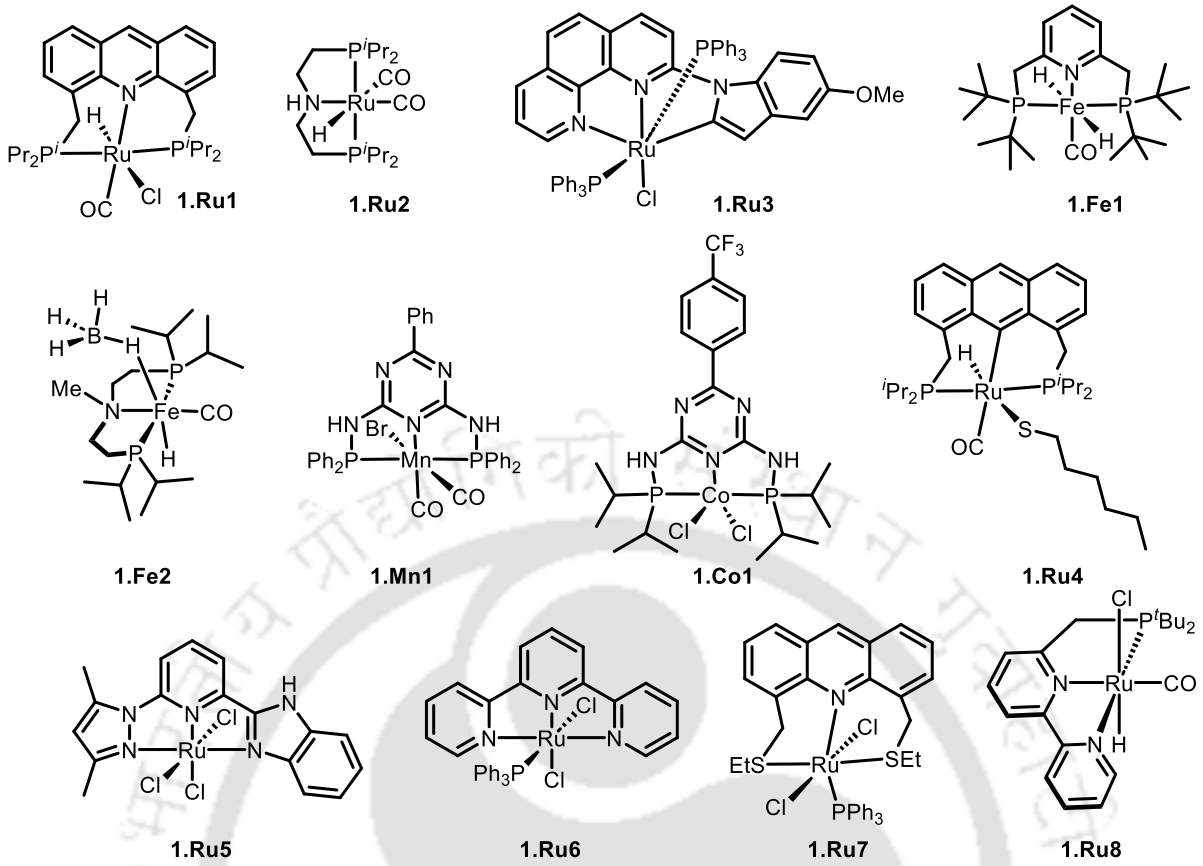

Figure 1.2. Different types of pincer-metal complexes reported in literature.

1.1.1. Catalytic application of various pincer-metal complexes

1.1.1.1. Alkane dehydrogenation reaction

Olefins are key chemical intermediates that may be converted to amines, alcohols, alkyl halides, aldehydes, ketones and esters or enchained into polymers with various commercial applications.[7] Pincer metal complexes play a huge role to convert the alkanes to the corresponding alkenes.

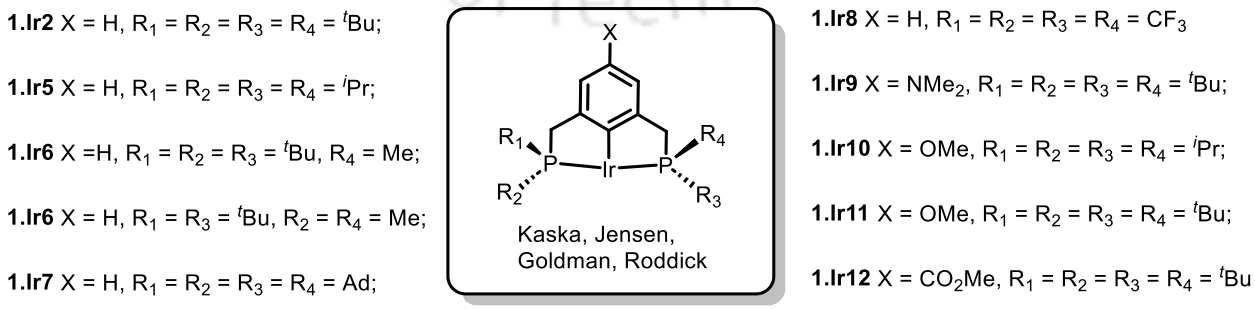

Figure 1.3. Pincer-Ir complexes reported for alkane dehydrogenation.

In 1996, Kaska and Jensen reported the use of PCP pincer-iridium complex (^{t}Bu4PCP)IrH$_2$ (**1.Ir3** = **1.Ir2-H$_2$**) as catalyst for the alkane transfer dehydrogenation (Figure 1.3).[34] The **1.Ir3** exhibited excellent activity for the dehydrogenation of COA that is driven by the periodic addition of TBE (increments of 0.4 M) at an elevated temperature (200 °C) giving up to 1000 TOs at 12 TON/min. Later, Kaska, Jensen and Goldman investigated that the **1.Ir3** (1 mM) itself catalyzed the dehydrogenation of cyclodecane without any acceptor and yielded 360 TON in 24 h at 200 °C.[35] Subsequently, Goldman group developed a active catalyst (^{i}Pr4PCP)IrH$_4$ (**1.Ir4 = 1.Ir5-H$_4$**) for the acceptorless cyclodecane dehydrogenation. The dehydrogenation of cyclodecane proceeded *via* double dehydrogenation of cyclodecene followed by isomerization to give *trans*, *trans*-1,5 cyclodecadiene which subsequently underwent a Cope rearrangement to give *trans*-1,2-divinylcyclohexane. This *trans*-1,2-divinylcyclohexane acted as hydrogen acceptor to complete the catalytic cycle with a net production of diethylcyclohexane from cyclodecane (Scheme 1.2).[7]

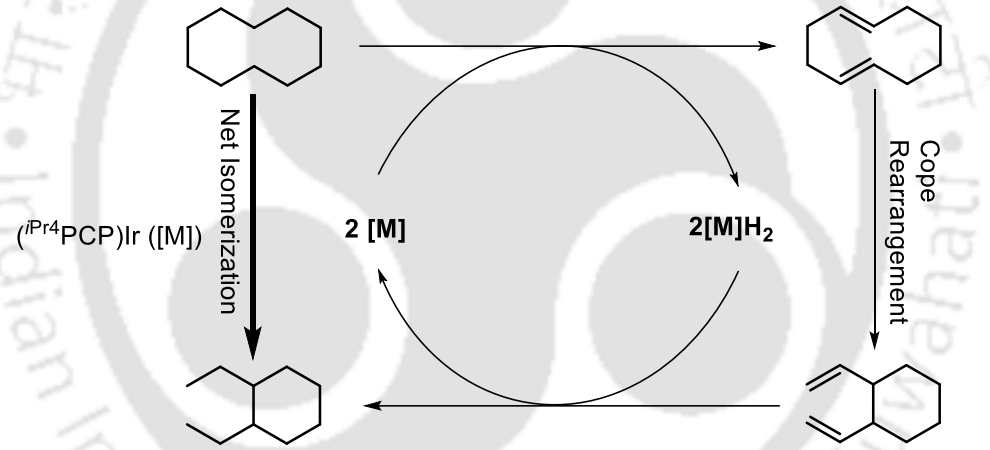

Scheme 1.2. Net isomerization of cyclodecane to diethylcyclohexane, catalyzed by (^{i}Pr4PCP)Ir.

Goldman has performed a detailed study on the effect of substituents in the catalytic dehydrogenation of alkanes. The bulkiness of the substituents hindered the progress of the reaction. In spite of the 'pincer effect' the bulkiness of the *tert*-butyl groups inhibits H_2 addition, i.e intermediates of dehydrogenation cycle are more favoured by isopropyl groups whereas it is sterically disfavoured by the *tert*-butyl groups. On this basis, the dehydrogenation of cyclooctane is more favoured with (^{i}Pr4PCP)IrH$_2$ (**1.Ir5-H$_2$**) than with (^{t}Bu4PCP)IrH$_2$ (**1.Ir2-H$_2$**).[36] The dehydrogenation of cyclooctane was carried out with both **1.Ir2-H$_2$** and **1.Ir5-H$_2$** at 150 °C at a similar loading of 1 mM). While in the case of **1.Ir5-H$_2$** more than 94 TON was achieved, only 11 TON was obtained when **1.Ir2-H$_2$** was used (Table 1.1). The rate of

acceptorless dehydrogenation rate is more for cyclodecane that has a high reflux temperature of 201 °C than that of low boiling cyclooctane (b.p 149°C). The **1.Ir5-H₂** catalyzed the cyclodecane dehydrogenation to cyclodecene with a *cis*: *trans* ratio of 4.6:1 with 460 TON after 1h. In case of **1.Ir2-H₂** lower TON of 170 after 4h was observed.[36]

Table 1.1. Dehydrogenation of cyclooctane with **1.Ir2** and **1.Ir5**

entry	catalyst [1.0 mM]	time	TON
1	**1.Ir2-H₂**	1 h	11
2	**1.Ir5-H₂**	30 min	47
3	**1.Ir5-H₂**	1 h	>94
4	**1.Ir5-H₂**	15 h	105

In 1999, Goldman reported the acceptorless dehydrogenation of *n*-alkanes with homogeneous catalyst **1.Ir5-H₂** that resulted in a mixture of internal isomers.[37] The catalyst ($^{i\text{Pr4}}$PCP)IrH$_2$ (**1.Ir5-H₂**) showed high efficiency for acceptorless dehydrogenation of *n*-alkanes compared with ($^{t\text{Bu4}}$PCP)IrH$_4$ (**1.Ir2-H₄**) and both the catalysts were selective towards 1-octene in the *n*-octane/1-decene transfer dehydrogenation at 150 °C. While ($^{i\text{Pr4}}$PCP)IrH$_2$ (**1.Ir5-H₂**) showed higher catalytic efficiency than ($^{t\text{Bu4}}$PCP)IrH$_4$ (**1.Ir2-H₂**), the latter showed higher selectivity than the former in the catalytic transfer dehydrogenation of *n*-octane/1-decene at 150 °C.

For the COA/TBE and *n*-octane/NBE dehydrogenation, Yamamoto developed fused tricyclic 7-6-7 type pincer-Ir complex (7-6-7^{R4}PCP)Ir (**1.Ir13**,R = ^{i}Pr ; **1.Ir14**, R = Cy; **1.Ir15**, R = Ph) complexes (Figure 1.4) [38]. These types of catalysts are highly efficient due to their flexible backbone and their fused nature of the bonds imparts rigidity and thermal stability to the iridium complex. The dehydrogenation rate of COA/TBE (1:1) was higher at both low and high temperature with phenyl analogue **1.Ir15**, while with the isopropyl analogue **1.Ir13**, the rate was higher only at high temperature. The catalyst **1.Ir15** showed a maximum of 4100 TON after 24 h at 200 °C for the transfer dehydrogenation of COA/TBE (1:1). In the case of *n*-octane/NBE dehydrogenation, **1.Ir13** showed higher activity compared with **1.Ir15** due to the poor solubility of **1.Ir15** in *n*-octane.

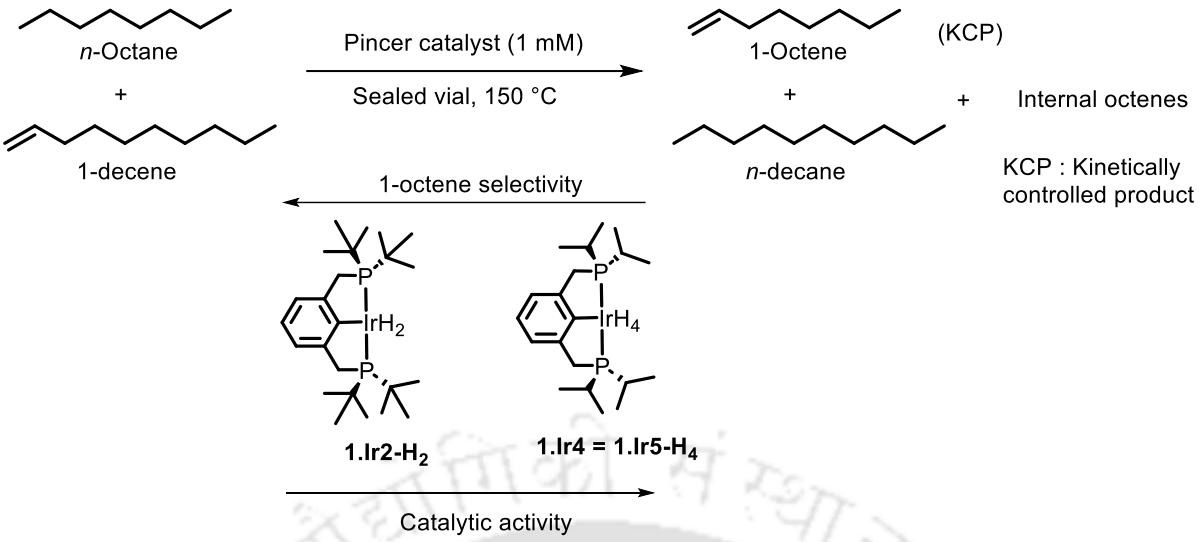

Scheme 1.3. Transfer dehydrogenation of *n*-octane catalyzed by **1.Ir2-H$_2$** and **1.Ir5-H$_4$**.

In a similar fashion, Kaska and co-workers developed tricyclic (PCP)-Ir complex (^{t}Bu^{4}Anthraphos)Ir, **1.Ir17** for the acceptorless dehydrogenation of alkanes (Figure 1.4).[39] The complex **1.Ir17** was thermally stable up to 250 °C due to its high rigidity. Later, Goldman and Brookhart observed that the isopropyl analogue (^{i}Pr^{4}Anthraphos)Ir, **1.Ir16** (Figure 1.4) was very effective towards alkane dehydrogenation [40, 41].

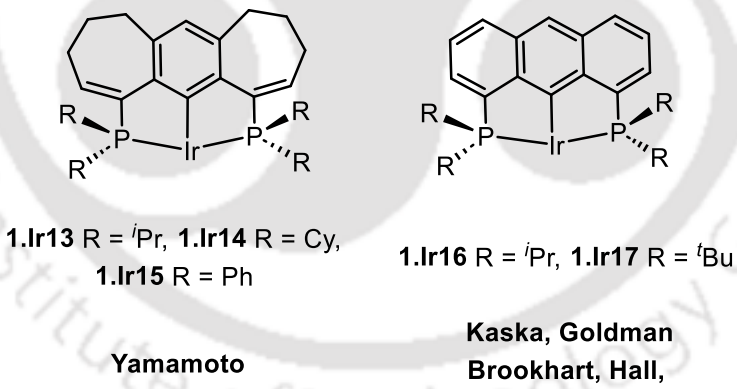

Figure 1.4. Fused tricyclic PC(sp^2)P pincer-Ir complexes reported for alkane dehydrogenation.

Brookhart and Jensen [42-45] independently developed (^{R4}POCOP)Ir type pincer complexes for dehydrogenation of alkanes (Figure 1.5). The reactivity in alkane dehydrogenation was changed due to introduction of heteroatom such as O, S in place of CH_2 of the PCP ligand framework. For the COA/TBE dehydrogenation, the catalyst (^{t}Bu^{4}POCOP)Ir (**1.Ir19**) **(**1583 TONs after 40 h) is more active than (^{t}Bu^{4}PCP)Ir (**1.Ir2**) **(**230 TONs after 20 h). However, for

the dehydrogenation of linear alkanes, ($^{t\text{Bu4}}$POCOP)Ir (**1.Ir19**) was less effective catalyst compared to ($^{t\text{Bu4}}$PCP)Ir (**1.Ir2**).[42]

Brookhart and co-workers tested fluoro containing pincer complexes (*p*-F-$^{t\text{Bu4}}$POCOP)Ir (**1.Ir24**) and (*p*-C_6F_5-$^{t\text{Bu4}}$POCOP)Ir (**1.Ir25**) for the COA/TBE (1:1) dehydrogenation at 200 °C. The catalyst (*p*-F-$^{t\text{Bu4}}$POCOP)Ir (**1.Ir24**) (1530 TONs after 40 h) showed comparable activity with ($^{t\text{Bu4}}$POCOP)Ir (**1.Ir19**), whereas (*p*-C_6F_5-$^{t\text{Bu4}}$POCOP)Ir (**1.Ir25**) showed a higher activity (2041 TONs after 40 h) (Figure 1.5).

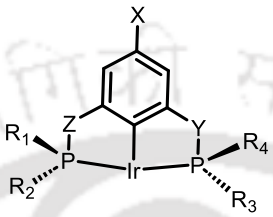

1.Ir18 X = H, Y = Z = O, $R_1 = R_2 = R_3 = R_4 = {}^{i}Pr$;

1.Ir19 X = H, Y = Z = O, $R_1 = R_2 = R_3 = R_4 = {}^{t}Bu$;

1.Ir20 X = H, Y = CH_2, Z = O, $R_1 = R_2 = R_3 = R_4 = {}^{i}Pr$;

1.Ir21 X = H, Y = CH_2, Z = O, $R_1 = R_2 = R_3 = R_4 = {}^{t}Bu$;

1.Ir22 X = H, Y = CH_2, Z = O, $R_1 = R_2 = {}^{i}Pr$, $R_3 = R_4 = {}^{t}Bu$;

1.Ir23 X = H, Y = S, Z = O, $R_1 = R_2 = R_3 = R_4 = {}^{i}Pr$

1.Ir24 X = F, Y = Z = O, $R_1 = R_2 = R_3 = R_4 = {}^{t}Bu$

1.Ir25 X = C_6F_5, Y = Z = O, $R_1 = R_2 = R_3 = R_4 = {}^{t}Bu$;

1.Ir26 X = OK, Y = Z = O, $R_1 = R_2 = R_3 = R_4 = {}^{t}Bu$;

1.Ir27 X = OMe, Y = Z = O, $R_1 = R_2 = R_3 = R_4 = {}^{t}Bu$;

Brookhart, Jensen, Goldman, Huang

Figure 1.5. PYCZP pincer-iridium complexes studied for alkane dehydrogenation.

Huang and co-workers observed that ($^{i\text{Pr4}}$PSCOP)Ir (**1.Ir23**) catalyzed the transfer dehydrogenation of COA/TBE (1:1) at 200 °C with at the rate of 2900 TOh^{-1} but for the similar reaction ($^{i\text{Pr4}}$POCOP)Ir (**1.Ir18**) showed 6900 TOh^{-1} whereas for ($^{t\text{Bu4}}$PCP)Ir (**1.Ir2**) TOF of 1200 TOh^{-1} was observed.[42] In case of ($^{t\text{Bu4}}$POCOP)Ir (**1.Ir19**) the dehydrogenation reactions levelled off after 6 h with only 62% conversion but ($^{i\text{Pr4}}$PSCOP)Ir (**1.Ir18**) catalyzed the dehydrogenation reactions with complete consumption of TBE after 8 h.

Huang reported 1400 TOh^{-1} in the ($^{i\text{Pr4}}$PSCOP)Ir (**1.Ir23**) catalyzed *n*-octane dehydrogenation using 0.5 M TBE, whereas ($^{t\text{Bu4}}$POCOP)Ir (**1.Ir19**) and ($^{t\text{Bu4}}$PCP)Ir (**1.Ir2**) demonstrated 220 TOh^{-1} and 820 TOh^{-1} respectively under identical conditions. Both ($^{i\text{Pr4}}$PSCOP)Ir (**1.Ir23**) and ($^{t\text{Bu4}}$PCP)Ir (**1.Ir2**) showed similar regioselectivity (30%) at comparable TON of 115.

Wendt group reported an efficient transfer dehydrogenation of COA/TBE (1:1) with ((*m*-$CF_3)_2$-$^{t\text{Bu4}}$POCOP)Ir (**1.Ir29**) at 170 °C [46]. The catalyst (*p*-((*m*-$CF_3)_2C_6H_3$)$^{t\text{Bu4}}$POCOP)Ir

(**1.Ir28**) achieved 2070 turnovers after 40 h at 200 °C for the transfer dehydrogenation of COA/TBE (1:1). While the catalyst (*p*-((*m*-CF_3)$_2$$C_6H_3$)^{tBu4}POCOP)Ir (**1.Ir28)** showed lower activity than ((*m*-CF_3)$_2$-^{tBu4}POCOP)Ir **(1.Ir29)**, it showed comparable activity as (*p*-C_6F_5-^{tBu4}POCOP)Ir (**1.Ir25)** (Figure 1.5) [42].

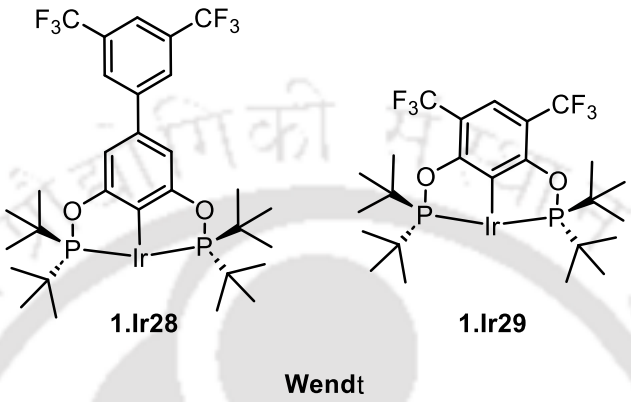

Figure 1.6. Fluorine containing POC(sp^2)OP pincer-Ir complexes reported for alkane dehydrogenation.

Over the last 4 decades, the catalytic alkane dehydrogenation using pincer metal complexes of group 9 has been extensively studied. In particular, pincer-iridium complexes played the most vital role as a catalyst for the transfer dehydrogenation of alkanes, demonstrating high TON and excellent regioselectivity. The pincer-iridium catalyzed dehydrogenation has various applications depending on substrates and acceptors. In the transfer dehydrogenation, the lighter alkene plays a dual role as both a sacrificial acceptor and a dienophiles in subsequent Diels-Alder cyclization, leading to the production of various precious BTX-chemicals.[46b] The alkyl group in cross metathesis selectively produces industrially valuable linear *n*-alkyl arenes.[46b] Additionally, the direct functionalization of alkyl-boronate esters, silanes, linear alkyl amines and linear alkyl aldehydes has also been achieved.[46b] However, achieving high yield of α-olefins starting from alkane remains a significant challenge. Though there are a plethora of pincer-metal catalysts based on Ir,[46b-c] Rh,[34,46d] Ru[46e] that have been reported for alkane dehydrogenation, only few of them has been discussed here to provide a glimpse of utility of pincer complexes in accomplishing this chemistry.

1.1.1.2. Reduction of CO_2

Carbon dioxide (CO_2) is a green-house gas and use of CO_2 as a renewable and cost-effective

C1 building block has received increasing attention from the scientific point of view in recent years.[47-53] The activation of CO_2 is very challenging due its high thermal and kinetic stability.[54-56] Hydrogenation of CO_2 leads to several useful chemicals like methanol, methane, formaldehyde and formic acid that are versatile starting materials to fuels and fine chemicals. In 1976, Hashimoto and co-workers first reported CO_2 hydrogenation to formic acid and its derivatives by using group VIII transition metal catalysts.[57a] Later, various methodologies were developed for the value-addition of CO_2 using homogeneous[57a] as well as heterogeneous[57b] catalytic systems.

For the first time, in 2009 Nozaki and co-workers carried out the hydrogenation of CO_2 with a pincer complex.[58] They developed PNP-Ir (**1.Ir30**) catalyst for the hydrogenation of CO_2 to formate salts at 60 bar (CO_2 : H_2 = 1:1) with 3,500,000 TON (Scheme 1.4).[58] Later, Hazari group introduced a new iridium complex **1.Ir31** for the hydrogenation of CO_2 to formate salt with 348000 TON at 55 bar (CO_2 : H_2 = 1:1) (Scheme 1.4). In 2011, Milstein and co-workers reported PNP pincer-iron complex **1.Fe1** and used it for the conversion of $NaHCO_3$ to sodium formate in the presence of molecular hydrogen (8.3 bar) and achieved 320 TON. This catalyst also demonstrated activity for the hydrogenation of carbon dioxide in the presence of molecular hydrogen under 10 bar of CO_2 and H_2 (2:1) and it produced formate with 788 TON (Scheme 1.4).[59] In 2015, Pidko and co-workers used **1.Ru9** for the hydrogenation of CO_2 to formate salt and obtained 1100000 TON at 40 bar (CO_2 : H_2 = 1:1) (Scheme 1.4).[60]

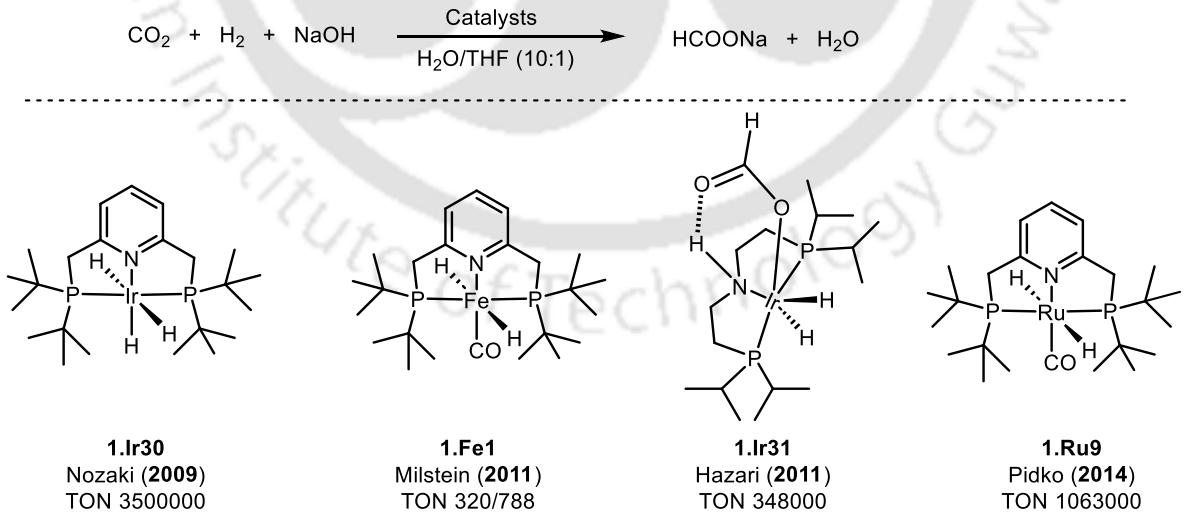

Scheme 1.4. Some initial reports on CO_2 hydrogention by pincer-metal catalysts.

In 2015, Bernskoetter and co-workers reported iron catalyzed CO_2 hydrogenation to formate salt (Scheme 1.5).[61] The catalyst **1.Fe2** showed the best result with 58990 TON whereas **1.Fe3**

(TON 46110) and **1.Fe5** (TON = 46130) exhibited almost similar activity. In contrast, **1.Fe4** catalyzed the hydrogenation of CO_2 with little less activity and exhibited TON of 38970 (Scheme 1.5).

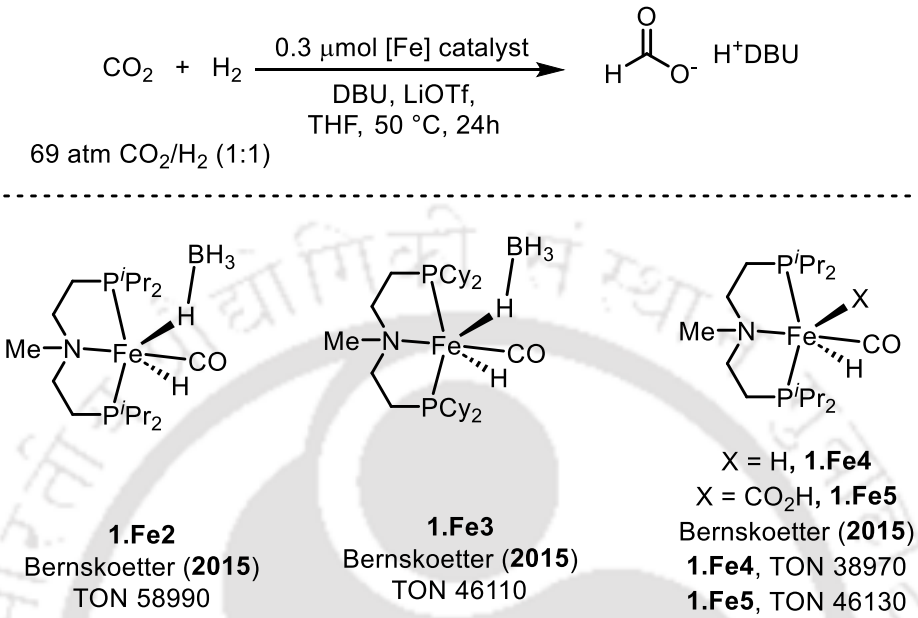

Scheme 1.5. Hydrogenation of CO_2 catalyzed by (PNP) pincer-iron complexes reported by Bernskoetter[61]

In 2016, hydrogenation of CO_2 with pincer catalyst was reported by Bernskoetter and co-workers. They developed PNP pincer-cobalt catalyst for the hydrogenation of CO_2 to formate as shown in Scheme 1.6.[62] The catalyst **1.Co2** showed quite high TON of 29000 (TOF = 5700 h^{-1}) with LiOTf as Lewis acid and DBU as a base. In the presence of Lewis acid, formate anion dissociated from metal centre,[61] but in absence of Lewis acid, catalytic activity decreased significantly, resulting in a TON of 460. Furthermore, the addition of one equivalent of ligand in the catalytic reaction mixture stabilized the metal complex and resulted in an increased TON. The analogous complexes of **1.Co2**, namely **1.Co3** and **1.Co4** were also employed for the hydrogenation of CO_2 as shown in Scheme 1.6. The catalyst **1.Co3** with a cyclohexyl ligand displayed similar catalytic activity as **1.Co2** with TON of 24000, whereas its NH analogue **1.Co4** displayed lower TON of 450.

A hypothetical catalytic mechanism for hydrogenation of CO_2 was proposed using **1.Co2** as shown in Scheme 1.7.[62] The complex **1.Co2** reacts with H_2 to form an intermediate **1.Co2a** In presence of base DBU, **1.Co2a** could be deprotonated to monohydride cobalt complex **1.Co2b**

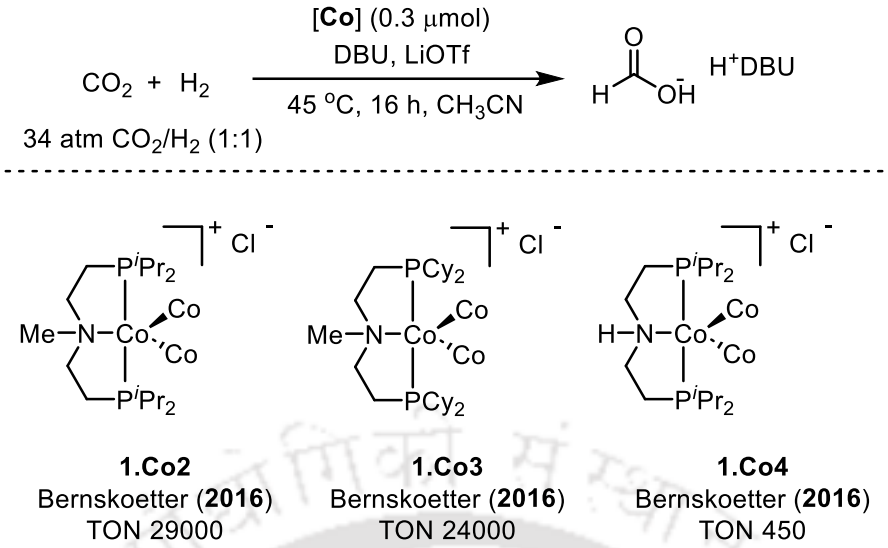

Scheme 1.6. Hydrogenation of CO_2 catalyzed by (PNP) pincer-cobalt complexes. [62]

and it could reversibly converted to **1.Co2c** with loss of one molecule of CO or react with CO_2 to form formate-coordinated cobalt intermediate **1.Co2d** *via* insertion mechanism. In the last step, dissociation occurs to produce the formate anion while regenerating **1.Co2**.[62]

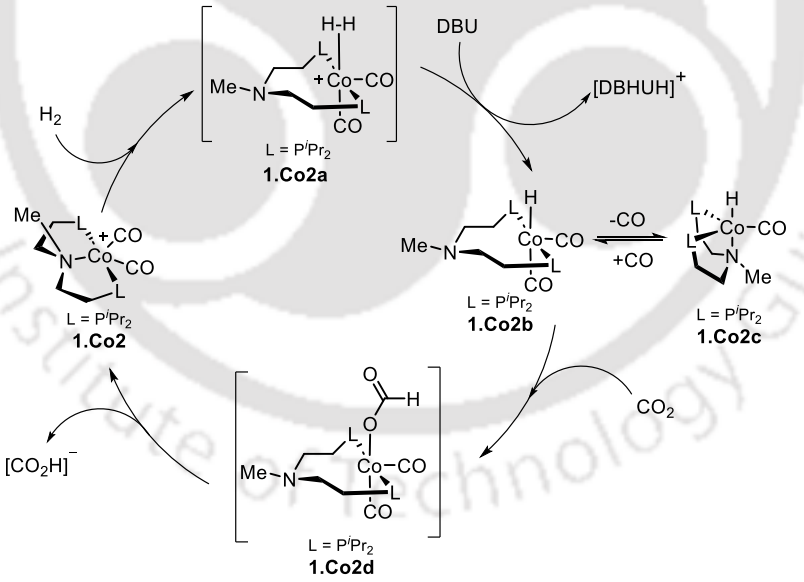

Scheme 1.7. Proposed mechanism for CO_2 hydrogenation using homogenous pincer-cobalt catalyst **1.Co2**.[62]

Recently in 2024, Ahmed and co-workers developed (CNC) carbene pincer-cobalt(I) complex for the hydrogenation of CO_2 to formate salt with 39800 TON (Scheme 1.8).[63]

Overall, significant progress has been made for the hydrogention of CO_2 to formic acid using

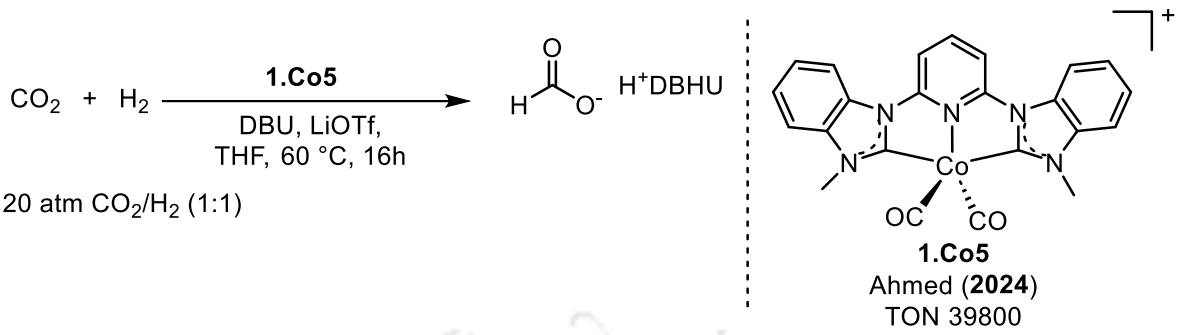

Scheme 1.8. Hydrogenation of CO_2 catalyzed by (CNC) pincer-cobalt(I) complex.[63]

homogeneous pincer complexes, few of which have been discussed above.[61,62] For CO_2 hydrogenation, utilizing inexpensive and earth-abundant metals that exhibit greater catalytic activity than their precious metal counterparts present a promising solution in near future.

1.1.1.3. Catalytic fixation of nitrogen gas to ammonia

Catalytic nitrogen fixation is an essential chemical revolution and one of the most important and challenging transformations.[10] The development in this field made with the molecular complexes has enabled the formation of the bioactive form of NH_3 from N_2.[10] The conventional Haber-Bosch methods requires very high pressure of 150-250 bar and high temperature of 400-500 °C for the transformation of N_2 to NH_3 which has very high demands in terms of cost.[10] In order to accomplish this very important transformation under milder conditions, there has been numerous efforts on development of homogeneous catalytic systems.[10]

In 2010, in a first example of a pincer catalyst for the N_2 to NH_3 reaction, Nishibayashi and co-workers introduced dinuclear molybdenum complex for molecular nitrogen fixation (Scheme 1.9).[64] The N_2 reduction was carried out in toluene at room temperature with [LutH]OTf (96 equivalents) and Cp_2Co (72 equivalents) as a proton and electron source respectively with **1.Mo1** as (pre)catalyst which resulted in 6.9 equivalents of NH_3 per Mo. Upon increasing the acid ([LutH]OTf) to 266 equivalents and reductant Cp_2Co to 72 equivalents, the NH_3 production increased to 11.6 equivalents per Mo. The substituents present on the phosphorous atom had significant influence on the PNP coordination mode, that has resulted in vast changes in the activity of the catalytic reaction.[65] While the (pre)catalyst **1.Mo2** with *tert*-butyl on one phosphine arm and phenyl on the other phosphine arm provided 2 equivalents of NH_3 per Mo,

1.Mo3 flanked with *tert*-butyl phosphine and adamantyl phosphine produced 14 equivalents of NH_3 per Mo (Scheme 1.9).[65]

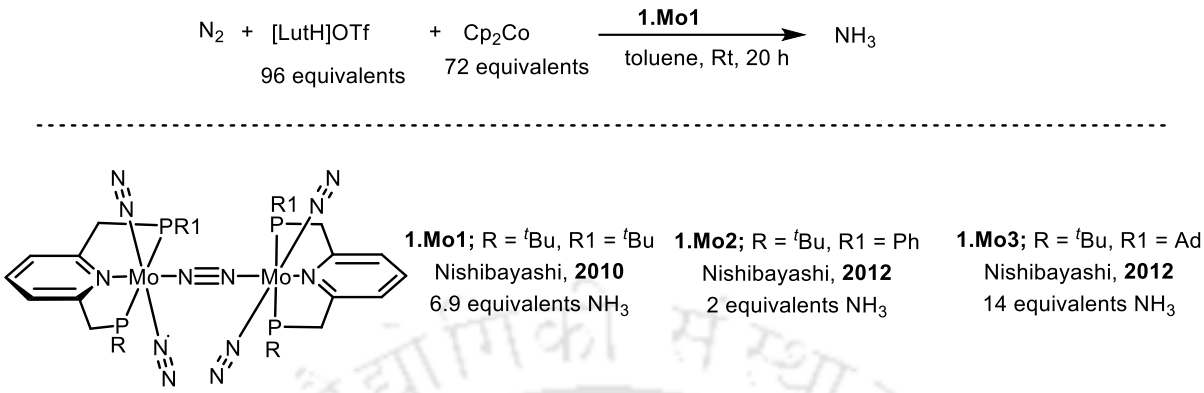

Scheme 1.9. The first report on pincer-Mo catalyzed activation of N_2 by Nishibayashi.[64, 65]

In 2017, Schrock and co-workers developed a geometrically distinct pincer ligand framework of diamido(pyridine) for N_2 fixation using Mo.[66] The catalyst **1.Mo4** in the presence of 108 equivalents of $[Ph_2NH_2]OTf$ and 54 equivalents of Cp^*_2Co produced 1.3 equivalents of NH_3 (Scheme 1.10).[66] The use of a large excess of base and Cp^*_2Co is the drawback of this protocol. Furthermore, upon using the *tert*-butyl methoxy substituted catalyst **1.Mo5** under similar reaction conditions, a significant enhancement in the yield of NH_3 (7.9 equivalents) was observed (Scheme 1.10).[66]

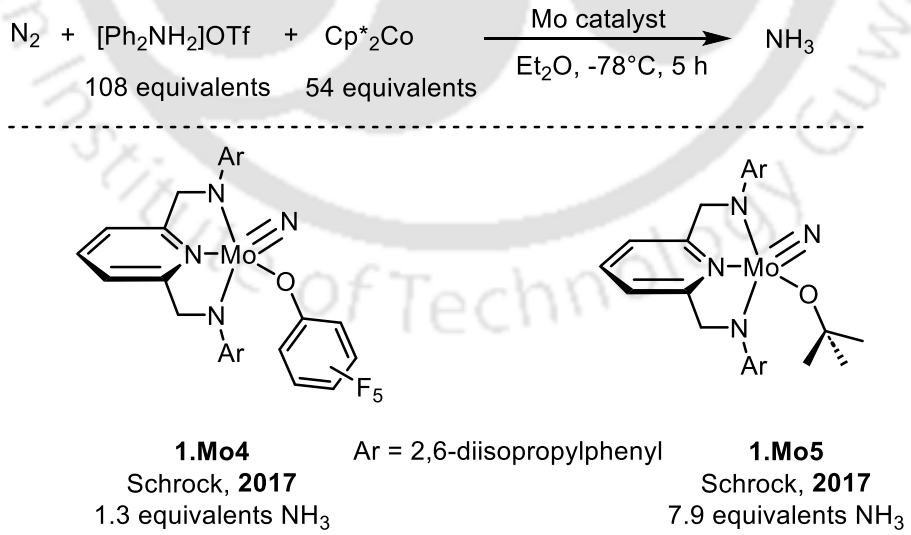

Scheme 1.10. Mo catalyzed activation of N_2 by Schrock.[66]

Nitrogen fixation, a six-electron/six-proton reduction process that produces NH_3 from N_2, is a

very crucial transformation, yet very challenging due to the inert nature of N_2.[10] The homogeneous pincer complexes have demonstrated high activity for the same and representative examples have been discussed above, as it is beyond the scope of the current chapter to cover all the reports. The recent investigations have focused on use of various metals such as Ru, Os, V, Ti and Co and have explored their mechanism in comparison to Mo.[10]

1.1.1.4. Hydrofunctionalization of alcohols

1.1.1.4.1. Guerbet reaction

In the age of fast-depleting fossil fuels, alternative energy source are very necessary to satisfy the energy demand of the society.[67, 68] Ethanol is acknowledged as a sustainable fuel, as it is very easy to access from fermentation process,[69] However, ethanol has poor energy density (70%)[69, 70] and higher absorptivity towards water.[71-73] Therefore *n*-butanol is the alternative energy source because of its high energy density (85%) and its immiscibility with water. [71-73] Guerbet reaction is one such potential solution that can transform ethanol to *n*-butanol.[74] Since, the last decade, the pincer catalytic system has been widely employed for such transformation. Transition metal catalyzed dehydrogenation of ethanol produces the corresponding acetaldehyde, which in the presence of a base undergoes aldol-condensation to produce *α*, *β* unsaturated aldehyde with water as a sole by-product. Hydrogenation of this *α*, *β* unsaturated aldehyde produces the *n*-butanol (Scheme 1.11).

In 2016, Szymczak and co-workers developed (NNN) type pincer-ruthenium complex **1.Ru10** for Guerbet reaction of ethanol to *n*-butanol.[75] The catalyst **1.Ru10** (0.1 mol%) in presence of 5 mol% NaOEt and 0.4 mol% PPh_3 showed 53% conversion of ethanol towards *n*-butanol wth 78% selectivity and 530 TON at 150 °C for 2 hours (Scheme 1.12). Under the same reaction conditions with only 0.001 mol% **1.Ru10** without 0.4 mol% PPh_3, 1.4% conversion of ethanol with 1.4% yield towards *n*-butanol was observed with 100% selectivity and 1400 TON (700 TOF).[75]

In the same year Milstein carried out the Guerbet reaction with PNP and NNP type pincer-ruthenium complexes.[76] The **1.Ru1** (0.02 mol%) catalyzed the *n*-butanol formation from ethanol in the presence of 4 mol% NaOEt at 110 °C for 16 h to give 18.2% conversion (14.6 % yield, 86. 1% selectivity) and 18209 TON (Scheme 1.12).[76] When the reaction was carried out at elevated temperature (150 °C) for 40 hours in the presence of 20 mol% NaOEt and 0.02

mol% **1.Ru**, 73.4% conversion (35.8% yield, 31.8% selectivity) of ethanol towards *n*-butanol was observed with 3671 TON.[76]

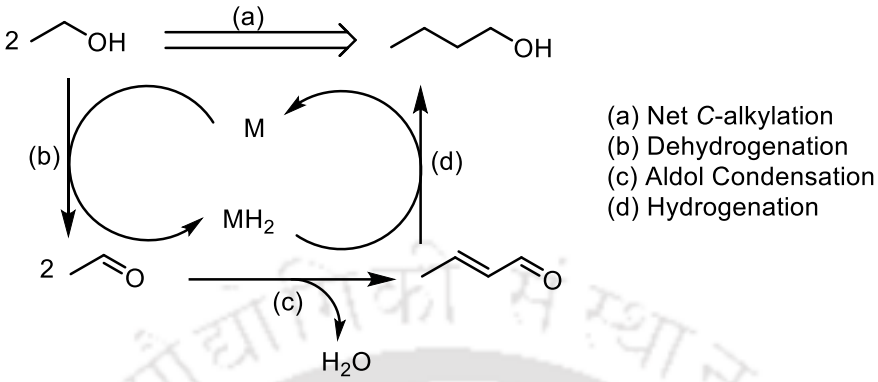

Scheme 1.11: Schematic representation of the transition metal catalyzed upgradation of ethanol to *n*-butanol.

In 2017, Liu and co-workers developed the PNP type pincer-manganese complexes for the conversion of ethanol to *n*-butanol.[77] The **1.Mn2** (0.00125 mmol) catalyzed the Guerbet reaction of ethanol (75 mL, 1275 mmol) in the presence of 12 mol% of NaOEt at 160 °C and after 7 days 11.2% conversion of ethanol with 9.8% yield of *n*-butanol with 92% selectivity and 114120 TON was observed (Scheme 1.12).[77] The Liu group reported the highest selectivity of 100% with 170 TON and 1.7% yield of *n*-butanol when the reaction was performed with **1.Mn2** (0.01 mmol), NaOAc (6 mol%) and EtOH (6 mL, 100 mmol) for 24 h at 160 °C.[77] They reported the highest yield of *n*-butanol of 22.7% with 87% selectivity and 286 TON using **1.Mn2** (0.1 mmol, 0.1 mol%), NaOEt (12 mol%) and EtOH (6 mL, 100 mmol) when the reaction was carried out at 160 °C for 96 h.[77]

In a similar parallel investigation, Jones and co-workers reported the formation of *n*-butanol from ethanol using (PNP) type pincer-Mn complexes.[78] The catalyst **1.Mn2** (0.5 mol%) catalyzed the Guerbet reaction with 25 mol% of NaOEt at 150 °C for 24 h and 34% yield of *n*-butanol was obtained with 68 TON in presence of 1g molecular sieves (Scheme 1.12).[78]

Recently, Kumar and co-workers developed a series of (NNN) type pincer-Ru complexes for the Guerbet reaction.[68, 79a] The *bis*(imino)pyridine based pincer ruthenium complex ^{Cy2}(NNN)RuCl$_2$(CO) (**1.Ru11**) (0.05 mol%) in presence of 10% NaOEt provided 335 TON with 170 TOF (TOh^{-1}) and 90% selectivity at 140 °C for the *n*-butanol formation from ethanol (Scheme 1.13). Subsequently, the 2,6-*bis*(benzimidazole-2-yl) pyridine based pincer ruthenium complex (^{Bim2}NNN)RuCl$_2$(CO) (**1.Ru12**) (0.025 mol%) in presence of 10% NaOEt provided

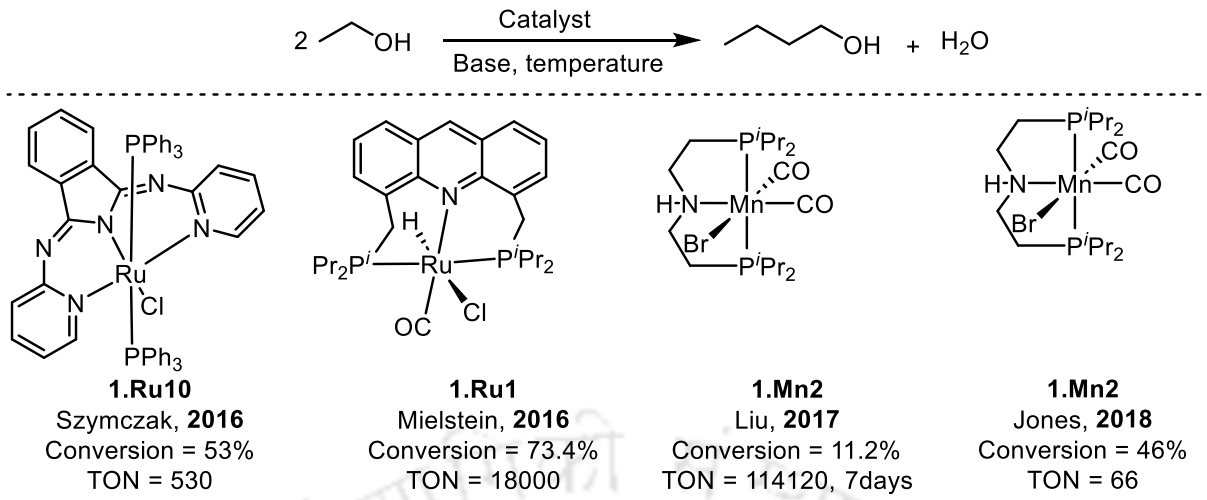

1.Ru10
Szymczak, **2016**
Conversion = 53%
TON = 530

1.Ru1
Mielstein, **2016**
Conversion = 73.4%
TON = 18000

1.Mn2
Liu, **2017**
Conversion = 11.2%
TON = 114120, 7days

1.Mn2
Jones, **2018**
Conversion = 46%
TON = 66

Scheme 1.12: Pincer-metal based homogeneous catalysts reported *n*-butanol formation from ethanol.

2100 TON with 710 TOF (TO h^{-1}) with 70% selectivity and 58% conversion at 140 °C for longer time (72 h) for the *n*-butanol formation from ethanol (Scheme 1.13).[79a] These pincer complexes are not only active under thermal conditions but also very active under microwave conditions. The 2,6-*bis*(benzimidazole-2-yl) pyridine based ruthenium pincer complex [(^{Bim2}NNN)RuCl(PPh_3)$_2$]Cl (**1.Ru13)** catalyzed the *n*-butanol formation from ethanol in presence of 10 mol% NaOEt at 110 °C under microwave irradiation at 75 W to obtain 8534 TO h^{-1} with 18% yield at 90% selectivity (Scheme 1.13). The 2,6-*bis*(benzimidazole-2-yl) pyridine based pincer ruthenium complex (^{Bim2}NNN)RuCl$_2$(CO) (**1.Ru12**) (0.025 mol%) in presence of 10% NaOEt provided 42% yield at 57% selectivity of *n*-butanol under microwave irridiation at 75 W at 110 °C , whereas in same reaction condtions, at low loading of **1.Ru12** 0.00225 mol%, 13022 TON with 22.8% yield of *n*-butanol at 78% selectivity was observed (Scheme 1.13).

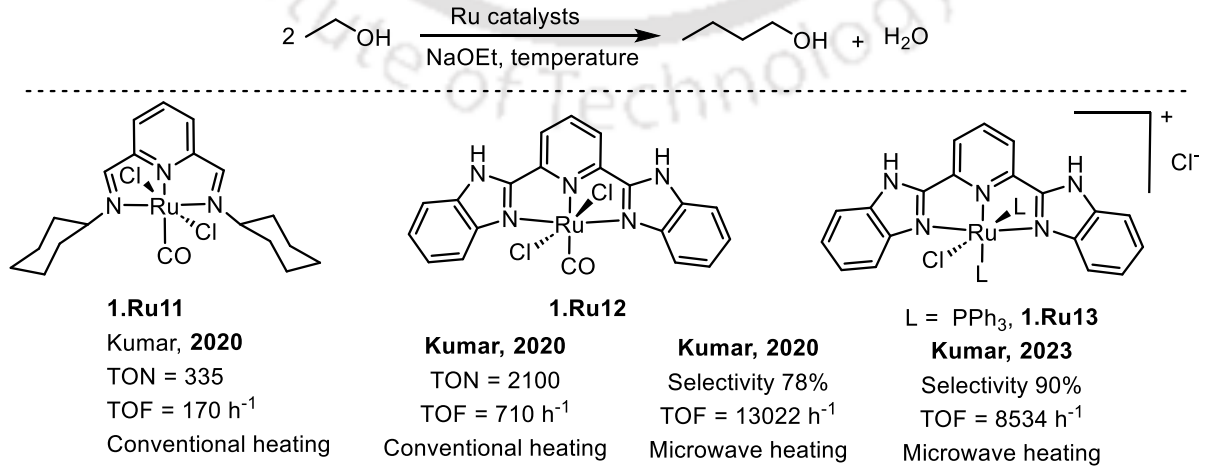

1.Ru11
Kumar, **2020**
TON = 335
TOF = 170 h^{-1}
Conventional heating

1.Ru12
Kumar, 2020
TON = 2100
TOF = 710 h^{-1}
Conventional heating

Kumar, 2020
Selectivity 78%
TOF = 13022 h^{-1}
Microwave heating

L = PPh_3, **1.Ru13**
Kumar, 2023
Selectivity 90%
TOF = 8534 h^{-1}
Microwave heating

Scheme 1.13: Catalysts reported for *n*-butanol formation from ethanol by Kumar.[68,79a]

The field of ethanol upgradation is very vast and there are some excellent reviews that provide a nice overview of the same.[79b, c] The effort of this section is to just provide a glimpse of the utility of pincer complexes in this interesting chemistry.

1.1.1.4.2. *β*-alkylation of alcohols

Transition metal catalyzed dehydrogenation of primary and secondary alcohol produces the corresponding aldehyde and ketone, which in the presence of a base undergoes aldol-condensation to produce *α*, *β*-unsaturated ketone with water as a sole by-product as observed in the Guerbet reaction. Hydrogenation of this *α*, *β*-unsaturated ketone produces the *β*-alkylated alcohol (Scheme 1.14).

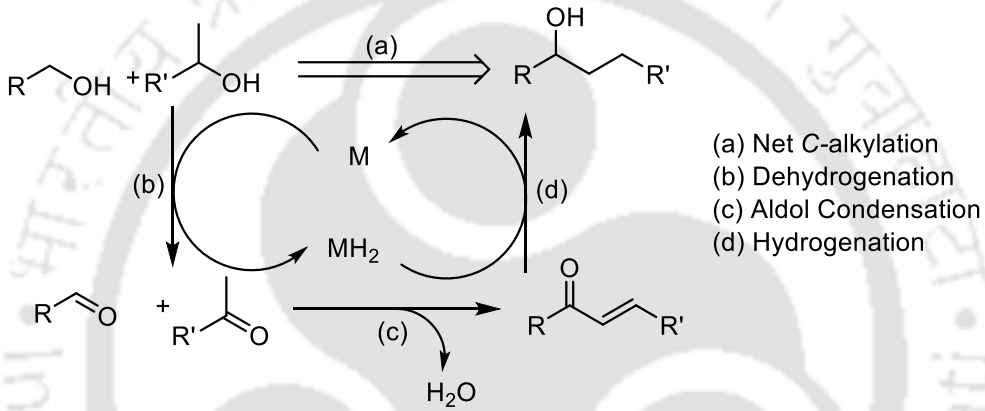

Scheme 1.14: Schematic representation of *C*-alkylation using alcohol as a starting material.

In 2003, Shim and co-workers first demonstrated the *β*-alkylation of secondary alcohols with primary alcohols by using dichloro *tris*(triphenylphosphine)ruthenium(II) [$RuCl_2(PPh_3)_3$] in presence of NaOH. This methodology afforded a variety of *β*-alkylated alcohol products.[80] Later, Carbtree,[81a] Yu,[82] Achard,[83a] Bera,[84] Kundu,[85, 86] Ghosh,[83b] Kumar,[79] Balaraman[81b] and others have developed the *β*-alkylated alcohols or *α*-alkylated ketones from the condensation of secondary alcohols/ketones with primary alcohols using pincer-metal complexes. Moreover, the cross coupling of the secondary alcohols to generate the ketones has also been described by Gunanathan in two independent reports using **1.Ru18b**.[83c,d]

Kundu and co-workers synthesized a series of pincer-ruthenium complexes and employed them for the *β*-alkylation of secondary alcohols with primary alcohols. The catalyst **1.Ru14** performed *β*-alkylation with 190 TON (Scheme 1.15).[86] The (NNN) based pincer-ruthenium catalyst **1.Ru16** showed metal ligand co-operativity and provided 31500 TON with 640 TO h^-

[1] for the *β*-alkylation of secondary alcohols with primary alcohols (Scheme 1.15).[87] The N-hetero cyclic carbene (NHC) based on NNC-pincer-ruthenium catalyst **1.Ru15** with very low loading exhibited very good TON of 288000 (TOF 24000 h^{-1}) for *β*-alkylation reaction

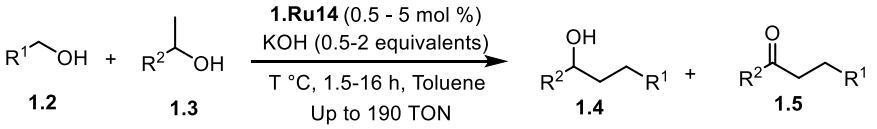

Derivatives of alcohol (**1.3**)

$R^1 = C_6H_5$, $R^2 = C_6H_5$; Yield = 94% at 115 °C (2 h)

$R^1 = H$, $R^2 = C_6H_5$; Yield = 88% at 135 °C (16 h)

$R^1 = C_6H_5$, $R^2 = 4'\text{-F-}C_6H_4$; Yield = 80% at 130 °C (1.5 h)

$R^1 = 4'\text{-F-}C_6H_4$, $R^2 = C_6H_5$; Yield = 92% at 130 °C (1.5 h)

$R^1 = C_6H_5$, $R^2 = 4'\text{-Me-}C_6H_4$; Yield = 95% at 115 °C (1.5 h)

$R^1 = 4'\text{-Me-}C_6H_4$, $R^2 = C_6H_5$; Yield = 94% at 115 °C (2 h)

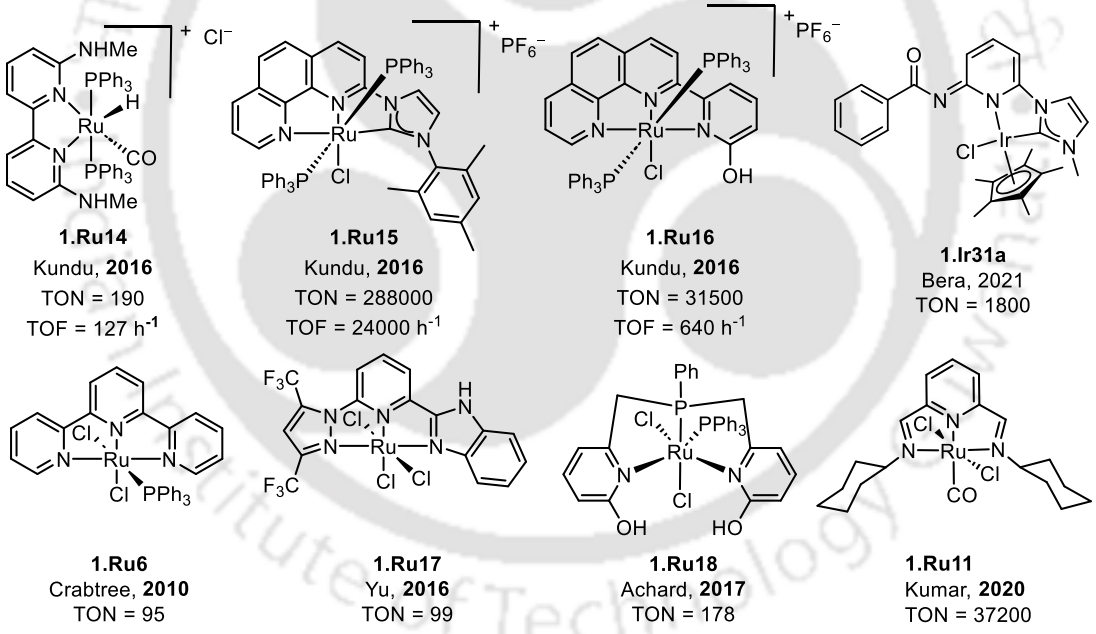

1.Ru14
Kundu, **2016**
TON = 190
TOF = 127 h^{-1}

1.Ru15
Kundu, **2016**
TON = 288000
TOF = 24000 h^{-1}

1.Ru16
Kundu, **2016**
TON = 31500
TOF = 640 h^{-1}

1.Ir31a
Bera, 2021
TON = 1800

1.Ru6
Crabtree, **2010**
TON = 95

1.Ru17
Yu, **2016**
TON = 99

1.Ru18
Achard, **2017**
TON = 178

1.Ru11
Kumar, **2020**
TON = 37200

Scheme 1.15: The homogeneous catalysts reported for *β*-alkylation of secondary alcohols with primary alcohols.[79, 81-83, 85, 86]

(Scheme 1.15). The reaction was carried out under solvent free condition and the optimized catalytic protocol was found to be efficient for a large variety of substrates.

In 2017, Achard group synthesized NPN tridentate pyridine based ruthenium complex (**1.Ru18**) (Scheme 1.15) for the *C*-alkylation of secondary alcohols with primary alcohols but

formation of α-alkylated ketones was observed as a major product instead of β-alkylated alcohol.[83a]

Bera group discovered the β-alkylation of secondary alcohols with primary alcohols using a

N-heterocyclic carbene based iridium catalyst **1.Ir31a**. Due to the pyridyl(benzamide)-functionalized NHC backbone, the catalytic system demonstrated very good activity towards the β-alkylation with 1800 TON (Scheme 1.15).[84]

In 2018, Yu and co-workers first reported Mn-catalyzed β-alkylation of secondary alcohols with primary alcohols. They have reported a series of pyridyl-supported pyrazolyl-imidazolyl ligand-based Mn(I) complexes for β-alkylation.[88] The complex **1.Mn3** among all the complexes showed highest activity for β-alkylation of secondary alcohols with primary alcohols. The **1.Mn3** (2.1 mol%) catalyzed the β-alkylation in presence of 30 mol% of KO^{t}Bu at 110 °C for 24 h in N_2 atmosphere and 92 % β-alkylated product was obtained in alkylation of secondary alcohols with primary alcohols (Scheme 1.16). Using the optimized methodology, a large library of substrates were tested. Additionally, this protocol was extended for β-alkylation of cholesterol and its derivatives and one pot synthesis of flavan derivatives.[88]

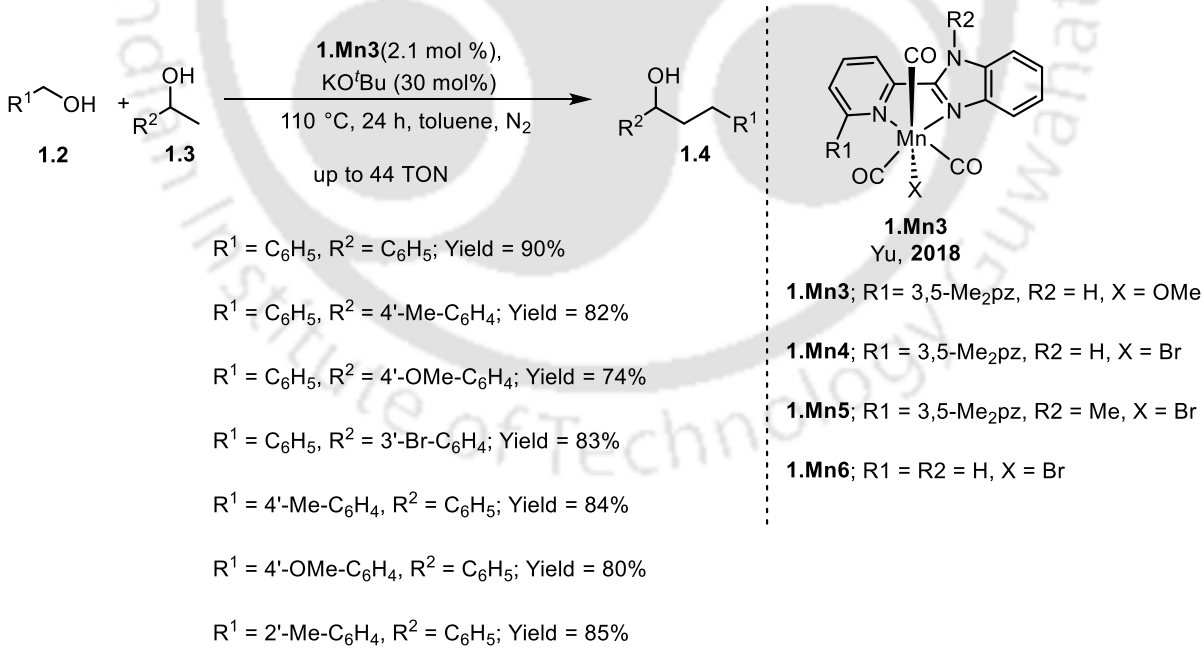

Scheme 1.16: The **1.Mn3** catalyzed β-alkylation of secondary alcohols with primary alcohols.[82]

In 2021, Ghosh group developed an amido-functionalized ruthenium carbene complexes for

the *β*-alkylation of secondary alcohols with primary alcohols. The **1.Ru18a** (1 mol%) catalyzed the *β*-alkylation in presence of 1 equivalent of NaO^{i}Pr at 110 °C after 3 hours to yield 72% of *β*-alkylated alcohol starting from benzyl alcohol and 1-phenylethanol as model substrates (Scheme 1.17).[83b] The cationic picolyl functionalized NHC ruthenium complex also showed similar reactivity for the *β*-alkylation of secondary alcohols with primary alcohols. The hydride intermediate of **1.Ru18a** was detected and remained active for 120 h. A variety of substrates scope was carried out with good to moderate yield.

Gunanathan and co-workers used Ru-MACHO **1.Ru18b** for the catalytic cross coupling of secondary alcohols to get ketone product **1.4'**. The **1.Ru18b** (1 mol%) catalyzed the cross coupling of secondary alcohols in presence of 5 mol% of KO^{t}Bu at 125 °C in toluene medium for 4 h to obtain selectively the crossed coupled ketone product **1.4'** (Scheme 1.18).[83c] A variety of substrates with different functional groups could be used to achieve the selective formation of ketones.

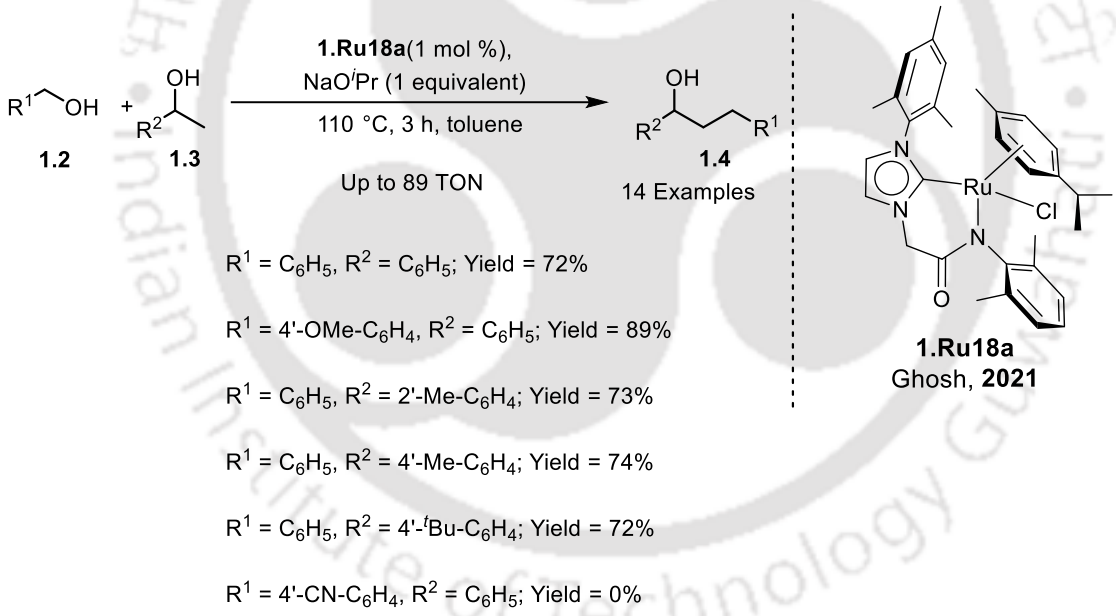

Scheme 1.17: Ruthenium-carbene catalyzed *β*-alkylation of secondary alcohols with primary alcohols. [83b]

The *β*-alkylation reaction is an excellent choice for the synthesis of C-C bonds, because it generates minimal amount of waste and requires only small amount of additives. This method has wide synthetic utility and leads to the production of valuable fine chemicals, fuel, agrochemicals and natural products.[82] In pharmaceutical industry, *β*-alkylation finds utility in the preparation of Ezetimite (which reduces the amount of cholesterol absorbed),[82] while in

cosmetics, this reaction is employed for the synthesis of Licochalcone A.[82] The homogeneous pincer complexes based on precious metal salts are highly active for *β*-alkylation and have enjoyed a huge application. Some of the representative examples have been discussed here for

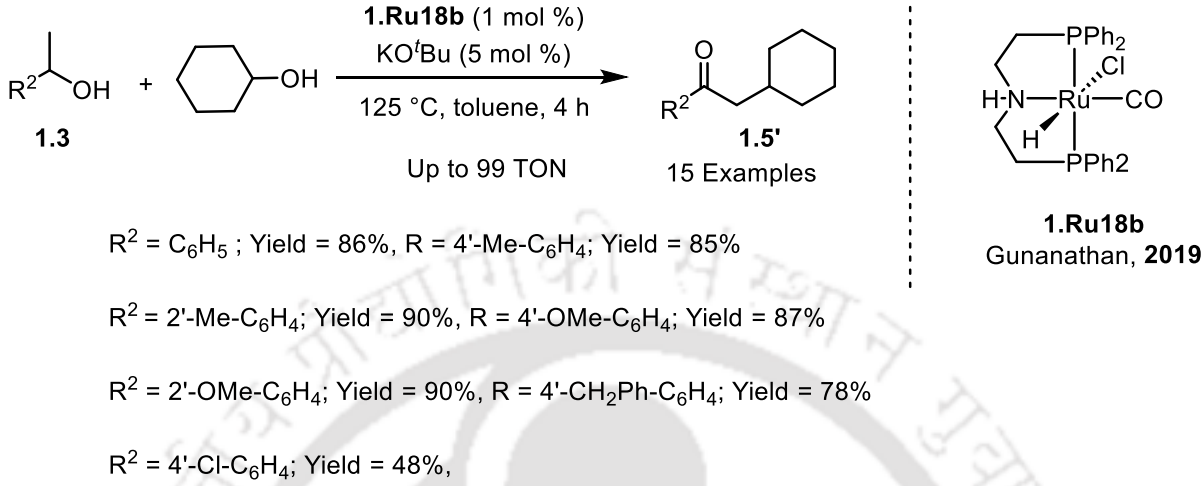

Scheme 1.18: Ruthenium catalyzed selective cross coupling of secondary alcohols.[83c]

the basic understanding of *β*-alkylation.[83e] The use of pincer complexes based on 3*d* metals is currently being explored for *β*-alkylation, however a detailed understanding of *β*-alkylation of secondary alcohols with primary alcohols has been discussed in Chapter-IV.

1.1.1.4.3. *N*-alkylation of alcohols

N-alkylated amines are versatile intermediates for organic transformation and also it has wide utility in dyes, polymers, pharmaceutical products and in the synthesis of fine chemicals.[89] Traditional methods involves the reaction of environmentally toxic alkyl halide with amines to produce *N*-alkylated amines.[90] Instead of using hazardous alkyl halide molecules, use of less hazardous alcohol molecules (precursor of alkyl halide) is more greener and atom economical for the transformation of amines and alcohols to *N*-alkylated amines.[91] The transition metal complex catalyzes the *N*-alkylation in presence of stoichiometric amounts of base. Transition metal complex catalyzed dehydrogenation of primary alcohol produces the corresponding aldehyde which reacts with amine and produces imine with water as a sole by-product.[92] Subsequent hydrogenation of imine produces the desired alkylated amine. (Scheme 1.19).[93-96]

The stoichiometric amounts of base or molecular sieves are used in *N*-alkylation to scavenge the by-product water which is formed in the reaction mixture.[92] The *N*-alkylation reaction has been well-explored by Meilstein[93] Kirchner[94] Kundu[95] Kumar[96a] and others. This reaction

proceeds *via* "hydrogen borrowing" strategy which involves transfer hydrogenation to mitigate the need of hydrogen gas, making it an overall atom efficient process (Scheme 1.19).

In 2016, Kirchner developed PNP pincer-Fe complexes and tested them for the *N*-Alkylation

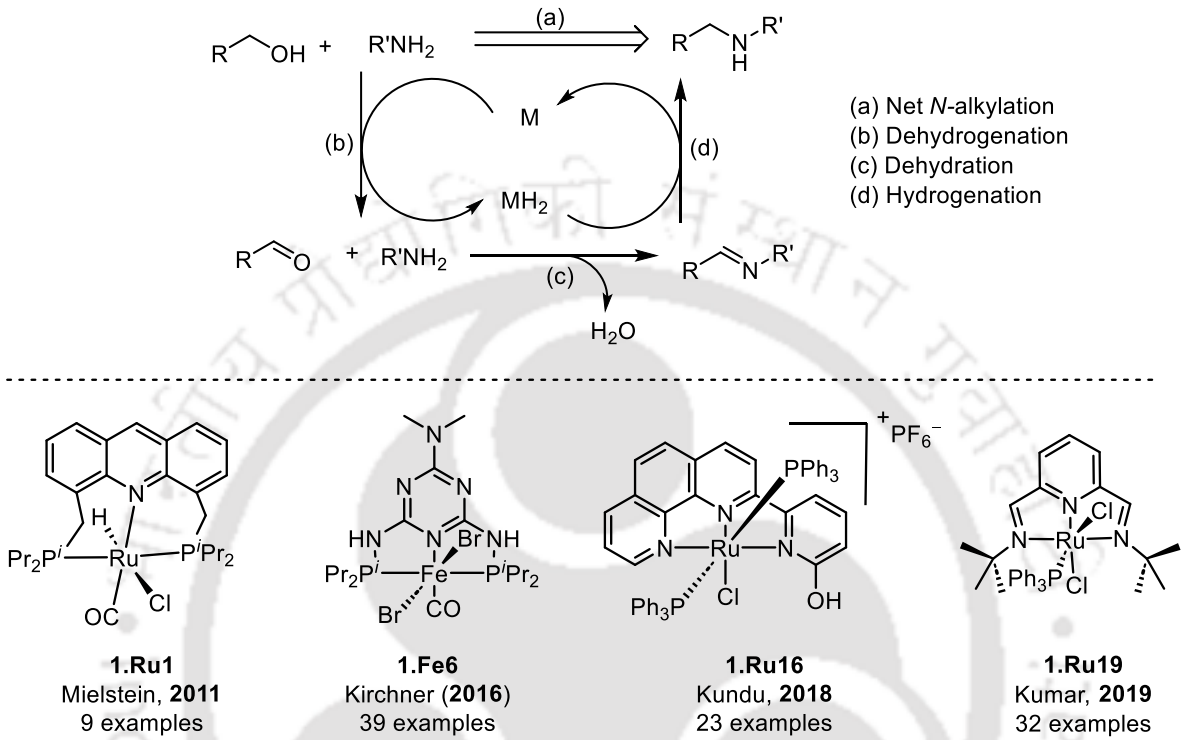

Scheme 1.19: Schematic representation of *N*-alkylation using alcohol and amine as a starting material, with representative examples of well-explored catalytic systems.

reaction of amines and alcohols.[94] The **1.Fe6** (2 mol%) catalyzed the *N*-alkylation reaction of alcohol and amine in presence of 1.3 equivalents of KO^{t}Bu in toluene medium (4 mL) at 80 °C for 16 hours. A large variety of substrates were *N*-alkylated with good to moderate yields (Scheme 1.20)[94] using the developed catalytic protocol.

In 2019, Kumar and co-workers developed a series of *bis*(imino)pyridine based pincer-Rucomplexes and tested for *N*-alkylation reaction of amines and alcohols.[96] Pincer-ruthenium complexes of the type (^{R2}NNN)RuCl$_2$(PPh$_3$) (**1.Ru19**; R = ^{t}Bu, **1Ru20**; R = ^{i}Pr **1.Ru21**; R = Cy, **1.Ru22**; R = Ph) have been used to accomplish *N*-alkylation of primary amines. For the first time, they reported the use of Na to generate the base *in-situ*, that made the reaction more favourable. The alcohol precursor was regenerated from sodium alkoxide by its reaction with water produced during the process. Thus, water formed in the reaction mixture enhanced the

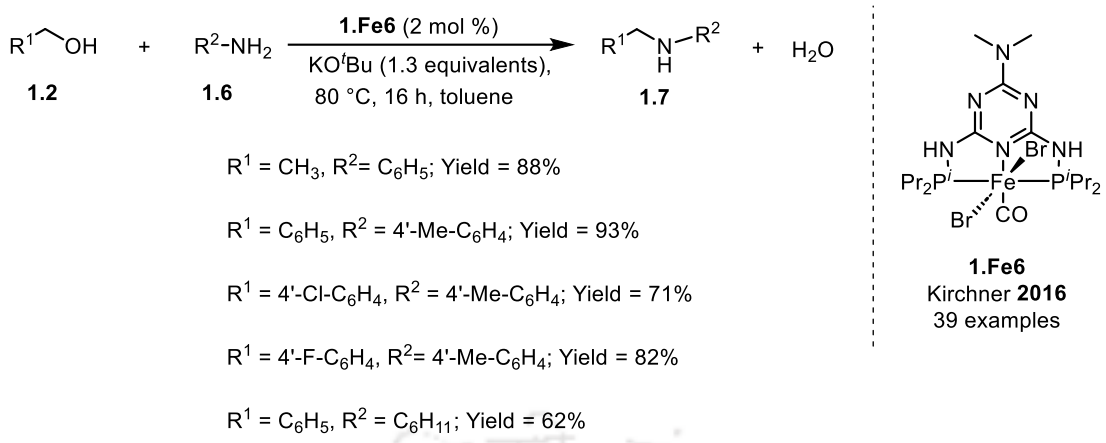

Scheme 1.20: The **1.Fe6** catalyzed *N*-alkylation of alcohols with amine.[94]

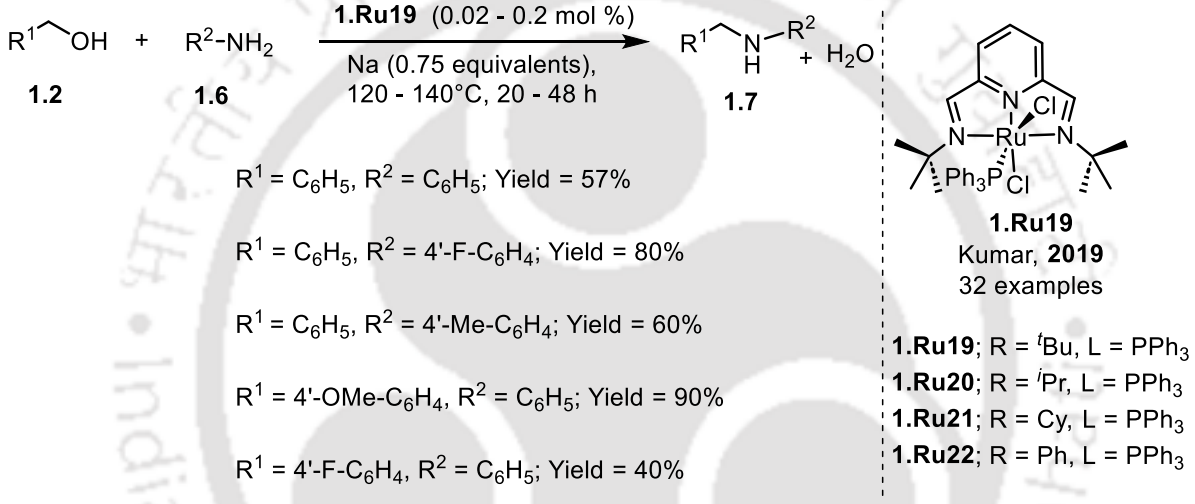

Scheme 1.21: The **1.Ru20** catalyzed *N*-alkylation of alcohols with amine.[96a]

rate of the catalytic cycle, making it more atom economical. The catalyst (^{t}Bu^{2}NNN)$RuCl_2(PPh_3)$ (**1.Ru19**) displayed highest TON of 29000 for *N*-alkylation of amine in solvent-free condition (Scheme 1.21).[96a]

The *N*-alkylation reaction has huge application in industry, specially in pharmaceutical [96b] and in medical chemistry.[96b] The *N*-alkylated amines are used to prepare various drug molecules like Sertraline,[96b] (effective antidepressant of various etiologies), Pramipexole, (agonist dopamine receptor and effective for Parkinson disease), Donepezil, (cholinesterase inhibitor) and Retigabine (used to normalize the potassium channel in neurons of the brain).[96b] The *N*-alkylation of amines has been explored using various complexes and specially pincer complexes have exhibited higher efficiency for the selective formation of higher amines instead of imines.[94] This section has attempted to shed light on some of the efficient amines *N*-

alkylation catalysts as representative examples.

1.1.1.4.4. Catalytic *β*-methylation of various alcohols

Methylation is a very useful technique among various C−C bond formation reactions, where access to branching provided by methyl groups is highly important as a structural motif in chemistry and biology,[97] ranging from synthetic lubricants[98] to drug molecules.[99] The dehydrogenation of methanol is very challenging though methylation reactions are attractive towards alkylation. The dehydrogenation of methanol is highly challenging due to its high enthalpy (ΔH = 84 kJ/mol). This highlights the importance to design and develop efficient catalysts and optimal catalytic methods for dehydrogenative functionalization using methanol as the alkylating agent.[100-102] Transition metal catalyzed dehydrogenation of methanol and 2-phenylethanol produces the corresponding aldehydes which in the presence of a base undergoes aldol-condensation to produce *α, β*-unsaturated aldehyde with water as a sole by-product. Hydrogenation of this *α, β*-unsaturated aldehyde produces the *β*-methylated alcohol (Scheme 1.22). A similar path for 1-phenylethanol can also be proposed (Scheme 1.22).

In 2014, Beller and co-workers reported the *β*-methylation of 2-phenylethanol (**1.7**) with a dual catalytic system Ru-MACHO (**1.Ru24**) (0.1 mol %) and Shvo's catalyst (**1.Ru23**) (0.05 mol %) that has resulted in 87% yield of **1.9** at 140 °C (Scheme 1.23).[103]

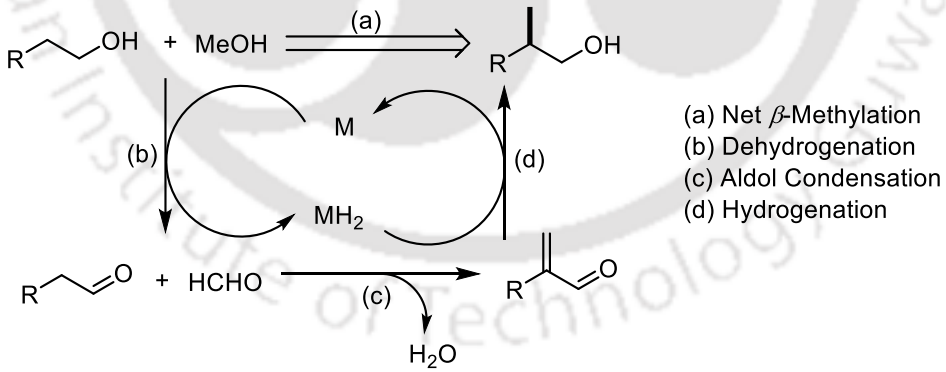

Scheme 1.22: A general schematic representation of the transition metal catalyzed *β*-methylation of 2-phenylethanol.

In 2019, Leitner and co-workers reported a Ru-MACHO-BH_4 (**1.Ru25**) (0.1 mol%) catalyzed *β*-methylation of 2-phenylethanol and 1-phenylethanol with 2 equivalents of NaOMe at 150 °C for 28 h to obtain 82% of 2-phenylpropan-1-ol and 84% 2-methyl-1-phenylpropan-1-ol respectively (Schemes 1.24 and 1.25).[104] The complex **1.Ru25** showed excellent catalytic

activity with 18000 TON for the *β*-methylation of alcohol. A variety of substrates based on both 2-phenylethanol and 1-phenylethanol were tested and good to moderate yields were observed.[104]

The *β*-methylation of alcohols has been explored independently by Renaud,[105] Kempe,[106] Leitner,[104, 107, 108] Srimani,[109] Kundu,[110] Morril[102, 111] and others using homogeneous complexes based on Fe, Mn, Ru. The selected pincer-metal complexes for *β*-methylation of alcohols have been shown in Scheme 1.23. The activation of methanol molecule is challenging but very useful for various C−C bond formation reactions. The synthesis of new carbon-methyl bond as a structural motif is very important in chemistry, biology,[97] and it is used in applications ranging from lubricants[98] to drug molecules.[99] The *β*-methylation of alcohols is challenging yet various homogeneous

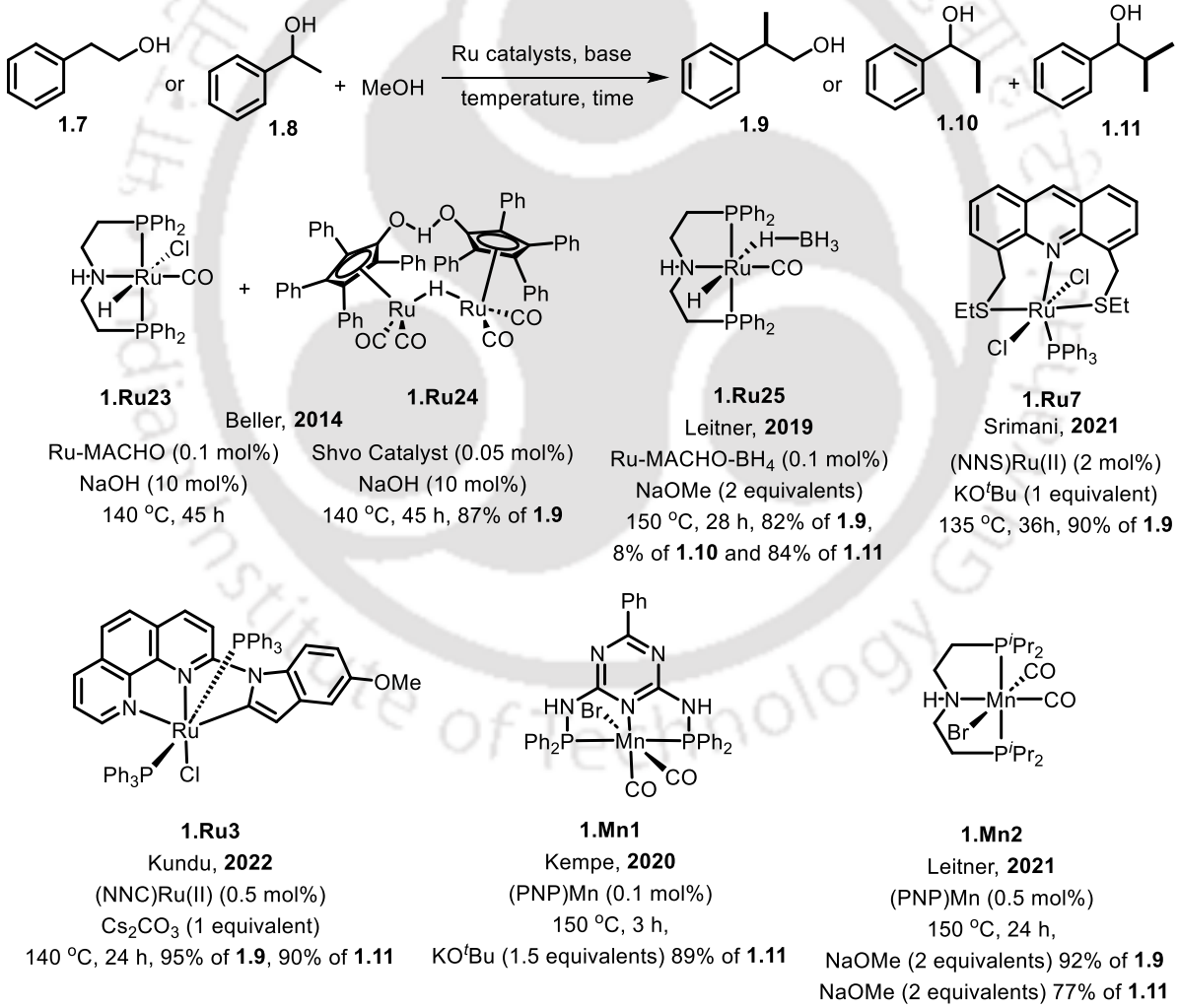

Scheme 1.23: Homogeneous pincer complexes reported for *β*-methylation of 2-phenylethanol and 1-phenylethanol.

pincer-metal complexes based on precious metals have been extensively reported that catalyse the *β*-methylation reaction effortlessly.[100-102] Here, some of the selected representative homogenous pincer-metal complexes have been discussed for *β*-methylation. The detailed reaction mechanism and other reports have been elaborately discussed in chapter-II. When the same reaction was carried out in the absence of methanol, the dehydrogenation product of 2-phenylethanol underwent self-coupling and produced alkane directly through decarboxylation coupling. There are very limited reports on decarboxylation of alcohol to alkane, therefore a detailed description is covered in chapter-III.

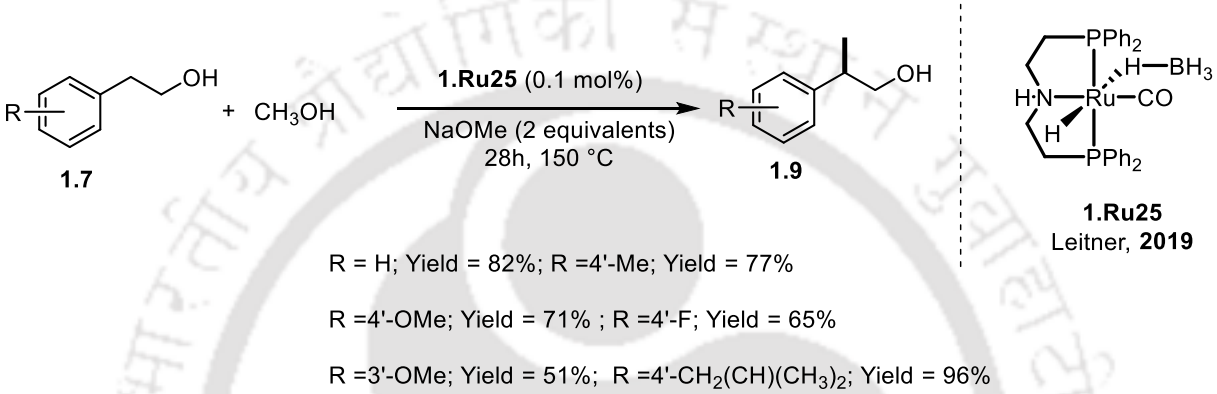

Scheme 1.24: The *β*-methylation of 2-phenylethanol and its derivatives catalyzed by **1.Ru28** catalyst.[104]

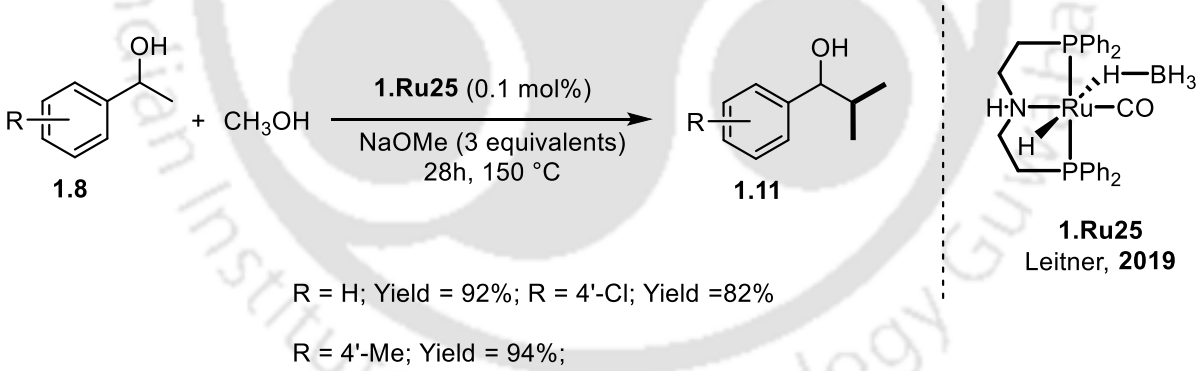

Scheme 1.25: The *β*-methylation of 1-phenylethanol and its derivatives catalyzed by **1.Ru25** catalyst.[104]

1.1.1.4.5. Alcohol reforming reaction: H_2 production

Hydrogen is regarded as one of the most efficient alternatives to non-renewable fuels.[112] In the of age of rapid depletion of fossil fuels, scientists are interested in the development of fuels based on renewable resources. Hydrogen is regarded as a clean fuel and an efficient energy carrier (120 MJ/Kg) that can be turned into electricity by utilising various fuel cell technologies

to get significant amount of energy per unit mass.[113-115] The use of hydrogen will extend the range of available energy sources and recently there is significant progress in the field of hydrogen generation using liquid organic hydrogen carrier (LOHC) systems due their high hydrogen storage capacity, easy transportation and environmental friendliness.[112] Recently, particular emphasis has been laid on alcohols as LOHCs to generate on-demand hydrogen.[112] Many potential LOHC candidates for hydrogen storage include methanol, ethanol, ethylene glycol, glycerol etc., which lead to the production of various value-added chemicals along with the concomitant generation of hydrogen.[112] However, this section will focus on the hydrogen generation from methanol as a representative example. For alcohol reforming, methanol has a high hydrogen storage capacity (12.6 wt%) and is therefore considered a promising candidate for H_2 generation.[116-119] Among the various alcohols, majority of the reports are based on aqueous reforming of methanol,[112] because of its easy availability. The reports with ethanol reforming are scarce due to the various side products formed during the reaction,[112, 76-78] thereby affecting the selectivity of the process. In case of ethylene glycol, it has only 6.5 wt% H_2 and a higher boiling point, which makes it less favourable to produce hydrogen under mild conditions.[112] Therefore, methanol is the most preferred candidate for the catalytic aqueous reforming employing homogeneous catalysts under mild conditions.[120]

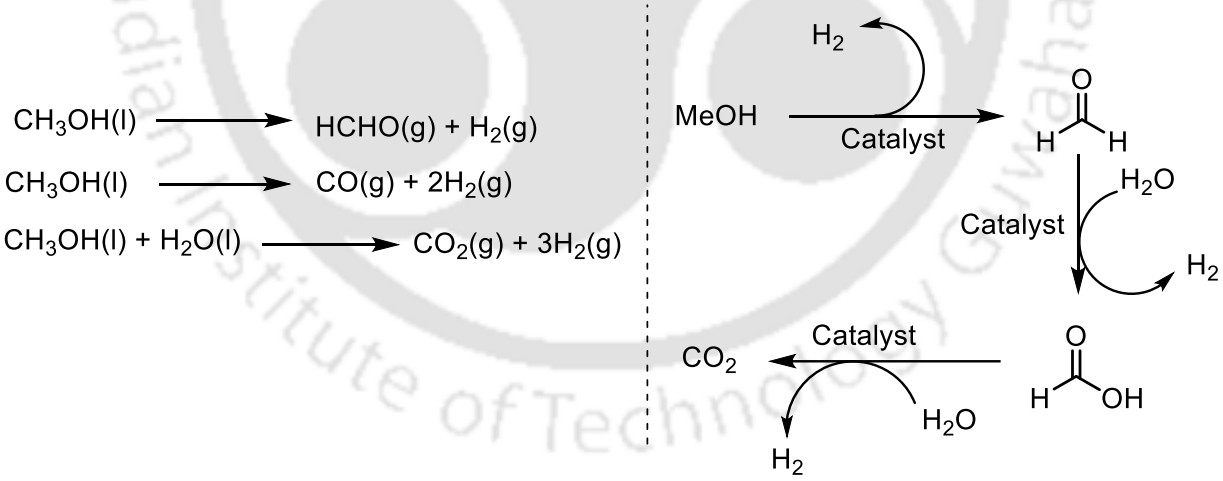

Scheme 1.26: Schematic representation of aqueous MeOH reforming reaction.

Depending upon reaction conditions, methanol can be converted to different products like HCHO, HCOOH, CO_2, CO and H_2 (Scheme 1.26). For the on-site hydrogen generation, aqueous methanol-reforming is an attractive method as it involves the complete dehydrogenation of methanol into CO_2 and H_2.[112, 121] A variety of homogeneous transition metal complexes can catalyze the aqueous reforming of methanol to H_2 (Scheme 1.27).[112, 121]

In 2013, Beller and co-workers reported the use of pincer-ruthenium complexes based on the MACHO ligand to catalyze MeOH/H_2O mixture to CO_2 (or CO_3^{2-}) and H_2.[121] The pincer-ruthenium complexes (**1.Ru23** and **1.Ru28**) (21 ppm) in presence of 0.5 M base dehydrogenated a 4:1 methanol-water mixture to formaldehyde. In presence of base and water it gets further dehydrogenated to formic acid and at last to CO_2 and H_2 (3 equivalents) (Scheme1.28). The complex **1.Ru23** and **1.Ru28** showed very good catalytic activity for the

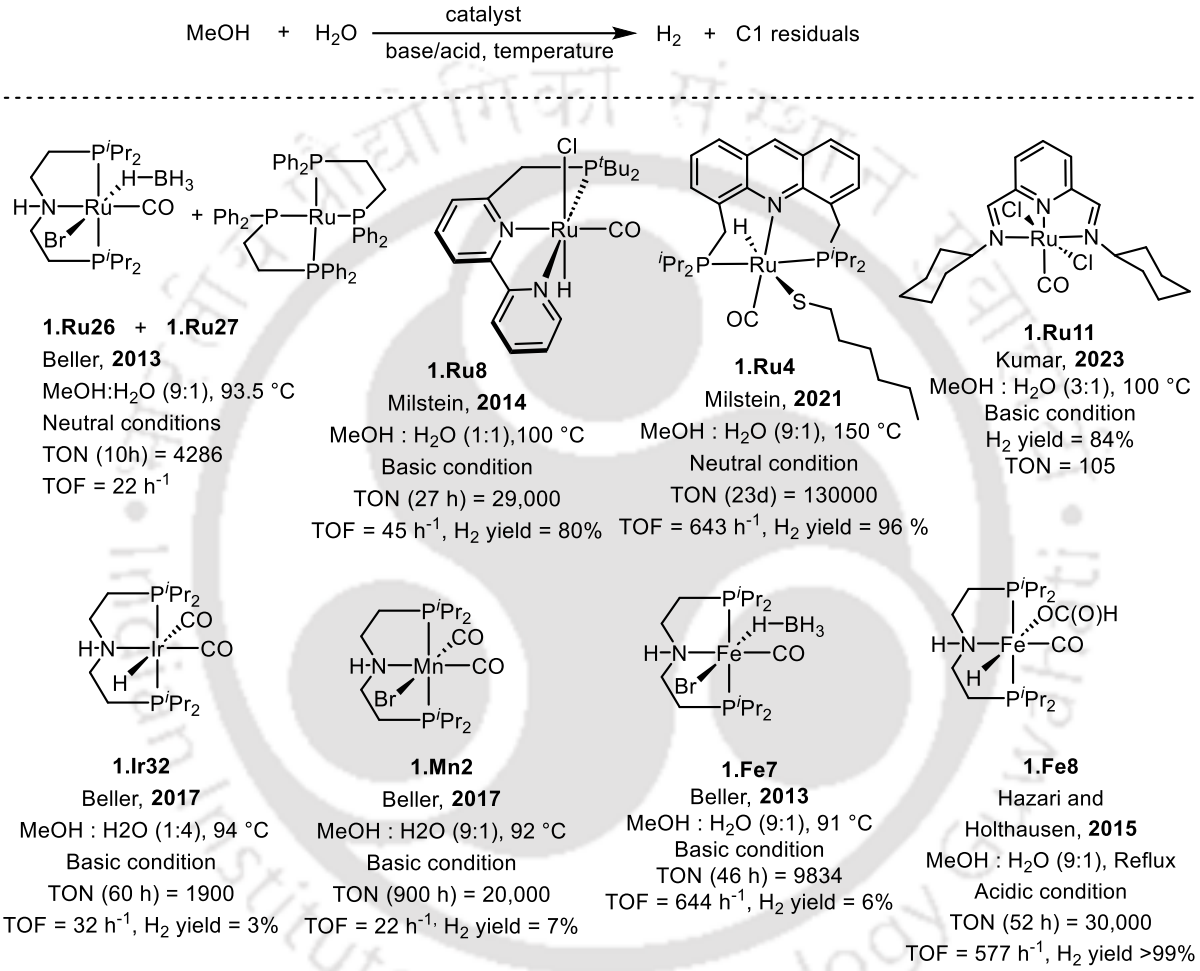

Scheme 1.27: Complexes reported for aqueous MeOH reforming reaction.

reforming of methanol to hydrogen (Scheme 1.28).[120] The **1.Ru23** (1.8 ppm, 0.008 mol%) with 8.0 M KOH (1.4 equivalents with respect to water) gave 8.23% yield of H_2 with 1051 TOF (h^{-1}). On the other hand, under similar reaction conditions the catalyst **1.Ru28** showed better activity towards dehydrogenation of 9:1 MeOH/H_2O with 16.6% yield of H_2 at 2678 h^{-1} after 3h at 91 °C. In neat methanol, after 3 hours an amazing TOF of 4734 h^{-1} was observed with 9.1 % yield of hydrogen under similar reaction conditions,[106] while using catalyst **1.Ru28**. The

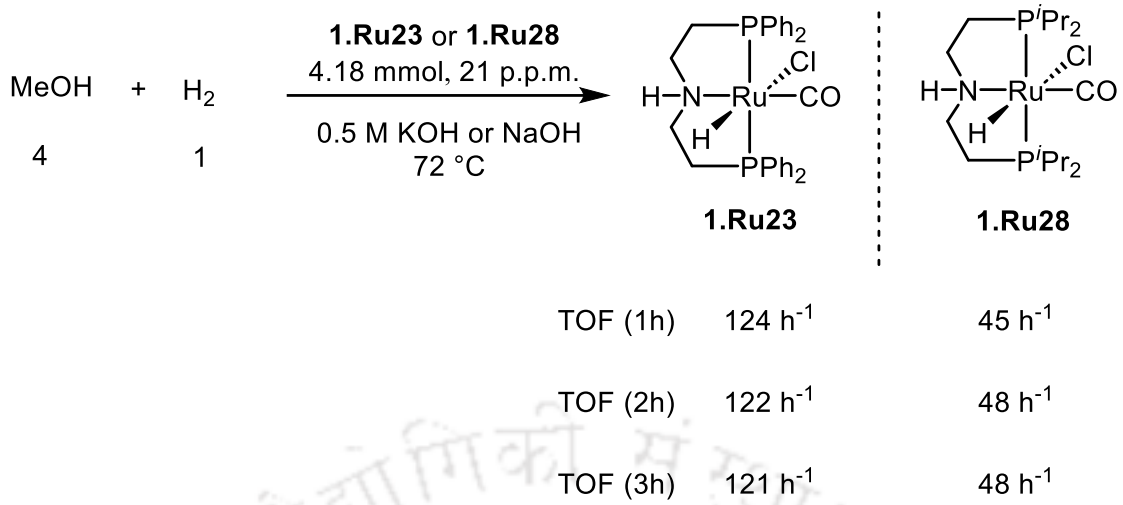

Scheme 1.28: **1.Ru23** and **1.Ru28** catalyzed aqueous reforming of methanol.[106]

studies by Beller laid the foundation for the systematic development on the MeOH reforming reaction with different complexes. Milstein,[122, 123] Beller, [124-126] Kumar,[127] Hazari[128] and others developed various efficient homogeneous pincer-catalytic systems for aqueous phase methanol reforming reaction (Scheme 1.27).

LOHC have many potential applications that involves the storage and transportation of hydrogen by eliminating the need of cooling or compressing H_2 in an energy intensive manner. [112] This makes the handling of hydrogen not only safer but cheaper as well. The hydrogen generated can be utilized in various applications such as fuel cell, power generation, hydrogen refuelling station, transportation and industrial sectors.[112] Hence, it is pivotal to expand the on-site production of hydrogen from LOHC in order to fulfil its ever-increasing demand as a fuel. In this context, this section has provided a brief overview of the application of pincer complexes towards H_2 generation from abundant alcohols.

1.2. Summary

The concept of pincer-metal complexes, emerged in 1976, introduced by Moulton and Shaw, marks a significant milestone in the field of catalysis that has continued to evolve over past five decades. These versatile complexes have been widely applied across various fields, particularly in catalysis where they have played a transformative role. Numerous pioneering reports are there in this field that has demonstrated the effectiveness of these pincer metal complexes. These complexes have showcased outstanding catalytic properties in

fundamentally important dehydrogenation and hydrogenation reactions such as *C*-alkylation,[79a, 81-86] *N*-alkylation,[93-96], alkane dehydrogenation,[7, 8] transformation of CO_2 to methanol[9] and nitrogen fixation[10] as well. Each of these areas have witnessed a significant growth, showcasing the wide utility of these complexes. While an in-depth discussion on each of the field is currently out of the scope of this thesis, we aim to provide a concise overview that highlights the most relevant reaction with representative example of these complexes. A detailed discussion on the literature for the relevant reactions has been provided in greater detail in the appropriate chapters. However, a significant amount of research is still ongoing globally that continues to lay emphasis on each of these reactions independently. All the observation presented above lay a solid foundation for the objectives of the current thesis.

1.3. Objective of the current thesis

The wide literature survey in this chapter discusses the role of pincer-metal complexes in various organic transformation that include the synthesis of fine chemicals, fuels, pharmaceuticals, and agrochemicals and, also the intermediates of various organic reactions. For a healthy global economy, energy self-sufficiency is essential. To satisfy the needs of energy of the society it is important to generate fine chemicals, fuel from abundant and cheap raw materials in an economical and environmentally-friendly fashion. The organometallic complexes with variety of metal-ligand combination under various optimized conditions have been successfully addressing the task to some extent. However, the expensive catalyst and sensitive reaction conditions are challenges that need to be addressed in the coming future. It would be beneficial if one could carry-out such transformation using an optimized reduced toxicity, low cost and less sensitive catalytic system. This thesis as a part of doctoral studies attempts to address the following questions,

1. Can we generate easy to synthesize *bis(*iminopyridine) based ligands instead of phosphine-based ligands and their corresponding pincer-ruthenium complexes?
2. Can we use these pincer-ruthenium catalysts to generate alkanes from alcohols *via* the challenging decarboxylative coupling?
3. Is it possible to use the simplest alcohol such as methanol as an alkylating agent in these pincer ruthenium catalysed reactions?
4. Can we substitute the ruthenium in these pincers catalytic systems with base metals such as cobalt and still obtain good activity in the C-C bond formation reactions using abundantly

available alcohols as alkylating agents?

1.4. References

(1) Morales-Morales, D.; Jensen, C. G., *The chemistry of pincer compounds*. Elsevier: 2011.
(2) van der Boom, M. E.; Milstein, D., Cyclometalated phosphine-based pincer complexes: mechanistic insight in catalysis, coordination, and bond activation. *Chem. Rev*. **2003,** *103*, 1759-1792.
(3) Moulton, C. J.; Shaw, B. L., Transition metal–carbon bonds. Part XLII. Complexes of nickel, palladium, platinum, rhodium and iridium with the tridentate ligand 2, 6-bis [(di-t-butylphosphino) methyl] phenyl. *J. Chem. Soc. Dalton Trans*. **1976**, *11*, 1020-1024.
(4) Gerber, R.; Blacque, O.; Frech, C. M., Suzuki Cross-Coupling Reactions Catalyzed by an Aliphatic Phosphine-Based Pincer Complex of Palladium: Evidence for a Molecular Mechanism. *ChemCatchem* **2009,** *1*, 393-400.
(5) Wang, W.; Gu, P.; Wang, Y.; Wei, H., Theoretical study of POCOP-pincer iridium (III)/Iron (II) hydride catalyzed hydrosilylation of carbonyl compounds: hydride not involved in the iridium (III) system but involved in the iron (II) system. *Organometallics* **2014**, *33*, 847-857.
(6) Miller, E. M.; Shaw, B. L., Kinetic and other studies on oxidative addition reactions of iridium phosphine complexes of the type trans-[IrCl (CO)(PMe 2 R) 2](R= Ph, o-MeO· C 6 H 4, or p-MeO· C 6 H 4). *J. Chem. Soc. Dalton Trans*. **1974**, *5*, 480-485.
(7) Kumar, A.; Bhatti, T. M.; Goldman, A. S., Dehydrogenation of Alkanes and Aliphatic Groups by Pincer-Ligated Metal Complexes. *Chem. Rev.* **2017,** *117* 12357-12384.
(8) Kumar, A.; Goldman, A. S., Recent Advances in Alkane Dehydrogenation Catalyzed by Pincer Complexes. In *The Privileged Pincer-Metal Platform: Coordination Chemistry & Applications*, van Koten, G.; Gossage, R. A., Eds. Springer International Publishing: Cham, 2016; pp 307-334.
(9) Manar, K. K.; Cheng, J.; Yang, Y.; Yang, X.; Ren, P., Promising Catalytic Application by Pincer Metal Complexes: Recent Advances in Hydrogenation of Carbon-Based Molecules. *Chem Cat Chem* **2023,** *15*, e202300004
(10) Chalkley, M. J.; Drover, M. W.; Peters, J. C., Catalytic N2-to-NH3 (or -N2H4) Conversion by Well-Defined Molecular Coordination Complexes. *Chem. Rev.* **2020,** *120*, 5582-5636.
(11) Reed-Berendt, B. G.; Latham, D. E.; Dambatta, M. B.; Morrill, L. C., Borrowing Hydrogen for Organic Synthesis. *ACS Cenl Sci.* **2021,** *7* , 570-585.
(12) Miller, E. M.; Shaw, B. L., Kinetic and other studies on oxidative addition reactions of iridium phosphine complexes of the type trans-[IrCl (CO)(PMe 2 R) 2](R= Ph, o-MeO· C 6 H 4, or p-MeO· C 6 H 4). *J. Chem. Soc. Dalton Trans*. **1974**, *5*, 480-485.
(13) Jones, C. E.; Shaw, B. L.; Turtle, B. L., O- and C-metallation of 2-alkoxyphenylphosphines by platinum(II). *J. Chem. Soc., Dalton Trans.* **1974**, 992-999.
(14) Moulton, C. J.; Shaw, B. L., Transition metal-carbon bonds. Part XLII. Complexes of nickel, palladium, platinum, rhodium and iridium with the tridentate ligand 2,6-bis[(di-t-butylphosphino)methyl]phenyl. *J. Chem. Soc., Dalton Trans.* **1976**, 1020-1024.
(15) Empsall, H. D.; Hyde, E. M.; Markham, R.; McDonald, W. S.; Norton, M. C.; Shaw, B. L.; Weeks, B., Synthesis and X-ray structure of an unusual iridium ylide or carbene complex. *J. Chem. Soc., Chem. Commun.* **1977**, 589-590.
(16) van Koten G., Tuning the reactivity of metals held in a rigid ligand environment. *Pure Appl Chem.* **1989**, *61*, 1681–1694.
(17) Altenhoff, G.; Glorius, F., A Domino Copper-Catalyzed C- N and C- O Cross-Coupling for the Conversion of Primary Amides into Benzoxazoles. *Adv. Syn. Catal.* **2004,** *346* , 1661-1664.
(18) Weissberg, A.; Portnoy, M., Unprecedented preparation of pincer bis(oxazolinyl)phenyl ligands on solid support and their use in the first heterogeneously-catalyzed enantioselective allylation of aldehydes. *Chem. Commun.* **2003**, 1538-1539.
(19) Kumar, A.; Bhatti, T. M.; Goldman, A. S., Dehydrogenation of Alkanes and Aliphatic Groups by Pincer-Ligated Metal Complexes. *Chem. Rev.* **2017,** *117*, 12357-12384.

(20) Gunanathan, C.; Milstein, D., Bond Activation and Catalysis by Ruthenium Pincer Complexes. *Chem. Rev.* **2014,** *114*, 12024-12087.
(21) Dani, P.; Karlen, T.; Gossage Robert, A.; Gladiali, S.; van Koten, G., Hydrogen-Transfer Catalysis with Pincer-Aryl Ruthenium(II) Complexes. *Angew. Chem. Int. Ed.* **2000,** *39*, 743-745.
(22) Krishnakumar, V.; Chatterjee, B.; Gunanathan, C., Ruthenium-Catalyzed Urea Synthesis by N–H Activation of Amines. *Inorg. Chem* **2017,** *56*, 7278-7284.
(23) Pelczar, E. M.; Emge, T. J.; Krogh-Jespersen, K.; Goldman, A. S., Unusual Structural and Spectroscopic Features of Some PNP-Pincer Complexes of Iron. *Organometallics* **2008,** *27*, 5759-5767.
(24) Zhang, J.; Gandelman, M.; Herrman, D.; Leitus, G.; Shimon, L. J. W.; Ben-David, Y.; Milstein, D., Iron(II) complexes based on electron-rich, bulky PNN- and PNP-type ligands. *Inorg. Chim. Acta* **2006,** *359*, 1955-1960.
(25) Poverenov, E.; Gandelman, M.; Shimon, L. J. W.; Rozenberg, H.; Ben-David, Y.; Milstein, D., Pincer "Hemilabile" Effect. PCN Platinum(II) Complexes with Different Amine "Arm Length". *Organometallics* **2005,** *24*, 1082-1090.
(26) Feichtner, K.-S.; Scherpf, T.; Gessner, V. H., Cooperative Bond Activation Reactions with Ruthenium Carbene Complex PhSO2(Ph2PNSiMe3)C═Ru(p-cymene): Ru═C and N–Si Bond Reactivity. *Organometallics* **2017,** *37*, 645–654.
(27) Gunanathan, C.; Ben-David, Y.; Milstein, D., Direct Synthesis of Amides from Alcohols and Amines with Liberation of H<sub>2</sub&gt. *Science* **2007,** *317*, 790.
(28) Sutter, J.-P.; James, S. L.; Steenwinkel, P.; Karlen, T.; Grove, D. M.; Veldman, N.; Smeets, W. J. J.; Spek, A. L.; van Koten, G., Versatile N,C,N Coordination Behavior of a Monoanionic Aryldiamine Ligand in Ruthenium(II) Complexes: Syntheses and Crystal Structures of [RuII{C6H3(CH2NMe2)2-2,6}X(L)] (L = Norbornadiene, X = Cl, SO3CF3; L = PPh3, X = I) and [RuII{C6H3(CH2NMe2)2-2,6}(2,2‘:6‘,2‘‘-terpyridine)]Cl. *Organometallics* **1996,** *15*, 941-948.
(29) Cao, X.-N.; Wan, X.-M.; Yang, F.-L.; Li, K.; Hao, X.-Q.; Shao, T.; Zhu, X.; Song, M.-P., NNN Pincer Ru(II)-Complex-Catalyzed α-Alkylation of Ketones with Alcohols. *J. Org. Chem.* **2018,** *83*, 3657-3668.
(30) Kiernicki, J. J.; Zeller, M.; Szymczak, N. K., Hydrazine Capture and N–N Bond Cleavage at Iron Enabled by Flexible Appended Lewis Acids. *J. Am. Chem. Soc.* **2017,** *139*, 18194-18197.
(31) Chirik, P. J., Carbon–Carbon Bond Formation in a Weak Ligand Field: Leveraging Open-Shell First-Row Transition-Metal Catalysts. *Angew. Chem. Int. Ed.* **2017,** *56*, 5170-5181.
(32) Poyatos, M.; Mata, J. A.; Falomir, E.; Crabtree, R. H.; Peris, E., New Ruthenium(II) CNC-Pincer Bis(carbene) Complexes: Synthesis and Catalytic Activity. *Organometallics* **2003,** *22*, 1110-1114.
(33) Danopoulos, A. A.; Winston, S.; Motherwell, W. B., Stable N-functionalised 'pincer' bis carbene ligands and their ruthenium complexes; synthesis and catalytic studies. *Chem. Commun.* **2002**, 1376-1377.
(34) Gupta, M.; Hagen, C.; Flesher, R. J.; Kaska, W. C.; Jensen, C. M., A highly active alkane dehydrogenation catalyst: stabilization of dihydrido rhodium and iridium complexes by a P–C–P pincer ligand. *Chem. Commun.* **1996,** 2083-2084.
(35) Xu, W.-w.; P. Rosini, G.; Krogh-Jespersen, K.; S. Goldman, A.; Gupta, M.; M. Jensen, C.; C. Kaska, W., Thermochemical alkane dehydrogenation catalyzed in solution without the use of a hydrogen acceptor. *Chem. Commun.* **1997,** 2273-2274.
(36) Liu, F.; S. Goldman, A., Efficient thermochemical alkane dehydrogenation and isomerization catalyzed by an iridium pincer complex. *Chem. Commun.* **1999,** 655-656.
(37) Liu, F.; Pak, E. B.; Singh, B.; Jensen, C. M.; Goldman, A. S., Dehydrogenation of n-Alkanes Catalyzed by Iridium "Pincer" Complexes: Regioselective Formation of α-Olefins. *J. Am. Chem. Soc.* **1999,** *121*, 4086-4087.
(38) Shi, Y.; Suguri, T.; Dohi, C.; Yamada, H.; Kojima, S.; Yamamoto, Y., Highly Active Catalysts for the Transfer Dehydrogenation of Alkanes: Synthesis and Application of Novel 7–6–7 Ring-Based Pincer Iridium Complexes. *Chem. Eur. J.* **2013,** *19* , 10672-10689.
(39) Haenel, M. W.; Oevers, S.; Angermund, K.; Kaska, W. C.; Fan, H.-J.; Hall, M. B., Thermally Stable Homogeneous Catalysts for Alkane Dehydrogenation. *Ang. Chem., Int. Ed.* **2001,** *40*, 3596-3600.

(40) Ahuja, R.; Punji, B.; Findlater, M.; Supplee, C.; Schinski, W.; Brookhart, M.; Goldman, A. S., Catalytic dehydroaromatization of n-alkanes by pincer-ligated iridium complexes. *Nat. Chem.* **2011,** *3*, 167-171.
(41) Lyons, T. W.; Guironnet, D.; Findlater, M.; Brookhart, M., Synthesis of p-Xylene from Ethylene. *J. Am. Chem. Soc.* **2012,** *134* , 15708-15711.
(42) Göttker-Schnetmann, I.; White, P.; Brookhart, M., Iridium Bis(phosphinite) p-XPCP Pincer Complexes: Highly Active Catalysts for the Transfer Dehydrogenation of Alkanes. *J. Am. Chem. Soc.* **2004,** *126*, 1804-1811.
(43) Göttker-Schnetmann, I.; White, P. S.; Brookhart, M., Synthesis and Properties of Iridium Bis(phosphinite) Pincer Complexes (p-XPCP)IrH2, (p-XPCP)Ir(CO), (p-XPCP)Ir(H)(aryl), and {(p-XPCP)Ir}2{μ-N2} and Their Relevance in Alkane Transfer Dehydrogenation. *Organometallics* **2004,** *23* , 1766-1776.
(44) Morales-Morales, D.; Redón, R. o.; Yung, C.; Jensen, C. M., Dehydrogenation of alkanes catalyzed by an iridium phosphinito PCP pincer complex. *Inorganica Chim. Acta* **2004,** *357* , 2953-2956.
(45) Göttker-Schnetmann, I.; Brookhart, M., Mechanistic Studies of the Transfer Dehydrogenation of Cyclooctane Catalyzed by Iridium Bis(phosphinite) p-XPCP Pincer Complexes. *J .Am. Chem. Soc.* **2004,** *126*, 9330-9338.
(46) (a) Kovalenko, O. O.; Wendt, O. F., An electron poor iridium pincer complex for catalytic alkane dehydrogenation. *Dalton Trans.* **2016,** *45* (40), 15963-15969. (b) Das, K.; Kumar, A. Alkane dehydrogenation reactions catalyzed by pincer-metal complexes. In *Advances in Organometallic Chemistry*, Vol. 72; Pérez, P. J., Ed.; Academic Press, 2019; Chapter 1, pp 1−57. (C) Kumar, A.; Zhou, T.; Emge, T. J.; Mironov, O.; Saxton, R. J.; Krogh-Jespersen, K.; Goldman, A. S., Dehydrogenation of n-Alkanes by Solid-Phase Molecular Pincer-Iridium Catalysts. High Yields of α-Olefin Product. *J. Am. Chem. Soc.* **2015,** *137*, 9894-9911. Wang, K.; Goldman, M. E.; Emge, T. J.; Goldman, A. S., Transfer-dehydrogenation of alkanes catalyzed by rhodium(I) phosphine complexes. *J. Organomet. Chem.* **1996,** *518*, 55-68. (e) Zhou, X.; Malakar, S.; Zhou, T.; Murugesan, S.; Huang, C.; Emge, T. J.; Krogh-Jespersen, K.; Goldman, A. S., Catalytic Alkane Transfer Dehydrogenation by PSP-Pincer-Ligated Ruthenium. Deactivation of an Extremely Reactive Fragment by Formation of Allyl Hydride Complexes. *ACS Catal.* **2019,** *9*, 4072-4083.
(47) Werkmeister, S.; Neumann, J.; Junge, K.; Beller, M., Pincer-type complexes for catalytic (De) hydrogenation and transfer (De) hydrogenation reactions: recent progress. *Chem. Eur. J.* **2015,** *21*, 12226-12250.
(48) Bernskoetter, W. H.; Hazari, N., Reversible hydrogenation of carbon dioxide to formic acid and methanol: Lewis acid enhancement of base metal catalysts. *ACC. Chem. Rev.* **2017,** *50* (4), 1049-1058.
(49) Behr, A.; Nowakowski, K., Catalytic hydrogenation of carbon dioxide to formic acid. In *Advances in Inorganic Chemistry*, Elsevier: 2014; Vol. 66, pp 223-258.
(50) Ai, W.; Zhong, R.; Liu, X.; Liu, Q., Hydride Transfer Reactions Catalyzed by Cobalt Complexes. *Chem. Rev.* **2019,** *119*, 2876-2953.
(51) Wang, W.-H.; Himeda, Y.; Muckerman, J. T.; Manbeck, G. F.; Fujita, E., CO2 Hydrogenation to Formate and Methanol as an Alternative to Photo- and Electrochemical CO2 Reduction. *Chem. Rev.* **2015,** *115*, 12936-12973.
(52) Artz, J.; Müller, T. E.; Thenert, K.; Kleinekorte, J.; Meys, R.; Sternberg, A.; Bardow, A.; Leitner, W., Sustainable conversion of carbon dioxide: an integrated review of catalysis and life cycle assessment. *Chem. Rev.* **2018,** *118* , 434-504.
(53) Dong, K.; Razzaq, R.; Hu, Y.; Ding, K., Homogeneous Reduction of Carbon Dioxide with Hydrogen. *Topics in Current Chemistry Collections. Springer, Cham.* **2017**, *375* , 23.
(54) Sakakura, T.; Choi, J.-C.; Yasuda, H., Transformation of Carbon Dioxide. *Chem. Rev.* **2007,** *107*, 2365-2387.
(55) Sanfilippo, D.; Rylander, P. N., Hydrogenation and dehydrogenation. In Ullmann's Encyclopedia of Industrial Chemistry, (Ed.). 2000.
(56) Riduan, S. N.; Zhang, Y., Recent developments in carbon dioxide utilization under mild conditions. *Dalton Trans.* **2010,** *39* (14), 3347-3357.

(57) (a) Inoue, Y.; Izumida, H.; Sasaki, Y.; Hashimoto, H., atalytic fixation of carbon dioxide to formic acid by transition-metal complexes under mild conditions. *Chem. Lett.* **1976,** *5*, 863-864. (b) Bulushev, D. A.; Ross, J. R. Heterogeneous catalysts for hydrogenation of CO2 and bicarbonates to formic acid and formates. *Catal. Rev.* **2018,** *60*, 566-593.
(58) Tanaka, R.; Yamashita, M.; Nozaki, K., Catalytic Hydrogenation of Carbon Dioxide Using Ir(III)−Pincer Complexes. *J. Am. Chem. Soc.* **2009,** *131*, 14168-14169.
(59) Langer, R.; Diskin-Posner, Y.; Leitus, G.; Shimon, L. J. W.; Ben-David, Y.; Milstein, D., Low-Pressure Hydrogenation of Carbon Dioxide Catalyzed by an Iron Pincer Complex Exhibiting Noble Metal Activity. *Angew. Chem.* **2011,** *123*, 10122-10126.
(60) Filonenko, G. A.; van Putten, R.; Schulpen, E. N.; Hensen, E. J. M.; Pidko, E. A., Highly Efficient Reversible Hydrogenation of Carbon Dioxide to Formates Using a Ruthenium PNP-Pincer Catalyst. *ChemCatChem* **2014**, 1526-1530.
(61) Zhang, Y.; MacIntosh, A. D.; Wong, J. L.; Bielinski, E. A.; Williard, P. G.; Mercado, B. Q.; Hazari, N.; Bernskoetter, W. H., Iron catalyzed CO2 hydrogenation to formate enhanced by Lewis acid co-catalysts. *Chem. Sci.* **2015,** *6* , 4291-4299.
(62) Spentzos, A. Z.; Barnes, C. L.; Bernskoetter, W. H., Effective Pincer Cobalt Precatalysts for Lewis Acid Assisted CO2 Hydrogenation. *Inorg. Chem.* **2016,** *55* , 8225-8233.
(63) Yao, W.; Olajide, G.; Boudreaux, C. M.; Wysocki, M. M.; Ahmed, M. K.; Qu, F.; Szilvási, T.; Papish, E. T., Cobalt(I) Pincer Complexes as Catalysts for CO2 Hydrogenation to Formate. *Organometallics* **2024,** *43*, 1447-1458.
(64) Arashiba, K.; Miyake, Y.; Nishibayashi, Y., A molybdenum complex bearing PNP-type pincer ligands leads to the catalytic reduction of dinitrogen into ammonia. *Nat. Chem.* **2011,** *3*, 120-125.
(65) Arashiba, K.; Sasaki, K.; Kuriyama, S.; Miyake, Y.; Nakanishi, H.; Nishibayashi, Y., Synthesis and Protonation of Molybdenum– and Tungsten–Dinitrogen Complexes Bearing PNP-Type Pincer Ligands. *Organometallics* **2012,** *31*, 2035-2041.
(66) Wickramasinghe, L. A.; Ogawa, T.; Schrock, R. R.; Müller, P., Reduction of Dinitrogen to Ammonia Catalyzed by Molybdenum Diamido Complexes. *J. Am.Chem. Soc.* **2017,** *139*, 9132-9135.
(67) Ragauskas, A. J.; Williams, C. K.; Davison, B. H.; Britovsek, G.; Cairney, J.; Eckert, C. A.; Frederick, W. J.; Hallett, J. P.; Leak, D. J.; Liotta, C. L.; Mielenz, J. R.; Murphy, R.; Templer, R.; Tschaplinski, T., The Path Forward for Biofuels and Biomaterials. *Science* **2006,** *311*, 484-489.
(68) Das, K.; Kathuria, L.; Jasra, R. V.; Dhole, S.; Kumar, A., Microwave-assisted pincer-ruthenium catalyzed Guerbet reaction for the upgradation of bio-ethanol to bio-butanol. *Catal. Sci. Technol.* **2023,** *13*, 1763-1776.
(69) Sheehan, J.; Aden, A.; Paustian, K.; Killian, K.; Brenner, J.; Walsh, M.; Nelson, R., Energy and Environmental Aspects of Using Corn Stover for Fuel Ethanol. *J. Ind. Ecol.* **2003,** *7* , 117-146.
(70) Hileman, J. I.; Stratton, R. W.; Donohoo, P. E., Energy content and alternative jet fuel viability. *J. Propuls. Power* **2010,** *26*, 1184-1196.
(71) Harvey, B. G.; Meylemans, H. A., Biotechnology, The role of butanol in the development of sustainable fuel technologies. *J. Chem. Technol. Biotechnol.***2011,** *86*, 2-9.
(72) Dürre, P., Biobutanol: an attractive biofuel. *Biotechnol. Healthc.* **2007,** *2*, 1525-1534.
(73) Jin, C.; Yao, M.; Liu, H.; Chia-fon, F. L.; Ji, J., Progress in the production and application of n-butanol as a biofuel. Renew. Sustain. *Energy. Rev.* **2011,** *15*, 4080-4106.
(74) Veibel, S.; Nielsen, J., On the mechanism of the Guerbet reaction. *Trtrahedron* **1967,** *23* , 1723-1733.
(75) Tseng, K.-N. T.; Lin, S.; Kampf, J. W.; Szymczak, N. K., Upgrading ethanol to 1-butanol with a homogeneous air-stable ruthenium catalyst. *Chem. Commun.* **2016,** *52*, 2901-2904.
(76) Xie, Y.; Ben-David, Y.; Shimon, L. J.; Milstein, D., Highly efficient process for production of biofuel from ethanol catalyzed by ruthenium pincer complexes. *J. Am. Chem. Soc.* **2016,** *138* , 9077-9080.
(77) Fu, S.; Shao, Z.; Wang, Y.; Liu, Q., Manganese-catalyzed upgrading of ethanol into 1-butanol. *J. Am. Chem. Soc.* **2017,** *139* 11941-11948.
(78) Kulkarni, N. V.; Brennessel, W. W.; Jones, W. D., Catalytic Upgrading of Ethanol to n-Butanol via Manganese-Mediated Guerbet Reaction. *ACS Catal.* **2018,** *8* 997-1002.

(79) (a) Das, K.; Yasmin, E.; Das, B.; Srivastava, H. K.; Kumar, A., Technology, Phosphine-free pincer-ruthenium catalyzed biofuel production: high rates, yields and turnovers of solventless alcohol alkylation. *Catal. Sci. Technol.* **2020,** *10*, 8347-8358. (b) Gabriëls, D.; Hernández, W. Y.; Sels, B.; Van Der Voort, P.; Verberckmoes, A., Review of catalytic systems and thermodynamics for the Guerbet condensation reaction and challenges for biomass valorization. *Catai. Sci. Technol* **2015,** *5* 3876-3902. (c) A. Messori, A. Gagliardi, C. Cesari, F. Calcagno, T. Tabanelli, F. Cavani and R. Mazzoni, Advances in the homogeneous catalyzed alcohols homologation: The mild side of the Guerbet reaction. *Catal. Today*, 2023, **423**, 114003.
(80) Cho, C. S.; Kim, B. T.; Kim, H.-S.; Kim, T.-J.; Shim, S. C., Ruthenium-Catalyzed One-Pot β-Alkylation of Secondary Alcohols with Primary Alcohols. *Organometallics* **2003,** *22* (17), 3608-3610.
(81) (a) Gnanamgari, D.; Leung, C. H.; Schley, N. D.; Hilton, S. T.; Crabtree, R. H., Alcohol cross-coupling reactions catalyzed by Ru and Ir terpyridine complexes. *Org. Biomol. Chem.* **2008,** *6*, 4442-4445. (b) Babu, R.; Subaramanian, M.; Midya, S. P.; Balaraman, E., Nickel-Catalyzed Guerbet Type Reaction: C-Alkylation of Secondary Alcohols via Double (de)Hydrogenation. *Org.let.* **2021,** *23*, 3320-3325.
(82) Wang, Q.; Wu, K.; Yu, Z., Ruthenium(III)-Catalyzed β-Alkylation of Secondary Alcohols with Primary Alcohols. *Organometallics* **2016,** *35*, 1251-1256.
(83) (a) Sahoo, A. R.; Lalitha, G.; Murugesh, V.; Bruneau, C.; Sharma, G. V.; Suresh, S.; Achard, M., Ruthenium phosphine–pyridone catalyzed cross-coupling of alcohols to form α-alkylated ketones. *J. Org. Let.* **2017,** *82*, 10727-10731. (b) Prakasham, A. P.; Ta, S.; Dey, S.; Ghosh, P., One pot tandem dual C-C and C-O bond reductions in the β-alkylation of secondary alcohols with primary alcohols by ruthenium complexes of amido and picolyl functionalized N-heterocyclic carbenes. *Dalton Trans.* **2021,** *50* , 15640-15654. (c) Thiyagarajan, S.; Gunanathan, C., Catalytic Cross-Coupling of Secondary Alcohols. *J. Am. Chem. Soc.* **2019,** *141*, 3822-3827. (d) Kumar, N.; Sankar, R. V.; Gunanathan, C., Ruthenium-Catalyzed Self-Coupling of Secondary Alcohols. *J.Org. Chem.* **2023,** *88*, 17155-17163. (e) Narjinari, H.; Bisarya, A.; Arora, V.; Nandi, P. G.; Das, K.; Kumar. In *Dehydrogenation Reactions with 3d Metals*, Sundararaju, B., Ed. Springer Nature: 2024; pp 93-127.
(84) Kaur, M.; U Din Reshi, N.; Patra, K.; Bhattacherya, A.; Kunnikuruvan, S.; Bera, J. K., A Proton-Responsive Pyridyl(benzamide)-Functionalized NHC Ligand on Ir Complex for Alkylation of Ketones and Secondary Alcohols. *Chem. Eur. J.* **2021,** *27*, 10737-10748.
(85) Shee, S.; Paul, B.; Panja, D.; Roy, B. C.; Chakrabarti, K.; Ganguli, K.; Das, A.; Das, G. K.; Kundu, S., Tandem Cross Coupling Reaction of Alcohols for Sustainable Synthesis of β-Alkylated Secondary Alcohols and Flavan Derivatives. *Adv. Syn. Catal.* **2017,** *359*, 3888-3893.
(86) Roy, B. C.; Debnath, S.; Chakrabarti, K.; Paul, B.; Maji, M.; Kundu, S., ortho-Amino group functionalized 2,2′-bipyridine based Ru(ii) complex catalysed alkylation of secondary alcohols, nitriles and amines using alcohols. *Org. Chem. Front.* **2018,** *5*, 1008-1018.
(87) Chakrabarti, K.; Paul, B.; Maji, M.; Roy, B. C.; Shee, S.; Kundu, S., Bifunctional Ru(ii) complex catalysed carbon–carbon bond formation: an eco-friendly hydrogen borrowing strategy. *Org. Biomol. Chem.* **2016,** *14*, 10988-10997.
(88) Liu, T.; Wang, L.; Wu, K.; Yu, Z., Manganese-Catalyzed β-Alkylation of Secondary Alcohols with Primary Alcohols under Phosphine-Free Conditions. *ACS Catal.* **2018,** *8*, 7201-7207.
(89) Kobayashi, S.; Ishitani, H., Catalytic Enantioselective Addition to Imines. *Chem. Rev.* **1999,** *99*, 1069-1094.
(90) Salvatore, R. N.; Yoon, C. H.; Jung, K. W., Synthesis of secondary amines. *Tetrahedron* **2001,** *57*, 7785-7811.
(91) Gunanathan, C.; Milstein, D., Applications of Acceptorless Dehydrogenation and Related Transformations in Chemical Synthesis. *Science* **2013,** *341*, 1229712.
(92) Filonenko, G. A.; van Putten, R.; Hensen, E. J. M.; Pidko, E. A., Catalytic (de)hydrogenation promoted by non-precious metals – Co, Fe and Mn: recent advances in an emerging field. *Chem. Soc. Rev.* **2018,** *47*, 1459-1483.
(93) Gunanathan, C.; Milstein, D., Metal–Ligand Cooperation by Aromatization–Dearomatization: A New Paradigm in Bond Activation and "Green" Catalysis. *Acc. Chem. Res.* **2011,** *44*, 588-602.

(94) Mastalir, M.; Stöger, B.; Pittenauer, E.; Puchberger, M.; Allmaier, G.; Kirchner, K., Air Stable Iron(II) PNP Pincer Complexes as Efficient Catalysts for the Selective Alkylation of Amines with Alcohols. *Adv. Synth. Catal.* **2016,** *358*, 3824-3831.
(95) Maji, M.; Chakrabarti, K.; Paul, B.; Roy, B. C.; Kundu, S., Ruthenium(II)-NNN-Pincer-Complex-Catalyzed Reactions Between Various Alcohols and Amines for Sustainable C−N and C−C Bond Formation. *Adv. Synth. Catal.* **2017,** *360*, 722-729.
(96) (a) Das, K.; Nandi, P. G.; Islam, K.; Srivastava, H. K.; Kumar, A., N–alkylation of amines catalyzed by a ruthenium–pincer complex in the presence of in situ generated sodium alkoxide. *Eur. J. Org. Chem.* **2019,** *2019*, 6855-6866. (b) Afanasyev, O. I.; Kuchuk, E.; Usanov, D. L.; Chusov, D., Reductive Amination in the Synthesis of Pharmaceuticals. *Chem. Rev.* **2019,** *119*, 11857-11911.
(97) Barreiro, E. J.; Kümmerle, A. E.; Fraga, C. A. M., The Methylation Effect in Medicinal Chemistry. *Chem. Rev.* **2011,** *111*, 5215-5246.
(98) Ray, S.; Rao, P. V.; Choudary, N. V., Poly-α-olefin-based synthetic lubricants: a short review on various synthetic routes. *Lub. Sci.* **2012,** *24*, 23-44.
(99) Schönherr, H.; Cernak, T., Profound Methyl Effects in Drug Discovery and a Call for New C-H Methylation Reactions. *Angew. Chem. Int. Edit.* **2013,** *52*, 12256-12267.
(100) Qian, M.; Liauw, M.; Emig, G., Formaldehyde synthesis from methanol over silver catalysts. *Appal. Catal. A Gen.* **2003,** *238*, 211-222.
(101) Wingad, R. L.; Bergström, E. J.; Everett, M.; Pellow, K. J.; Wass, D. F., Catalytic conversion of methanol/ethanol to isobutanol–a highly selective route to an advanced biofuel. *Chem. Commun.* **2016,** *52*, 5202-5204.
(102) Polidano, K.; Allen, B. D.; Williams, J. M.; Morrill, L. C., Iron-catalyzed methylation using the borrowing hydrogen approach. *ACS Catal.* **2018,** *8* , 6440-6445.
(103) Li, Y.; Li, H.; Junge, H.; Beller, M., Selective ruthenium-catalyzed methylation of 2-arylethanols using methanol as C1 feedstock. *Chem. Coummun.* **2014,** *50*, 14991-14994.
(104) Kaithal, A.; Schmitz, M.; Hölscher, M.; Leitner, W., Ruthenium (II)-Catalyzed β-Methylation of Alcohols using Methanol as C1 Source. *Chem coummun* **2019,** *11* 5287-5291.
(105) Bettoni, L.; Gaillard, S.; Renaud, J.-L., Iron-catalyzed β-alkylation of alcohols. *Org. lett.***2019,** *21*, 8404-8408.
(106) Schlagbauer, M.; Kallmeier, F.; Irrgang, T.; Kempe, R., Manganese-catalyzed β-methylation of alcohols by methanol. *Angew. Chem. Int. Ed.* **2020,** *59*, 1485-1490.
(107) Kaithal, A.; Schmitz, M.; Hölscher, M.; Leitner, On the Mechanism of the Ruthenium-catalyzed β-methylation of Alcohols with Methanol. *ChemCatChem* **2020,** *12*, 781-787.
(108) Kaithal, A.; van Bonn, P.; Hölscher, M.; Leitner, W., Manganese (I)-Catalyzed β-Methylation of Alcohols Using Methanol as C1 Source. *Angew. Chem. Int. Ed*. **2020,** *59*, 215-220.
(109) Biswas, N.; Srimani, D., Ru-catalyzed selective catalytic methylation and methylenation reaction employing methanol as the C1 source. *J. Org. Chem.* **2021,** *86*, 10544-10554.
(110) Ganguli, K.; Belkova, N. V.; Kundu, S., Cyclometalated (NNC) Ru (ii) complex catalyzed β-methylation of alcohols using methanol. *Dalton Trans.* **2022,** *51*, 4354-4365.
(111) Polidano, K.; Williams, J. M.; Morrill, L. C., Iron-catalyzed borrowing hydrogen β-C (sp3)-methylation of alcohols. *ACS Catal.* **2019,** *9*, 8575-8580.
(112) Bisarya, A.; Karim, S.; Narjinari, H.; Banerjee, A.; Arora, V.; Dhole, S.; Dutta, A.; Kumar, A., Production of hydrogen from alcohols via homogeneous catalytic transformations mediated by molecular transition-metal complexes. *Chem. Commun.* **2024,** *60*, 4148-4169.
(113) El-Shafie, M.; Kambara, S.; Hayakawa, Y., Hydrogen production technologies overview. *J. Energy Eng.* **2019,** *07*, 107-154.
(114) Singh, S.; Jain, S.; Venkateswaran, P.; Tiwari, A. K.; Nouni, M. R.; Pandey, J. K.; Goel, S. J. R.; reviews, s. e., Hydrogen: A sustainable fuel for future of the transport sector. *Renew. Sustain. Energy Rev.* **2015,** *51*, 623-633.
(115) Satyapal, S.; Read, C.; Ordaz, G.; Stetson, N.; Thomas, G.; Petrovic, J. In *The US Department of Energy's National Hydrogen Storage Project: Goal, Progress and Future Plans*, The Fourth US-Korea Forum on Nanotechnology: Sustainable Energy, Honolulu, 2007.
(116) Olah, G. A.; Goeppert, A.; Prakash, G. S., *Beyond oil and gas: the methanol economy*. John Wiley & Sons: 2011.

(117) Reed, T. B.; Lerner, R. M., Methanol: A Versatile Fuel for Immediate Use: Methanol can be made from gas, coal, or wood. It is stored and used in existing equipment. *Science* **1973,** *182*, 1299-1304.
(118) Asinger, F.; Asinger, F., *Methanol—Chemie und Energierohstoff*. Springer: 1986.
(119) Perry, J. H.; Perry, C. P., *Methanol: Bridge to a renewable energy future*. University Press of America: 1990.
(120) Levin, D. B.; Chahine, R., Challenges for renewable hydrogen production from biomass. *Int. J. Hydrogen Energy* **2010,** *35*, 4962-4969.
(121) Nielsen, M.; Alberico, E.; Baumann, W.; Drexler, H.-J.; Junge, H.; Gladiali, S.; Beller, M., Low-temperature aqueous-phase methanol dehydrogenation to hydrogen and carbon dioxide. *Nature* **2013,** *495*, 85-89.
(122) Hu, P.; Diskin-Posner, Y.; Ben-David, Y.; Milstein, D., Reusable Homogeneous Catalytic System for Hydrogen Production from Methanol and Water. *ACS Catal.* **2014,** *4*, 2649-2652.
(123) Luo, J.; Kar, S.; Rauch, M.; Montag, M.; Ben-David, Y.; Milstein, D., Efficient base-free aqueous reforming of methanol homogeneously catalyzed by ruthenium exhibiting a remarkable acceleration by added catalytic thiol. *J. Am. Chem. Soc.* **2021,** *143*, 17284-17291.
(124) Monney, A.; Barsch, E.; Sponholz, P.; Junge, H.; Ludwig, R.; Beller, M., Base-free hydrogen generation from methanol using a bi-catalytic system. *Chem. Commun.* **2014,** *50*, 707-709.
(125) Alberico, E.; Sponholz, P.; Cordes, C.; Nielsen, M.; Drexler, H. J.; Baumann, W.; Junge, H.; Beller, M., Selective hydrogen production from methanol with a defined iron pincer catalyst under mild conditions. *Angew. Chem.* **2013,** *125*, 14412-14416.
(126) Andérez-Fernández, M.; Vogt, L. K.; Fischer, S.; Zhou, W.; Jiao, H.; Garbe, M.; Elangovan, S.; Junge, K.; Junge, H.; Ludwig, R., A stable manganese pincer catalyst for the selective dehydrogenation of methanol. *Angew. Chem.* **2017,** *129*, 574-577.
(127) Arora, V.; Yasmin, E.; Tanwar, N.; Hathwar, V. R.; Wagh, T.; Dhole, S.; Kumar, A., Pincer–Ruthenium-Catalyzed Reforming of Methanol─ Selective High-Yield Production of Formic Acid and Hydrogen. *ACS Catal.* **2023,** *13*, 3605-3617.
(128) Bielinski, E. A.; Förster, M.; Zhang, Y.; Bernskoetter, W. H.; Hazari, N.; Holthausen, M. C., Base-free methanol dehydrogenation using a pincer-supported iron compound and Lewis acid co-catalyst. *ACS Catal.* **2015,** *5*, 2404-2415.

Chapter- II

Pincer-Ru Catalyzed β-Methylation of Alcohols

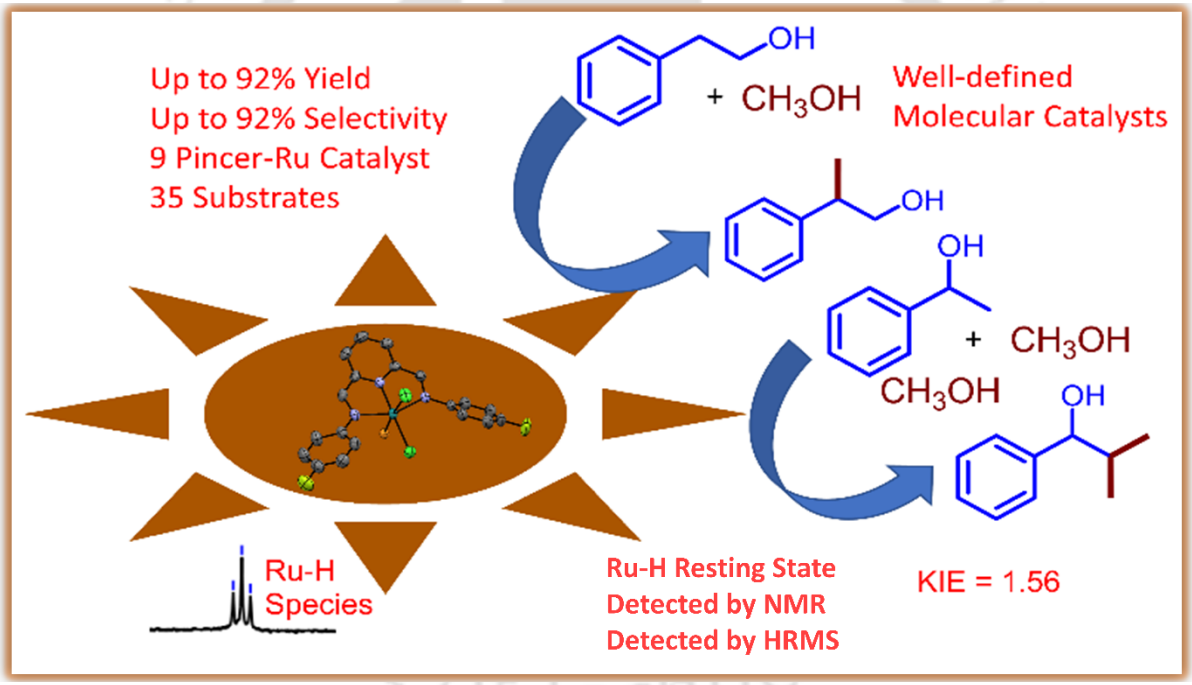

The contents of this chapter have been adapted from "*Pincer-Ru Catalyzed β-Methylation of Alcohols*" by Nandi, P. G.; Jasra, R. V.; Kumar, A. *Organometallics* **2023,** *42*, 3138-3152.

2.1 Introduction

The formation of C−C bonds serves as one of the key processes in the synthesis of natural products,[1] fine chemicals,[1] fuels,[1] pharmaceuticals,[1] and agrochemicals.[1] Conventionally, these C−C bond-forming reactions are accomplished via transition-metal-catalyzed activation of C−X (X = Cl, Br, I) bonds that typically involve organometallic[2] or radical pathways.[3] In a bid to move away from stoichiometric hazardous waste generation,[2] global research has recently intensified its focus on the use of readily available alcohols as potential alkylating agents for the generation of versatile C−C bonds. Such alcohol refunctionalization reactions are known to proceed via the hydrogen auto-transfer[4] or hydrogen-borrowing[5] pathways, which have garnered greater research interest worldwide due to their green and atom economical nature with water as the only by-product.

Among various C−C bond formation reactions, methylation is a very useful tool where access to branching provided by methyl groups is highly important as a structural motif in chemistry and biology,[6] ranging from drug molecules[7] to synthetic lubricants.[8] Though methylation reactions are attractive, the use of methanol as an alkylating agent requires one to accomplish the challenging dehydrogenation of methanol, which has a very high enthalpy (ΔH = 84 kJ/mol). This underlines the importance of the need to design and develop efficient catalysts and catalytic methods for dehydrogenative functionalization using methanol as the alkylating agent.[9]

Transition metal catalyzed dehydrogenation of methanol and 2-phenylethanol produces the corresponding aldehydes which in the presence of a base undergoes aldol-condensation to produce α, β-unsaturated aldehyde with water as a sole by-product. Hydrogenation of this α, β -unsaturated aldehyde produces the β-methylated alcohol (Scheme 2.1). A similar path for 1-phenylethanol can also be proposed (Scheme 2.2).

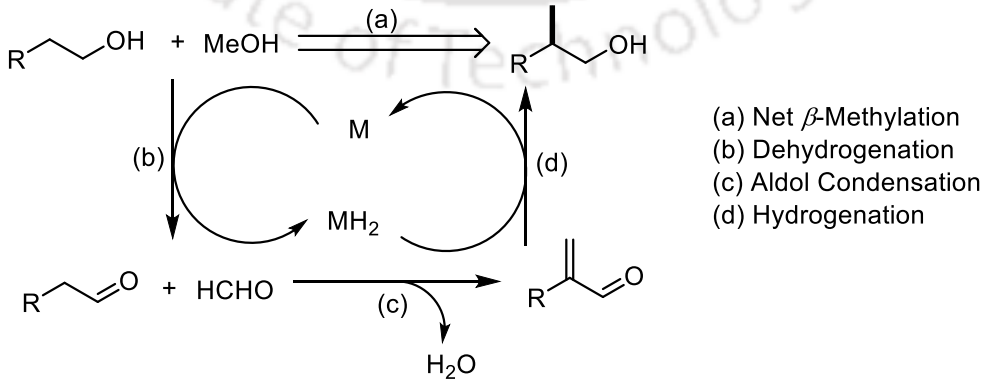

Scheme 2.1: A general schematic representation of the transition metal catalyzed β-methylation of 2-phenylethanol.

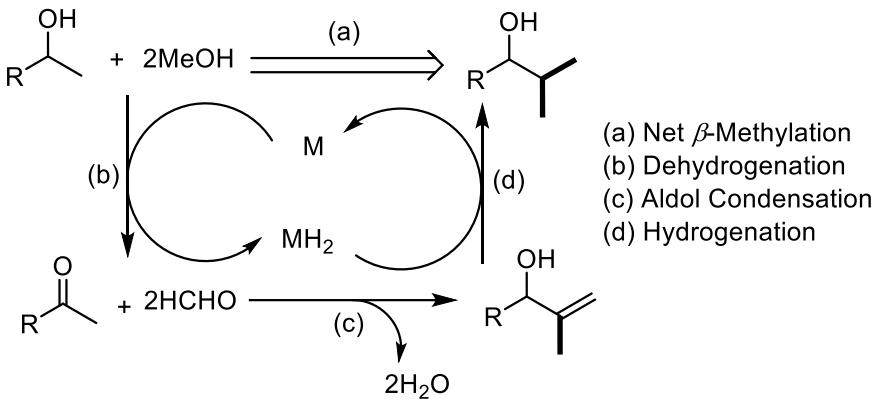

Scheme 2.2: A general schematic representation of the transition metal catalyzed *β*-methylation reaction of 1-phenylethanol.

Among the catalysts that are known for the dehydrogenative functionalization, such as *α*- and *β*-alkylation of secondary alcohols using aliphatic primary alcohols as alkylating agents, catalysts based on Rh,[10c] Ru,[10a,f,j] and Ir[10d,i] have enjoyed great success.[10] However, for the methylation of alcohols at the sp^3 carbon, only a few catalytic systems have been reported.[11]

Recently the *β*-methylation reaction has been explored independently by Tu,[12] Beller,[11c] Renaud,[13c] Kempe,[4] Leitner,[13a,14] and Morril,[9b,13b] using homogeneous complexes[4,9b,13] based on either Fe(0) or Mn(I). Apart from these few attempts to accomplish the *β*-methylation using catalysts based on earth-abundant 3*d* metals, there has been an equal emphasis toward identification of Ru-based *β*-methylation catalytic systems.

In 2019, Leitner and co-workers reported *β*-methylation of primary and secondary alcohols catalyzed by a borane adduct of the Ru−dihydrido complex [RuH(CO)(BH_4)(HN-($C_2H_4PPh_2$)$_2$)] (abbreviated as Ru-MACHO-BH) (**2.10Ru3**).[11a,14] The Guerbet-type coupling of methanol with ethanol leading to isobutanol was reported by Wass using [$RuCl_2(L)_2$] (L = *bis*(diphenylphosphino)methane) as a catalyst.[15] Recently Srimani reported a maximum yield of 90% in the methylation of 2-phenylethanol (**2.1**) catalyzed by 2 mol % (SNS)Ru(II) (**2.10Ru4**) after 36 h at 135 °C.[16] The Kundu group have studied the methylation of both 2-phenylethanol (**2.1**) and 1-phenylethanol (**2.2**) resulting in up to 95% yield and 90% yield of **2.3** and **2.5**, respectively, in the reaction catalyzed by (NNC)Ru(II) (0.5 mol %) in the presence of Cs_2CO_3 (1 equivalent) at 140 °C for 24 h.[17]

Leitner and co-workers reported the highly selective *β*-methylation of alcohols using an earth-abundant first-row transition metal complex [$Mn(CO)_2Br(HN(C_2H_4P^iPr_2)_2)$] **2.10Mn1**

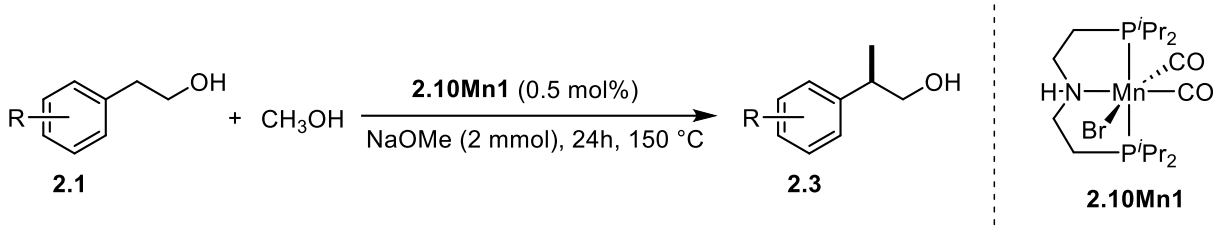

R = H, Yield = 92%; R =4'-Me; Yield = 94%

R =4'-Cl, Yield = 81%; R =4'-OMe; Yield = 91%

R= 3'-OMe; Yield = 77%; R =4'-F; Yield = 87%

Scheme 2.3: *β*-methylation reaction of 2-phenylethanol (**2.1**) and its derivatives by the Mn(I) catalyst **2.10Mn1**.[13a]

((HN($C_2H_4P^iPr_2)_2$) = MACHO-^{i}Pr).[13a] The best yield 94% of 2-(*p*-tolyl)propan-1-ol was obtained at 0.5 mol% loading of **2.10Mn1** in the presence of 2 equivalents of NaOMe at 150 ^oC after 24h in 1 mL methanol (Scheme 2.3). Alternatively, at a high loading of NaOMe (4 equivalents), double methylation of 1-phenylethanol (**2.2**) was achieved with 77% yield of 2-methyl-1-phenylpropan-1-ol **(2.5)** (Scheme 2.4). Excellent activity of the catalyst **2.10Mn1** was observed in the case of methylation of 2-phenylethanol. However moderate to good activity was observed for the **2.10Mn1** catalyzed methylation of 1-phenylethanol and its derivatives.[13a]

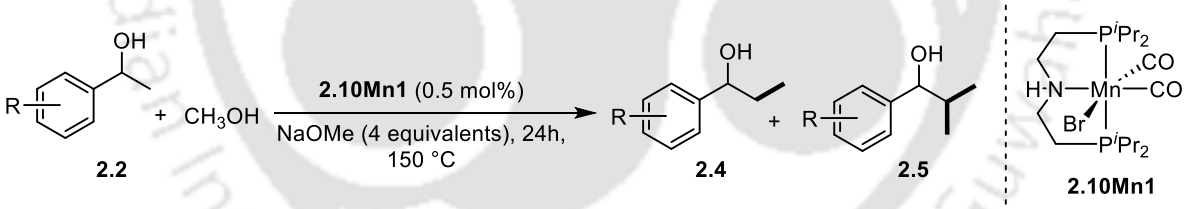

R = H, Yield = 77%; R =4'-F, Yield =61%

R = 4'-Me, Yield = 73%; R = 4'-OMe, Yield =57%

R = 2'-Me, Yield = 29%

Scheme 2.4: The *β*-methylation of 1-phenylethanol (**2.2**) and its derivatives catalyzed by Mn(I) catalyst **2.10Mn1**[13a]

In 2020, Kempe and co-workers reported the earth abundant metal catalyzed double and single methylation of 2-phenyl ethanol and 1-phenyl ethanol.[4] The highest catalytic activity was observed with **2.10Mn2**. The best yield of 89% 2-methyl-1-phenylpropan-1-ol was obtained in the presence of 1.5 equivalents KO^{t}Bu, at a loading of 0.1 mol% **2.10Mn2** and 3 equivalents methanol in 2 mL diglyme after 3h at 140 °C. A large number of substrates could be methylated using this protocol (Scheme 2.5).[4]

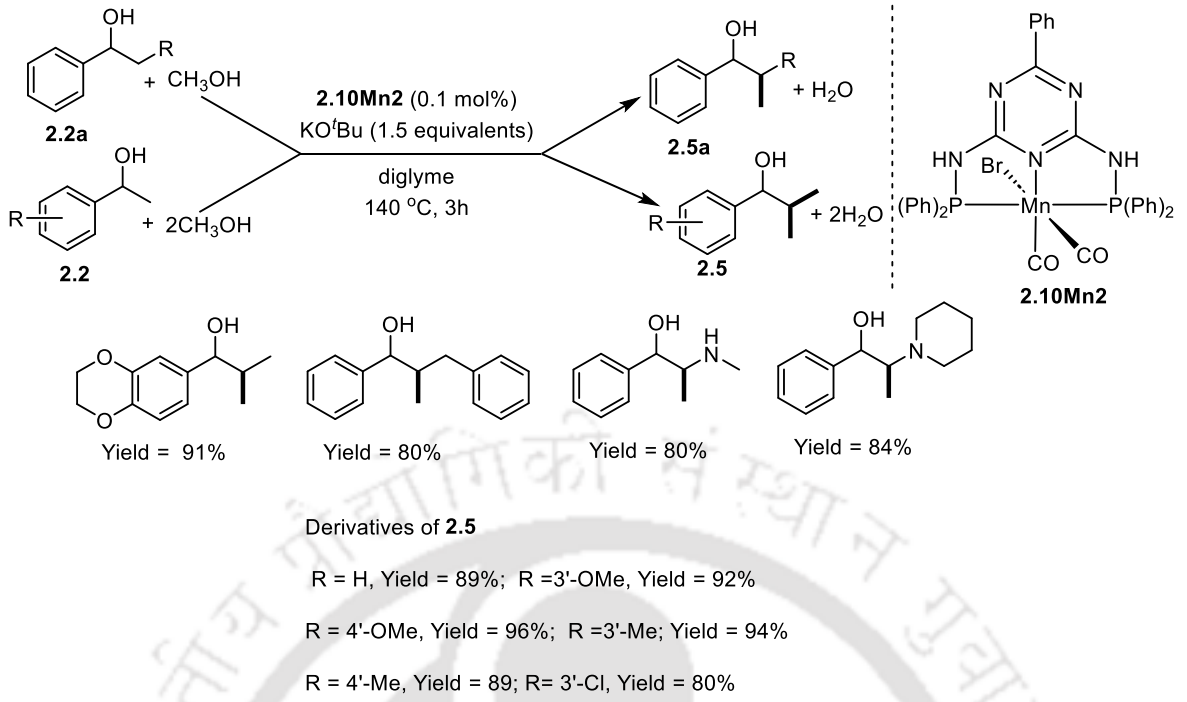

Scheme 2.5: The *β*-methylation of 1-phenylethanol (**2.2**) and its derivatives catalyzed by Mn(I) catalyst **2.10Mn2**[4]

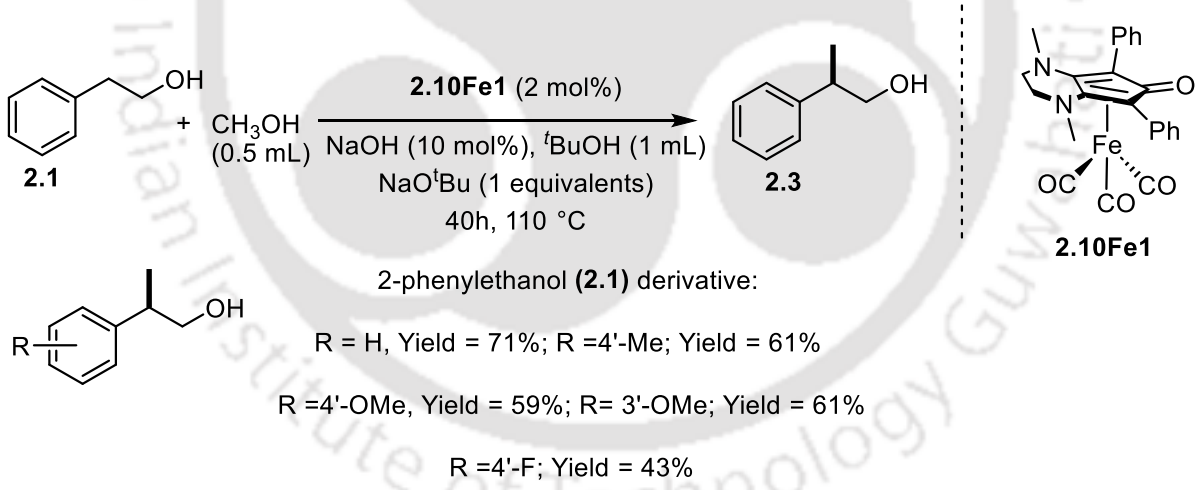

Scheme 2.6: The *β*-methylation of 2-phenylethanol (**2.2**) and its derivative catalyzed by **2.10Fe1**.[13c]

In 2019 Renaud and co-workers carried out the *β*-methylation of 2-phenylethanol in the presence of 2 mol% **2.10Fe1**, NaOH (10 mol%), ^{t}BuOH (1 mL) and NaO^{t}Bu (1 equivalent) at 150 °C for 40h to get 71% of 2-methyl-1-phenylpropan-1-ol (**2.2a**) (Scheme 2.6). Notably the catalyst is moderately active for other 2-phenylethanol substrates.[13c]

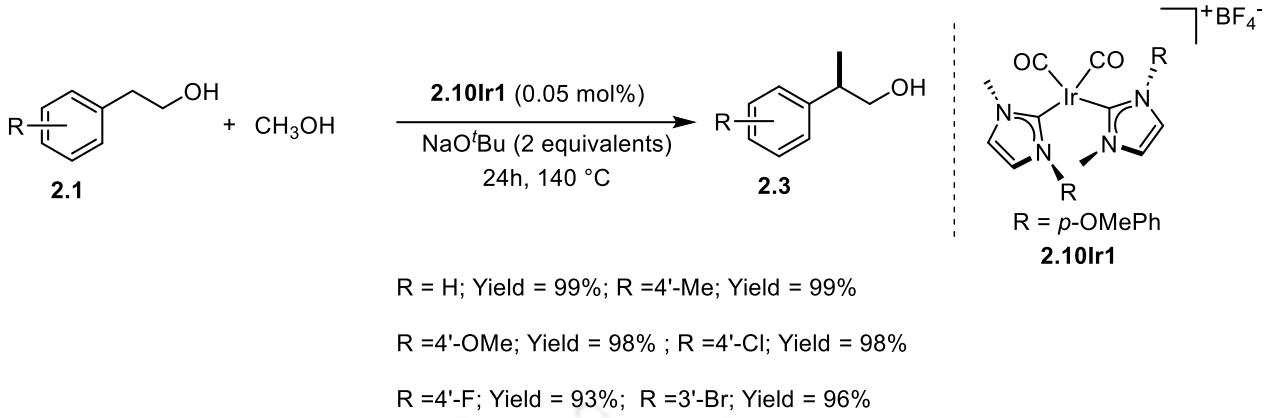

R = H; Yield = 99%; R =4'-Me; Yield = 99%

R =4'-OMe; Yield = 98% ; R =4'-Cl; Yield = 98%

R =4'-F; Yield = 93%; R =3'-Br; Yield = 96%

Scheme 2.7: The *β*-methylation of 2-phenylethanol and its derivatives catalysed by **2.10Ir1** catalyst.[12]

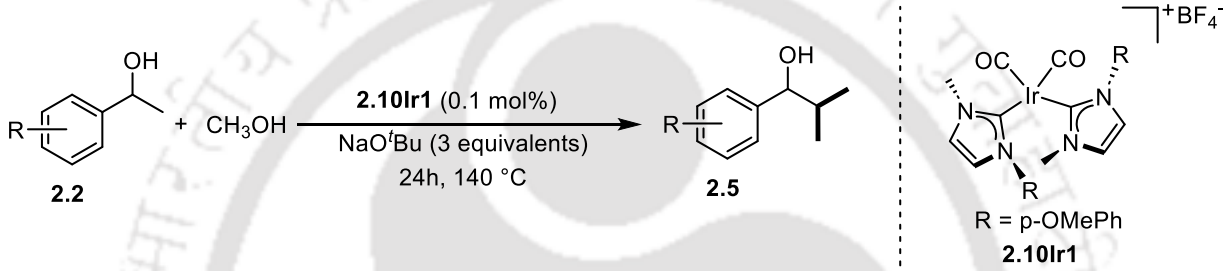

R = H; Yield = 99%; R = 4'-OMe; Yield =90%

R =3'-Me; Yield = 87%; R = 4'-Me; Yield = 82%

R =2'-Me; Yield = 99%; R =4'-Br; Yield = 78%

Scheme 2.8: The *β*-methylation of 1-phenylethanol and its derivatives catalyzed by **2.10Ir1** catalyst.[12]

Tu and co-workers carried out the methylation reaction using *bis*-N-heterocyclic carbene based iridium (*bis*-NHC-Ir) complex at a low catalyst loading, broad substrates scope was achieved with excellent yields (Scheme 2.7 and Scheme 2.8). They carried out the *β*-methylation of 2-phenylethanol catalyzed by *bis*-NHC Ir complex (**2.10Ir1**) (0.05 mol %) in the presence of 2 equivalents of NaO^{t}Bu and obtained up to 99% yield at 140 °C.[12] DFT studies and other control experiments revealed that the ligand effect is critical for achieving an excellent catalytic activity towards the methylation of 2-phenylethanol and 1-phenylethanol.[12]

Beller and co-workers developed a catalytic system based on Ru-MACHO for the methylation of 2-phenyl ethanol under drastic condition (200 ^{o}C, 1.6 equivalents NaOMe) to achieve sufficient conversion. However co-operativity of two ruthenium complexes namely **2.10Ru1** (Shvo catalyst) and **2.10Ru2** (Ru-MACHO) is a key to success for the methylation of 2-aryl ethanols.[11c] The dual catalytic system based on Ru-MACHO (0.1 mol %) (**2.10Ru2**) in conjug-

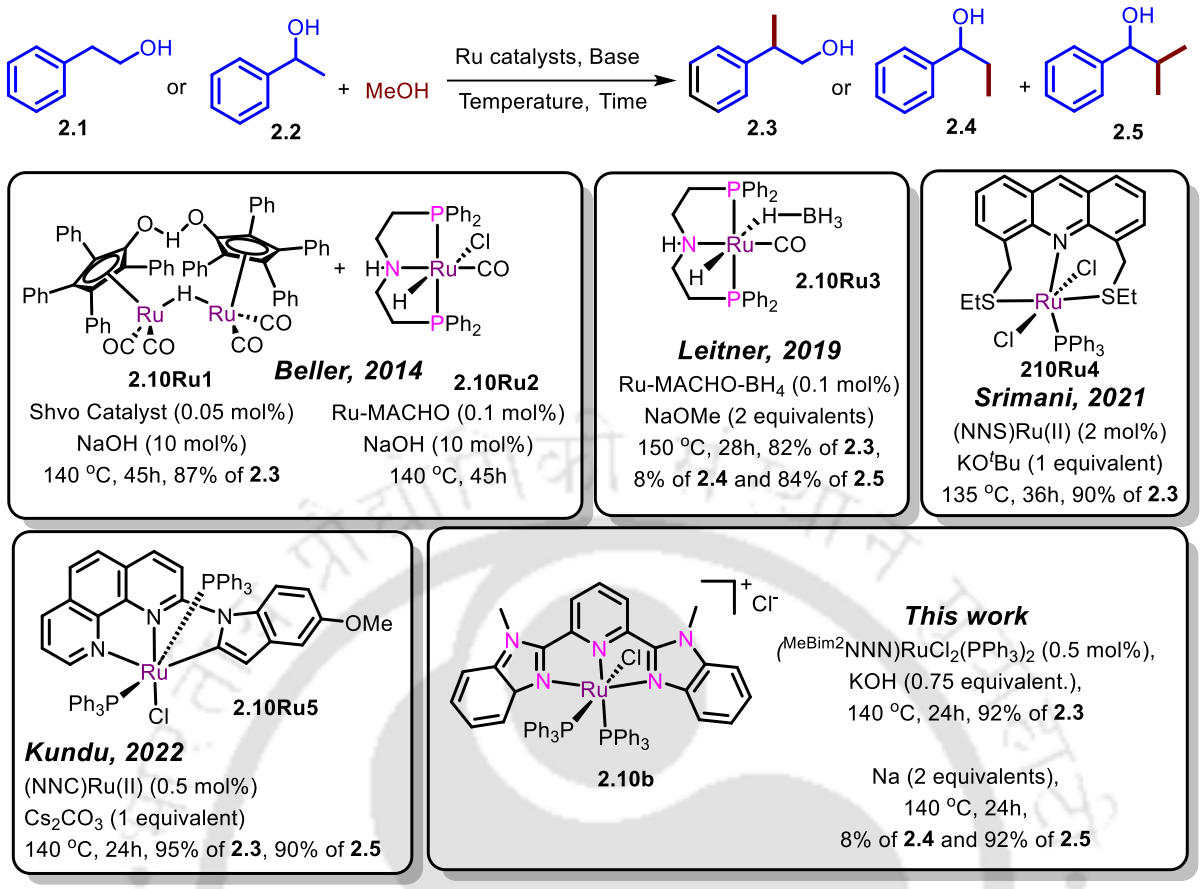

Figure 2.1. Homogeneous ruthenium catalysts reported for the *β*-methylation of 2-phenylethanol (**2.1**) and 1-phenylethanol (**2.2**).

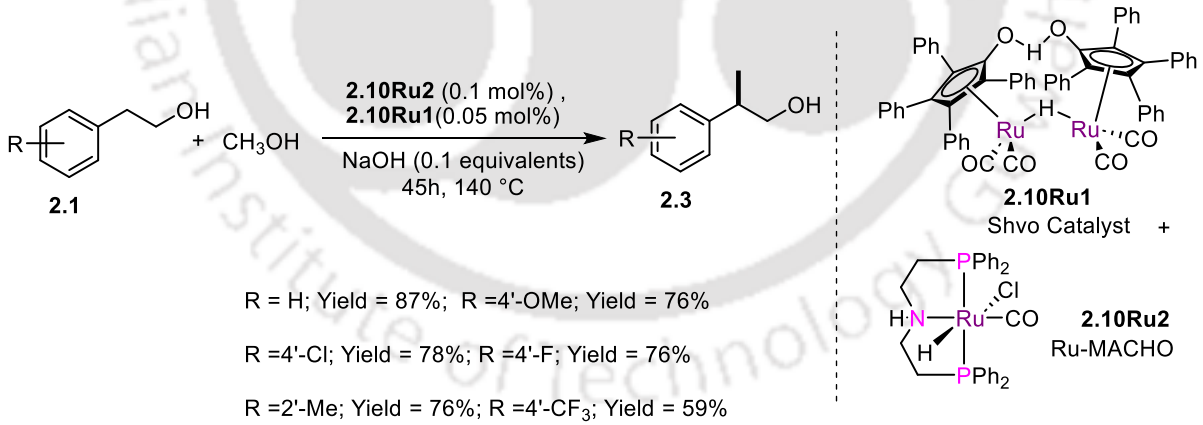

Scheme 2.9: The *β*-methylation of 1-phenylethanol and and it's derivatives catalyzed by **2.10Ru1** in the presence of **2.10Ru2** as co-catalyst.[11c]

-ation with Shvo's catalyst (**2.10Ru1**) (0.05 mol %) (Figure 2.1) for the *β*-methylation of 2-phenylethanol (**2.1**) that resulted in up to 87% yield of **2.3** at 140 °C.[11c] Using these co-catalysts a large library of substrates were transformed to corresponding products with moderate to good yields (Scheme 2.9, Figure 2.1).

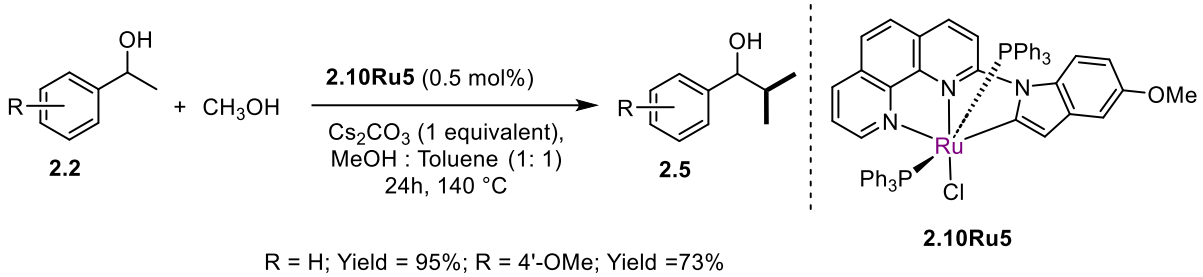

R = H; Yield = 95%; R = 4'-OMe; Yield =73%

R = 4'-Me; Yield = 82%; R =4'-F; Yield =0%

R = 2'-OMe; Yield = 68%; R =4'-Br; Yield =0%

Scheme 2.10: The *β*-methylation reaction of 1-phenylethanol and it's derivatives catalyzed by **2.10Ru5**.[17]

Recently Kundu and co-workers developed (NNC)Ru(II) pincer complexes which show very good activity for the *β*-methylation reaction for wide range of substrates (Scheme 2.10, Figure 2.1). [17]

2.2. Objectives of the current work

A comprehensive literature survey reveals that the pincer complexes are very much active for the activation of alcohols molecules. Our recent success in the synthesis of a series of NNN pincer-ruthenium complexes (**2.6a**–**d** and **2.10a**–**b**; Figure 2.2) based on *bis*(imino)pyridine and 2,6-*bis*(benzimidazol-2-yl)- pyridine ligands for accomplishing catalytic reactions like N-alkylation, [18] glycerol transformation to lactic acid,[19] *β*- alkylation,[20] methanol reforming,[21a] ethanol reforming,[21b] and Guerbet reactions[20,22a] prompted us to test these catalysts for potential *β*-methylation reactions that involve dehydrogenation as a key step in the presence of base. To the best of our knowledge there are no reports on the *β*-methylation reaction using *bis*(imino)pyridine and 2,6-*bis*(benzimidazol-2-yl)pyridine based pincer complexes. On the basis of these facts, the current work attempts to address the following questions

- Can we utilize the pincer-Ru complexes based on *bis*(imino)pyridine and 2,6 *bis*(benzimidazol-2-yl)pyridine ligands for the *β*-methylation of alcohols?
- Can we extrapolate the catalytic activity towards *β*-methylation of alcohols from Guerbet reaction?
- Are various functional groups tolerated?
- Can we get better activity with *bis*(benzimidazol-2-yl)pyridine ligand based pincer-Ru complexes instead of those based on *bis*(imino)pyridine ligand?

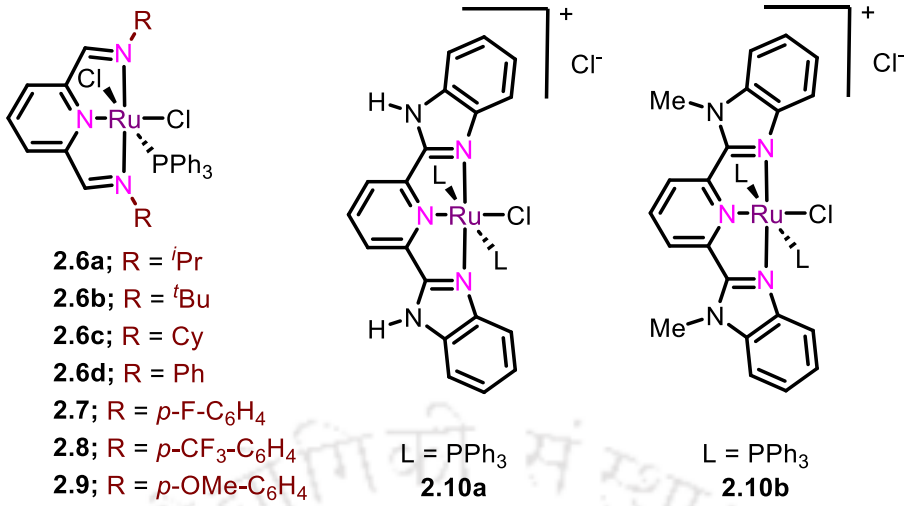

Figure 2.2. Pincer-ruthenium complexes investigated in the current study for the *β*-methylation of alcohols**.**

Gratifyingly, in this chapter, apart from the previously reported complexes, three new pincer−ruthenium complexes (**2.7**, **2.8**, and **2.9**; Figure 2.2) were synthesized and were employed towards the catalytic *β*-methylation reaction. After 24 h at 140 °C, we were able to obtain up to 92% yield of **2.3** in the methylation of 2-phenylethanol (**2.1**) catalyzed by **2.10b** (0.5 mol %) in the presence of 0.75 equivalents of KOH and up to 92% yield of dimethylated product **2.5** in the methylation of 1-phenylethanol (**2.2**) catalyzed by **2.10b** (0.5 mol %) in the presence of 2 equivalents of Na. Both protocols were used to efficiently accomplish the synthesis of several derivatives of **2.3** and **2.5.**

2.3. Results and discussion

2.3.1. Synthesis and characterization of pincer-ruthenium complexes 2.7−2.9 based on *bis*(imino)pyridine ligands

The NNN pincer-Ru phosphine complexes **2.7** and **2.8** containing the *p*-F and *p*-CF_3 groups were synthesized in good yields by treatment of the corresponding ligands[2e,18–20,23] with $RuCl_2(PPh_3)_3$ under an argon atmosphere at reflux for 12 h, and the NNN pincer−Ru phosphine complex **2.9** with a *p*-OMe moiety was synthesized in a similar fashion but at room temperature, followed by washing with diethyl ether and hexane (Scheme 2.11). Complexes **2.7**−**2.9** were fully characterized by HRMS, ^{1}H NMR, ^{31}P NMR, and ^{13}C NMR studies. HRMS analysis of **2.7**, **2.8**, and **2.9** (Figures 2.S58−2.S66) demonstrated prominent peaks at *m*/*z* 720.0725, *m*/*z* 820.0675, and *m*/*z* 744.1131 that correspond to [**2.7** − Cl],$^+$ [**2.8** − Cl]$^+$ and [**2.9**

− Cl]$^+$ respectively. The ^{31}P NMR spectrum exhibited a single peak for each of the complexes **2.7** and **2.8** at δ = 31.90 ppm and at δ = 30.74 ppm. However, for **2.9** two peaks were observed at δ = 29.09 ppm (minor amounts, ca 33% where PPh_3 is *trans* to pyridyl N) and at δ = 33.20 ppm (major amounts, 67 %, PPh_3 *trans* to chloride).

Good quality crystals of **2.7**, **2.8**, and **2.9** were obtained for SCXRD analysis by slow evaporation of their solutions (10 mg each in 1 mL) from a methanol/hexane mixture, a methanol/DCM mixture, and DCM, respectively. Notably, **2.7**, **2.8**, and **2.9** crystallized in space groups *P*21/*c*, *Pna*21, and $P\bar{1}$, respectively (Table 2.1 and 2.S1).

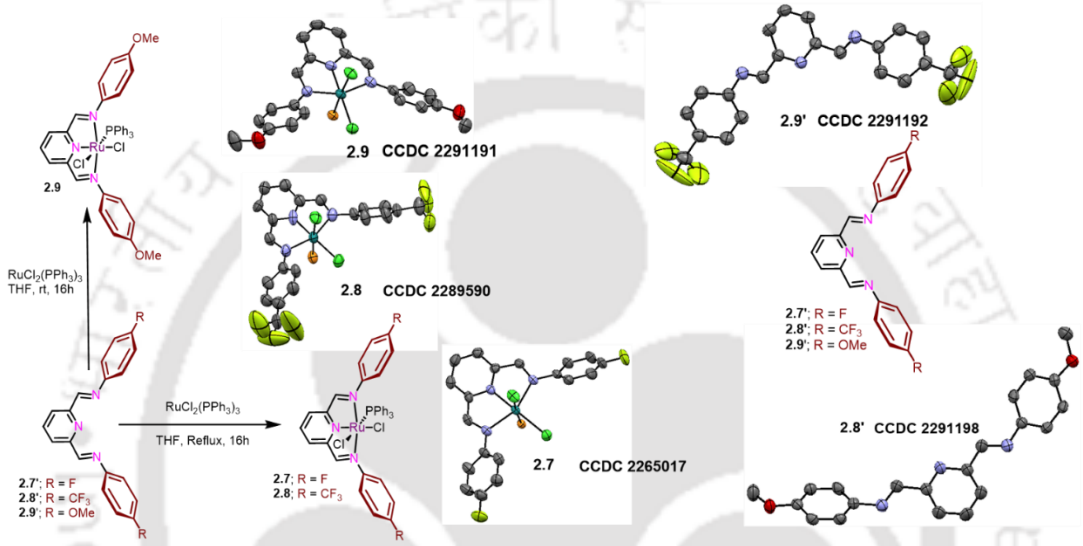

Scheme 2.11. General synthetic route to NNN pincer-ruthenium complexes[a]

[a]The molecular structures of **2.8′**, **2.9′**, **2.7**, **2.8**, and **2.9** are provided as ORTEPs drawn at 50% probability. The phenyl groups on the P atoms and all of the hydrogen atoms in **2.7**, **2.8**, and **2.9** have been omitted for the sake of clarity.

2.3.2. Pincer-ruthenium-catalyzed methylation of 2-phenylethanol

The catalytic methylation reactions of 2-phenylethanol (**2.1**) as a model alcohol was initiated using 0.5 mol % (^{iPr2}NNN)$RuCl_2(PPh_3)$ (**2.6a**) in the presence of various bases at 140 °C. In the presence of 19.2 equivalents of methanol at 140 °C, the yield of the **2.6a**-catalyzed methylation of **2.1** increased with an increase in the amount of NaOH used, giving methylated product **2.3** in a maximum yield of 54% (entries 1−5, Table 2.3). As the **2.6a** catalyzed methylation levelled off at a loading of NaOH higher than 0.75 equivalents (entry 3, Table 2.3), further optimization of the **2.6a**-catalyzed methylation of **2.1** was performed with 0.75 equivalents of NaOH at 140 °C. While increased loading of **2.6a** resulted in a marginal rise in the yield of **2.3** (entry 8, Table 2.3), at lower catalyst loadings there was a concomitant decrease in the yield of **2.3** (entries 6 and 7, Table 2.3).

Table 2.1. Crystal structure and refinement parameters of 2.7, 2.8 and 2.9

Complex	**2.7**	**2.8**	**2.9**
Empirical formula	$C_{37}H_{28}Cl_2F_2N_3PRu$	$C_{40}H_{30}Cl_4F_6N_3PRu$	$C_{78}H_{68}Cl_4N_6O_4P_2Ru_2$
Formula weight	755.56	940.51	1559.26
Temperature/K	298.00	297.0	296.00
Crystal system	monoclinic	orthorhombic	triclinic
Space group	$P2_1/c$	$Pna2_1$	P-1
a/Å	18.353(5)	20.562(3)	15.826(5)
b/Å	12.641(3)	14.706(2)	16.155(6)
c/Å	15.899(4)	14.128(2)	18.092(6)
α/°	90	90	100.222(12)
β/°	107.835(7)	90	103.786(12)
γ/°	90	90	111.712(12)
Volume/Å^3	3511.4(16)	4272.3(12)	3989(2)
Z	4	4	2
ρ_{calc}g/cm^3	1.429	1.462	1.298
μ/mm^{-1}	0.685	0.712	0.602
F(000)	1528.0	1888.0	1592.0
Crystal size/mm^3	0.34 × 0.26 × 0.23	0.32 × 0.24 × 0.21	0.32 × 0.26 × 0.21
Radiation	MoKα (λ = 0.71073)	MoKα (λ = 0.71073)	MoKα (λ = 0.71073)
2Θ range for data collection/°	4.384 to 49.996	3.998 to 49.996	4.242 to 50.17
Index ranges	-21 ≤ h ≤ 21, -15 ≤ k ≤ 15, -18 ≤ l ≤ 18	-24 ≤ h ≤ 24, -17 ≤ k ≤ 17, -16 ≤ l ≤ 16	-18 ≤ h ≤ 18, -19 ≤ k ≤ 19, -21 ≤ l ≤ 21
Reflections collected	70564	82137	50546
Independent reflections	6133 [R_{int} = 0.0357, R_{sigma} = 0.0157]	7519 [R_{int} = 0.0525, R_{sigma} = 0.0267]	14034 [R_{int} = 0.0466, R_{sigma} = 0.0462]
Data/restraints/parameters	6133/0/415	7519/401/530	14034/292/919
Goodness-of-fit on F^2	1.130	1.016	1.023
Final R indexes [I>=2σ (I)]	R_1 = 0.0473, wR_2 = 0.1054	R_1 = 0.0811, wR_2 = 0.1925	R_1 = 0.0600, wR_2 = 0.1412
Final R indexes [all data]	R_1 = 0.0529, wR_2 = 0.1083	R_1 = 0.1087, wR_2 = 0.2323	R_1 = 0.0838, wR_2 = 0.1644
Largest diff. peak/hole / e Å^{-3}	1.39/-0.82	0.15/-0.08	1.09/-0.73
Flack parameter	-	0.08(12)	-

Table 2.2. Selected bond lengths and bond angles around metal (Ru) centre

Parameters	**2.7**	**2.8**	**2.9**
Ru-N (Å) (Pyridyl)	1.941(3)	1.957(15)	1.948 (4), 1.936 (5)
Ru –N (imine) (Å)	2.109 (3), 2.134 (3)	2.111(13), 2.106 (14)	2.126 (4), 2.102 (4), 2.118 (5), 2.101 (4)
Ru – P (Å)	2.3049 (11)	2.330 (4)	2.43192 (15), 2.3334 (15)
Ru – Cl (Å)	2.4425 (12), 2.4471 (12)	2.434 (4), 2.439 (4)	2.4482 (16), 2.4317 (15), 2.4675 (17), 2.4643 (15)
(Imine)N-Ru-N(Imine) (°)	155.18 (13)	157.0 (5)	155.33 (17), 156.2 (2)
(Pyridyl)N -Ru-N(Imine) (°)	77.34 (13),78.18 (13)	77.7(6),79.3(5)	78.10 (17), 77.92 (18), 77.8 (2), 78.55 (19)
Cl (cis) – Ru – P (°)	87.81 (4)	90.31 (16)	88.63 (5), 91.42 (12)
Cl (trans) – Ru – P (°)	174.73 (4)	176.77 (17)	176.26 (5), 179.70 (5)
Cl (cis) – Ru – N (°)	89.00 (10)	87.8 (4)	89.05 (13), 86.46 (13)
Cl (trans) – Ru – N(°)	176.63 (10)	174.2 (4)	176.81 (13), 174.48 (13)

Notably, no methylation of **2.1** was observed in the absence of the catalyst (entries 9 and 10, Table 2.3). The yield of the **2.6a** catalyzed methylation of **2.1** in the presence of 0.75 equivalents of NaOH was lower when the reaction was performed at 120 °C (entry 11, Table 2.3). Upon repeating the **2.6a**-catalyzed methylation of **2.1** under the optimized conditions (entry 3, Table 2.1), but with varying amounts of methanol (entries 12− 15, Table 2.3), the best results (ca. 76% yield of 3 after 24 h) were obtained with 7.5 equivalents of methanol (entry 14, Table 2.3) at 140 °C. Shortening the duration of the **2.6a**-catalyzed methylation of **2.1** using 7.5 equivalents of methanol in the presence of 0.75 equivalents of NaOH at 140 °C to 12 h lowered the yield of **2.3** (entry 16, Table 2.3). Under these new optimized conditions (entry 14, Table 2.3), good yields were obtained either by the use of KOH or by the use of Na (to generate the base *in-situ*)[18] (entries 17 and 24, Table 2.3). While the yields of **2.3** were appreciable when KO^{t}Bu and NaO^{t}Bu were used (entries 18 and 21, Table 2.3), very poor yields were observed with the use of bases based on the carbonate and bicarbonate salts of potassium and sodium (entries 19, 20, 22, and 23, Table 2.3). Among the pincer−ruthenium catalysts **2.6**−**2.9** based on *bis*(imino)pyridine ligands, only **2.6a** provided good yields of methylated product **2.3** under the optimized conditions (entry 1 vs entries 2−7, Table 2.4). When the pincer−ruthenium catalysts **2.10a** and **2.10b** based on 2,6-*bis*(benzimidazol-2- yl)pyridine ligands were

Table 2.3. Pincer-ruthenium-catalyzed methylation of 2- phenylethanol under varying conditions[a]

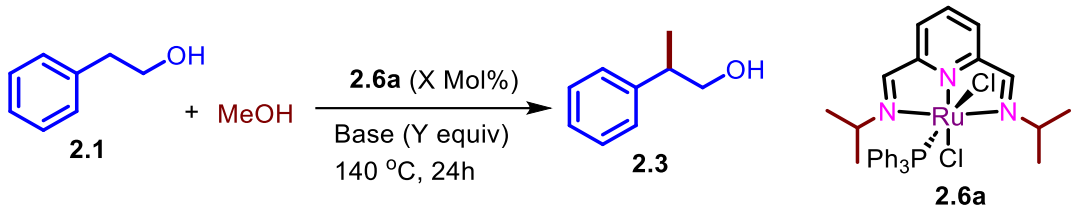

Entry	**2.6a** (X mol%)	Base (Y)	MeOH (equivalents)	%Yield of **2.3** [b]
1	0.5	NaOH (0.25)	19.2	16
2	0.5	NaOH (0.50)	19.2	36
3	0.5	NaOH (0.75)	19.2	47
4	0.5	NaOH (1.00)	19.2	50/55[c]
5	0.5	NaOH (4.00)	19.2	54
6	0.25	NaOH (0.75)	19.2	44
7	0.1	NaOH (0.75)	19.2	27
8	1	NaOH (0.75)	19.2	55
9	–	NaOH (0.75)	19.2	0
10	–	Na (0.75)	19.2	0
11[d]	0.5	NaOH (0.75)	19.2	22
12	0.5	NaOH (0.75	12.4	62
13	0.5	NaOH (0.75)	24.8	42
14	0.5	NaOH (0.75)	7.5	76
15	0.5	NaOH (0.75)	5.0	68
16[e]	0.5	NaOH (0.75)	7.5	65
17	0.5	KOH (0.75)	7.5	83
18	0.5	KO^{t}Bu (0.75)	7.5	70
19	0.5	K_2CO_3 (0.75)	7.5	21
20	0.5	Na_2CO_3 (0.75)	7.5	7
21	0.5	NaO^{t}Bu (0.75)	7.5	60
22	0.5	$NaHCO_3$ (0.75)	7.5	0
23	0.5	$KHCO_3$ (0.75)	7.5	0
24	0.5	Na (0.75)	7.5	83

[a]Reaction conditions, unless specified otherwise: 1 mmol of **2.1**, 19.2−7.5 mmol of MeOH, Y equivalents of Base, and X mol % **2.6a** at 140 °C for 24 h in a 5 mL Schlenk flask under an argon atmosphere. [b]Determined by ^{1}H NMR analysis using toluene as the standard. [c]Reaction time = 48 h. [d]The reaction was performed at 120 °C. [e]The reaction was performed for 12 h.

considered, the *N*-methylated analogue **2.10b** outperformed not only **2.10a** but also **2.6a** and resulted in up to 92% yield of the methylated product **2.3** (entry 9 vs entries 8 and 1, Table 2.4). Typical Ru(II) precursors $RuCl_2(PPh_3)_3$, [Ru(*p*-cymene)Cl_2]$_2$, and [Ru(*p*-benzene)Cl_2]$_2$ exhibited lower reactivity in comparison to the pincer−Ru catalyst **2.10b** (entry 9 vs entries 10−12, Table 2.4).

Table 2.4. Methylation of 2-phenylethanol catalyzed by various ruthenium catalysts[a]

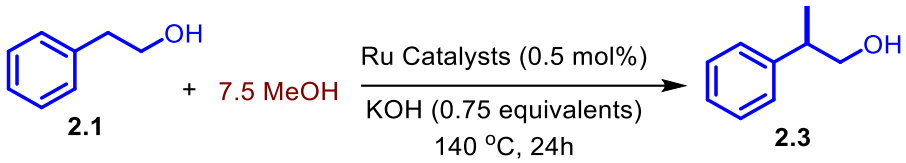

Entry	Ru catalyst	Equivalents of KOH	Equivalents of MeOH	%Yield of **2.3**[b]
1	**2.6a**	0.75	7.5	83
2	**2.6b**	0.75	7.5	57
3	**2.6c**	0.75	7.5	74
4	**2.6d**	0.75	7.5	64
5	**2.7**	0.75	7.5	61
6	**2.8**	0.75	7.5	73
7	**2.9**	0.75	7.5	73
8	**2.10a**	0.75	7.5	27
9	**2.10b**	0.75	7.5	92
10	$RuCl_2(PPh_3)_2$	0.75	7.5	52
11	$[Ru(p\text{-cymene})Cl_2]_2$	0.75	7.5	10
12	$[Ru(p\text{-benzene})Cl_2]_2$	0.75	7.5	19

[a]Reaction conditions, unless specified otherwise: 1 mmol of **2.1**, 7.5 mmol of MeOH, 0.75 equivalents of KOH, and 0.5 mol % Ru catalyst at 140 °C for 24 h in a 5 mL Schlenk flask under an argon atmosphere. [b]Determined by ^1H NMR analysis using toluene as the standard. [c]Average of two runs.

The generic nature of the **2.10b**-catalyzed synthetic protocol was demonstrated by applying it for the catalytic methylation of close to 18 derivatives of 2-phenylethanol (Table 2.5). In general, 2-phenylethanol derivatives with electron-donating and electron-withdrawing groups at the *para* position gave yields that were slightly lower than the corresponding yields obtained when 2-phenylethanol was used (**2.3a**, **2.3b**, **2.3k**, **2.3m**, and **2.3p** vs **2.3**, Table 2.5). While the 2-phenylethanol derivative with a *p*-nitro group was inactive toward methylation (**2.3n**, Table 3), the methylation of the corresponding *p*-bromo derivative resulted in debromination leading to a mixture of **2.3d** and **2.3** (Table 2.5).

The yields of methylated products obtained from the *meta*-substituted 2-phenylethanol derivatives (**2.3c**, **2.3f**, **2.3h**, and **2.3l**, Table 2.5) were comparable to the yield of **2.3**. On the other hand, *ortho*-substituted 2-phenylethanol derivatives and 2-thiopheneethanol performed very poorly (**2.3i**, **2.3j**, and **2.3e**) in the **2.10b** catalysed methylation reaction, presumably due

Table 2.5. Methylation of various 2-phenylethanol derivatives catalyzed by 2.10b[a]

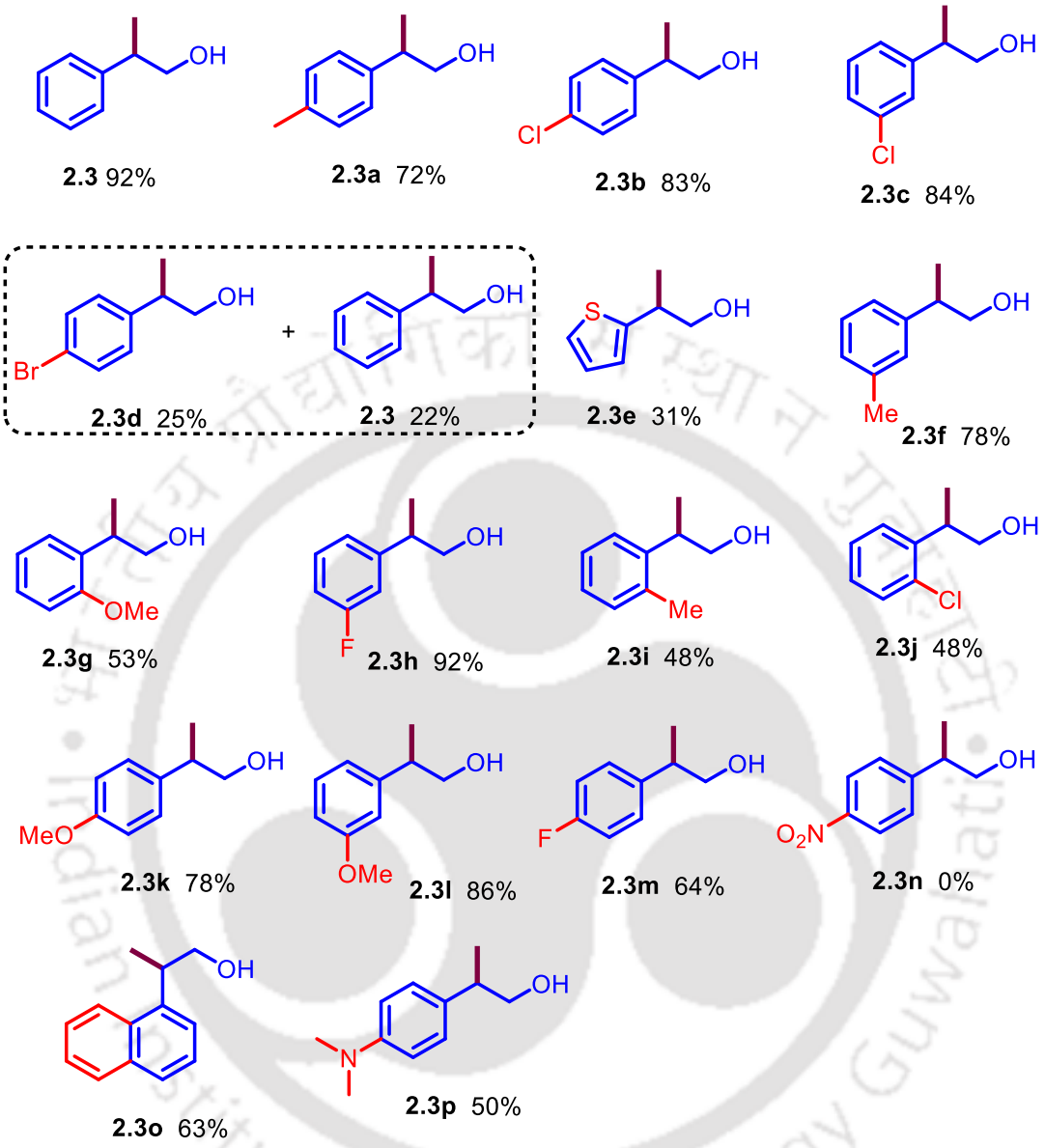

[a]Reaction conditions, unless specified otherwise: 1 mmol of **2.1**, 7.5 mmol of MeOH, 0.75 equivalents of KOH, and 0.5 mol % **2.10b** at 140 °C for 24 h in a 5 mL Schlenk flask under an argon atmosphere. The yields were determined by ^{1}H NMR analyses using toluene as the standard.

to steric effects and deactivation via chelation, respectively. A moderate yield of **2.3o** was obtained in the methylation reaction of 1- naphthaleneethanol catalyzed by **2.10b** at 140 °C in the presence of 0.75 equivalents of KOH after 24 h (Table 2.5).

Efforts were then focused on optimizing a synthetic protocol for the methylation of 1-phenylethanol (**2.2**) using **2.10b** as a catalyst. Upon employing the conditions that gave the best

Table 2.6. Pincer−ruthenium-catalyzed methylation of 1- phenylethanol under varying conditions[a]

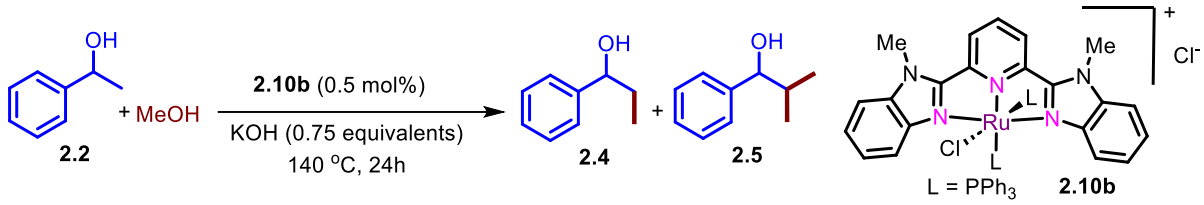

Entry	Ru catalyst (X)	Base (Y)	Equivalents of MeOH	Yield (%) [b]	
				2.4	**2.5**
1	**2.10b** (0.5)	KOH (0.75)	7.5	48	30
2	**2.10b** (0.5)	KOH (0.75)	24.8	27	44
3	**2.10b** (0.5)	Na (0.75)	12. 4	32	55
4	**2.10b** (0.5)	Na (0.75)	24.8	23	59
5	**2.10b** (0.5)	Na (0.75)	49.6	20	9
6	**2.10b** (0.5)	Na (1)	24.8	17	73
7	**2.10b** (0.5)	Na (1.5)	24.8	11	72
8	**2.10b** (0.5)	Na (2)	24.8	8	92
9	**2.10b** (0.5)	Na (3)	24.8	16	77
10	**2.10b** (0.5)	NaOH (2)	24.8	17	78
11	**2.10b** (0.5)	KOH (2)	24.8	14	76
12	**2.10b** (0.5)	NaO^{t}Bu (2)	24.8	12	87
13	**2.10b** (0.5)	KO^{t}Bu (2)	24.8	17	63
14	**2.10b** (0.5)	Cs_2CO_3 (2)	24.8	24	58
15	**2.10b** (0.5)	Na_2CO_3 (2)	24.8	0	0
16	**2.10b** (0.5)	K_2CO_3 (2)	24.8	25	12
17	$RuCl_2(PPh_3)_3$ (0.5)	Na (2)	24.8	12	41
18	**2.6a** (0.5)	Na (2)	24.8	17	71
19	**2.10b** (0.05)	Na (2)	24.8	10	05
20	**2.10b** (0.1)	Na (2)	24.8	20	65
21	**2.10b** (0.2)	Na (2)	24.8	22	64

[a]Reaction conditions, unless specified otherwise: 1 mmol of **2.2**, 7.5− 49.6 mmol of MeOH, Y equivalents of base, and X mol % Ru catalyst at 140 °C for 24 h in a 5 mL Schlenk flask under an argon atmosphere. [b]Determined by ^{1}H NMR analyses using toluene as the standard.

results for the methylation of 2-phenylethanol (entry 9, Table 2.4), the **2.10b** (0.5 mol %)-catalyzed methylation of **2.2** at 140 °C in the presence of 0.75 equivalents of KOH for 24 h resulted in a mixture of monomethylated product **2.4** (48%) and demethylated product **2.5**

(30%) (entry 1, Table 2.6). Repeating the reaction with a higher amount of methanol (24.8 equivalents rather than 7.5 equivalents) resulted in dimethylated **2.5** as the major product (44%; entry 2, Table 2.6). Switching to use Na (to generate the base *in-situ*) resulted in higher selectivity toward **2.5** in the **2.10b** (0.5 mol %)-catalyzed methylation reaction of 1-phenylethanol at 140 °C (entries 3 and 4, Table 2.6). However, the reactivity (29% total yield) and selectivity dropped at very high dilutions in methanol (49.6 equivalents; entry 5, Table 2.6).

Considering 24.8 equivalents as an optimized methanol amount (entry 4, Table 2.6), the loading of Na was then increased to obtain **2.5** with a maximum yield and selectivity of about 92% (compare entry 8 with entries 6, 7, and 9, Table 2.6). At this optimized Na loading of 2 equivalents in the **2.10b** (0.5 mol %)-catalyzed methylation reaction of 1-phenylethanol at 140 °C using 24.8 equivalents of methanol, the yield and selectivity of **2.5** obtained upon using other bases such as NaOH, KOH, NaO^{t}Bu, KO^{t}Bu, Cs_2CO_3, Na_2CO_3, and K_2CO_3 were less as compared to the corresponding results obtained with Na (entry 8 vs entries 10−16, Table 2.6). The loading of 0.5 mol % **2.10b** was found to be optimal (entry 8 vs entries 19−21, Table 2.6), and **2.10b** clearly outperformed both **2.6a** and the precursor $RuCl_2(PPh_3)_3$ (entry 8 vs entries 17 and 18, Table 2.6).

The optimized catalytic system for the dimethylation of 1- phenylethanol was then applied for the screening of about 24 1-phenylethanol derivatives (Table 2.7). In general, good yields of dimethylated products were obtained in the **2.10b**-catalyzed dimethylation of 1-phenylethanol derivatives in the presence of 2 equiv of Na at 140 °C after 24 h using 24.8 equivalents of methanol (**2.5**, **2.5f**, **2.5g**, **2.5j**, **2.5l**, **2.5o**, **2.5q**, and **2.5r**, Table 2.7).

In stark contrast to the methylation of the *p*-bromo derivative of 2-phenylethanol, the corresponding demethylation of the *p*-bromo derivative of 1-phenylethanol did not result in debromination, and about 78% yield of dimethylated product **2.5a** was observed (Table 2.7). However, debromination leading to a mixture of **2.5h** and **2.5** was observed when the *m*-bromo derivative of 1-phenylethanol was used (Table 2.7). The **2.10b** catalyzed dimethylation of 1-(furan-2-yl)ethanol could be achieved in the presence of 2 equivalents of Na leading to the formation of **2.5c** in 64% yield at 140 °C after 24 h using 24.8 equivalents of methanol (Table 2.7). The performance of **2.10b** in accomplishing the dimethylation of 1-(pyridin-2-yl)ethanol was not appreciable and led to only a 20% yield of **2.5d**. The low reactivity of 1-(pyridin-2-yl)ethanol may be attributed to catalyst deactivation via chelation. In contrast, **2.10b** could

catalyze the dimethylation of 1-(pyridin-3-yl)ethanol and 1-(pyridin-4-yl)ethanol with moderate efficiency and resulted in 49% and 51% yields of **2.5m** and **2.5s**, respectively. The

Table 2.7. Methylation of various 1-phenylethanol derivatives catalyzed by 2.10b[a]

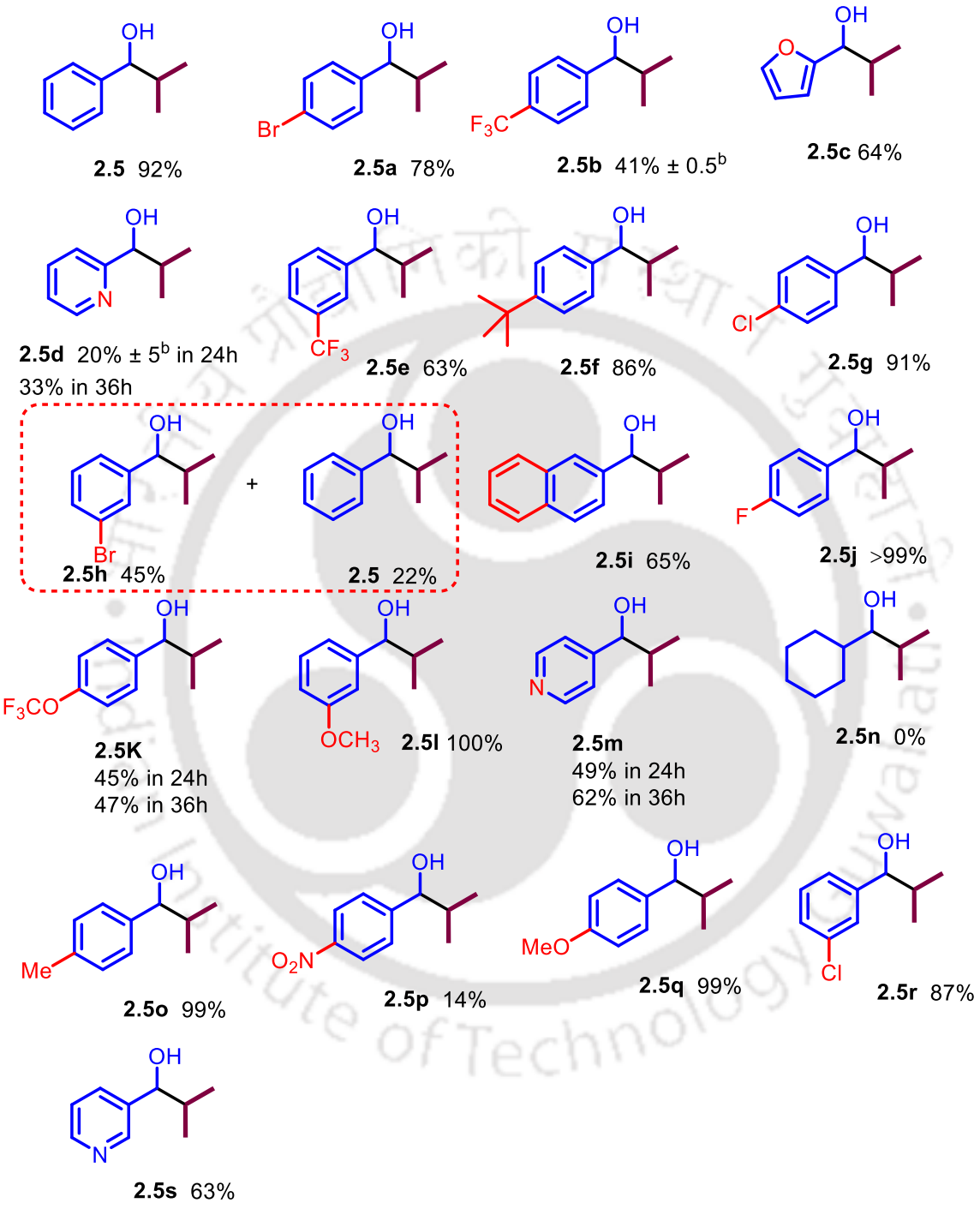

[a]Reaction conditions, unless specified otherwise: 1 mmol of **2.2**, 24.8 mmol of MeOH, 2 mmol of Na, and 0.5 mol % **2.10b** at 140 °C for 24 h in a 5 mL Schlenk flask under an argon atmosphere. The yields were determined by ^{1}H NMR analyses using toluene as the standard. [b]Average of two runs.

presence of $-CF_3$, $-OCF_3$, and $-NO_2$ groups at the *para* position resulted in lower yields of dimethylated products (**2.5b**, **2.5k** and **2.5p**, Table 2.7).

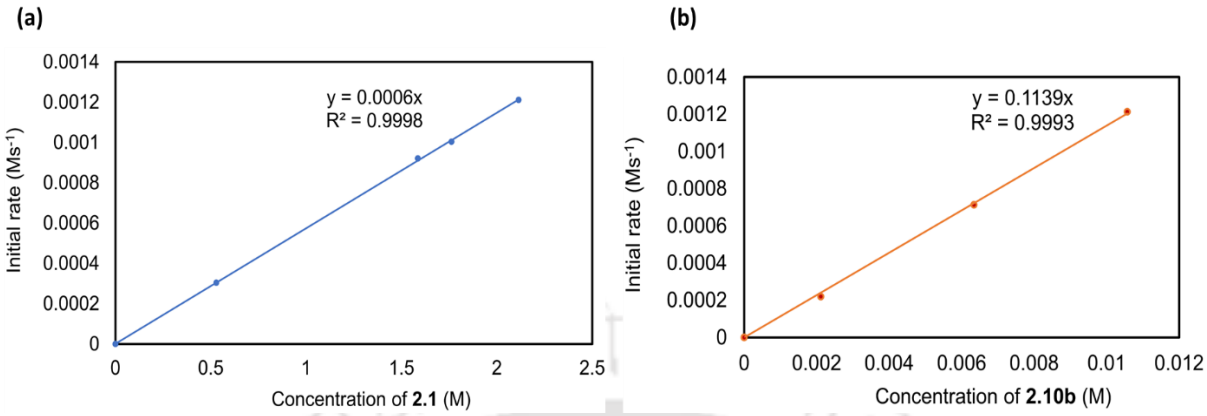

Figure 2.3. (a) Variation of the initial rate of formation of **2.3** with the concentration of **2.1**, reaction conditions: (0.25−1.00 mmol of **2.1**, 7.5 mmol of MeOH, 0.75 mmol of KOH, and 0.5 mol % **2.10b** at 140 °C for 24 h in a 5 mL Schlenk flask under an argon atmosphere). Also see Figures 2.S73−2.S76 and Figure 2.9 (b) Variation of the initial rate of formation of **2.3** with the concentration of **2.10b** (reaction conditions: 1 mmol of **2.1**, 7.5 mmol of MeOH, 0.75 mmol of KOH, and 0.1−0.5 mol % **2.10b** at 140 °C for 24 h in a 5 mL Schlenk flask under an argon atmosphere). Also see Figures 2.S76−2.S78 and Figure 2.10.

2.3.3. Control experiments

The ^{1}H NMR experiments performed during the current studies (Figures 2.5 and 2.S82) and the HRMS analysis along with the mercury-drop experiments previously reported by us[21a] are indicative of the integrity of the pincer fragment and show that the imino groups are intact during catalysis. The bonding of the *bis*(imino)pyridine fragment in a meridional fashion to Ru imparts a very high stability to the resulting pincer. In addition, the steric encumbrance around the imino groups bound to the metal strongly disfavors any reactivity such as insertion into M−H bonds and σ-bond metathesis reactions. Hence, the destruction/ reduction of the imino groups of the pincer fragment is highly unlikely.

In the current studies, detailed mechanistic studies were performed with the most efficient catalyst **2.10b** based on the 2,6-*bis*(benzimidazol-2-yl)pyridine ligand. Kinetic experiments were carried out to determine the order of the **2.10b**-catalyzed methylation of **2.1** in the presence of 0.75 equivalents of KOH using 7.5 equivalents of methanol at 140 °C (Figure 2.3). Using the initial rate method, a first-order dependence of the rate was observed on the

concentrations of both **2.1** and **2.10b**, which points to the homogeneous nature of the reaction. Additional evidence for the homogeneous nature of the reaction involving well-defined

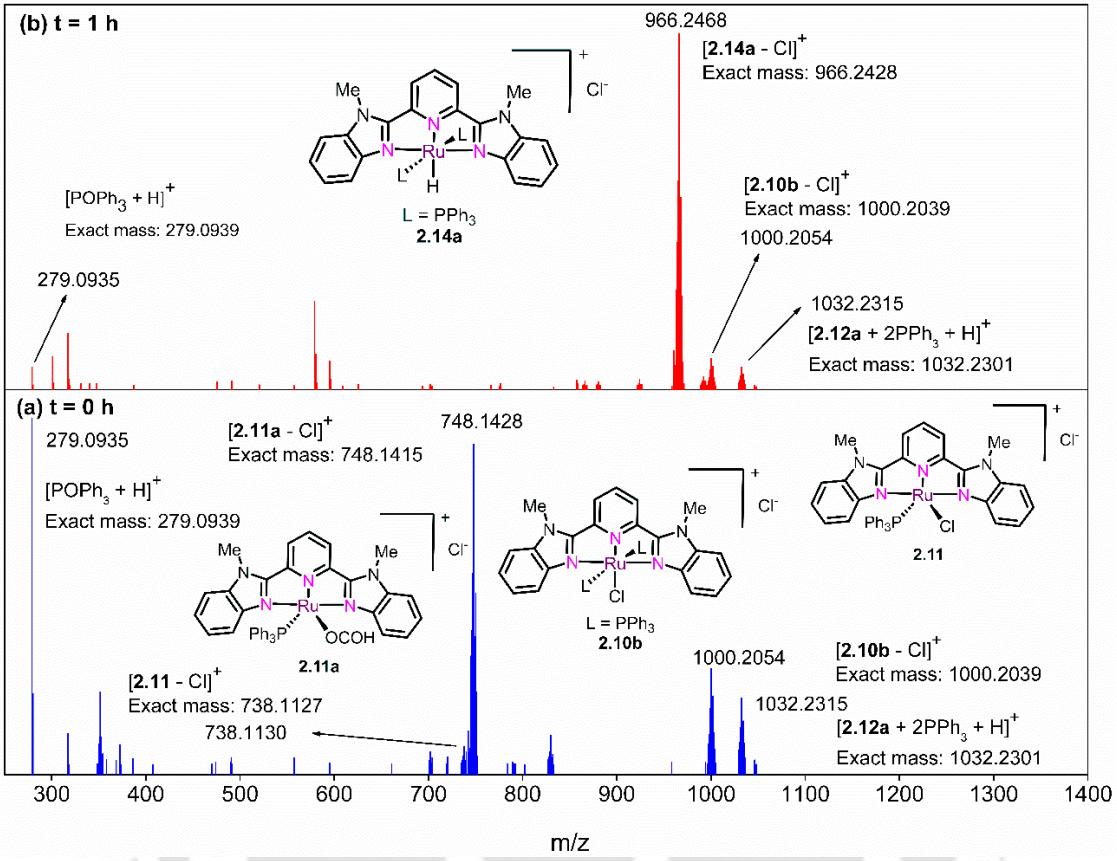

Figure 2.4. HRMS of the reaction mixture containing 2-phenylethanol (0.120 mL, 1 mmol), methanol (0.303 mL, 7.5 mmol), KOH (0.042 g, 0.75 mmol), and **2.10b** (5.16 mg, 5 μmol) maintained at (a) room temperature (t = 0 h) and (b) 140 °C for 1 h. Also see Figures 2.S68−S72.

molecular catalysts was obtained from mercury poisoning experiments that led to hardly any change in reactivity (equation 9, Scheme 2.12). Analysis of the headspace of the reaction vessel of the **2.10b** catalyzed methylation of either **2.1** or **2.2** under the optimized conditions (entry 9, Table 2.4 and entry 8, Table 2.6) revealed the evolution of hydrogen (equation 1, 5 and 6, Scheme 2.12 and Figures 2.S79−2.S8 and 2.6-2.8). The involvement of formaldehyde during the reaction was confirmed by its independent experiment with 2- phenylethanol under the optimized conditions which led to the β-methylated product **2.3** (equation 2, Scheme 2.12). This validates the likely formation of formaldehyde as the dehydrogenation product of methanol (equation 6, Scheme 2.12).

Methylation of acetophenone (**2.2a**) under the optimized conditions led to formation of monomethylated product **2.4**, dimethylated product **2.5**, and hydrogenated product **2.2** in 10%, 88%, and 2% yield, respectively (equation 3, Scheme 2.12). This observation is indicative of

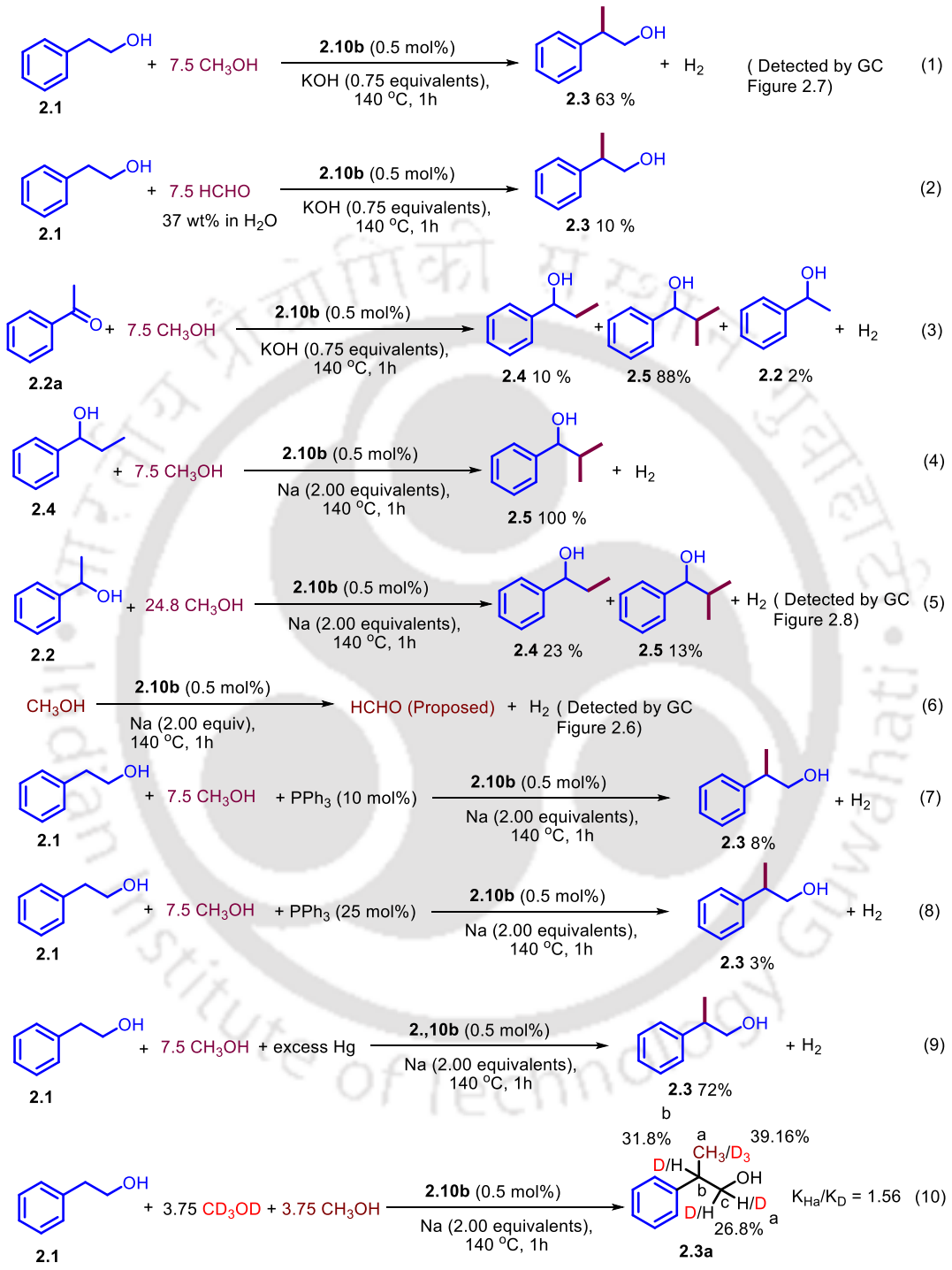

Scheme 2.12. Control experiments

the intermediacy of **2.2a** in the **2.10b** catalyzed methylation of **2.2**. Further, the intermediacy of **2.4** in the **2.10b**-catalyzed methylation of **2.2** was also confirmed by independently

performing its methylation under the optimized conditions, which gave rise to **2.5** in quantitative yield (equation 4, Scheme 2.12). Competitive deuterium labeling studies reveal a secondary kinetic isotope effect (KIE) of 1.56[21] (equation 10, Scheme 2.12). It is hence unlikely that C−H activation is a part of the rate-determining step (RDS), though it is involved in the catalytic cycle. The productivity of the **2.10b**-catalyzed methylation of **2.1** was greatly affected by the presence of externally added PPh_3 (equation 7 and 8, Scheme 2.12), which highlights the importance of the dissociation of PPh_3 from the pincer−ruthenium complex in generating the catalytically active species (Scheme 2.13).

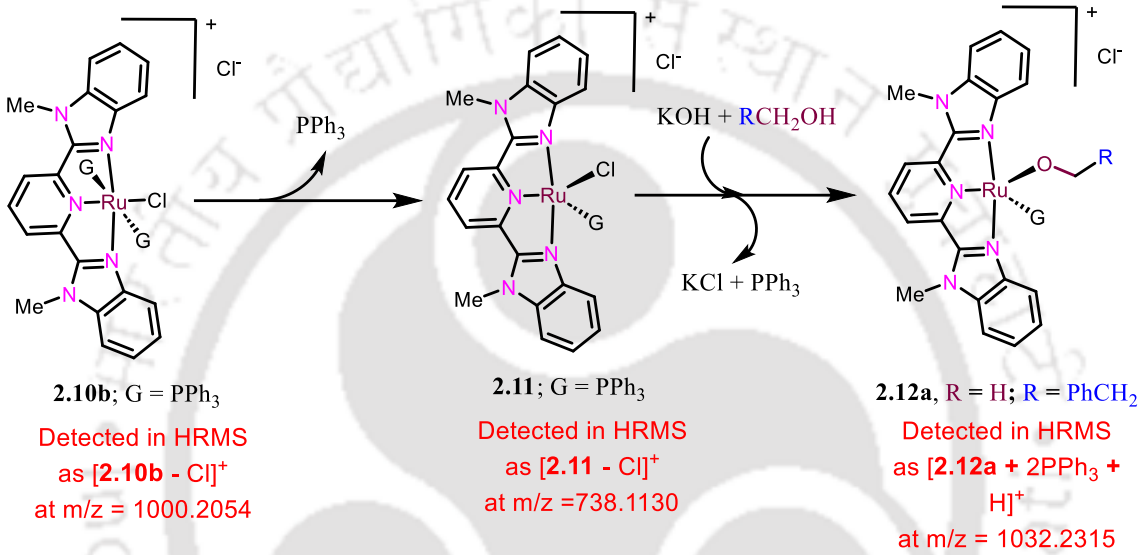

Scheme 2.13. Generation of catalytically active species **2.12a** via dissociation of PPh_3 from **2.10b** followed by salt metathesis.

2.3.4. Plausible mechanism involved in the 2.10b-catalyzed methylation reaction

A catalytic cycle has been proposed employing the most efficient catalyst **2.10b** for the methylation of **2.1** as a model alcohol (Schemes 2.13−2.16). This catalytic cycle has also been probed computationally using the PBE method with the LANL2DZ basis set for metal atoms and the 6-311G(d,p) basis set for non-metal atoms (Schemes 2.14−2.16). The generation of 16-electron five-coordinate dichloride species **2.11** (Scheme 2.13) is likely to be the first step via the dissociation of the ancillary ligand (PPh_3 from **2.10b**). The loss of PPh_3 was detected as Ph_3PO both in the HRMS analysis (*m/z* 279.0935; Figure 2.4) and in the ^{31}P NMR spectrum (δ = 31.37 ppm; Figure 2.5b,c) of the reaction catalyzed by **2.10b**. As the NMR spectrum and HRMS analysis were performed under air, the pincer−ruthenium is likely to have catalyzed the oxidation of the dissociated PPh_3 to PPh_3O. This observation is very common for Ru(II)-based catalysts under air.[21a,22] The salt metathesis of 16-electron five-coordinate dichloride species

2.11 with KOR (R = Me or CH_2CH_2Ph) results in the formation of the active Ru−alkoxide species **2.12** (Scheme 2.13).[19] Interestingly, only **2.12a** was detected not only in HRMS analysis (*m*/*z* 1032.2315; Figure 2.4) but also in NMR studies (^{31}P: δ = 50.65 ppm; Figure 2.5b) as its phosphine adduct, which apparently points to it being one of the resting-state species.

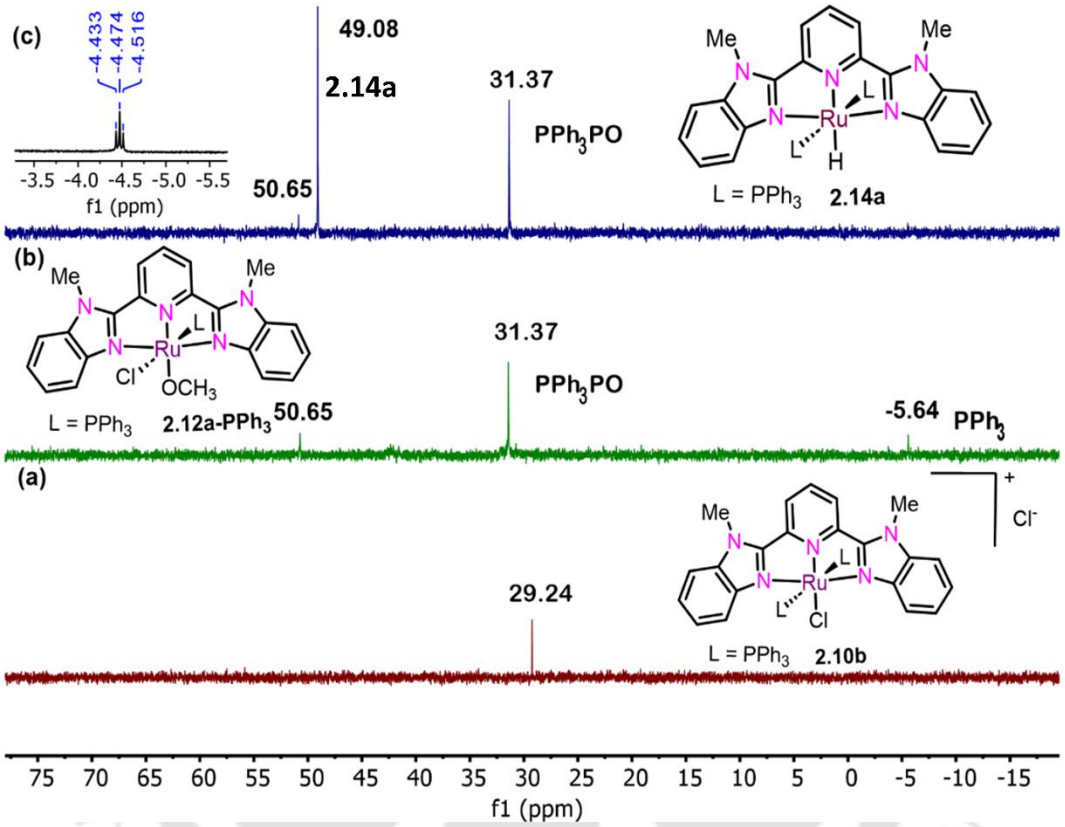

Figure 2.5. (a) ^{31}P NMR spectrum of **2.10b** in $CDCl_3$. (b) ^{31}P NMR spectrum of the reaction mixture containing containing methanol (1 mL, 24.8 mmol), KOH (0.056 g, 1.0 mmol), and **2.10b** (10.35 mg, 0.01 mmol) maintained at room temperature (t = 0 h) under air. (c) ^{31}P NMR spectrum of the reaction mixture containing methanol (1 mL, 24.8 mmol), KOH (0.056 g, 1.0 mmol), and **2.10b** (10.35 mg, 0.01 mmol) maintained at 140 °C for 5 min under air. The hydride region of the ^{1}H NMR spectrum is given in the inset.

The catalytic cycle begins with the β-hydride elimination from **2.12a**/**2.12b** via **TS-2.13a**/**TS-2.13b** to yield Ru−H species **2.14** along with the formation of carbonyl compound **2.1′** and/or formaldehyde (Scheme 2.14). Subsequent σ-bond metathesis of the O−H of methanol or **2.1** with the Ru−H bond in **2.14** regenerates **2.12a**/**2.12b** along with the production of hydrogen, going through **TS-2.15a**/**TS-2.15b** (Scheme 2.14). Interestingly, the Ru−H species **2.14** is detected as its phosphine adduct **2.14a** both in NMR (^{31}P: δ = 49.08 ppm; ^{1}H: triplet at δ =

−4.47 ppm; Figure 2.5c) and HRMS analysis (*m*/*z* 966.2468; Figure 2.4b), indicating that it is a resting state of the reaction. This is well in agreement with the comparison of the energetics of the dehydrogenation of methanol and **2.1**, which reveals that the overall dehydrogenation of the former is more endergonic by 7.05 kcal/mol. Further, for both the dehydrogenation of methanol and **2.1**, the *σ*-bond metathesis (**2.14** → **TS-2.15a**/**TS- 2.15b** → **2.12a**/**2.12b**) is the rate-determining step, with the overall RDS lying in the dehydrogenation segment of the former $\Delta G_{140}^{\ddagger}$ = 24.06 kcal/mol) (Scheme 2.14).

The catalytic dehydrogenation cycle is followed by an uncatalyzed base-mediated condensation of formaldehyde with **2.1′** leading to the formation of **2.16**. The olefinic bond in **2.16** can insert into the Ru−H bond in **2.14** to yield **2.18** via **TS-2.17** (Scheme 2.15). This step can undergo *σ*-bond metathesis either with hydrogen is exergonic (ΔG_{140} = −7.05 kcal/mol) with a barrier of 9.46 kcal/mol. The intermediate **2.18** (hydrogenolysis) or with the O−H bond of methanol/**2.1** (alcoholysis) to result in the regeneration of **2.14**/**2.12a**/**2.12b** along with the formation of **2.22**, going through **TS- 2.19**/**TS-2.20**/**TS-2.21** (Scheme 2.15). Apparently, the hydrogenolysis step is both thermodynamically ($\Delta\Delta G_{140}$ = −9.54 kcal/mol with H_2 vs $\Delta\Delta G_{140}$ = −0.68 kcal/mol with methanol and $\Delta\Delta G_{140}$ = 0.85 kcal/mol kcal/mol with **2.1**) and kinetically ($\Delta G_{140}^{\ddagger}$ = 21.51 kcal/ mol with H_2 vs $\Delta G_{140}^{\ddagger}$ = 23.12 kcal/mol with methanol and $\Delta G_{140}^{\ddagger}$ = 24.97 kcal/mol with **2.1**) favored in comparison with the alcoholysis step (Scheme 2.15).

In a similar fashion, insertion of a carbonyl group in **2.22** into the Ru−H bond of **2.14** followed by hydrogenolysis/alcoholysis would result in the formation of the product **2.3** via the path (**2.14** → **TS-2.23** → **2.24** → **TS-2.25**/**TS-2.26**/**TS-2.27** → **2.14**/**2.12a**/**2.12b**) (Scheme 2.16). The insertion of **2.22** into the Ru−H bond of **2.14** is endergonic (ΔG_{140} = 6.03 kcal/mol) with a barrier of 18.25 kcal/mol (**TS-2.23**). We were not able to locate **TS-2.26** and **TS- 2.27** for the alcoholysis step (Figure 2.S83). However, while step **2.24** → **2.12a** is endergonic ($\Delta\Delta G_{140}$ = 1.52 kcal/mol), the corresponding step **2.24** → **2.12b** is thermodynamically neutral ($\Delta\Delta G_{140}$ = 0.00 kcal/mol). In comparison, the hydrogenolysis step **2.24** → **2.14** is exergonic ($\Delta\Delta G_{140}$ = -8.87 kcal/mol) with a barrier of 13.69 kcal/mol (**TS-2.25**). The thermodynamics of the alcoholysis step in this segment (Scheme 2.16) is very much comparable to that of the corresponding alcoholysis steps **2.18** → **2.12a** ($\Delta\Delta G_{140}$ = −0.68 kcal/mol) and **2.18** → **2.12b** ($\Delta\Delta G_{140}$ = 0.85 kcal/mol) in the previous segment (Scheme 2.15). Taking a cue from the previous step, one may infer that hydrogenolysis is the favored pathway in the overall transformation of **2.22** to **2.3**, which is exergonic (ΔG_{140} = −2.84 kcal/mol) with a rate

determining hydrogenolysis barrier of 13.69 kcal/mol (Scheme 2.16).

A comparison of the individual RDSs of the segments related to the transformation of methanol/**2.1** → formaldehyde/**2.1′** (Scheme 2.14), **2.16** → **2.22** (Scheme 2.15) and **2.22** → **2.3** (Scheme 2.16) suggests that the overall RDS is the dehydrogenolysis step (**TS-2.15a**; $\Delta G_{140}^{\ddagger}$ = 24.06 kcal/mol) that lies in the methanol → formaldehyde dehydrogenation segment (Scheme 2.14). This is in line with the observed secondary KIE of 1.56[21b] (equation 9, Scheme 2.12). Not surprisingly, none of the intermediates involved in the cycles **2.1** → **2.1′** (Scheme 2.14), **2.16** → **2.22** (Scheme 2.15), and **2.22** → **2.3** (Scheme 2.16) are observed in the HRMS analysis. Furthermore, in the overall RDS **2.14** → **TS-2.15a** → **2.12a**, as **2.14** (ΔG_{140} = −1.18 kcal/mol) has a lower energy than **2.12a** (ΔG_{140} = 9.21 kcal/mol) (Scheme 2.14), its phosphine adduct **2.14a** is observed as the resting state, which was detected by both NMR (^{31}P: δ = 49.08 ppm; ^{1}H: triplet at δ = −4.47 ppm; Figure 2.5c) and HRMS analysis (*m*/*z* 966.2468; Figure 2.4b). The comparable energies of **2.14** (ΔG_{140} = −1.18 kcal/mol) and **2.12** (ΔG_{140} = 0.00 kcal/mol) mean that the step **2.12a** → **TS-2.13** → **2.14** may be reversible, and not surprisingly, **2.12a** is also the resting state, as it was detected in the HRMS analysis (*m*/*z* 1032.2315; Figure 2.4) and NMR studies (^{31}P: δ = 50.65 ppm; Figure 2.5b) as its phosphine adduct.

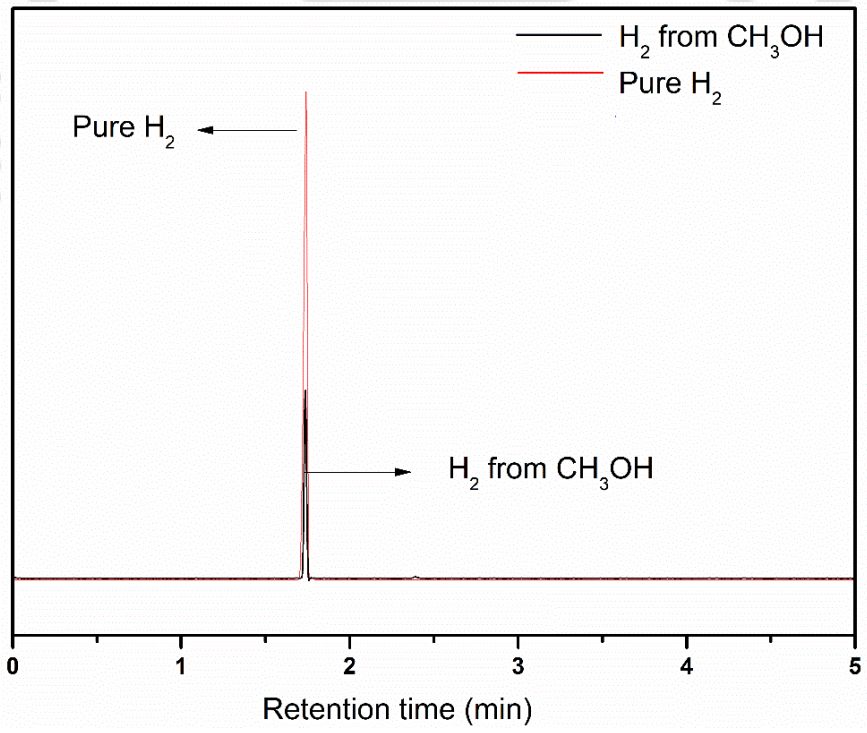

Figure 2.6: Evidence for the evolution H_2 in dehydrogenation of methanol catalyzed by **2.10b** (0.5 mol %) at 140 °C via GC analysis.

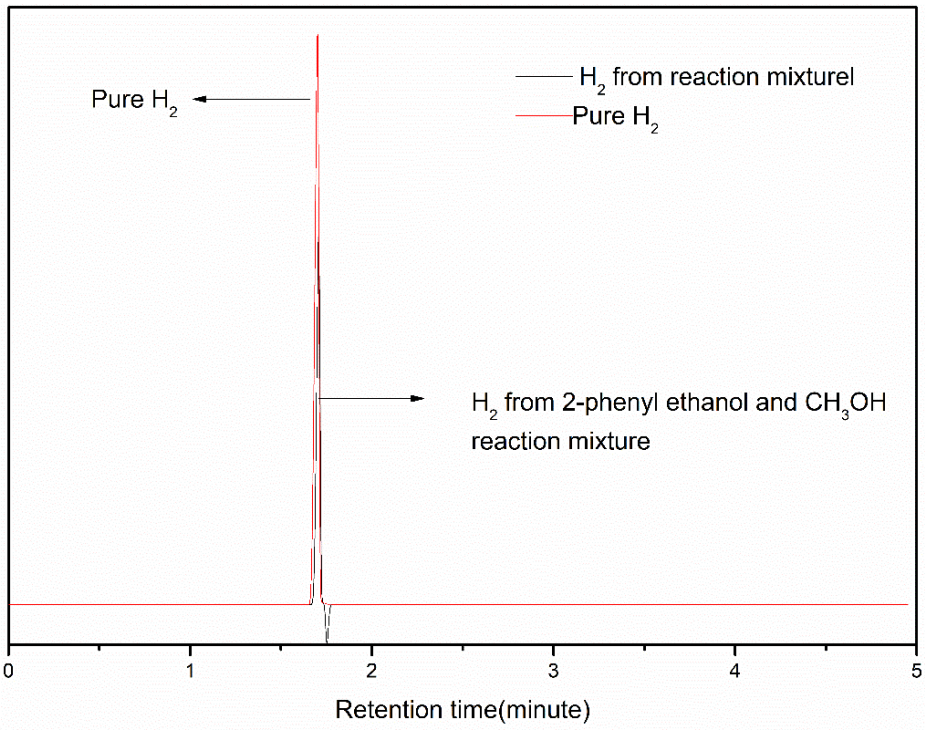

Figure 2.7: Evidence for the evolution H_2 in dehydrogenation of 2-phenyl ethanol (**2.1**) and methanol catalyzed by **2.10b** (0.5 mol %) at 140 °C via GC analysis.

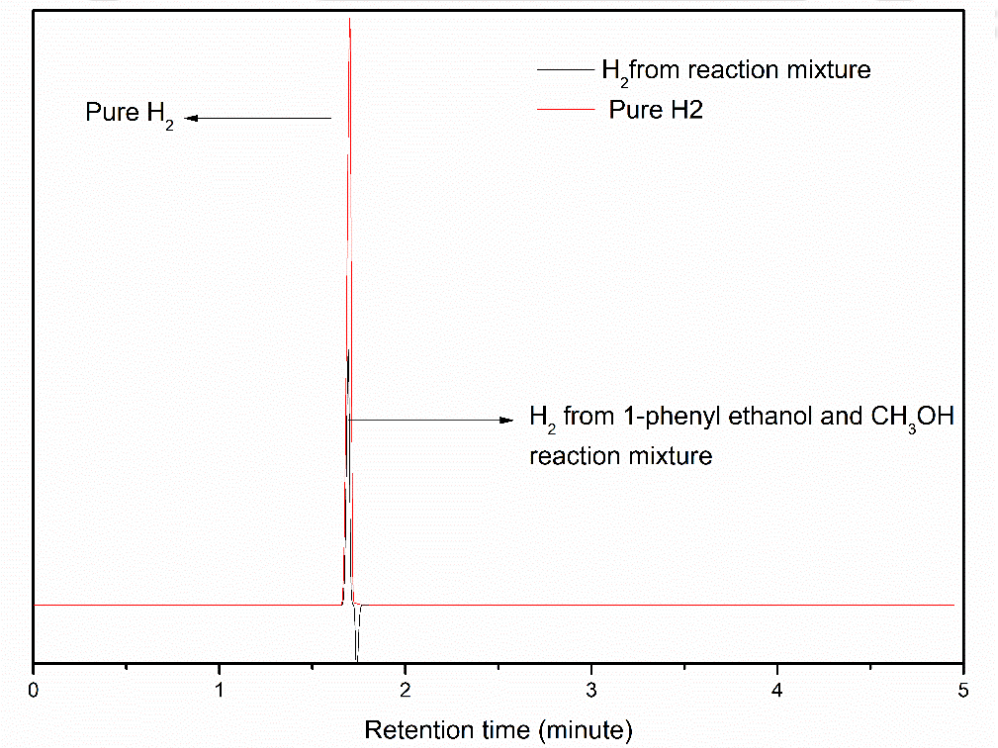

Figure 2.8: Evidence for the evolution H_2 in dehydrogenation of 1-phenyl ethanol (**2.2**) and methanol catalyzed by **2.10b** (0.5 mol %) at 140 °C via GC analysis.

2.4. Conclusion

We have reported the synthesis and characterization of three NNN pincer−ruthenium complexes based on *bis*(imino)-pyridine ligands. The *β*-methylation of 2-phenylethanol and selective *β*-dimethylation of 1-phenylethanol using methanol as an alkylating agent have been accomplished using pincer−ruthenium catalysts based on *bis*(imino)pyridine and 2,6-*bis*(benzimidazol-2-yl)pyridine ligands. Among the considered catalysts, the pincer−ruthenium complex [(^{MeBim2}NNN)RuC(PPh_3)$_2$]Cl based on the dimethyl-substituted 2,6-*bis*-(benzimidazol-2-yl)pyridine ligand was found to be the most efficient. In particular, up to 92% yield of *β*-methylated 2-phenylethanol was obtained at 140 °C in the [(^{MeBim2}NNN)-RuCl(PPh_3)$_2$]Cl (0.5 mol %)-catalyzed reactions in the presence of 0.75 equivalents of KOH using 7.5 equivalents of methanol. Additionally, selective *β*-dimethylation of 1-phenylethanol could be achieved in the [(^{MeBim2}NNN)RuCl(PPh_3)$_2$]Cl (0.5 mol %)-catalyzed reactions in the presence of 2 equivalents of Na using 24.8 equivalents of methanol at 140 °C. The synthetic protocol could be successfully implemented to bring about the *β*-methylation and selective *β*-dimethylation of about 35 substrates.

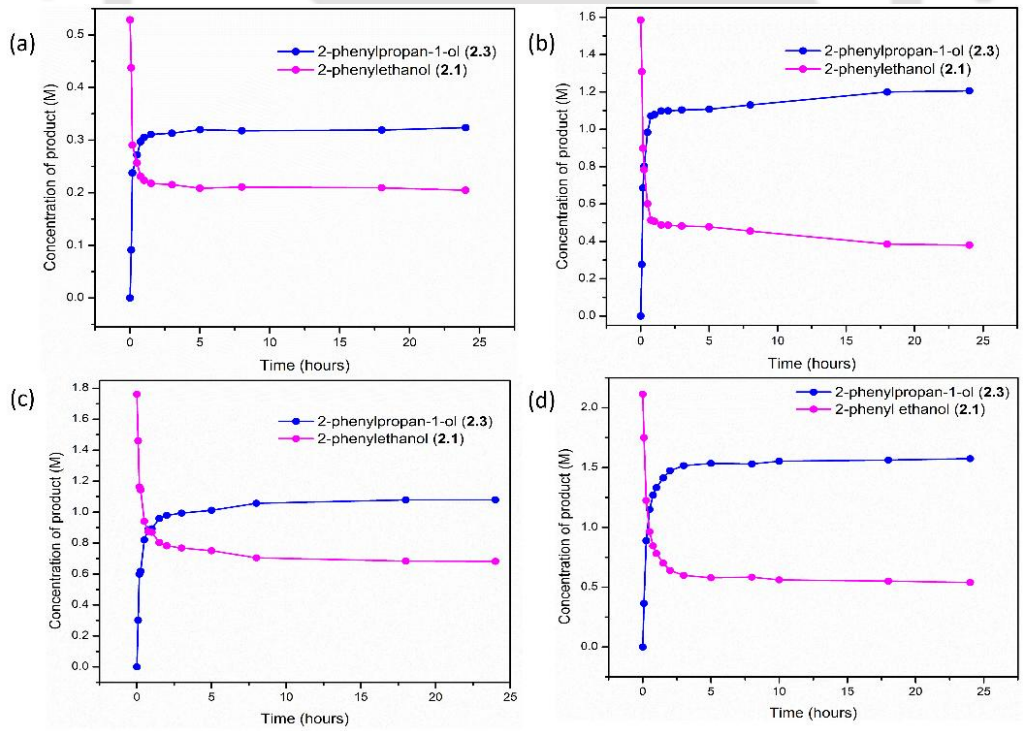

Figure 2.9: Time-profile of the methylation of 2-phenyl ethanol, Reaction condition: 7.5 mmol of CH_3OH, 5 µmol (5.2 mg, 0.5 mol%) **2.10b**, 0.75 mmol KOH at 140 °C and (a) 0.25 mmol of **2.1**, 90 µL 1,4 dioxane was added, (b) 0.75 mmol of **2.1** 30 µL 1,4 dioxane was added, (c) 0.833 mmol of **2.1**, 20 µL 1,4 dioxane was added and (d) 1 mmol of **2.1**.

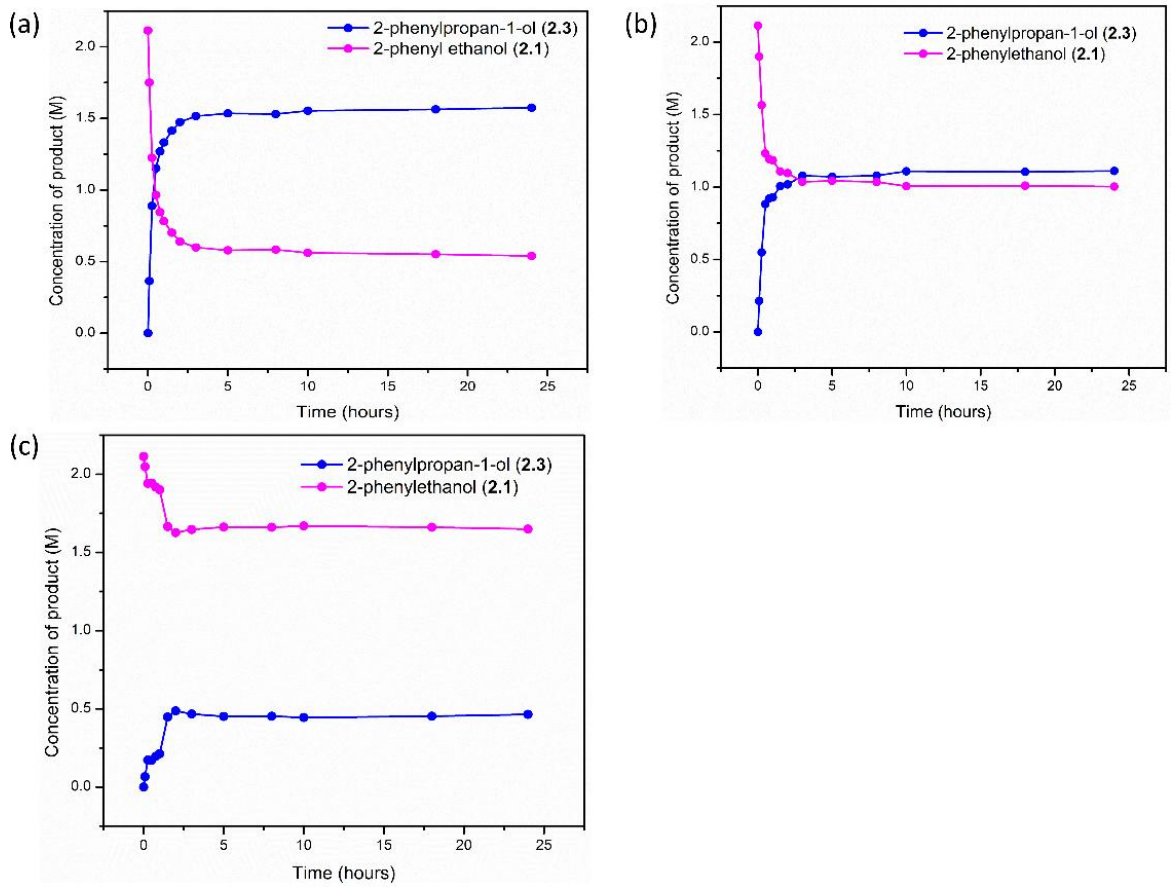

Figure 2.10: Time-profile of the methylation of 2-phenyl ethanol, Reaction condition: 1 mmol of **2.1**, 7.5 mmol of CH_3OH, 0.75 mmol KOH and (a) 5 µmol (5.2 mg, 0.5 mol%) **2.10b**, (b) 3 µmol (3.12 mg, 0.3 mol%) **2.10b** and (c) 1µmol (1.04 mg, 0.1 mol%) **2.10b** at 140 °C.

Valuable information has been obtained from detailed and systematic mechanistic studies. The reactions are catalyzed by well-defined molecular catalysts as inferred from mercury-drop experiments, which are further fortified by kinetic experiments that indicate linear dependenceof the rate of product formation on the concentrations of both the pincer−ruthenium catalyst and 2-phenylethanol. Deuterium labeling studies indicate a secondary KIE of 1.56, which is suggestive of the unlikely participation of C−H activation in the rate-determining step (RDS), though it is involved in the catalytic cycle. Not surprisingly, DFT studies demonstrate that the dehydrogenolysis involving σ-bond metathesis of methanol with the Ru−H species with concomitant evolution of hydrogen is the RDS with a barrier of 24.06 kcal/mol. The evolved hydrogen was detected by GC during the analysis of the contents of the headspace of the reaction vessel. The resting state of the cycle comprises the lowest-energy intermediates, including the Ru−H species and the Ru−OMe species, which were detected by NMR and HRMS analysis.

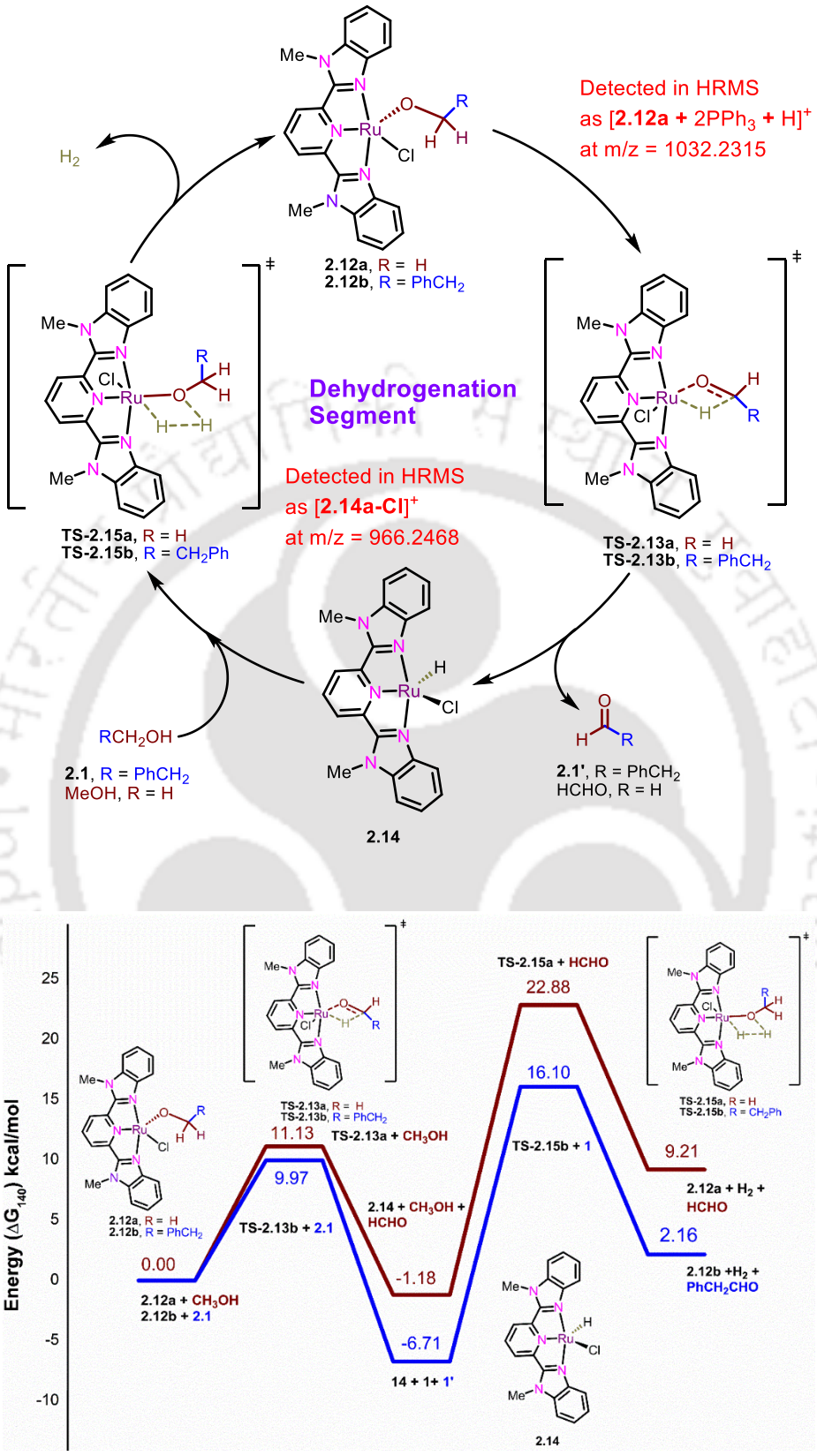

Scheme 2.14. Plausible mechanism involved in the **2.10b**-catalyzed dehydrogenation of **2.1** and methanol and associated energy (ΔG_{140}) profile.

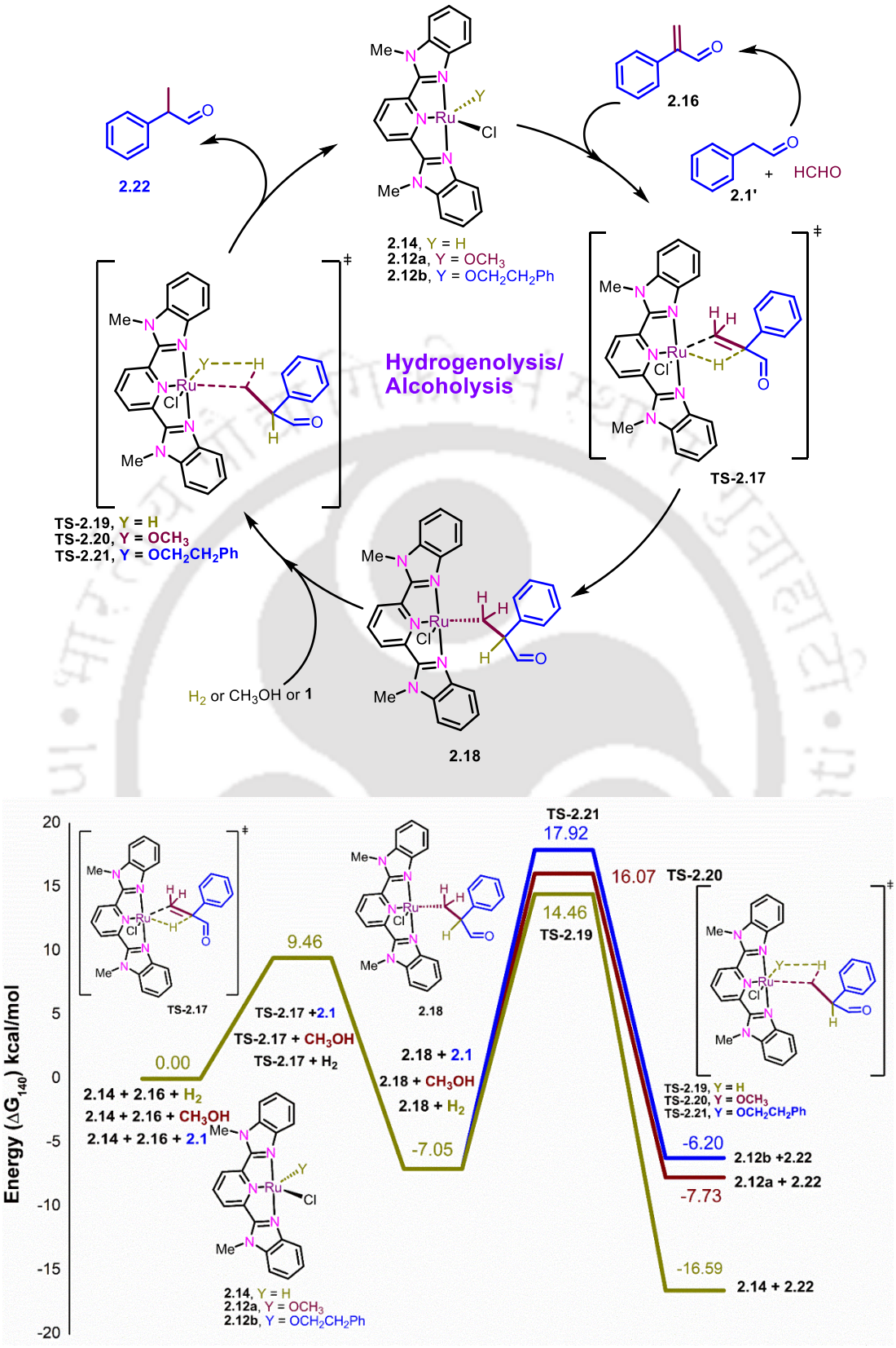

Scheme 2.15. Plausible mechanism involved in the **2.10b**-catalyzed transformation of **2.16** to **2.22** and associated energy (ΔG_{140}) profile.

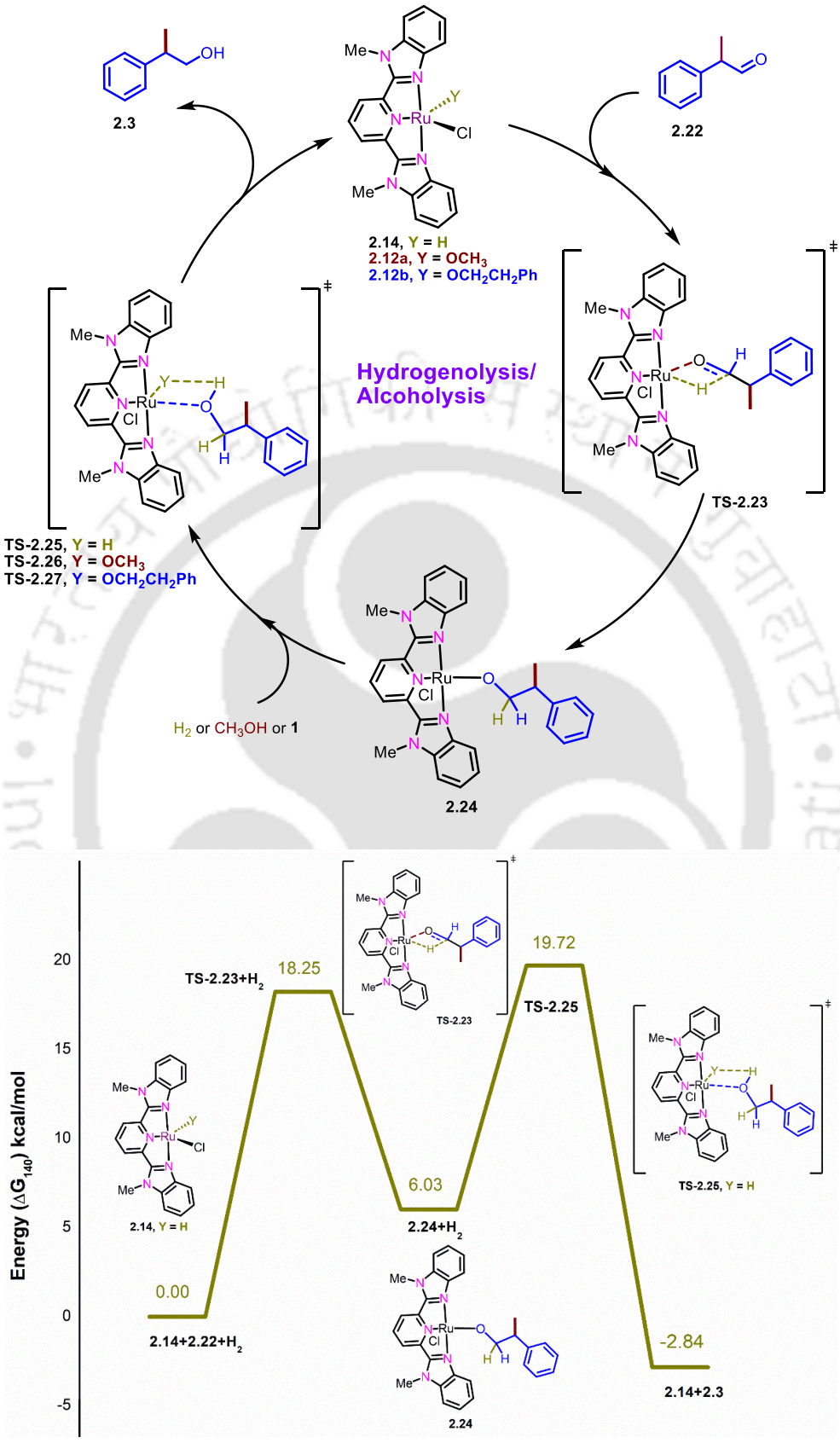

Scheme 2.16. Plausible mechanism involved in the **2.10b**-catalyzed transformation of **2.22** to **2.3** and associated energy (ΔG_{140}) profile.

2.5. Experimental Section

2.5.1. General procedures and materials

All manipulations were carried out under an argon atmosphere. All the chemicals, including NaOH, KOH, NaO^{t}Bu, KO^{t}Bu, Na_2CO_3, K_2CO_3, Na, $CDCl_3$, CD_3OD, 1- and 2-phenylethanol and their derivatives, and the ruthenium precursors $RuCl_3.xH_2O$ and $[RuCl_2(p\text{-cymene})]_2$, were purchased either from Sigma-Aldrich, Merck, or Alfa Aesar and used as such. All catalytic reactions were carried out in argon using ovendried glassware. The 1-phenylethanol derivatives that were not commercially available were prepared according to the literature procedure.[26] Methanol was dried and distilled under argon according to the literature procedure.[27] Solvents such as toluene, tetrahydrofuran, and hexane were dried via double distillation over Na/ benzophenone prior to the experiment.[27] The ruthenium precursor $RuCl_2(PPh_3)_3$ and complexes **2.6a**−**d**, **2.10a**, and **2.10b** were prepared according to the literature protocol.[23f]

2.5.2. Physical measurements

^1H, $^{13}C\{^1H\}$, ^{19}F, and ^{31}P NMR spectra were recorded on a Bruker ASCEND 600 operating at 600 MHz for ^1H, 150 MHz for $^{13}C\{^1H\}$, 564 MHz for ^{19}F, and 243 MHz for ^{31}P; on a Bruker AVANCE 500 operating at 500 MHz for ^1H, 125 MHz for $^{13}C\{H\}$, 470 MHz for 19F, and 203 MHz for ^{31}P; or on a Bruker AVANCE 400 operating at 400 MHz for ^1H, 100 MHz for $^{13}C\{^1H\}$, 377 MHz for ^{19}F, and 162 MHz for ^{31}P. Chemical shifts (δ) are reported here in parts per million, and spin−spin coupling constants (J) are reported in Hertz. The multiplicity data are reported as s−singlet, d−doublet, t−triplet, m−multiplet, q−quartet, and brs−broad singlet. X-ray crystallographic data were acquired on a Bruker D8 Venture single-crystal X-ray diffractometer using graphite-monochromatized Mo Kα radiation. The data refinement and cell reductions were carried out by the Bruker SAINT program.[24] Structures were further solved and refined by the full matrix leastsquares method using SHELXL-14.[25] HRMS measurements were done using an Agilent Accurate-Mass Q-TOF ESI-MS 6520 spectrometer. GC-MS analysis was carried out on an Agilent 5977B GC/MSD instrument. GC analysis was performed on an Agilent 7820 GC instrument fitted with an Agilent Front SS7 inlet N_2 HP-PLOT Q column (30 m × 530 μm × 40 μm) using the following methods: Agilent 7820 GC back detector; detector temperature (TCD), 250 °C; detector temperature (FID), 300 °C; inlet temperature, 40 °C; time at starting temperature, 0 min; ramp, 40 °C/min up to 250 °C; hold time, 5 min; flow rate (carrier), 25 mL/min (N_2); split ratio, 195. The derivatives of 3 and 5 were separated using a Combi*Flash* NextGen 100 system.

2.5.3. General procedure for pincer−ruthenium-catalyzed methylation of 2-phenylethanol (2.1)

A 5 mL Schlenk flask containing **2.10b** (5.2 mg, 5 μmol), KOH (42 mg, 0.75 mmol), 2-phenylethanol (120 μL, 1 mmol), and CH_3OH (0.303 mL, 7.5 mmol) under an argon atmosphere was heated at 140 °C for 24 h. The reaction mixture was then cooled to room temperature, and toluene (50 μL, 4.7 μmol) was added with constant stirring. An aliquot (typically 10 mg) was withdrawn from reaction mixture and added into an NMR tube containing $CDCl_3$ (0.5 mL). The yield of **2.3** was determined by ^{1}H NMR spectroscopy using toluene as a standard.[28] Methanol from the reaction mixture was removed under reduced pressure. The mixture was then diluted with dichloromethane and H_2O followed by separation of the organic layer, which was subsequently dried over anhydrous Na_2SO_4 prior to removal under reduced pressure. The crude mixture was then purified on a flash chromatography system with a column containing 230−400 mesh silica using hexane and ethyl acetate as the eluent.

2.5.4. General procedure for pincer−ruthenium-catalyzed methylation of 1-phenylethanol (2.2)

To a 5 mL Schlenk flask containing 1-phenylethanol (120 μL, 1 mmol), and CH_3OH (1 mL, 24.8 mmol) Na (45.96 mg, 2 mmol) was added under ice-cold condition under an argon atmosphere. (***Caution***: Na reacts with water violently to produce H_2 gas, which is highly flammable. The Na metal should be handled under the surface of paraffin oil under argon and stored in paraffin oil in a tightly sealed container to avoid contact with skin and eyes.) After the exothermic reaction had ceased, the reaction mixture was brought to room temperature then **2.10b** (5.2 mg, 5 μmol) was added and subsequently heated at 140 °C for 24 h. The reaction mixture was then cooled to room temperature, and toluene (50 μL, 0.470 mmol) was added with constant stirring. An aliquot (typically 10 mg) was withdrawn from reaction mixture and added into an NMR tube containing $CDCl_3$ (0.5 mL). The yields of **2.4** and **2.5** were determined by ^{1}H NMR spectroscopy using toluene as a standard.[28] Methanol from the reaction mixture was removed under reduced pressure. The mixture was then diluted with dichloromethane and H_2O followed by separation of the organic layer, which was subsequently dried over anhydrous Na_2SO_4 prior to removal under reduced pressure. The crude mixture was then purified on a flash chromatography system with a column containing 230−400 mesh silica using hexane and ethyl acetate as the eluent.

2.5.5. General procedure for the kinetic study of the 2.10b-catalyzed methylation of alcohols

(a) Variation in the amount of 2.1

To four 5 mL Schlenk flasks containing **2.10b** (5.2 mg, 5 μmol), KOH (42 mg, 0.75 mmol), CH_3OH (0.303 mL, 7.5 mmol), and the standard mesitylene (50 μL, 0.359 mmol) under an argon atmosphere were added various amounts of 2-phenylethanol (30−120 μL, 0.25−1 mmol) using 1,4-dioxane (0.0−90 μL) as a makeup solvent to maintain a total volume of 0.473 mL. The reaction mixture was then heated at 140 °C. At regular intervals (Figures 2.S73−76, Figure 2.9), an aliquot (typically 10 mg) was withdrawn from reaction mixture and added to an NMR tube containing $CDCl_3$ (0.5 mL). The yield of **2.3** was determined by ^{1}H NMR spectroscopy using mesitylene as the standard.[28]

(b) Variation in the catalyst 2.10b loading

To three 5 mL Schlenk flasks containing 2-phenylethanol (120 μL, 1 mmol), KOH (42 mg, 0.75 mmol), CH_3OH (0.303 mL, 7.5 mmol), and the internal standard mesitylene (50 μL, 0.359 mmol) under an argon atmosphere, were added various amounts of catalyst **2.10b (**1.0−5.2 mg, 1−5 μmol). The reaction mixture was then heated at 140 °C. At regular intervals (Figures 2.S76−78, Figure 2.10), an aliquot (typically 10 mg) was withdrawn from reaction mixture and added to an NMR tube containing $CDCl_3$ (0.5 mL). The yield of **2.3** was determined by ^{1}H NMR spectroscopy using mesitylene as the standard.[28]

2.5.6. Synthesis of complex ((p-F-C6H4)2NNN)RuCl2(PPh3) (2.7)

In a 10 mL pear-shaped Schlenk flask, $RuCl_2(PPh_3)_3$ (0.298 g, 0.311 mmol) and ligand **2.7′** (0.100 g, 0.311 mmol) were dissolved in dry, distilled THF (5 mL), and the solution was refluxed for 16 h. The solvent was evaporated under reduced pressure, and the deep-red-colored solid was washed with diethyl ether (5 × 4 mL) followed by hexane (5 × 4 mL). The resulting solid was then dried under vacuum and isolated as a deep-red solid in 88% yield (0.207 g). ^{1}H NMR (400 MHz, $CDCl_3$, 25 °C): δ 7.99 (s, 2H, N=CH), 7.57 (dd, J = 8.3, 4.9 Hz, 4H, Ar), 7.35 (d, J = 7.6 Hz, 2H, Ar), 7.20 (q, J = 6.9 Hz, 1H, Ar), 7.11−7.06 (m, 9H, Ar), 6.98 (t, J = 8.4 Hz, 4H, Ar), 6.85 (t, J = 6.9 Hz, 6H, Ar). ^{13}C{^{1}H} NMR (151 MHz, DMSO-d_6, 25 °C): δ 167.17, 162.43, 160.98, 160.81, 147.03, 132.36 (d, J = 9.6 Hz), 130.49 (d, J = 43.8 Hz), 128.88, 127.23 (d, J = 9.2 Hz), 126.58 (d, J = 8.4 Hz), 126.13, 114.42 (d, J = 22.5 Hz) (Ar). ^{31}P NMR (162 MHz, $CDCl_3$): δ 31.90. ^{19}F NMR (377 MHz, CDCl3): δ −113.19. HRMS (ESI): *m/z*

calculated for [**2.7** − Cl]$^+$ = [$C_{37}H_{28}ClF_2N_3PRu$]$^+$: 720.0721, found 720.0725; *m*/*z* calculated for [(**2.7** − Cl + CH_3CN]$^+$ = [$C_{39}H_{31}ClF_2N_4PRu$]$^+$: 761.0986, found 761.0982.

2.5.7. Synthesis of complex ((p-CF3-C6H4)$_2$NNN)RuCl$_2$(PPh$_3$) (2.8)

In a 10 mL pear-shaped Schlenk flask, $RuCl_2(PPh_3)_3$ (0.205 g, 214 mmol) and ligand **2.8′** (0.090 g, 214 mmol) were dissolved in dry, distilled THF (5 mL), and the solution was refluxed for 16 h. The solvent was evaporated under reduced pressure, and the blackish-colored solid was washed with diethyl ether (5 × 4 mL) followed by hexane (5 × 4 mL). The resulting solid was dried under vacuum and isolated as a blackish solid in 88% yield (0.207 g). ^{1}H NMR (600 MHz, $CDCl_3$, 25 °C): δ 8.08 (s, 2H, N=CH), 7.65 (d, J = 8.0 Hz, 4H, Ar), 7.54 (d, J = 8.1 Hz, 4H, Ar), 7.40 (d, J = 7.8 Hz, 2H, Ar), 7.13 (t, J = 7.8 Hz, 1H, Ar), 7.12−7.01 (m, 9H, Ar), 6.80 (t, J = 7.6 Hz, 6H, Ar). ^{13}C{^{1}H} NMR (151 MHz, $CDCl_3$): δ 165.74, 161.57, 153.28, 132.70 (d, J = 9.6 Hz), 130.45 (d, J = 4.2 Hz), 130.19 (d, J = 8.8 Hz), 129.51, 128.31, 127.79 (d, J = 9.8 Hz), 126.21, 125.74 (q, J = 3.6 Hz), 125.47, 125.04, 123.24 (Ar). ^{31}P NMR (243 MHz, $CDCl_3$, 25 °C): δ 30.74. ^{19}F NMR (565 MHz, $CDCl_3$, 25 °C): δ −62.25. HRMS (ESI): *m*/*z* calculated for [**2.8** − Cl]$^+$ = [$C_{39}H_{28}ClF_6N_3PRu$]$^+$: 820.0657, found 820.0675; *m*/*z* calculated for [(**2.8** − Cl + CH_3CN]$^+$ = [$C_{41}H_{31}F_6N_4PRu$]$^+$: 861.0922, found 861.0939.

2.5.8. Synthesis of complex ((p-OMe-C6H4)$_2$NNN)RuCl$_2$(PPh$_3$) (2.9)

In a 10 mL pear-shaped Schlenk flask, $RuCl_2(PPh_3)_3$ (0.167 g, 0.174 mmol) and ligand **2.9′** (0.060 g, 0.174 mmol) were dissolved in dry, distilled THF (5 mL), and the solution was stirred for 16 h at room temperature. The solvent was evaporated under reduced pressure, and the blackish-colored solid was washed with diethyl ether (5 × 4 mL) followed by hexane (5 × 4 mL). The resulting solid was dried under vacuum and isolated as a blackish solid in 78% yield (0.105 g). NMR analysis showed the presence of two isomers, *cis* (major) and *trans* (minor), in a 2:1 ratio. ^{1}H NMR (400 MHz, $CDCl_3$, 25 °C): δ 8.14 (s, 2H, N=CH), 7.95 (s, 1H, Ar), 7.74 (d, J = 7.9 Hz, 2H, Ar), 7.58 (d, J = 8.9 Hz, 2H, Ar), 7.35−7.27 (m, 8H, Ar), 7.18 (dd, J = 13.6, 8.2 Hz, 7H, Ar), 7.12−7.03 (m, 10H, Ar), 6.83 (t, J = 7.2 Hz, 6H, Ar), 6.37 (d, J = 8.8 Hz, 4H, Ar), 3.88 (s, 3H, OMe), 3.68 (s, 6H, OMe). ^{13}C{^{1}H} NMR (151 MHz, $CDCl_3$, 25 °C): δ 166.44 (d, J = 2.2 Hz), 162.93, 161.77, 160.04, 159.74, 158.73, 148.37, 144.57, 135.45 (d, J = 9.7 Hz), 134.26, 134.02, 132.94 (d, J = 9.3 Hz), 132.77, 132.20 (d, J = 10.0 Hz), 132.05 (d, J = 2.8 Hz), 130.91, 130.61, 129.02, 128.68 (d, J = 7.4 Hz), 128.57, 128.35, 127.54 (d, J = 9.7 Hz), 127.10 (d, J = 8.9 Hz), 126.34, 124.92, 123.70, 123.32, 113.79, 113.63 (Ar), 55.82 (OMe), 55.42. ^{31}P

NMR (243 MHz, $CDCl_3$): δ 33.21, 29.10. HRMS (ESI): *m/z* calculated for [**2.9** − Cl]$^+$ = [$C_{39}H_{34}ClN_3O_2PRu$]$^+$: 744.1121, found 744.1131; *m/z* calculated for [**2.9** − Cl + CH_3CN]$^+$ = [$C_{41}H_{37}ClN_4O_2PRu$]$^+$:785.1386, found 785.1381.

2.5.9. Characterization of the products

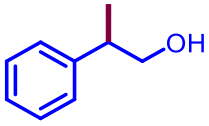

2.3

2-Phenylpropane-1-ol(2.3).[11c] Colorless liquid. ^{1}H NMR (600 MHz, $CDCl_3$): δ 7.27−7.24 (m, 2H, Ar), 7.20−7.14 (m, 3H, Ar), 3.61 (d, *J* = 7.1 Hz, 2H, -CH_2), 2.89−2.84 (m, 1H, -CH), 1.70 (br s, 1H, -OH), 1.21 (d, *J* = 7.1 Hz, 3H,-CH_3). ^{13}C{^{1}H} NMR (151 MHz, $CDCl_3$): δ 143.83, 128.72, 127.59, 126.75 (Ar), 68.76 (-CH_2), 42.52 (-CH), 17.69 (-CH_3).

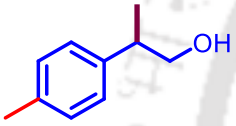

2.3a

2-(p-Tolyl)propan-1-ol (2.3a).[11a] Colorless liquid. ^{1}H NMR (600 MHz, $CDCl_3$): δ 7.18−7.11 (m, 4H), 3.68 (d, *J* = 7.2 Hz, 2H, -CH_2), 2.94− 2.89 (m, 1H, -CH), 2.33 (s, 3H, -CH_3), 1.54 (br s, 1H, -OH), 1.26 (d, *J* = 7.0 Hz, 3H,). ^{13}C{^{1}H} NMR (151 MHz, $CDCl_3$): δ 140.68, 136.38, 129.49, 127.49 (Ar), 77.37, 68.91 (-CH_2), 42.16 (-CH_3), 21.13 (-CH_3 (C_6H_4)), 17.79 (-CH_3).

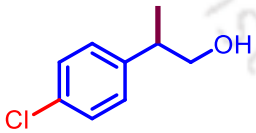

2.3b

2-(4-Chlorophenyl)propan-1-ol (2.3b).[11c] Colorless liquid. ^{1}H NMR (600 MHz, $CDCl_3$): δ 7.32−7.28 (m, 2H), 7.20−7.13 (m, 2H), 3.93−3.47 (m, 2H), 2.96−2.90 (m, 1H), 1.62 (brs, 1H), 1.26 (d, *J* = 7.0 Hz, 3H). ^{13}C {^{1}H} NMR (151 MHz, $CDCl_3$): δ 142.35, 132.47, 128.97, 128.85 (Ar), 68.63 (-CH_2), 41.99 (-CH), 17.67 (-CH_3).

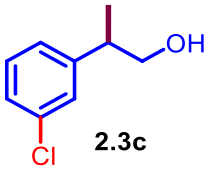

2.3c

2-(3-Chlorophenyl)propan-1-ol (2.3c).[11f] Colorless liquid. ^{1}H NMR (600 MHz, $CDCl_3$): δ 7.30−7.20 (m, 3H, Ar), 7.14 (m, 1H, Ar), 3.70 (d, 2H, -CH_2), 2.97−2.91 (m, 1H, -CH), 1.76 (brs, 1H, -OH), 1.28 (d, J = 7.0 Hz, 3H, -CH_3). ^{13}C{^{1}H} NMR (151 MHz, $CDCl_3$): δ 146.09, 134.50, 129.94, 127.74, 126.91, 125.89 (Ar), 68.46, (-CH_2), 42.32 (-CH), 17.58 (-CH_3).

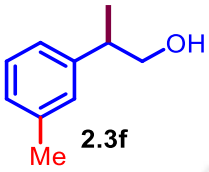

2.3f

2-(m-Tolyl)propan-1-ol (2.3f).[13b] Colorless liquid. ^{1}H NMR (600 MHz, $CDCl_3$): δ 7.31−7.17 (m, 1H, Ar), 7.11−6.98 (m, 3H, Ar), 3.69 (d, J = 6.9 Hz, 2H, -CH_2), 2.94−2.89 (m, 1H, -CH), 2.36 (s, 3H, -CH_3(C_6H_4)), 1.65 (brs, 1H, -OH), 1.27 (d, J = 7.0 Hz, 3H, -CH_3). ^{13}C{^{1}H} NMR (151 MHz, $CDCl_3$): δ 143.74, 138.30, 128.63, 128.39, 127.53, 124.55 (Ar), 68.75 (-CH_2), 42.47 (CH), 21.57 (-CH_3(C_6H_4)), 17.73 (-CH_3).

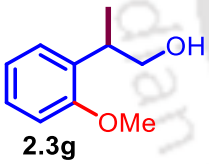

2.3g

2-(2-Methoxyphenyl)propan-1-ol (2.3g). Colorless liquid. ^{1}H NMR (600 MHz, $CDCl_3$): δ 7.23−7.20 (m, 2H, Ar), 6.96 (td, J = 7.5, 1.1 Hz, 1H, Ar), 6.88 (d, J = 8.0 Hz, 1H, Ar), 3.83 (s, 3H, -OMe), 3.77−3.66 (m, 2H, -CH_2), 3.47−3.41 (m, 1H, -CH), 1.69 (brs, 1H, -OH), 1.26 (d, J = 7.1 Hz, 3H, -CH_3). ^{13}C{^{1}H} NMR (151 MHz, $CDCl_3$): δ 157.46, 131.89, 127.57, 127.46, 120.95, 110.73 (Ar), 68.00 (-OMe), 55.53 (-CH_2), 35.32 (-CH), 16.68, -CH_3).

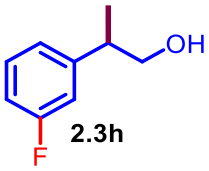

2.3h

2-(3-Fluorophenyl)propan-1-ol (2.3h).[32] Colorless liquid. ^{1}H NMR (600 MHz, $CDCl_3$): δ 7.30−7.27 (m, 1H, Ar), 7.02 (d, J = 7.7 Hz, 1H, Ar), 6.98−6.89 (m, 2H, Ar), 3.79−3.56 (m, 2H,

-CH_2), 2.99−2.93 (m, 1H, -CH), 1.62 (brs, 1H, -OH), 1.27 (d, *J* = 7.0 Hz, 3H, -CH_3). $^{13}C\{^1H\}$ NMR (151 MHz, $CDCl_3$): *δ* 164.02, 162.40, 146.64, 130.19, 130.13, 123.35, 123.33, 114.48, 114.34, 113.73, 113.59 (Ar), 68.58 (-CH_2), 42.38 (-CH), 17.60 (-CH_3). ^{19}F NMR (565 MHz, $CDCl_3$): *δ* −113.11.

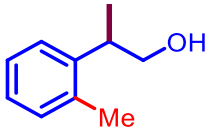

2.3i

2-(o-Tolyl)propan-1-ol (2.3i).[11c] Colorless liquid. ^1H NMR (600 MHz, $CDCl_3$): *δ* 7.24−7.09 (m, 4H, Ar), 3.95−3.50 (m, 2H, -CH_2), 3.29−3.23 (m, 1H, -CH), 2.37 (s, 3H, -$CH_3(C_6H_4)$), 1.50 (brs, 1H, -OH), 1.25 (d, *J* = 6.9 Hz, 3H, -CH_3). $^{13}C\{^1H\}$ NMR (151 MHz, $CDCl_3$): *δ* 141.86, 136.57, 130.71, 126.52, 126.42, 125.56 (Ar), 68.16 (-CH_2), 37.34 (-CH), 19.76 (-$CH_3(C_6H_4)$), 17.67 (-CH_3).

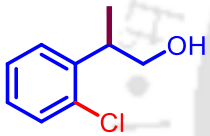

2.3j

2-(2-Chlorophenyl)propan-1-ol (2.3j). Colorless liquid. ^1H NMR (600 MHz, $CDCl_3$): *δ* 7.37 (dd, *J* = 8.0, 1.3 Hz, 1H, Ar), 7.30−7.23 (m, 2H, Ar), 7.18−7.15 (m, 1H, Ar), 3.80 (dd, *J* = 10.8, 6.5 Hz, 1H, -CH_2), 3.71 (dd, *J* = 10.8, 6.3 Hz, 1H, -CH_2), 3.57−3.51 (m, 1H, -CH), 1.69 (brs, 1H, -OH), 1.29 (d, *J* = 7.0 Hz, 3H, -CH_3). $^{13}C\{^1H\}$ NMR (151 MHz, $CDCl_3$): *δ* 141.02, 134.42, 129.88, 127.74, 127.71, 127.18 (Ar), 67.33 (-CH_2), 38.20 (-CH). 17.61 (-CH_3).

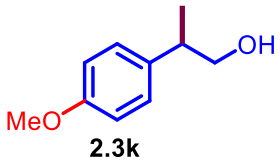

2.3k

2-(4-Methoxyphenyl)propan-1-ol (2.3k).[11c] Colorless liquid. ^1H NMR (600 MHz, $CDCl_3$): *δ* 7.20−7.05 (m, 2H, Ar), 6.97−6.59 (m, 2H, Ar), 3.79 (s, 3H, -OMe), 3.77−3.45 (m, 2H, -CH_2), 3.16−2.69 (m, 1H, -CH), 1.63 (brs, 1H, -OH), 1.25 (d, *J* = 7.0 Hz, 3H, -CH_3). $^{13}C\{^1H\}$ NMR (151 MHz, $CDCl_3$): *δ* 158.45, 135.73, 128.51, 114.16 (Ar), 68.91 (-OMe), 55.39 (-CH_2), 41.68 (-CH), 17.85 (-CH_3).

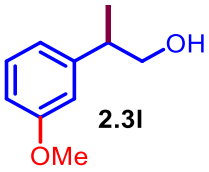

2.3l

2-(3-Methoxyphenyl)propan-1-ol (23l).[11a] Colorless liquid. ^{1}H NMR (600 MHz, $CDCl_3$): δ 7.26 (t, J = 7.6 Hz, 1H, Ar), 6.87−6.75 (m, 3H, Ar), 3.82 (s, 3H, -OMe), 3.69 (d, 2H, $-CH_2$), 2.95−2.90 (m, 1H, -CH), 1.87 (brs, 1H, -OH), 1.27 (d, J = 7.1 Hz, 3H, $-CH_3$). ^{13}C{^{1}H} NMR (151 MHz, $CDCl_3$): δ 159.87, 145.55, 129.68, 119.89, 113.56, 111.77 (Ar), 68.65 (-OMe), 55.24 ($-CH_2$), 42.57 (-CH), 17.66 ($-CH_3$)

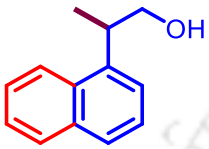

2.3o

2-(Naphthalen-1-yl)propan-1-ol (2.3o).[11c] Off-white solid. ^{1}H NMR (600 MHz, $CDCl_3$): δ 8.16 (d, J = 8.6 Hz, 1H, Ar), 7.89 (d, J = 8.1 Hz, 1H, Ar), 7.76 (d, J = 8.1 Hz, 1H, Ar), 7.56−7.46 (m, 3H, Ar), 7.42 (d, J = 7.3 Hz, 1H, Ar), 3.97−3.80 (m, 3H, $-CH_2$, -CH), 1.77 (brs, 1H, -OH), 1.55−1.33 (m, 3H). ^{13}C{^{1}H} NMR (151 MHz, $CDCl_3$): δ 139.67, 134.10, 132.05, 129.09, 127.15, 126.13, 125.64, 123.16, 123.13 (Ar), 68.17 ($-CH_2$), 36.45 (-CH), 17.94 ($-CH_3$).

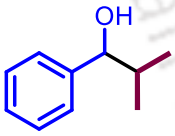

2.5

2-Methyl-1-phenylpropan-1-ol (2.5).[11a,13b] Colorless liquid. ^{1}H NMR (600 MHz, $CDCl_3$): δ 7.36−7.25 (m, 5H, Ar), 4.36 (d, J = 6.9 Hz, 1H, -CHOH), 2.00−1.92 (m, 1H, -CH), 1.88 (brs, 1H, -OH), 1.01 (d, J = 6.7 Hz, 3H, $-CH_3$), 0.80 (d, J = 6.8 Hz, 3H, $-CH_3$). ^{13}C{^{1}H} NMR (151 MHz, $CDCl_3$): δ 143.77, 128. 30, 127.53, 126.69 (Ar), 80.17 (-CHOH) 35.38 (-CH), 19.12 ($-CH_3$), 18.36 ($-CH_3$).

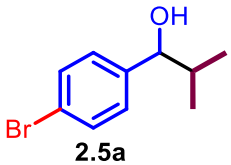

2.5a

1-(4-Bromophenyl)-2-methylpropan-1-ol (55a).[17] Colorless liquid. ^{1}H NMR (600 MHz, $CDCl_3$): δ 7.36−7.25 (m, 4H, Ar), 4.36 (d, J = 6.9 Hz, 1H, -CHOH), 1.99−1.92 (m, 1H, -CH), 1.75 (brs, 1H, -OH), 1.00 (d, J = 6.7 Hz, 3H, $-CH_3$), 0.80 (d, J = 6.8 Hz, 3H, $-CH_3$). ^{13}C{^{1}H} NMR (151 MHz, $CDCl_3$): δ 143.78, 128.31, 127.53, 126.70 (Ar), 80.17 (-CHOH), 35.38 (-CH), 19.12 ($-CH_3$), 18.36 ($-CH_3$).

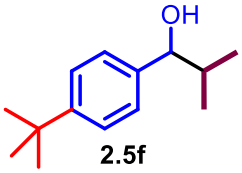

2.5f

1-(4-(tert-Butyl)phenyl)-2-methylpropan-1-ol (5.5f). Colorless liquid. ^{1}H NMR (600 MHz, $CDCl_3$): δ 7.36−7.35 (m, 2H, Ar), 7.26− 7.23 (m, 2H, Ar), 4.32 (d, J = 7.1 Hz, 1H, -CHOH), 1.99−1.91 (m, 1H, -CH), 1.79 (brs, 1H, -OH), 1.324 (s, 9H, $-C(CH_3)_3$) 1.02 (d, J = 6.6 Hz, 3H, $-CH_3$), 0.80 (d, J = 6.8 Hz, 3H, $-CH_3$). ^{13}C{^{1}H} NMR (151 MHz, $CDCl_3$): δ 150.45, 140.81, 126.42, 126.40, 125.22 (Ar), 80.06 (-CHOH), 35.30 (-CH), 34.63 ($-C(CH_3)_3$), 31.51 ($-C(CH_3)_3$), 19.24 ($-CH_3$), 18.52 ($-CH_3$).

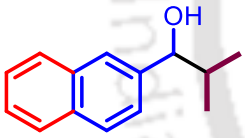

2.5i

2-Methyl-1-(naphthalen-2-yl)propan-1-ol (5.5i).[13b] Off-white solid. ^{1}H NMR (400 MHz, $CDCl_3$): δ 7.87−7.80 (m, 3H, Ar), 7.76 (d, J = 1.7 Hz, 1H, Ar), 7.51−7.44 (m, 3H, Ar), 4.54 (d, J = 6.9 Hz, 1H, -CHOH), 2.12−2.03 (m, 1H, -CH), 1.80 (brs, 1H, -OH), 1.05 (d, J = 6.7 Hz, 3H, $-CH_3$), 0.85 (d, J = 6.9 Hz, 3H, $-CH_3$). ^{13}C{^{1}H} NMR (151 MHz, $CDCl_3$): δ 141.25, 133.31, 133.10, 128.09, 128.06, 127.79, 126.19, 125.86, 125.54, 124.77 (Ar), 80.29 (-CHOH), 35.33 (-CH), 19.27 (-OH), 18.36 ($-CH_3$).

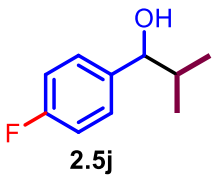

2.5j

1-(4-Fluorophenyl)-2-methylpropan-1-ol (5.5j).[17] Colorless liquid. ^{1}H NMR (600 MHz, $CDCl_3$): δ 7.36−7.30 (m, 3H, Ar), 7.29−7.25 (m, 1H, Ar), 4.37 (d, J = 6.9 Hz, 1H, -CHOH),

2.0−1.92 (m, 1H, -CH), 1.61 (brs, 1H, -OH), 1.00 (d, J = 6.7 Hz, 3H, -CH_3), 0.80 (d, J = 6.8 Hz, 3H, -CH_3). $^{13}C\{^1H\}$ NMR (151 MHz, $CDCl_3$): δ 143.77, 128.34, 127.57, 126.70 (Ar), 80.21 (-CHOH), 35.41 (-CH), 19.15 (-CH_3), 18.38 (-CH_3). ^{19}F NMR (565 MHz, $CDCl_3$): δ −121.88.

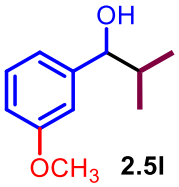

2.5l

1-(3-Methoxyphenyl)-2-methylpropan-1-ol (5.5l).[4] Colorless liquid. ^1H NMR (600 MHz, $CDCl_3$): δ 7.28−7.24 (m, 1H, Ar), 6.90−6.83 (m, 2H, Ar), 6.85−6.81 (m, 1H, Ar), 4.34 (d, J = 6.9 Hz, 1H, -CHOH), 1.99−1.91 (m, 1H, -CH), 1.88 (brs, 1H, -CHOH), 1.01 (d, J = 6.7 Hz, 3H, -CH_3), 0.82 (d, J = 6.8 Hz, 3H, -CH^3). $^{13}C\{^1H\}$ NMR (151 MHz, $CDCl_3$): δ 159.69, 145.56, 129.28, 119.11, 112.93, 112.21 (Ar), 55.33 (-CHOH), 35.34 (-CH), 19.20 (-CH_3), 18.33 (CH_3).

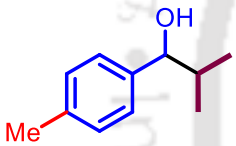

2.5o

2-Methyl-1-(p-tolyl)propan-1-ol (5.5o).[11a,17] Colorless liquid. ^1H NMR (600 MHz, $CDCl_3$): δ 7.21−7.13 (m, 4H, Ar), 4.31 (d, J = 7.0 Hz, 1H, -CHOH), 2.35 (s, 3H, -$CH_3(C_6H_4)$), 1.98−1.90 (m, 1H, -CH), 1.86 (brs, 1H, -OH), 1.01 (d, J = 6.7 Hz, 3H, -CH_3), 0.79 (d, J = 6.8 Hz, 3H, -CH_3). $^{13}C\{^1H\}$ NMR (151 MHz, $CDCl_3$): δ 140.82, 137.13, 128.99, 126.63 (Ar), 80.07 (-CHOH), 35.32 (-CH), 21.22 (-$CH_3(C_6H_4)$), 19.12 (-CH_3), 18.48 (-CH_3).

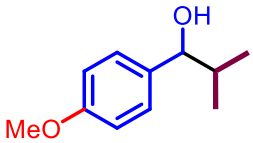

2.5q

1-(4-Methoxyphenyl)-2-methylpropan-1-ol (5.5q).[17] Colorless liquid. ^1H NMR (600 MHz, $CDCl_3$): δ 7.24−7.20 (m, 2H, Ar), 6.89− 6.85 (m, 2H, Ar), 4.28 (d, J = 7.2 Hz, 1H, -CHOH), 3.80 (s, 3H, -OCH_3), 1.98−1.88 (m, J = 6.7 Hz, 1H, -CH), 1.75 (brs, 1H, -OH), 1.00 (d, J = 6.7 Hz, 3H, -CH3), 0.76 (d, J = 6.8 Hz, 3H, -CH_3). $^{13}C\{^1H\}$ NMR (151 MHz, $CDCl_3$): δ 159.05,

135.98, 127.83, 113.69 (Ar), 79.87 (-OMe), 55.37 (-CHOH), 35.39 (-CH), 19.07 (-CH_3), 18.63 (-CH_3).

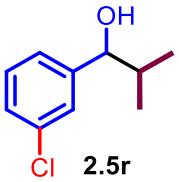

2.5r

1-(3-Chlorophenyl)-2-methylpropan-1-ol (5.5r).[4] Colorless liquid. ^{1}H NMR (600 MHz, $CDCl_3$): δ 7.22−7.17 (m, 3H, Ar), 7.13−7.11 (m, 1 Hz, 1H, Ar), 4.31 (d, J = 6.6 Hz, 1H, -CHOH), 1.93−1.83 (m, 1H, -CH), 1.63 (brs, 1H, -OH), 0.91 (d, J = 6.7 Hz, 3H, -CH_3), 0.76 (d, J = 6.8 Hz, 3H, -CH_3). ^{13}C{^{1}H} NMR (151 MHz, $CDCl_3$): δ 145.85, 134.28, 129.58, 127.65, 126.83, 124.86 (Ar), 79.41 (-CHOH), 35.40 (-CH), 19.09 (-CH_3), 18.02 (-CH_3).

2.5.10. Computational details

The geometries of all the considered complexes were fully optimized using the DFT (PBE)[29] method with the Gaussian-09 package.[30] The LANL2DZ[31] and 6-311G(d,p) basis sets with a polarization function were used for the metal (Ru) and nonmetal atoms, respectively. The method and basis set were selected according to previous reports on pincer-ruthenium complexes.[18,20,22] The transition states were located using the synchronous transit-guided quasi-Neon (QST2) Genecp (gen keyword with the effective core potential) to define the basis set. The empirical dispersion-GD3 was used in all molecular geometry optimization and energy computations. Frequency calculations were used to characterize the obtained stationary points as minimum-energy structures or transition states based on the number of imaginary frequencies. Single-point calculations were performed to calculate the relative free energy values at 140 °C (ΔG_{140}).

Supporting information (containing NMR spectra and of pure compound and metal-complexes, HRMS data, GC plot) for chapter II is available as appendix I and can be found at https://drive.google.com/file/d/1nRhwGf9bdDny5-1W_ZrfScmF2e7tI0ZP/view?usp=sharing

2.6. References

(1)(a) Akhtar, W. M.; Armstrong, R. J.; Frost, J. R.; Stevenson, N. G.; Donohoe, T. J., Stereoselective Synthesis of Cyclohexanes via an Iridium Catalyzed (5 + 1) Annulation Strategy. *J. Am. Chem. Soc.* **2018**, *140*, 11916-11920. (b) Kumar, A.; Bhatti, T. M.; Goldman, A. S., Dehydrogenation of Alkanes and Aliphatic Groups by Pincer-Ligated Metal Complexes. *Chem. Rev.* **2017,** *117*, 12357-12384.
(2)(a) Nandi, P. G.; Kumar, P.; Kumar, A., Ligand-free Guerbet-type reactions in air catalyzed by in situ formed complexes of base metal salt cobaltous chloride. *Catal. Sci. Technol.* **2022**, *12*, 1100-1108. (b) Das, K.; Kumar, A., Chapter One - Alkane dehydrogenation reactions catalyzed by pincer-metal complexes. In *Advances in Organometallic Chemistry*, Pérez, P. J., Ed. Academic Press: 2019; Vol. 72, pp 1-57. (c) Kumar, A.; Goldman, A. S., Recent Advances in Alkane Dehydrogenation Catalyzed by Pincer Complexes. In *The Privileged Pincer-Metal Platform: Coordination Chemistry & Applications*, van Koten, G.; Gossage, R. A., Eds. Springer International Publishing: Cham, 2016; pp 307-334. (d) Kumar, A.; Bhatti, T. M.; Goldman, A. S., Dehydrogenation of Alkanes and Aliphatic Groups by Pincer-Ligated Metal Complexes. *Chem. Rev.* **2017**, *117* , 12357-12384. (e) Nandi, P. G.; Thombare, P.; Prathapa, S. J.; Kumar, A., Pincer-Cobalt-Catalyzed Guerbet-Type β-Alkylation of Alcohols in Air under Microwave Conditions. *Organometallics* **2022**, *41*, 3387-3398.
(3) Yi, H.; Zhang, G.; Wang, H.; Huang, Z.; Wang, J.; Singh, A. K.; Lei, A., Recent Advances in Radical C–H Activation/Radical Cross-Coupling. *Chem. Rev.* **2017,** *117*, 9016-9085.
(4) Schlagbauer, M.; Kallmeier, F.; Irrgang, T.; Kempe, R., Manganese-Catalyzed β-Methylation of Alcohols by Methanol. *Angew. Chem., Int. Ed.* **2020**, *59* , 1485-1490.
(5) Watson, A. J.; Williams, J. M., The give and take of alcohol activation. *Science* **2010**, *329*, 635-636.
(6) Barreiro, E. J.; Kümmerle, A. E.; Fraga, C. A. M., The Methylation Effect in Medicinal Chemistry. *Chem. Rev.* **2011**, *111*, 5215-5246.
(7) Schönherr, H.; Cernak, T., Profound Methyl Effects in Drug Discovery and a Call for New C-H Methylation Reactions. *Angew. Chem., Int. Ed.* **2013**, *52*, 12256-12267.
(8) Ray, S.; Rao, P. V.; Choudary, N. V., Poly-α-olefin-based synthetic lubricants: a short review on various synthetic routes. *Lubr. Sci.* **2012**, *24*, 23-44.
(9) (a) Qian, M.; Liauw, M.; Emig, G., Formaldehyde synthesis from methanol over silver catalysts. *App. Catal. A: Gen.* **2003**, *238*, 211-222. (b) Polidano, K.; Allen, B. D.; Williams, J. M.; Morrill., Iron-catalyzed methylation using the borrowing hydrogen approach. *ACS Catal.* **2018**, *8* , 6440-6445. (c) Wingad, R. L.; Bergström, E. J.; Everett, M.; Pellow, K. J.; Wass, D. F., Catalytic conversion of methanol/ethanol to isobutanol–a highly selective route to an advanced biofuel. *Chem. Commun.* **2016**, *52* , 5202-5204.
(10) (a) Cheung, H. W.; Lee, T. Y.; Lui, H. Y.; Yeung, C. H.; Lau, C. P., Ruthenium-Catalyzed β-Alkylation of Secondary Alcohols with Primary Alcohols. *Adv. Synth. Catal.* **2008**, *350*, 2975-2983. (b) Bower, J. F.; Kim, I. S.; Patman, R. L.; Krische, M. J., Catalytic Carbonyl Addition through Transfer Hydrogenation: A Departure from Preformed Organometallic Reagents. *Angew. Chem., Int. Ed.* **2009**, *48*, 34-46. (c) Zweifel, T.; Naubron, J.-V.; Grützmacher, H., Catalyzed Dehydrogenative Coupling of Primary Alcohols with Water, Methanol, or Amines. *Angew. Chem., Int. Ed.* **2009**, *48* , 559-563. (d) Suzuki, T., Organic Synthesis Involving Iridium-Catalyzed Oxidation. *Chem. Rev.* **2011,** *111*, 1825-1845. (e) Cano, R.; Yus, M.; Ramón, D. J., First practical cross-alkylation of primary alcohols with a new and recyclable impregnated iridium on magnetite catalyst. *Chem. Commun.* **2012**, *48*, 7628-7630. (f) Balaraman, E.; Khaskin, E.; Leitus, G.; Milstein, D., Catalytic transformation of alcohols to carboxylic acid salts and H2 using water as the oxygen atom source. *Nat. Chem.* **2013**, *5* , 122-125. (g) Nielsen, M.; Alberico, E.; Baumann, W.; Drexler, H.-J.; Junge, H.; Gladiali, S.; Beller, M., Low-temperature aqueous-phase methanol dehydrogenation to hydrogen and carbon dioxide. *Nature* **2013**, *495* , 85-89. (h) Wang, Q.; Wu, K.; Yu, Z., Ruthenium(III)-Catalyzed β-Alkylation of Secondary Alcohols with Primary Alcohols. *Organometallics* **2016**, *35*, 1251-1256. (i) Akhtar, W. M.; Cheong, C. B.; Frost, J. R.; Christensen, K. E.; Stevenson, N. G.; Donohoe, T. J., Hydrogen Borrowing Catalysis with Secondary Alcohols: A New Route for the Generation of β-Branched Carbonyl Compounds. *J. Am. Chem. Soc.* **2017**, *139* , 2577-2580. (j) Sarbajna, A.; Dutta, I.; Daw, P.; Dinda, S.; Rahaman, S. M. W.; Sarkar, A.; Bera, J. K., Catalytic Conversion of Alcohols to Carboxylic Acid

Salts and Hydrogen with Alkaline Water. *ACS Catal.* **2017**, *7*, 2786-2790. (k) Thiyagarajan, S.; Gunanathan, C., Facile Ruthenium(II)-Catalyzed α-Alkylation of Arylmethyl Nitriles Using Alcohols Enabled by Metal–Ligand Cooperation. *ACS Catal.* **2017**, *7* , 5483-5490.
(11) (a) Kaithal, A.; Schmitz, M.; Hölscher, M.; Leitner, W., Ruthenium (II)-Catalyzed β-Methylation of Alcohols using Methanol as C1 Source. *ChemCatChem* **2019**, *11*, 5287-5291. (b) Chan, L. K. M.; Poole, D. L.; Shen, D.; Healy, M. P.; Donohoe, T. J., Rhodium-Catalyzed Ketone Methylation Using Methanol Under Mild Conditions: Formation of α-Branched Products. *Angew. Chem., Int. Ed.* **2014**, *53*, 761-765. (c) Li, Y.; Li, H.; Junge, H.; Beller, M., Selective ruthenium-catalyzed methylation of 2-arylethanols using methanol as C1 feedstock. *Chem. Commun.* **2014**, *50*, 14991-14994. (d) Natte, K.; Neumann, H.; Beller, M.; Jagadeesh, R. V., Transition-Metal-Catalyzed Utilization of Methanol as a C1 Source in Organic Synthesis. *Angew. Chem., Int. Ed.* **2017**, *56*, 6384-6394. (e) Ogawa, S.; Obora, Y., Iridium-catalyzed selective α-methylation of ketones with methanol. *Chem. Commun.* **2014**, *50*, 2491-2493. (f) Oikawa, K.; Itoh, S.; Yano, H.; Kawasaki, H.; Obora, Y., Preparation and use of DMF-stabilized iridium nanoclusters as methylation catalysts using methanol as the C1 source *Chem. Commun.* **2017**, *53*, 1080-1083. (g) Shen, D.; Poole, D. L.; Shotton, C. C.; Kornahrens, A. F.; Healy, M. P.; Donohoe, T. J., Hydrogen-Borrowing and Interrupted-Hydrogen-Borrowing Reactions of Ketones and Methanol Catalyzed by Iridium. *Angew. Chem., Int. Ed.* **2015**, *54*, 1642-1645. (h) Beydoun, K.; Ghattas, G.; Thenert, K.; Klankermayer, J.; Leitner, W., Ruthenium-Catalyzed Reductive Methylation of Imines Using Carbon Dioxide and Molecular Hydrogen. *Angew. Chem., Int. Ed.* **2014**, *53*, 11010-11014.
(12) Lu, Z.; Zheng, Q.; Zeng, G.; Kuang, Y.; Clark, J. H.; Tu, T., Highly efficient NHC-iridium-catalyzed β-methylation of alcohols with methanol at low catalyst loadings. *Sci. China Chem.* **2021**, *64*, 1361-1366.
(13) (a) Kaithal, A.; van Bonn, P.; Hölscher, M.; Leitner, W., Manganese (I)-Catalyzed β-Methylation of Alcohols Using Methanol as C1 Source. *Angew. Chem., Int. Ed.* **2020**, *59*, 215-220. (b) Polidano, K.; Williams, J. M.; Morrill, L. C., Iron-catalyzed borrowing hydrogen β-C (sp3)-methylation of alcohols. *ACS Catal.* **2019,** *9*, 8575-8580. (c) Bettoni, L.; Gaillard, S.; Renaud, J.-L. J., Iron-Catalyzed β-Alkylation of Alcohols. *Org. Lett.* **2019**, *21*, 8404-8408.
(14) Kaithal, A.; Schmitz, M.; Hölscher, M.; Leitner, W., On the Mechanism of the Ruthenium-catalyzed β-methylation of Alcohols with Methanol. *ChemCatChem* **2020,** *12*, 781-787.
(15) Wingad, R. L.; Bergström, E. J. E.; Everett, M.; Pellow, K. J.; Wass, D. F., Catalytic conversion of methanol/ethanol to isobutanol – a highly selective route to an advanced biofuel. *Chem. Commun.* **2016**, *52*, 5202-5204.
(16) Biswas, N.; Srimani, D., Ru-Catalyzed Selective Catalytic Methylation and Methylenation Reaction Employing Methanol as the C1 Source. *J. Org. Chem.* **2021**, *86*, 10544-10554.
(17) Ganguli, K.; Belkova, N. V.; Kundu, S., Cyclometalated (NNC)Ru(ii) complex catalyzed β-methylation of alcohols using methanol. *Dalton Trans.* **2022,** *51*, 4354-4365.
(18) Das, K.; Nandi, P. G.; Islam, K.; Srivastava, H. K.; Kumar, A., N–Alkylation of Amines Catalyzed by a Ruthenium–Pincer Complex in the Presence of in situ Generated Sodium Alkoxide. *Eur. J. Org. Chem.* **2019**, *2019*, 6855-6866.
(19) Dutta, M.; Das, K.; Prathapa, S. J.; Srivastava, H. K.; Kumar, A., Selective and high yield transformation of glycerol to lactic acid using NNN pincer ruthenium catalysts. *Chem. Commun.* **2020**, *56*, 9886-9889.
(20) Das, K.; Yasmin, E.; Das, B.; Srivastava, H. K.; Kumar, A., Phosphine-free pincer-ruthenium catalyzed biofuel production: high rates, yields and turnovers of solventless alcohol alkylation. *Catal. Sci. Technol.* **2020**, *10*, 8347-8358.
(21) (a)Arora, V.; Yasmin, E.; Tanwar, N.; Hathwar, V. R.; Wagh, T.; Dhole, S.; Kumar, A., Pincer–Ruthenium-Catalyzed Reforming of Methanol─Selective High-Yield Production of Formic Acid and Hydrogen. *ACS Catal.* **2023**, *13*, 3605-3617. (b) Arora, V.; Dhole, S.; Kumar, A., Reforming of ethanol to hydrogen and acetic acid catalyzed by pincer-ruthenium complexes. *Catal. Sci. Technol* **2023,** *13*, 6699-6711.

(22) Das, K.; Kathuria, L.; Jasra, R. V.; Dhole, S.; Kumar, A., Microwave-assisted pincer-ruthenium catalyzed Guerbet reaction for the upgradation of bio-ethanol to bio-butanol. *Catal. Sci. Technol.* **2023**, *13*, 1763-1776.
(23) (a) Narjinari, H.; Tanwar, N.; Kathuria, L.; Jasra, R. V.; Kumar, A. Guerbet-type β-alkylation of secondary alcohols catalyzed by chromium chloride and its corresponding NNN pincer complex. *Catal. Sci. Technol.* **2022**, *12*, 4753-4762. (b) Das, K.; Yasmin, E.; Kumar, A., Pincer-Ruthenium Catalyzed Oxygen Mediated Dehydrative Etherification of Alcohols and Ortho-Alkylation of Phenols. *Adv. Synth. Catal.* **2022**, *364*, 3895-3909. (c) Nandi, P. G.; Jadi, P. K.; Das, K.; Prathapa, S. J.; Mandal, B. B.; Kumar, A., Synthesis of NNN Chiral Ruthenium Complexes and Their Cytotoxicity Studies. *Inorg. Chem.* **2021**, *60*, 7422-7432. (d) Arora, V.; Narjinari, H.; Kumar, A., Pincer-Nickel Catalyzed Selective Guerbet-Type Reactions. *Organometallics* **2021**, *40*, 2870-2880. E Arora, V.; Dutta, M.; Das, K.; Das, B.; Srivastava, H. K.; Kumar, A., Solvent-Free N-Alkylation and Dehydrogenative Coupling Catalyzed by a Highly Active Pincer-Nickel Complex. *Organometallics* **2020**, *39*, 2162-2176. (f) Das, K.; Dutta, M.; Das, B.; Srivastava, H. K.; Kumar, A., Efficient Pincer-Ruthenium Catalysts for Kharasch Addition of Carbon Tetrachloride to Styrene. *Adv. Synth. Catal.* **2019**, *361*, 2965-2980.

Chapter- III

Pincer-Ruthenium Catalyzed Direct Formation of Fuel-Grade Alkanes via Decarboxylative Coupling of Alcohols

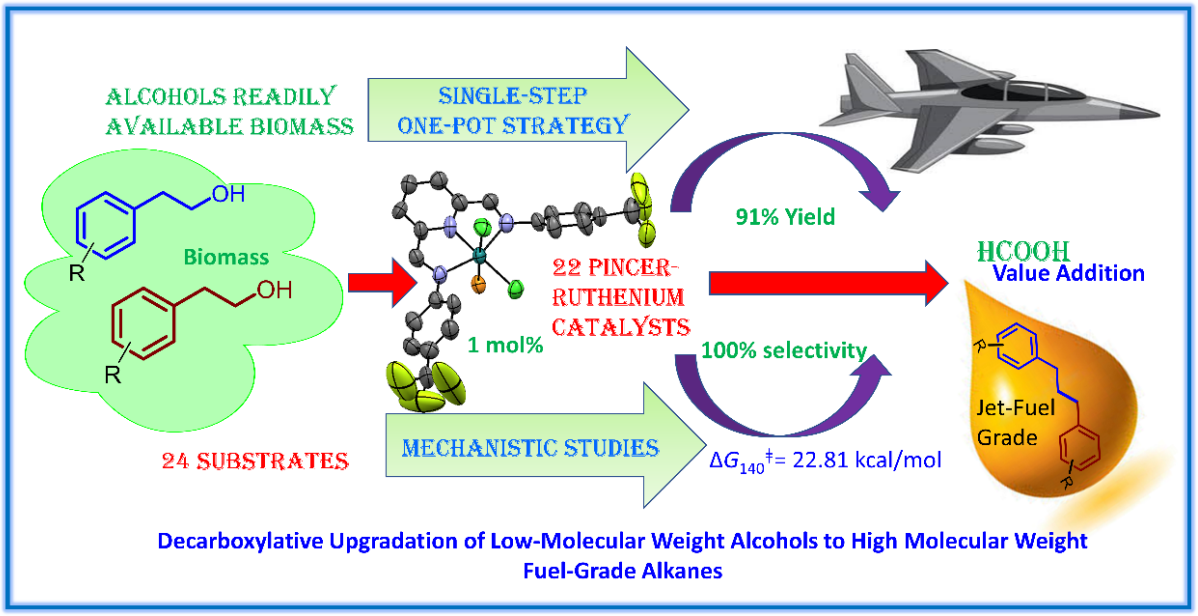

The contents of this chapter have been adapted from "*Pincer-Ruthenium-Catalyzed Direct Formation of Fuel-Grade Alkanes via a Net-Decarboxylative Coupling of Alcohols*" by Nandi, P. G.; Maity, P.; Kumar, A. *ACS Catat* **2025,** *15*, 543-556.

3.1. Introduction

There has been a flurry of activities towards sustainable conversion of easily available biomass into biofuels and chemical feedstock to counter the raw-material deficit that is inevitable owing to the rapid depletion of fossil fuels.[1] Towards this end, the chemistry of C-C bond formation has been an evergreen area of synthetic organic chemistry that provides a convenient and versatile route to natural products, fine chemicals, fuels, pharmaceuticals and agrochemicals.[2] Typically, these otherwise unsurmountable C-C bond formation reactions are mainly accomplished by organometallic[3-7] and radical pathways[8] *via* transition metal-catalyzed activation of C-X (X = Cl, Br and I) bonds. Another convenient route to C-C bond formation that has received special attention recently due to its atom-economical and green nature has been the alcohol re-functionalization reaction *via* hydrogen auto-transfer[9] or the hydrogen-borrowing strategy[10] where water is the only by-product. In particular, the direct transformation of alcohols derived from biomass into biofuel and long chain alkanes are not only sustainable but also attractive despite its tremendously challenging nature owing to the difficult to achieve hydrogenation of the decarboxylated alkene.[11,12]

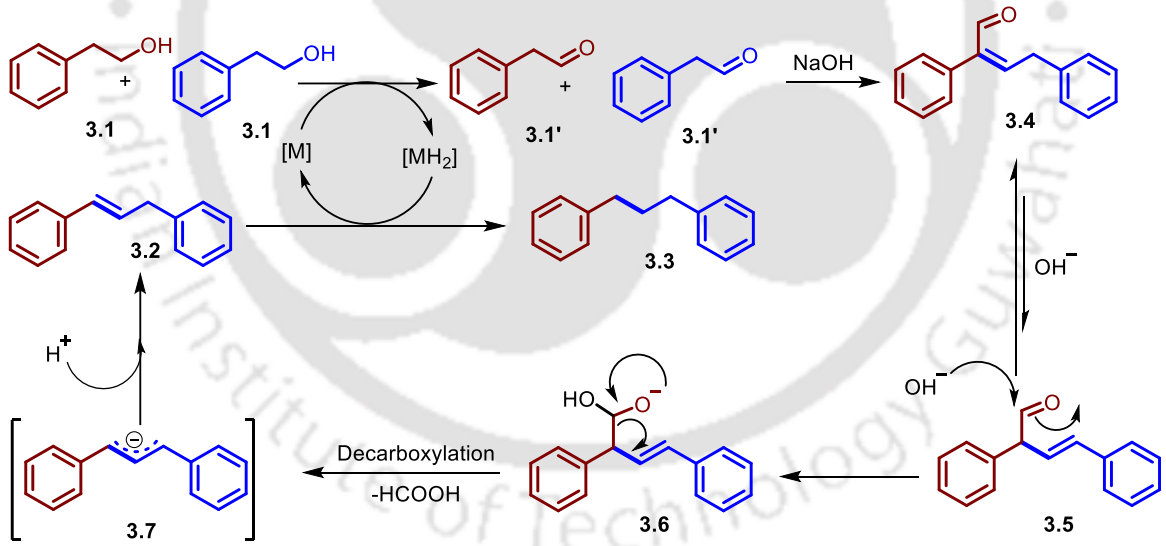

Scheme 3.1. General mechanistic pathway for the transformation of low-molecular weight alcohols to high-molecular weight alkanes *via* decarboxylative coupling.

The first step of these low-molecular weight alcohol to higher-molecular weight alkane transformations involve the dehydrogenation of the low-molecular weight alcohol to produce aldehydes which couple in presence of a base to give α, β-unsaturated aldehyde *via* aldol-condensation (Scheme 3.1). This is followed by decarboxylation to produce allyl anion and

then alkene which ideally then should react with the H_2 released in the previous step in a metal

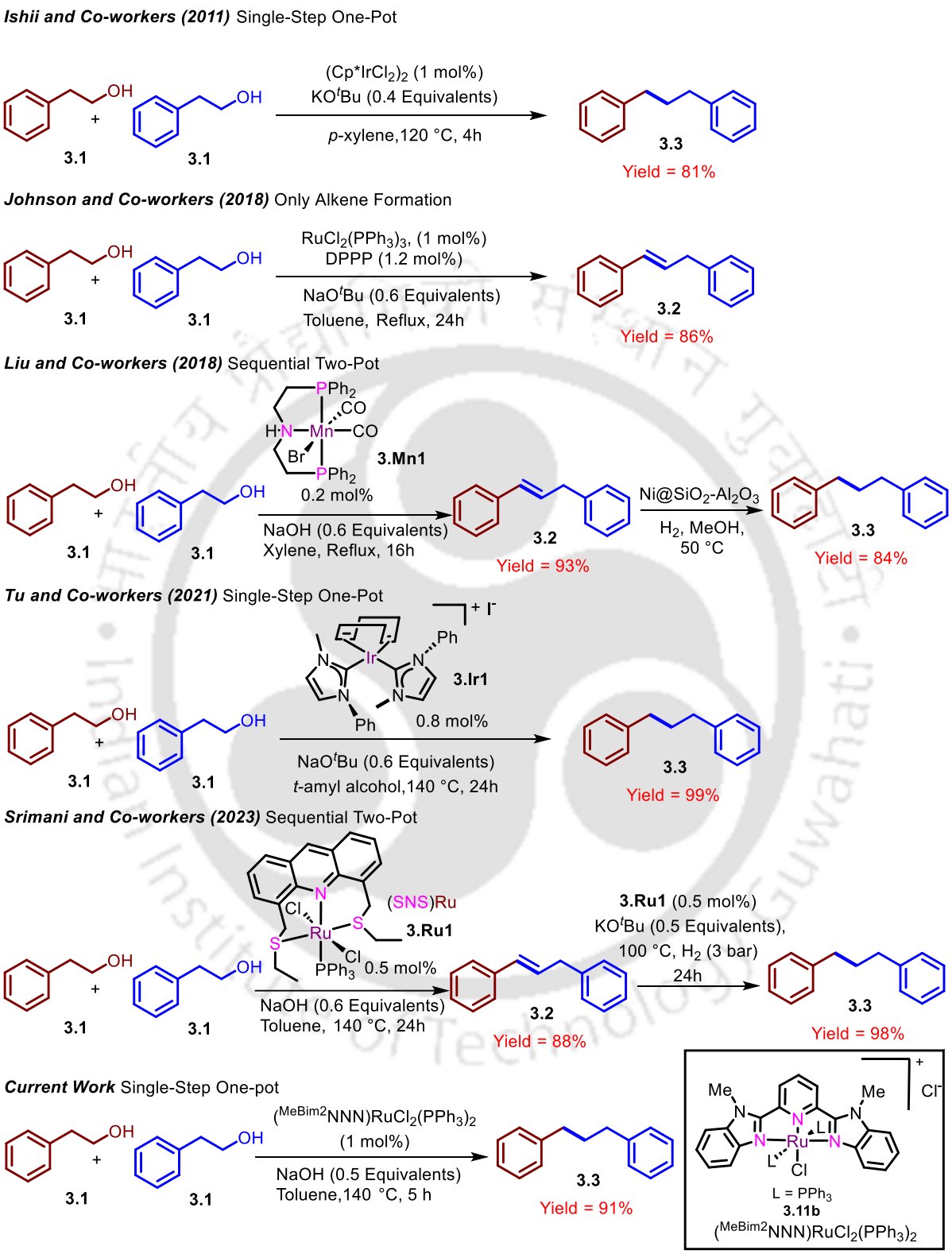

Scheme 3.2. Catalytic methods reported for the decarboxylative coupling of alcohols.

catalyzed reaction to produce fuel-grade higher molecular weight alkane as the desired product (Scheme 3.1).

A majority of the reported catalytic systems (Scheme 3.2) halt at the stage of formation of higher-molecular weight alkene and an additional effort is required to hydrogenate the alkene to alkane (Scheme 3.2). Efficient catalytic methods are hence vital to selectively produce alkane without the need of additional hydrogen and/or catalysts. The decarboxylation of alcohols to alkene or alkane has been reported in past by Ishii and Obora,[13] Liu,[14] Srimani,[15] Jhonson [16] and Tu.[17]

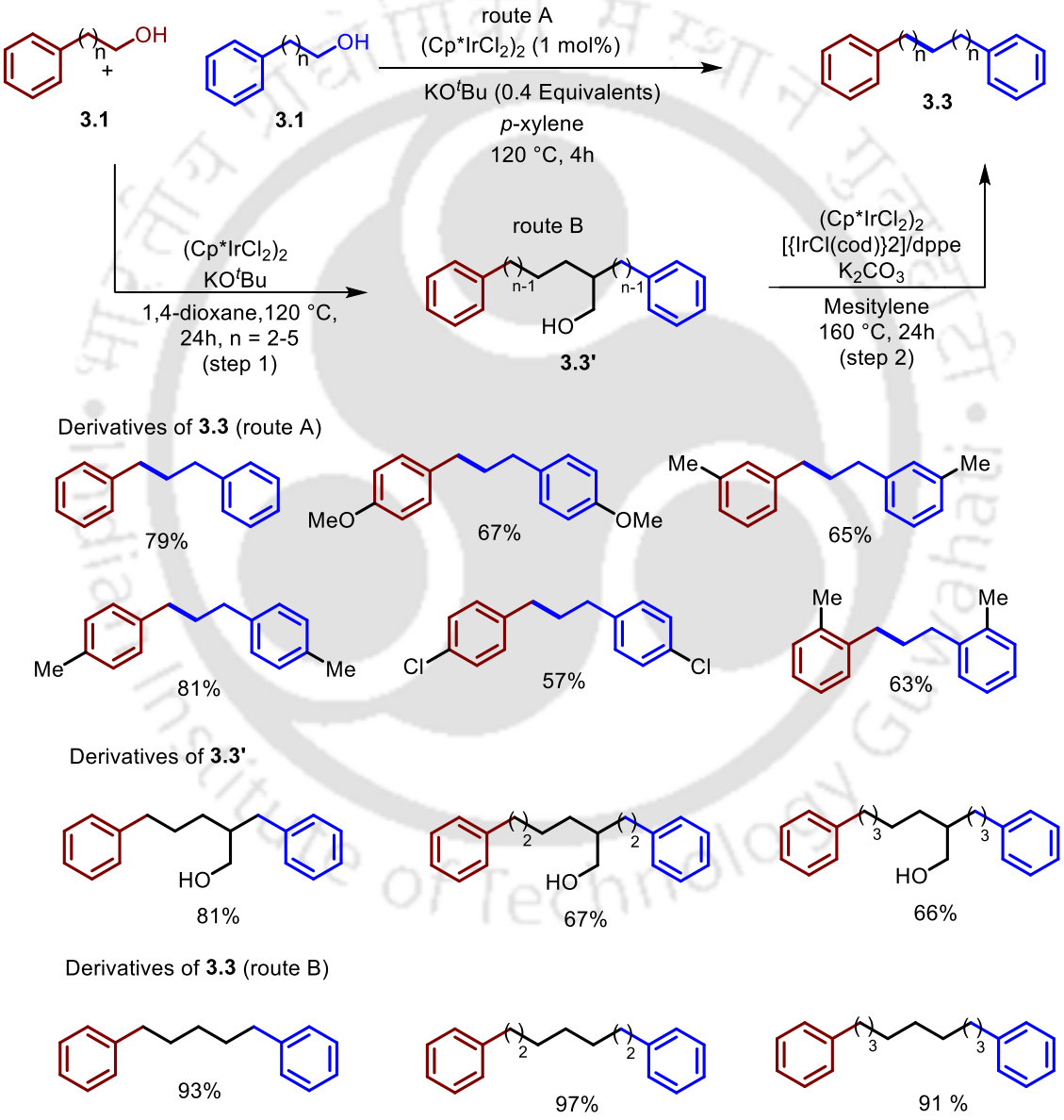

Scheme 3.3. Iridium catalyzed decarboxylative coupling of 2-phenylethanol to 1,3-diphenylpropane.[13]

In 2011, Ishii and Obora carried out the formation of fluorescent active *α*, *ω*-diaryl alkanes from ω-aryl alcohols as the model substrates using iridium salt $(Cp^*IrCl_2)_2$ (Scheme 3.3).[13] They have reported *α*, *ω*-diarylalkane (**3.3**) formation from *ω*-arylethanol (**3.1**) by dehydrogenation/*β*-alkylation (step1) and subsequent dehydrogenation/decarboxylation (step 2) either by one step (direct) (route A) or sequential step (route B) (Scheme 3.3). The *α*, *ω*-diaryl propanes were synthesized in good to moderate yield from the homo-coupling of 2-aryl ethanols using commercially available iridium catalyst $(Cp^*IrCl_2)_2$ (1 mol%), KO^{t}Bu (0.4 equivalents) in *p*-xylene (0.5 mL) at 120 °C for 4 hours. Similarly, when the reaction was carried out in 1,4 dioxane (1 mL) for 24 h, **3.3'** was observed instead of **3.3** in good to moderate yield. In presence of $[(Cp^*IrCl_2)_2]$ (2)/ $[\{IrCl(cod)\}_2]$ (2) **3.3'** was converted to **3.3** with dppe ligand, K_2CO_3 (20 mol%) in mesitylene (1.5 mL) at 160 °C for 24 h with good to moderate yields (Scheme 3.3).

In 2018, Johnson and co-workers used commercially available $RuCl_2(PPh_3)_3$ (1 mol%) for the conversion of a variety of 2-phenylethanols to the corresponding alkenes using 1.2 mol% of +DPPP ((1,3-*bis*(diphenylphosphino) propane) ligand, 0.6 equivalents NaO^{t}Bu in toluene under reflux for 24 h (Scheme 3.4).[16]

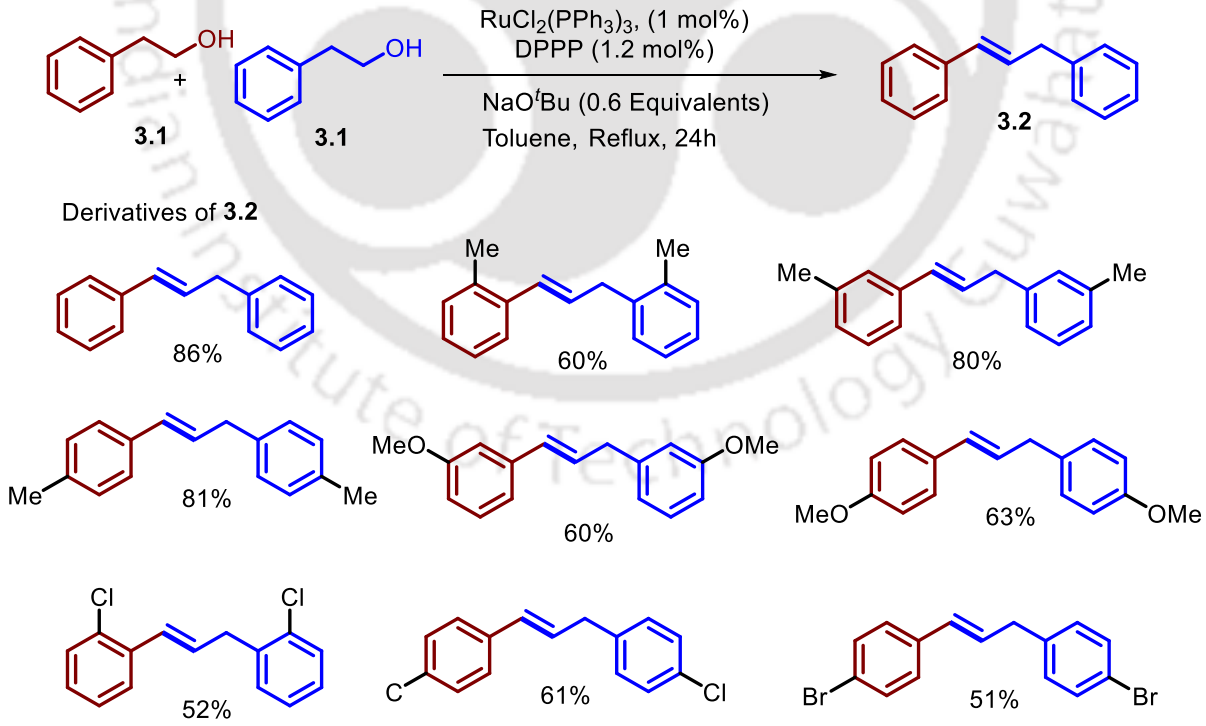

Scheme 3.4. Ruthenium catalyzed decarboxylative coupling of 2-phenylethanol to 1,3-diphenylpropene.[16]

In 2018, Liu and co-workers, for the first time studied the homo as well as hetero coupling of alcohols to corresponding alkenes using PNP pincer-Mn catalysts **3.Mn1**. In the first step 2-phenylethanols were converted to the corresponding alkenes with very good yields, using **3.Mn1 (**0.2 mol%), NaOH (0.6 equivalents) in xylene under reflux conditions for 16 hours (Scheme 3.5).[14] A follow-up hydrogenation catalyzed by $Ni@SiO_2$-Al_2O_3 under 20 bar H_2 in methanol was carried out at 50 °C in a separate pot to get good to moderate yield of alkanes (Scheme 3.5).

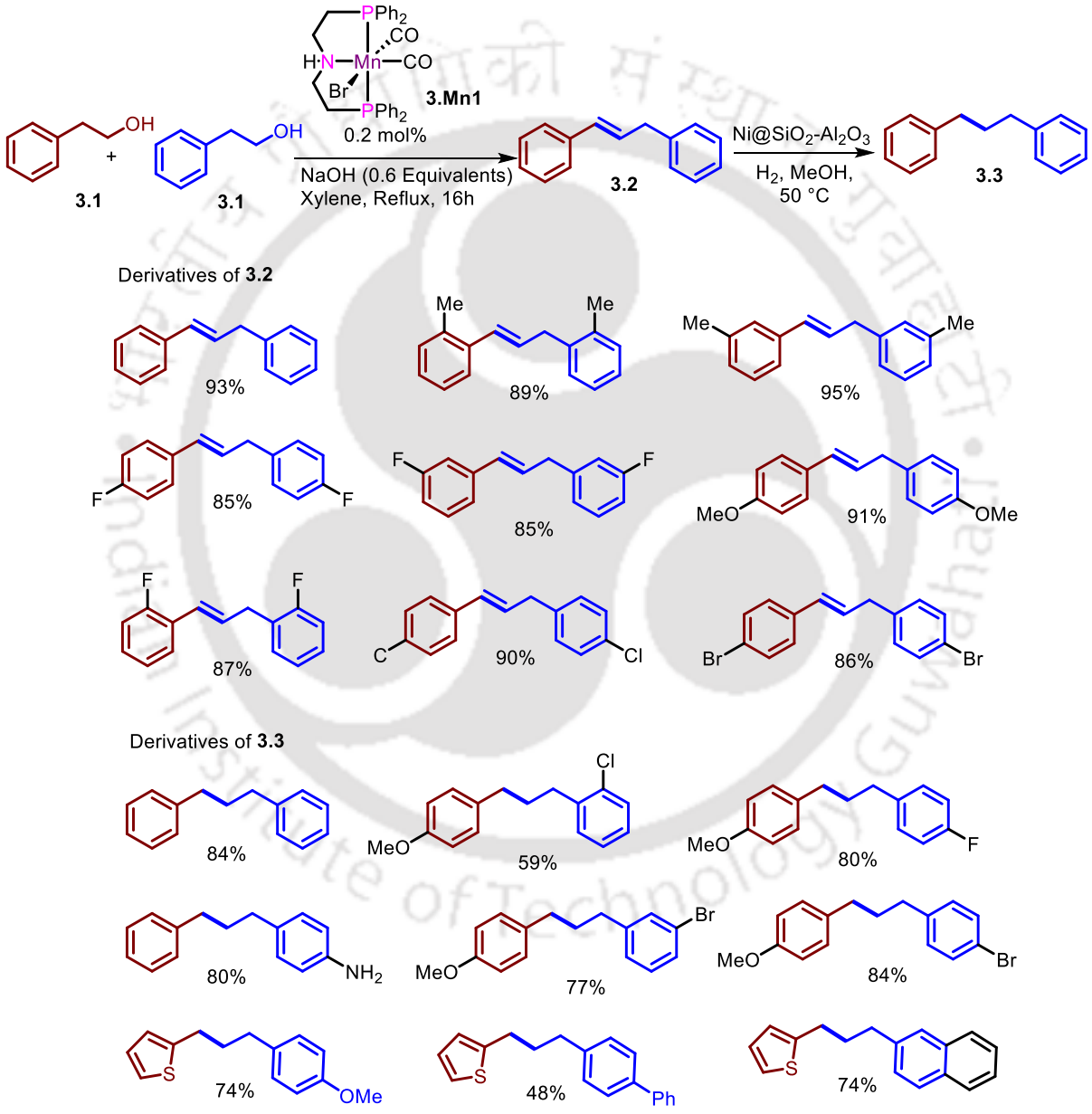

Scheme 3.5. The **3.Mn1** catalyzed decarboxylative coupling of 2-phenylethanol to 1,3-diphenylpropenes and $Ni@SiO_2$-Al_2O_3 catalyzed formation of 1,3-diphenylpropane and its derivatives.[14]

In 2021, Tu and co-workers carried out the direct formation of 1,3-diphenylpropane from 2-phenylethanol using **3.Ir1** (0.8 mol%) in presence of 0.6 equivalents NaOH in *tert*-amyl alcohol for 24 h in 140 °C (Scheme 3.6).[17] The catalyst **3.Ir1** catalyzed the hydrogenation of 1,3-diphenylpropene without any additional molecular hydrogen (H_2) and also the catalytic system is very suitable for both homo and hetero coupling of alcohols. Using the highly selective protocol a variety of alcohol substrates were upgraded to corresponding alkanes with good to moderate yield.

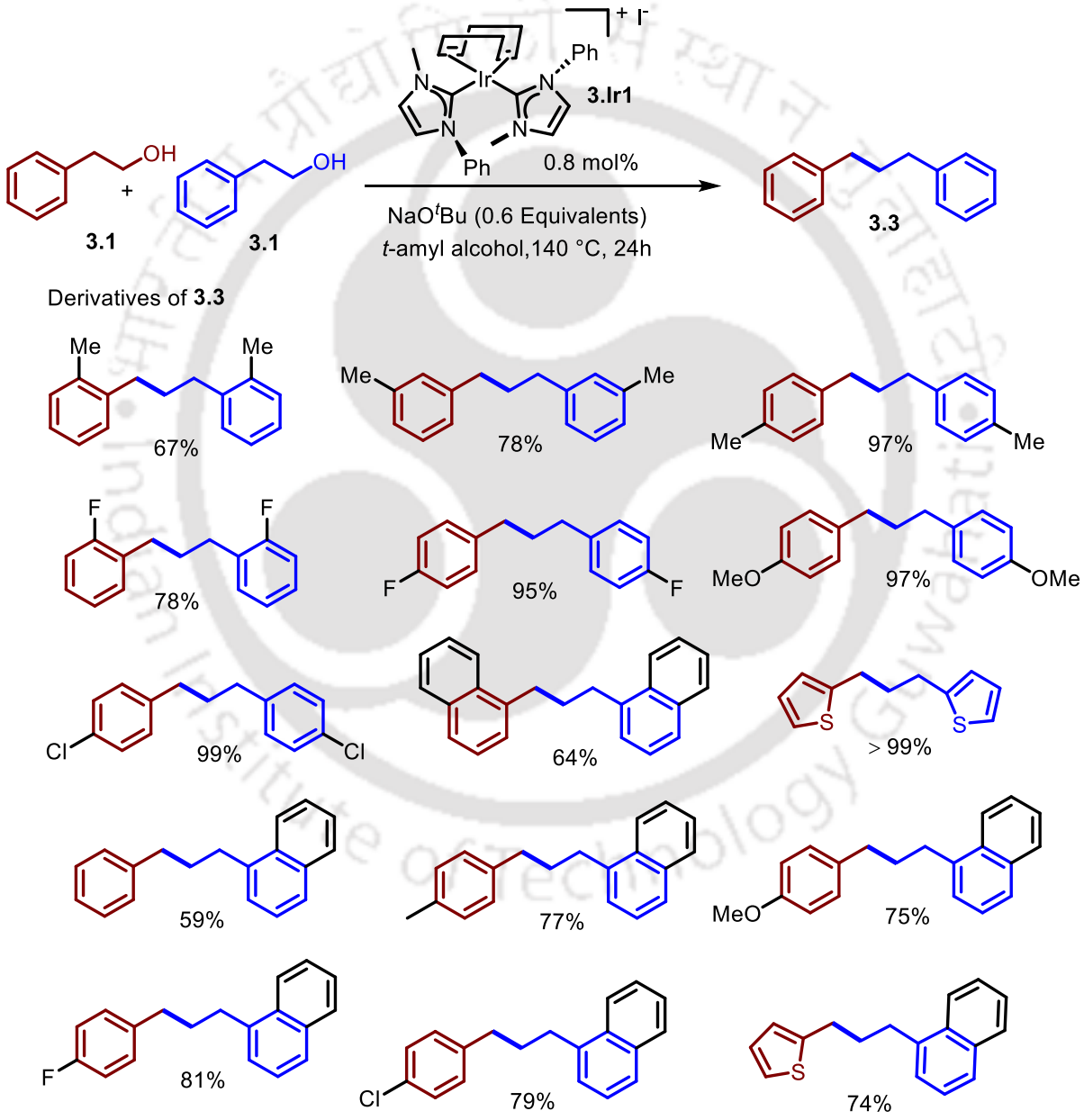

Scheme 3.6. The **3.Ir1** catalyzed direct formation of 1,3-diphenylpropanes from 2-phenylethanols.[17]

Recently, Srimani developed a methodology for the transformation of 2-phenylethanols to the corresponding alkanes using (SNS)Ru (**3.Ru1**) catalytic system in two sequential steps (Scheme 3.7).[15] In the first step **3.Ru1**(0.5 mol%) catalyzed the transformation of 2-phenylethanol to 1,3-diphenylpropene with 0.6 equivalents NaOH in toluene at 140 °C for 24 h. In the second step, **3.Ru1**(0.5 mol%) catalyzed the transformation 1,3-diphenylpropene to 1,3-diphenylpropane with 0.5 equivalents of KO^{t}Bu at 100 °C in presence of externally added molecular H_2 (3 bar). This methodology was useful for the both homo and hetero coupling of a variety of alcohol substrates (Scheme 3.7).[15]

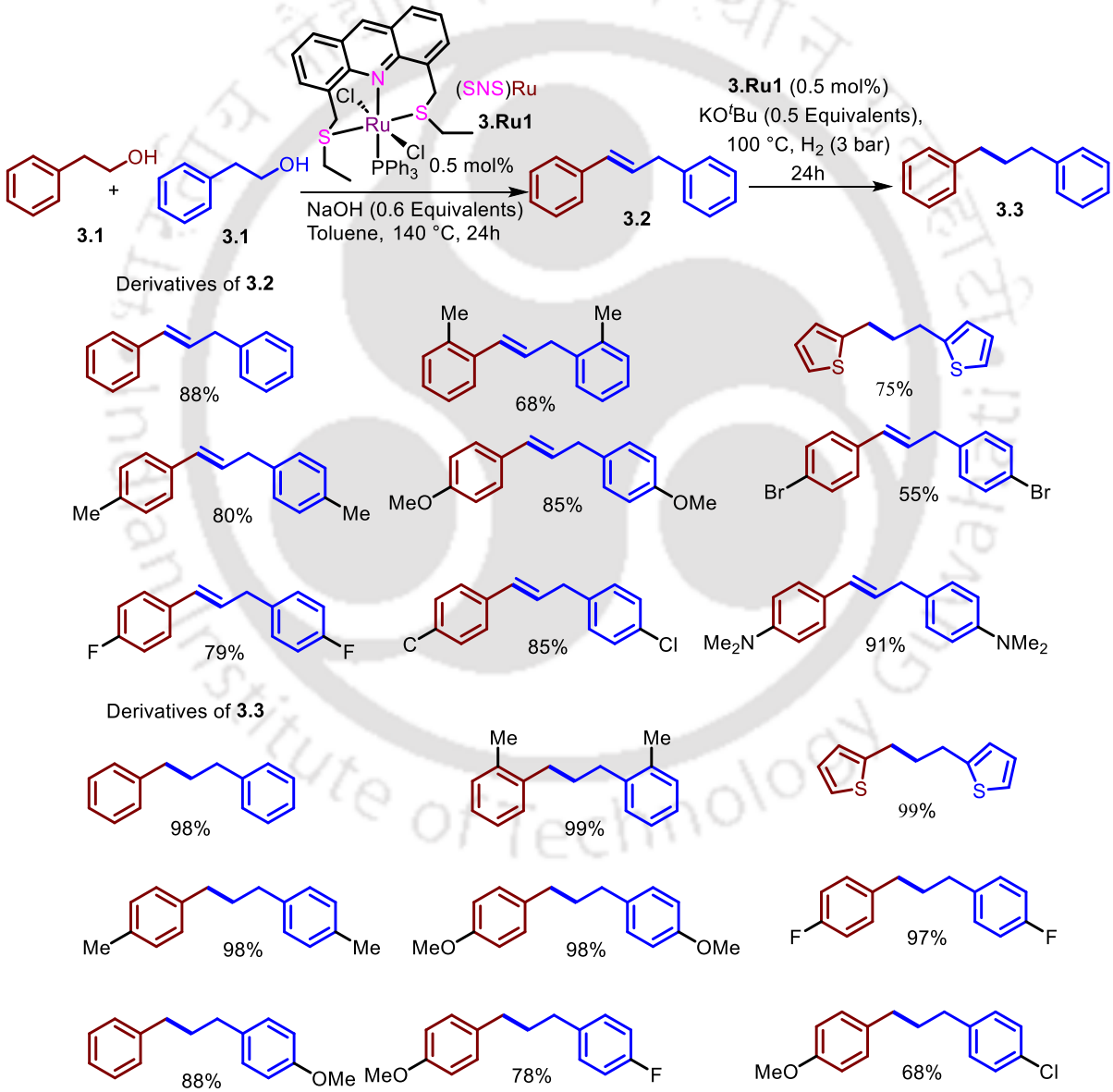

Scheme 3.7. The **3.Ru1** catalyzed decarboxylative coupling of 2-phenylethanol to 1,3-diphenylpropenes and sequential hydrogenation of 1,3-diphenylpropane and its derivatives .[15]

3.2. Objectives of the current work

A comprehensive literature survey reveals that the pincer complexes are very much active for the activation of alcohol molecules. Other than the independent reports by Ishi[13] and Tu[17] with Ir based catalysts, there are no investigations on the formation of alkanes starting from alcohols using a single-step one-pot strategy, to the best of our knowledge. In particular, all the reported Ru[15,16] based catalysts have led to the formation of alkenes starting from alcohols and wherever alkanes were reported, these were accomplished in an additional[15] hydrogenation step with molecular hydrogen (Scheme 3.2).

We have demonstrated the utility of NNN pincer-Ru catalysts based on *bis*(imino)pyridine ligands and 2,6-*bis*(benzimidazole- 2-yl)pyridine ligands in catalyzing various value addition of alcohols such as N-alkylation,[18] alcohol reforming,[19] *β*-alkylation,[20] *β*- methylation[21] and Geurbet reactions.[20,22] Notably, all of these reactions involved a dehydrogenation step[18-22] while some of the reactions involved a secondary hydrogenation step[18,20-22] utilizing the hydrogen evolved during the former step. It would be interesting to examine the activity of these NNN pincer-Ru catalysts based on *bis*(imino)pyridine ligands and 2,6-*bis*(benzimidazole- 2-yl)pyridine ligands towards decarboxylative coupling of alcohols to higher alkanes which also requires a very similar tandem occurrence of dehydrogenation and hydrogenation reactions.

In this context, in the current work, the activity of a series of new and known NNN pincer-Ru catalysts of the type (^{R2}NNN)RuCl$_2$L (R = ^{i}Pr, ^{t}Bu, Cy, Ph, *p*-F-C$_6$H$_4$, *p*-OMe-C$_6$H$_4$ and L = PPh$_3$, CO and CH$_3$CN) based on *bis*(imino)pyridine ligands and (^{RBim2}NNN)RuCl$_2$L$_2$ (R = H and Me, L = PPh$_3$ and CO) based on 2,6-*bis*(benzimidazole-2-yl)pyridine ligands have been investigated towards the decarboxylative coupling of alcohols to alkanes. While most of the complexes were unselective giving alkene/alkane mixtures, the complex (^{MeBim2}NNN)RuCl$_2$(PPh$_3$)$_2$ based on 2,6-*bis*(benzimidazole-2- yl)pyridine ligand demonstrated high activity (ca. 88 ± 3% yield) with exclusive formation of the alkane (1,3-diphenyl propane) starting from 2-phenyl ethanol in the presence of 0.5 equivalents of NaOH in toluene at 140 °C within 5 h of reaction. The (^{MeBim2}NNN)RuCl$_2$(PPh$_3$)$_2$ catalyzed transformation of 2- phenyl ethanol to 1,3-diphenyl propane has been probed in detail from both synthetic and mechanistic point of view. To the best of our knowledge, this has been the first example of a Ru based catalyst for the direct upgradation of alcohols to alkanes using a single-step one-pot decarboxylative tandem transfer hydrogenation strategy.

3.3. Result and discussions

3.3.1. Synthesis and characterization of pincer-ruthenium complexes based on *bis*(imino)pyridine ligands

The NNN pincer ruthenium complexes **3.8a-f**, **3.9a-d**, **3.10a**, **3.10c-d**, **3.11a-b** and **3.12a-b** (Figure 3.1) were synthesized following our previously reported protocol.[19a, 20-24] The new complexes **3.9e-f** with CO as ancillary ligands were synthesized in good yields by treatment of the corresponding ligands[21] with $[Ru(p\text{-cymene})Cl_2]_2$ under CO atmosphere with THF at reflux for 16h (Scheme 3.8). Similarly, **3.10b** and **3.10e-f** with $NCCH_3$ as ancillary ligand were synthesized in acetonitrile under argon atmosphere (Scheme 3.8).

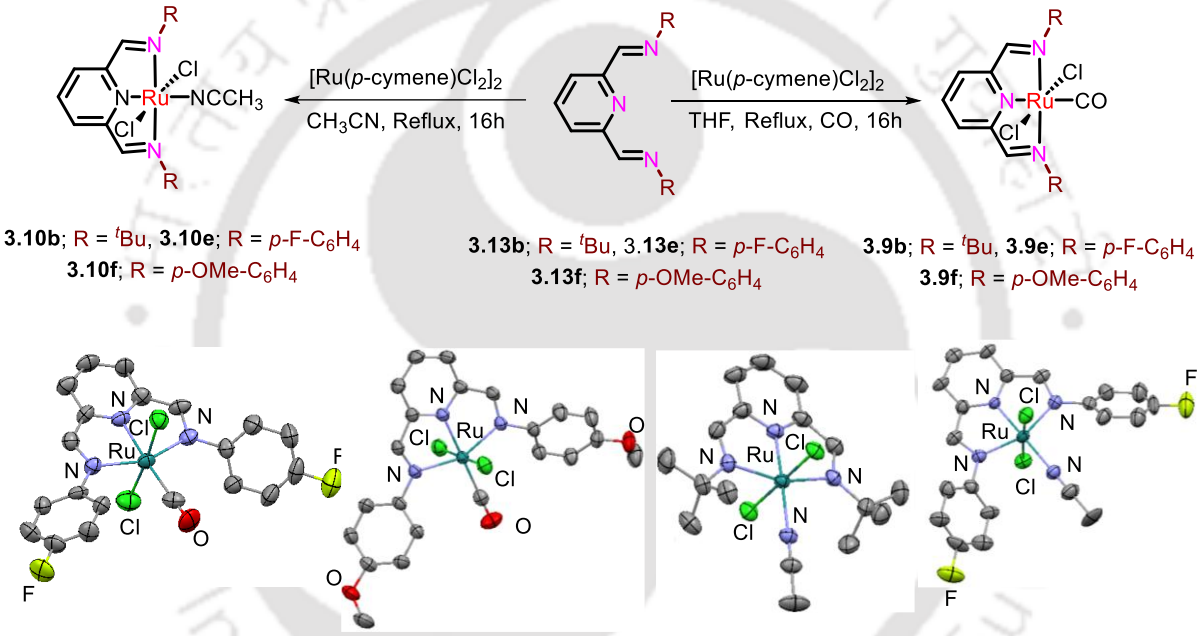

Scheme 3.8. Protocol for the synthesis of **3.9e-f** and **3.10b**,**e-f**[a].

[a]The molecular structures of **3.9e**, **3.9f**, **3.10b** and **3.10e** are provided as ORTEP figures drawn at 50% probability. All the hydrogen atoms are omitted for the sake of clarity.

All the new complexes **3.9e-f**, **3.10b** and **3.10e-f** were fully characterized by ^{1}H, $^{13}C\{^{1}H\}$, ^{19}F NMR spectroscopy and HRMS studies. The $^{13}C\{^{1}H\}$ NMR spectrum of **3.9e** and **3.9f** exhibited the chemical shift of CO group at δ = 201 ppm and δ = 204 ppm respectively (Figure 3.S3 and 3.S5). The FT-IR studies revealed prominent bands at 1967 $cm^{-1}$and 1945 cm^{-1} that correspond to the CO stretching in **3.9e** and **3.9f** respectively (Figure 3.7, 3.8 and 3.S13, 3.S14). While the complexes **3.10b** and **3.10f** exists as a single isomer with the $NCCH_3$ ligand *trans* to the pyridyl N, the ^{1}H NMR studies revealed that the complex **3.10e** exists as two isomers in the ratio 1.00: 0.75 where the major isomer has the $NCCH_3$ ligand *trans* to the pyridyl N and the minor isomer

has the $NCCH_3$ ligand *trans* to one of the chloride ligands. The HRMS analysis of **3.9e**, **3.9f**, **3.10b**, **3.10e** and **3.10f** demonstrated prominent peaks at m/z = 485.9749, 510.0155, 423.0893, 499.0051and 523.0460 that correspond to [**3.9e** – Cl]$^+$, [**3.9f** – Cl]$^+$, [**3.10b** – Cl]$^+$, [**3.10e** – Cl]$^+$ and [**3.10f** – Cl]$^+$ (Figure 3.S15-3.S32). For SCXRD studies, good quality crystals of **3.9e** was obtained by layering its solution in $CDCl_3$+DCM with hexane, while suitable crystals of **3.9f**, **3.10b** and **3.10e** were obtained by slow evaporation of the corresponding solvent from their solution in DMSO, $CDCl_3$ and DCM respectively. The complexes **3.9e**, **3.9f**, **3.10b** and **3.10e** crystallized with a space-group of P21/c, C2/c, P -1 and C2/c respectively (Table 3.4 and 3.S1).

3.3.2. Pincer-ruthenium catalyzed decarboxylative coupling of 2-phenylethanol to 1,3-diphenyl propane

The catalytic upgradation of lower-molecular weight alcohols to higher-molecular weight alkanes were initiated using 2-phenylethanol (**3.1**) as model substrate using 0.5 mol% (^{MeBim2}NNN)$RuCl_2(PPh_3)_2$ (**3.11b**) in presence of various bases at 140 °C in toluene (Table 3.1). In the presence of an equivalent of NaOH at 140 °C, the yield of 1,3-diphenylpropane (**3.3**) increases to >99% with increase in the loading of **3.11b** from 0.25 mol% to 1 mol% (entries 1-4, Table 3.1).

At 1 mol% loading of **3.11b** in 0.5 mL toluene, though the exclusive selectivity towards **3.3** was retained, the yield of **3.3** however decreased upon lowering the NaOH loading (entries 4-8, Table 3.1). To strike a good balance between the high yield of **3.3** and minimal base loading, the optimization was continued at a NaOH loading of 0.5 equivalents as in entry 6, Table 3.1.

Further studies with 1 mol% loading of **3.11b** in the presence of 0.5 equivalents of NaOH at varying dilutions in toluene revealed that the catalytic decarboxylation of **3.1** to **3.3** was more efficient in 0.5 mL toluene (entry 6 *vs.* entries 9-11, Table 3.1). Upon repeating the reaction under the new optimized conditions (1 mol% **3.11b**, 0.5 equivalent NaOH in 0.5 mL solvent), it was observed that productivity of **3.11b** in toluene was superior than the corresponding productivity of **3.11b** in other solvents such as 1, 4 dioxane, *tert*-butanol, THF, *m*-xylene and *tert*-amyl alcohol (entry 6 *vs.* entries 12-16, Table 3.1). Entry 6, Table 3.1 thus continues to be the optimized condition till this stage. While the performance of **3.11b** was relatively poor in the presence of bases such as NaO^tBu, KO^tBu and KOH (entries 18-20, Table 3.1), no reactivity was observed when the **3.11b** catalysed decarboxylation was carried out in the presence of

presence of Na_2CO_3, K_2CO_3, Cs_2CO_3, $NaHCO_3$ and $KHCO_3$ (entries 21-25, Table 3.1).

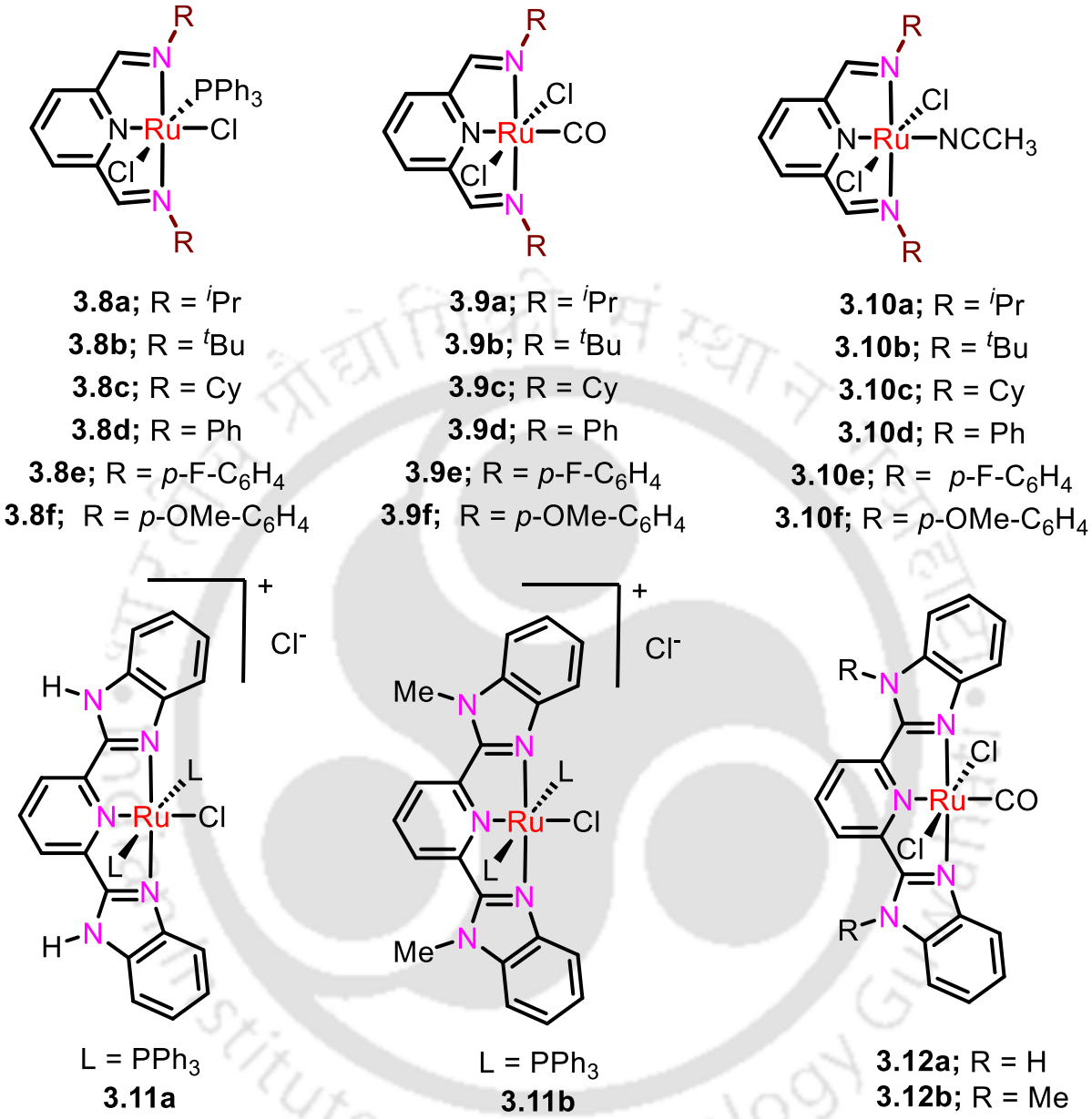

Figure 3.1. Pincer-Ru complexes investigated in the current study.

The **3.11b** catalyzed decarboxylation of **3.1** to **3.3** in the presence of 0.5 equivalents of NaOEt resulted in a selectivity and productivity that was comparable to the corresponding results obtained in the presence of 0.5 equivalents of NaOH (entry 6 *vs.* entry 17, Table 3.1 and Table 3.S3). As the latter is readily available and more economical, further studies on the **3.11b** catalyzed decarboxylation was carried out in the presence of 0.5 equivalents of NaOH in 0.5 mL toluene at 140 °C.

Table 3.1. The 3.11b catalyzed decarboxylation of 2-phenyethanol to 1,3-diphenylpropane under varying conditions[a]

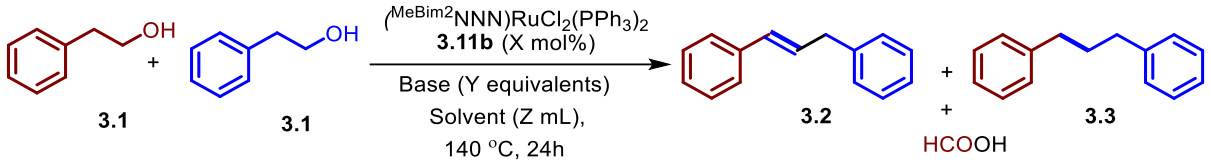

Entry	Catalyst (X mol %)	Base (Y equivalents)	Solvent (Z mL)	% Yield[b] **3.2**	**3.3**	Selectivity of **3.3** (%)[d]
1	**3.11b** (0.25)	NaOH (1.0)	Toluene (0.5)	15	12	44
2	**3.11b** (0.5)	NaOH (1.0)	Toluene (0.5)	15	59	80
3	**3.11b** (0.75)	NaOH (1.0)	Toluene (0.5)	0	63	100
4	**3.11b** (1.0)	NaOH (1.0)	Toluene (0.5)	0	>99	100
5	**3.11b** (1.0)	NaOH (0.75)	Toluene (0.5)	0	89	100
6	**3.11b** (1.0)	NaOH (0.5)	Toluene (0.5)	0	88±3	100
7	**3.11b** (1.0)	NaOH (0.4)	Toluene (0.5)	0	56	100
8	**3.11b** (1.0)	NaOH (0.3)	Toluene (0.5)	0	15±1	100
9	**3.11b** (1.0)	NaOH (0.5)	Toluene (0.3)	0	39	100
10	**3.11b** (1.0)	NaOH (0.5)	Toluene (0.4)	0	61	100
11	**3.11b** (1.0)	NaOH (0.5)	Toluene (1.0)	0	65	100
12	**3.11b** (1.0)	NaOH (0.5)	1,4 Dioxane (0.5)	26	20	43
13	**3.11b** (1.0)	NaOH (0.5)	*tert*-butanol (0.5)	22	24	52
14	**3.11b** (1.0)	NaOH (0.5)	THF (0.5)	0	42±3	100
15	**3.11b** (1.0)	NaOH (0.5)	*m*-Xylene (0.5)	0	37	100
16	**3.11b** (1.0)	NaOH (0.5)	*tert*-Amyl alcohol (0.5)	0	41	100
17	**3.11b** (1.0)	NaOEt (0.5)	Toluene (0.5)	0	91	100
18	**3.11b** (1.0)	NaO^{t}Bu (0.5)	Toluene (0.5)	0	63	100
19	**3.11b** (1.0)	KO^{t}Bu (0.5)	Toluene (0.5)	15	37	71
20	**3.11b** (1.0)	KOH (0.5)	Toluene (0.5)	15	61	80
21	**3.11b** (1.0)	Na_2CO_3 (0.5)	Toluene (0.5)	0	0	-
22	**3.11b** (1.0)	K_2CO_3 (0.5)	Toluene (0.5)	0	0	-
23	**3.11b** (1.0)	$NaHCO_3$ (0.5)	Toluene (0.5)	0	0	-
24	**3.11b** (1.0)	$KHCO_3$ (0.5)	Toluene (0.5)	0	0	-
25	**3.11b** (1.0)	Cs_2CO_3 (0.5)	Toluene (0.5)	0	0	-
26[c]	**3.11b** (1.0)	NaOH (0.5)	Toluene (0.5)	9	68	88
27	No catalyst	NaOH (0.5)	Toluene (0.5)	27	0	0
28	**3.11b** (1.0)	No Base	Toluene (0.5)	0	0	-

[a]Reaction conditions, unless specified otherwise: 0.5 mmol of **3.1**, Y equivalents of Base, and X mol % **3.11b** at 140 °C for 24 h in a 15 mL high pressure tube with 0.5 mL solvent under air. [b]Determined by ^{1}H NMR analysis using mesitylene as the standard. [c]Reaction performed at 120 °C. [d]Selectivity is calculated as Selectivity = (**3.3***100)/(**3.3**+**3.2**).

Table 3.2 depicts the efforts towards catalytic decarboxylation of **3.1** to **3.3** in the presence of 0.5 equivalents of NaOH in 0.5 mL toluene at 140 °C using various pincer-ruthenium catalysts

and their precursors. Clearly, the catalyst **3.11b** based on 2,6-*bis*(benzimidazole- 2-yl)pyridine

Table 3.2. Decarboxylation of 2-phenyethanol to 1,3-diphenylpropane catalyzed by various ruthenium complexes[a]

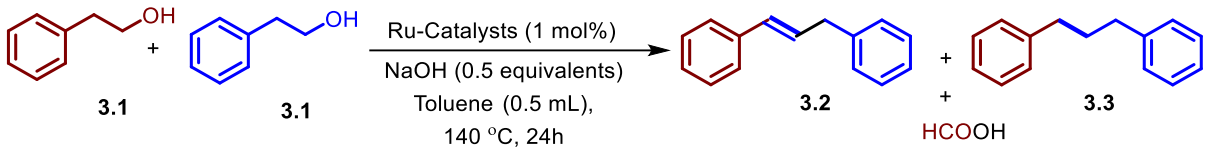

Entry	Catalyst (1.0 mol %)	%Yield[b]		Selectivity of **3.3** (%)[c]
		3.2	**3.3**	
1	**3.8a**	43	14	25
2	**3.8b**	18	20	53
3	**3.8c**	53	29	35
4	**3.8d**	11	73	87
5	**3.8e**	17	53	76
6	**3.8f**	71	0	0
7	**3.9a**	42	25	37
8	**3.9b**	40	32	44
9	**3.9c**	54±3	18±4	28
10	**3.9d**	63	22	26
11	**3.9e**	68	11	14
12	**3.9f**	56	Trace	-
13	**3.10a**	61	3	5
14	**3.10b**	82	14	15
15	**3.10c**	61	38	38
16	**3.10d**	69	7	9
17	**3.10e**	8	27	77
18	**3.10f**	6	69	92
19	**3.11a**	50	16	24
20	**3.11b**	0	88±3	100
21	**3.12a**	1	38	97
22	**3.12b**	0	21	100
23	$RuCl_2(PPh_3)_3$	16	7	30
24	$[Ru(benzene)Cl_2]_2$	32	18	36
25	$[Ru(p\text{-cymene})Cl_2]_2$	60	8	12

[a]Reaction conditions, unless specified otherwise: 0.5 mmol of **3.1**, 0.5 equivalents of NaOH and 1 mol % ruthenium catalysts at 140 °C for 24 h in a 15 mL high pressure tube with toluene (0.5 mL) under air. [b]Determined by ^1H NMR analysis using mesitylene as the standard. [c]Selectivity is calculated as Selectivity = (**3.3***100)/(**3.3**+**3.2**).

ligand demonstrated the excellent activity among all the considered pincer-Ru complexes and

their precursors both in terms of selectivity and productivity (entry 20 *vs.* rest of the entries in Table 3.2 and Table 3.S4).

Table 3.3. Decarboxylation of 2-phenylethanol to 1,3-diphenyl propane catalyzed by various ruthenium complexes[a]

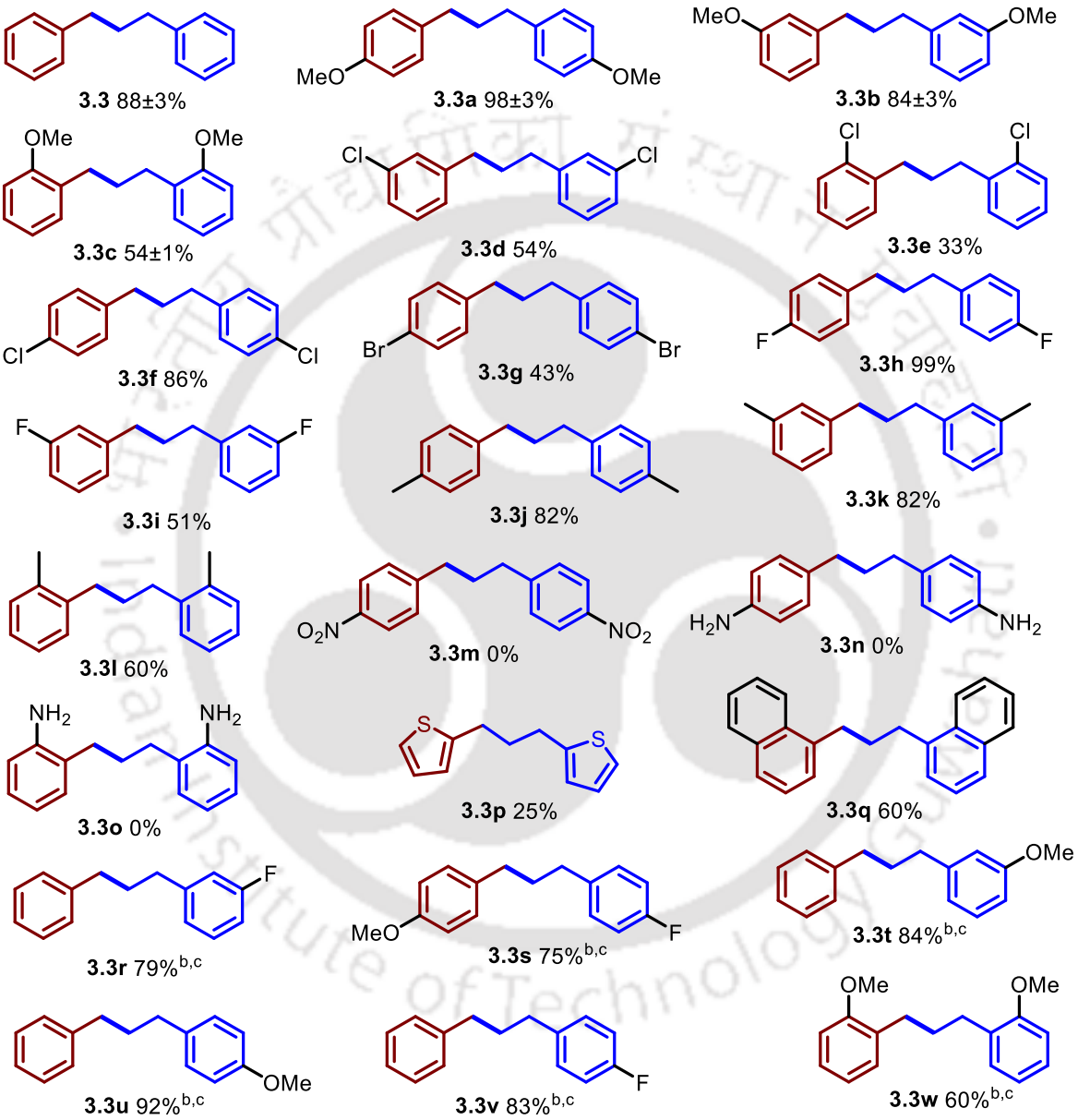

[a]Reaction conditions, unless specified otherwise: 0.5 mmol of **3.1**, 0.5 equivalents (10 mg, 0.25 mmol) of NaOH and 1 mol % (5.2 mg, 5 µmol) **3.11b** at 140 °C for 24 h in a 15 mL high pressure tube with toluene (0.5 mL) under air. Yields determined by ^{1}H NMR analysis using mesitylene as the standard. [b]Isolated yields. [c]Ratio of precursor alcohols of structures marked in maroon to corresponding structures marked in blue are 4:1.

Notably, reaction of **3.1** under the optimized conditions but in the absence of any catalyst lead

to exclusive formation of the alkene **3.2** in 27% yield (entry 27, Table 3.1). However, there was no reactivity when the reaction was repeated under the optimized conditions, but this time without using a base (entry 28, Table 3.1). These observations along with the inference obtained from control experiments (*vide infra*) sheds light on the key role that the catalyst **3.11b** plays in leading to the selective formation of alkane **3.3** in high yields.

The formulated protocol on the **3.11b** catalyzed decarboxylation was then investigated for various derivatives of 2-phenylethanol not only for homocoupling but also for heterocoupling (Table 3.3). In general, functional groups at *p*-position of the arene ring on the derivatives of **3.1** gave good yields of the corresponding **3.3** based alkanes (**3.3a**, **3.3f**, **3.3h** and **3.3j**) with **3.3g**, **3.3m** and **3.3n** being the only exceptions. The yields of alkane derivatives **3.3b**, **3.3c**, **3.3d**, **3.3e**, **3.3i**, **3.3k** and **3.3l** which had substituents either in the *m*-position or in the *o*-position were slightly lower than the corresponding alkanes with *p*-substituents. A variety of heterocoupled alkane products **3.3r**-**3.3w** could also be accessed in moderately good yields (Table 3.3).

3.3.3. Control experiments and mechanistic insight

Various control experiments were performed with an objective to attain a clear understanding on the plausible mechanism involved in the **3.11b** (1 mol%) catalyzed decarboxylation of **3.1** to **3.3** in the presence of 0.5 equivalents of NaOH. Analysis of the head space of the vessel containing the reaction mixture under the optimized conditions (entry 6, Table 3.1 and entry 20, Table 3.2) revealed the evolution of hydrogen during the reaction (equation 1, Scheme 3.4 and Figures 3.9) essentially pointing towards dehydrogenation of **3.1** to the corresponding aldehyde **3.1'** as one of the primary steps. Apart from the formation of **3.3**, the generation of formic acid is also observed from the ^{1}H NMR analysis of the crude reaction mixture corresponding to equation **3.1** of Scheme 3.9 which is indicative of an associated decarboxylative step in the upgradation of **3.1** to **3.3** The aldehyde **3.1'** which is the dehydrogenated version of **3.1** when subjected to optimized reaction conditions in the absence of a base leads to *α*,*β*-unsaturated aldehyde **3.4** (equation 2, Scheme 3.9) which when treated with NaOH under the optimized conditions but in the absence of **3.11b** resulted in the formation of the alkene **3.2** (equation 5, Scheme 3.9). Notably alkene **3.2** could be accessed exclusively in 92% yield by treating the aldehyde **3.1'** under the optimized conditions either in the presence

Table 3.4. Crystal structure and refinement parameters of 3.9e, 3.9f, 3.10b and 3.10e

Complex	**3.9e**	**3.9f**	**3.10b**	**3.10e**
Empirical formula	$C_{21}H_{14}Cl_5F_2N_3ORu$	$C_{22}H_{19}Cl_2N_3O_3Ru$	$C_{19}H_{30}Cl_8N_4Ru$	$C_{21}H_{16}Cl_2F_2N_4Ru$
Formula weight	640.67	545.37	699.14	534.35
Temperature/K	296.00	295(2)	301(2)	303.00
Crystal system	monoclinic	monoclinic	triclinic	monoclinic
Space group	$P2_1/c$	C2/c	P-1	C2/c
a/Å	10.189(3)	20.670(4)	8.9381(18)	17.8541(11)
b/Å	15.341(4)	11.1071(17)	12.039(3)	14.1751(11)
c/Å	15.361(4)	11.4435(17)	14.400(3)	8.6101(6)
α/°	90	90	105.072(5)	90
β/°	96.044(10)	121.238(5)	101.269(4)	101.573(3)
γ/°	90	90	92.727(5)	90
Volume/$Å^3$	2387.8(11)	2246.4(7)	1459.5(5)	2134.8(3)
Z	4	4	2	4
$\rho_{calc}g/cm^3$	1.782	1.613	1.591	1.663
μ/mm^{-1}	1.252	0.965	1.285	1.017
F(000)	1264.0	1096.0	704.0	1064.0
Crystal size/mm^3	0.24 × 0.21 × 0.18	0.28 × 0.25 × 0.20	0.25 × 0.21 × 0.18	0.25 × 0.21 × 0.18
Radiation	MoKα (λ = 0.71073)	MoKα (λ = 0.71073)	MoKα (λ = 0.71073)	MoKα (λ = 0.71073)
2Θ range for data collection/°	3.762 to 48.812	8.424 to 49.984	3.95 to 54.27	3.698 to 51.996
Index ranges	$-11 \le h \le 11, -17 \le k \le 17, -12 \le l \le 17$	$-24 \le h \le 24, -13 \le k \le 13, -13 \le l \le 13$	$-11 \le h \le 11, -15 \le k \le 15, -18 \le l \le 18$	$-22 \le h \le 22, -17 \le k \le 17, -10 \le l \le 10$
Reflections collected	10123	23305	37089	21632
Independent reflections	3766 [R_{int} = 0.0673, R_{sigma} = 0.0916]	1935 [R_{int} = 0.0231, R_{sigma} = 0.0103]	6283 [R_{int} = 0.0241, R_{sigma} = 0.0158]	2107 [R_{int} = 0.0526, R_{sigma} = 0.0263]
Data/restraints/parameters	3766/0/298	1935/0/144	6283/0/296	2107/6/140
Goodness-of-fit on F^2	1.041	0.980	0.950	1.150
Final R indexes [I>=2σ (I)]	R_1 = 0.0749, wR_2 = 0.1907	R_1 = 0.0186, wR_2 = 0.0490	R_1 = 0.0422, wR_2 = 0.1109	R_1 = 0.0519, wR_2 = 0.1068
Final R indexes [all data]	R_1 = 0.1233, wR_2 = 0.2245	R_1 = 0.0199, wR_2 = 0.0511	R_1 = 0.0446, wR_2 = 0.1134	R_1 = 0.0728, wR_2 = 0.1168
Largest diff. peak/hole / e $Å^{-3}$	0.64/-0.77	0.20/-0.33	1.18/-0.98	0.76/-0.86

Table 3.5. Selected bond lengths and bond angles around metal (Ru) centre

Parameters	**3.9e**	**3.9f**	**3.10b**	**3.10e**
Ru-N (Å) (Pyridyl)	2.017 (8)	2.012 (2)	1.921 (2)	1.923 (5)
Ru –N (imine) (Å)	2.090 (9), 2.068 (9)	2.1129 (14), 2.1130 (14)	2.104 (3), 2.108 (3)	2.073 (4), 2.073 (4)
Ru – C (CO) (Å)	1.934 (13)	1.895 (3)	-	-
Ru – N ($NCCH_3$) (Å)	-	-	2.078 (3)	2.070 (5)
Ru – Cl (Å)	2.381(3), 2.393 (4)	2.3861(6), 2.3861(6)	2.3904 (8), 2.3990 (8)	2.3819 (13), 2.3820 (13)
(Imine)N-Ru-N(Imine) (°)	155.7 (3)	154.34 (8)	157.82 (10)	157.2 (2)
(Pyridyl)N -Ru-N(Imine) (°)	77.8 (3), 77.9 (4)	77.17 (4), 77.17 (4)	79.06 (11), 78.77 (11)	78.58 (11), 78.58 (11)
Cl – Ru – CO (°)	91.2 (3), 92.2 (3)	91.016 (13), 91.016 (13)	-	-
Cl – Ru – $NCCH_3$ (°)	-	-	89.75 (7), 90.60 (7)	87.61 (3)
(Pyridile)N-Ru – N ($NCCH_3$) (Å)	-	-	178.36 (10)	180.0
(Pyridile)N-Ru – CO (°)	176.7 (4)	180.0	-	-

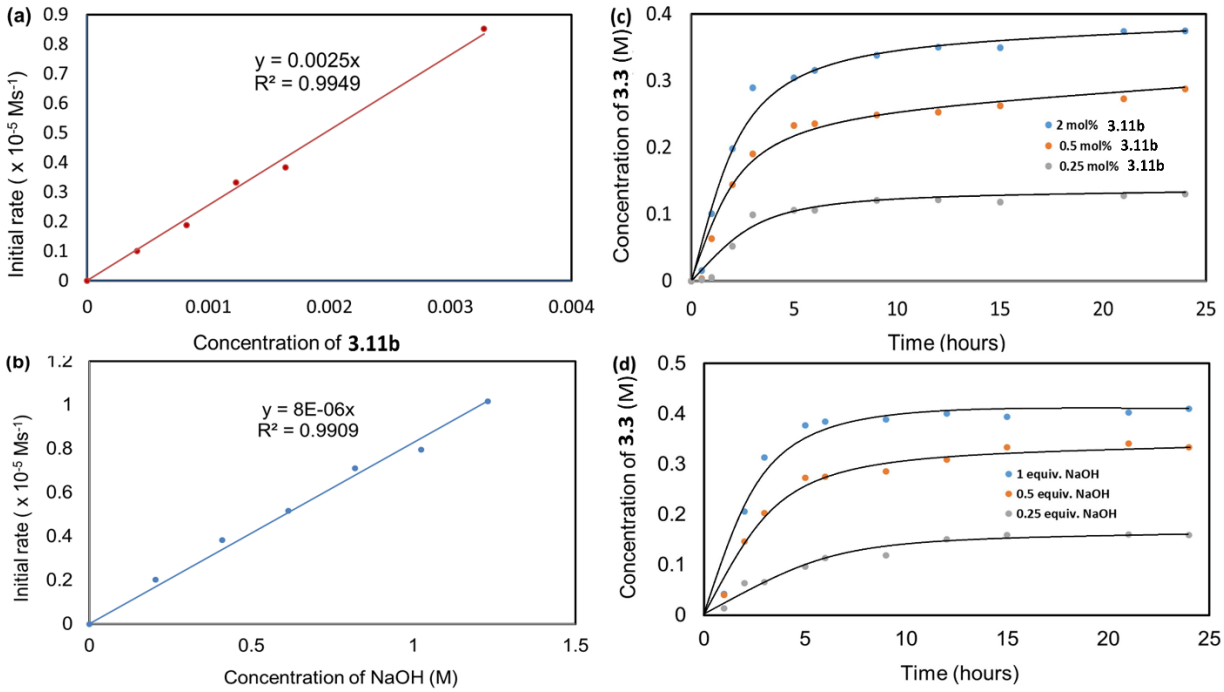

Figure 3.2. (a) Variation of the initial rate of formation of **3.3** with the concentration of **3.11b**(reaction conditions: 0.5 mmol of **3.1**, 0.25 mmol (10 mg) of NaOH, 0.5 mL toluene and 0.25 – 2 mol% (1.3 mg – 10.4 mg, 1.25 µmol - 10 µmol) **3.11b** at 140 °C for 24 h in a 15 mL pressure tube) (b) Variation of the initial rate of formation of **3.3** with the concentration of NaOH (reaction conditions: 0.5 mmol of **3.1**, 1 mol% (5.2 mg, 5µmol) **3.11b**, 0.5 mL toluene and 0.125 – 0.75 mmol (5 mg – 30 mg) of NaOH at 140 °C for 24 h in a 15 mL pressure tube). (c) Time profile for formation of **3.3** at various loadings to **3.11b** corresponding to reaction conditions described in (a) *vide supra*. (d) Time profile for formation of **3.3** at various loadings to NaOH corresponding to reaction conditions described in (b) *vide supra*.

(equation 3, Scheme 3.9) or in the absence (equation 4, Scheme 3.9) of catalyst **3.11b**. These observations indicate that the formation of alkene **3.2** starting from the aldehyde **3.1'** is typically uncatalyzed and base mediated.

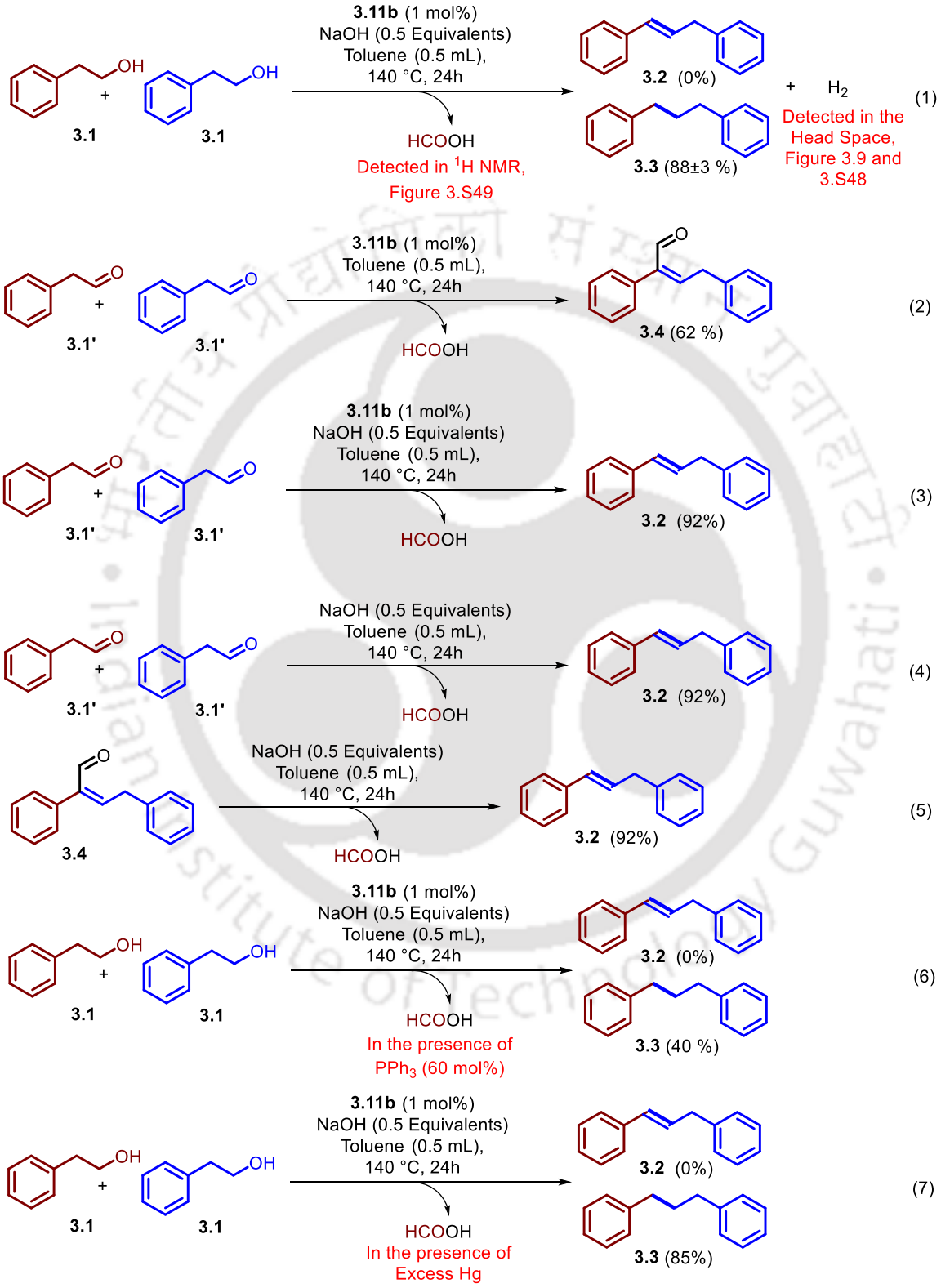

Scheme 3.9. Control experiments.

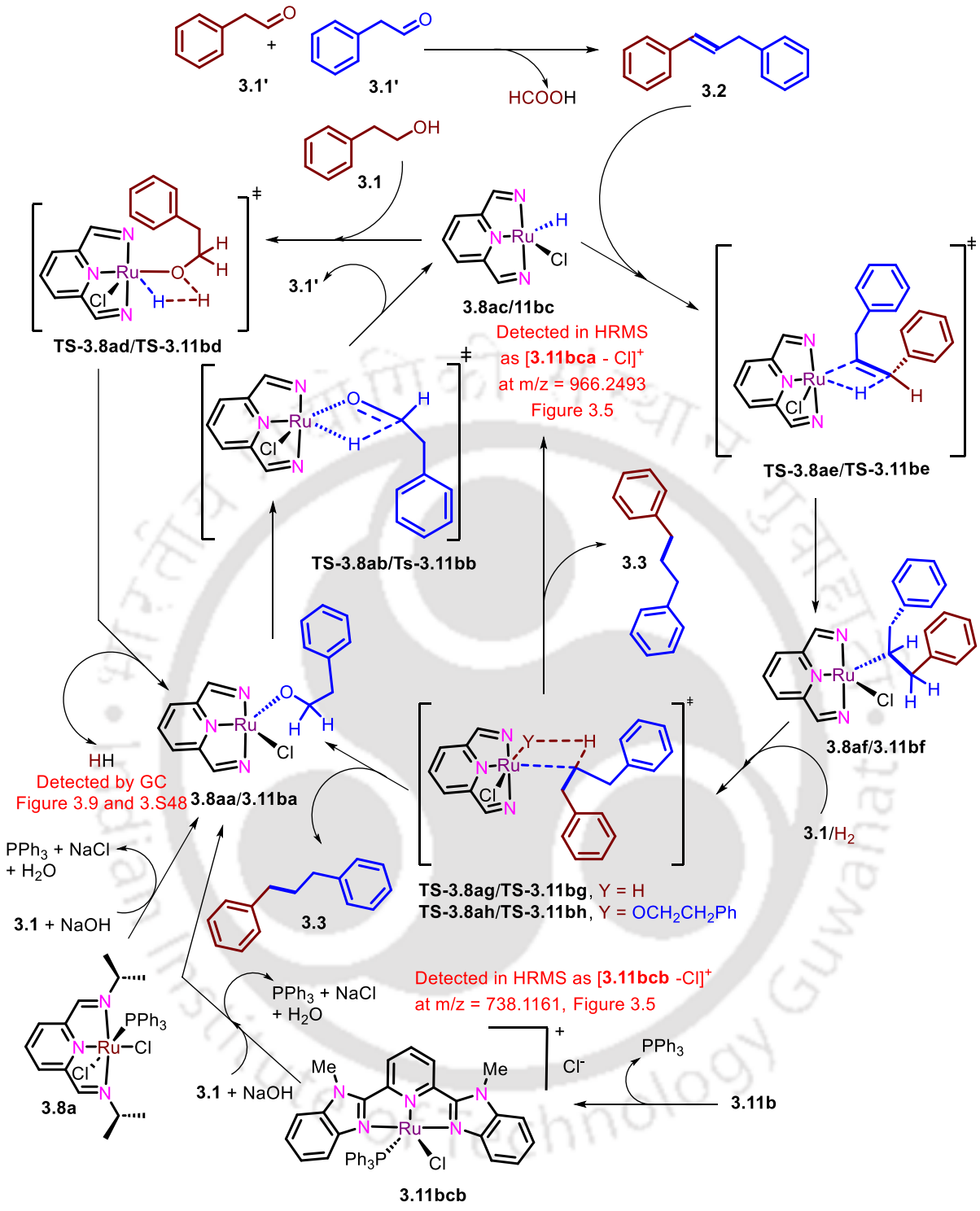

Scheme 3.10. Plausible mechanism involved in the **3.8a** and **3.11b** catalyzed decarboxylative transformation of **3.1** to **3.3**.

In the **3.11b** (1 mol%) catalyzed decarboxylation of **3.1** to **3.3** mediated by 0.5 equivalents of NaOH, while the presence of PPh_3 had a detrimental effect on the productivity (equation 6, Scheme 3.9), there was a negligible effect on overall activity upon addition of excess mercury

(equation 7, Scheme 3.9). The former observation is indicative of the key role that phosphine dissociation plays in the generation of the active catalyst **3.8ac**/**3.11bc** (Scheme 3.10) while the latter highlights the exclusively molecular homogeneous nature of the catalytic system.

Further evidence for the exclusive role of well-defined molecular nature of the catalyst system has been obtained from kinetic experiments that were conducted by varying the concentration of **3.11b**. Using the initial-rate method, it was observed that the rate of the **3.11b** catalyzed decarboxylation of **3.1** to **3.3** had a first-order dependence on the concentration of **3.11b** (Figure 3.2a and Figures 3.S38-S42). A linear dependence of rate on the concentration of NaOH was also observed by employing the initial rate method (Figure 3.2b and Figures 3.S43-S47).

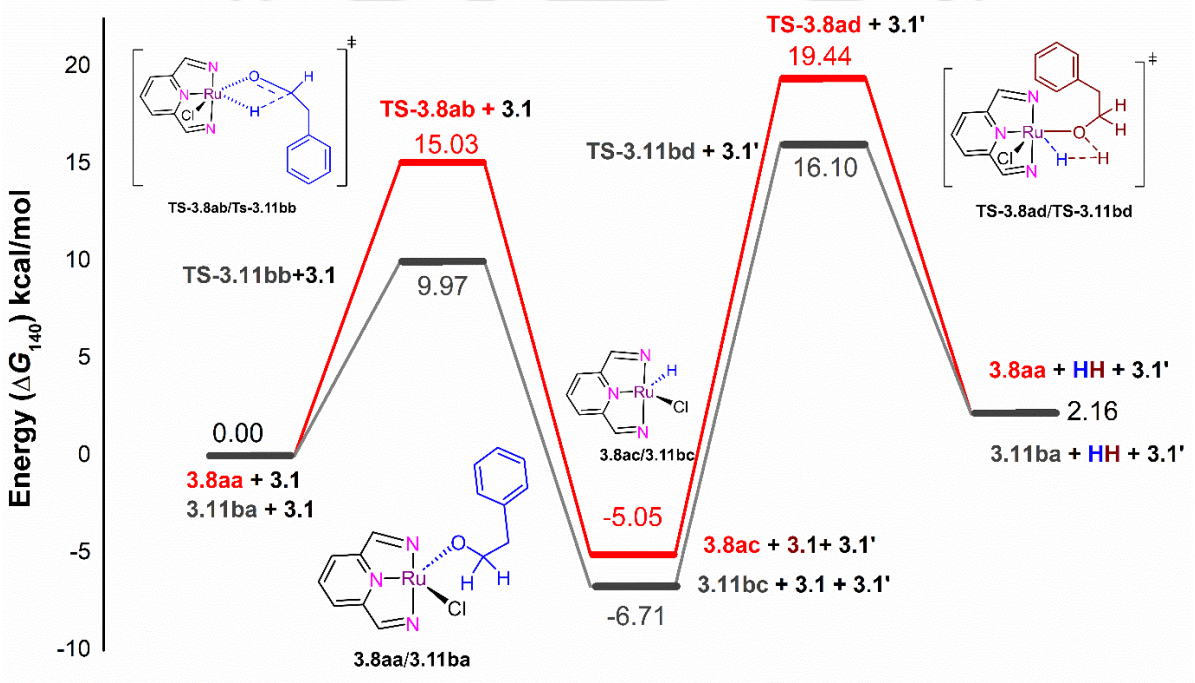

Figure 3.3. Free energy (ΔG_{140}) profile for the **3.8a** and **3.11b** catalyzed dehydrogenation of **3.1**.

The inferences drawn from the catalytic studies and control experiments have been instrumental in arriving at a plausible mechanism which is depicted in Scheme 3.10 where the pincer framework of the most efficient catalyst **3.11b** and the least efficient catalyst **3.8a** are represented only by their NNN ligating section for the sake of simplicity. One of the key events in the **3.8a**/**3.11b** decarboxylative upgradation of **3.1** to **3.3** is the dehydrogenation of **3.1** to the corresponding aldehyde **3.1'** which involves sequential *β*-hydride elimination from **3.8aa**/**3.11ba** followed by dehydrogenolysis (*σ*-bond metathesis) of **3.8ac**/**3.11bc** with **3.1** *via*

TS-3.8ab/**TS-3.11bb** and **TS-3.8ad**/**TS-3.11bd** respectively (Scheme 3.10). For the overall endergonic reaction (ΔG_{140} = 2.16 kcal/mol), both the β-hydride elimination and the σ-bond metathesis are kinetically favorable with the most efficient catalyst **3.11b** by 5.06 kcal/mol and 3.34 kcal/mol respectively when compared with the least efficient system based on **3.8a** (Figure 3.3). Notably, for the dehydrogenation of **3.1** catalyzed by **3.11b** and **3.8a**, the dehydrogenolysis is the rate-determining step (RDS) with a barrier of 22.81 kcal/mol and 24.49 kcal/mol respectively (Figure 3.3).

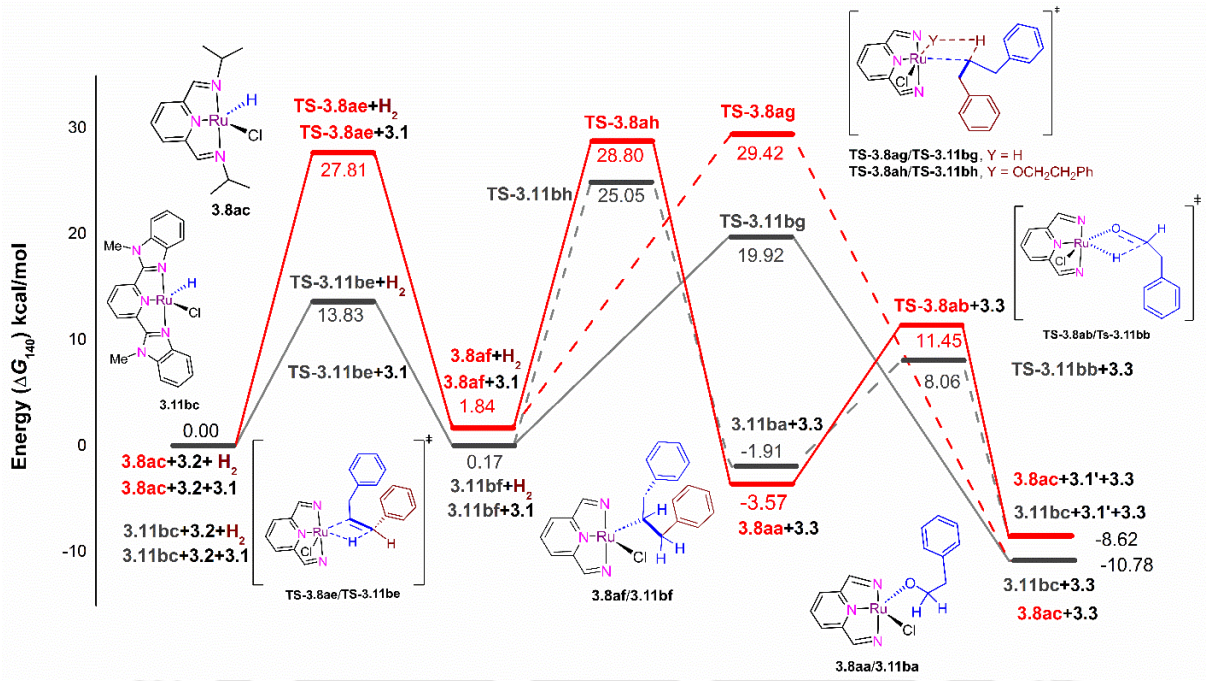

Figure 3.4. Free energy (ΔG_{140}) profile for the **3. 8a** and **3.11b** catalyzed hydrogenation of **3.2**.

In the presence of NaOH, the aldehyde **3.1'** undergoes a decarboxylative coupling (Scheme 3.1) to yield the internal olefin **3.2**. The olefin **3.2** could then insert into the Ru-H bond in **3.8ac**/**3.11bc** to yield the intermediate **3.8af**/**3.11bf** *via* **TS-3.8ae**/**TS-3.11be** (Scheme 3.10). While using **3.11b**, this step is almost thermodynamically neutral with a barrier of 13.83 kcal/mol. On the other hand, use of **3.8a** leads to an endergonic step (ΔG_{140} = 1.84 kcal/mol) with a high barrier of 27.81 kcal/mol (Figure 3.4). The intermediate **3.8af**/**3.11bf** either undergo an alcoholysis (**3.8af**/**3.11bf**→**TS-3.8ah**/**TS-11bh**→**8aa**/**11ba**→**TS-8ab**/**TS 11bb**→**8ac**/**11bc**) with a molecule of **3.1** or a hydrogenolysis (**3.8af**/**3.11bf**→**TS-3.8ag**/**TS-3.11bg**→**3.8ac**/**3.11bc**) with hydrogen to complete the catalytic cycle. Figure 3.4 shows that both the sub-steps **3.8af**/**3.11bf**→**TS-3.8ah**/**TS-3.11bh**→**3.8aa**/**3.11ba** and **3.8aa**/**3.11ba**→**TS-3.8ab**/**TS- 3.11bb**→**3.8ac**/**3.11bc** involved in the alcoholysis fragment are clearly kinetically more favored with **3.11b**.

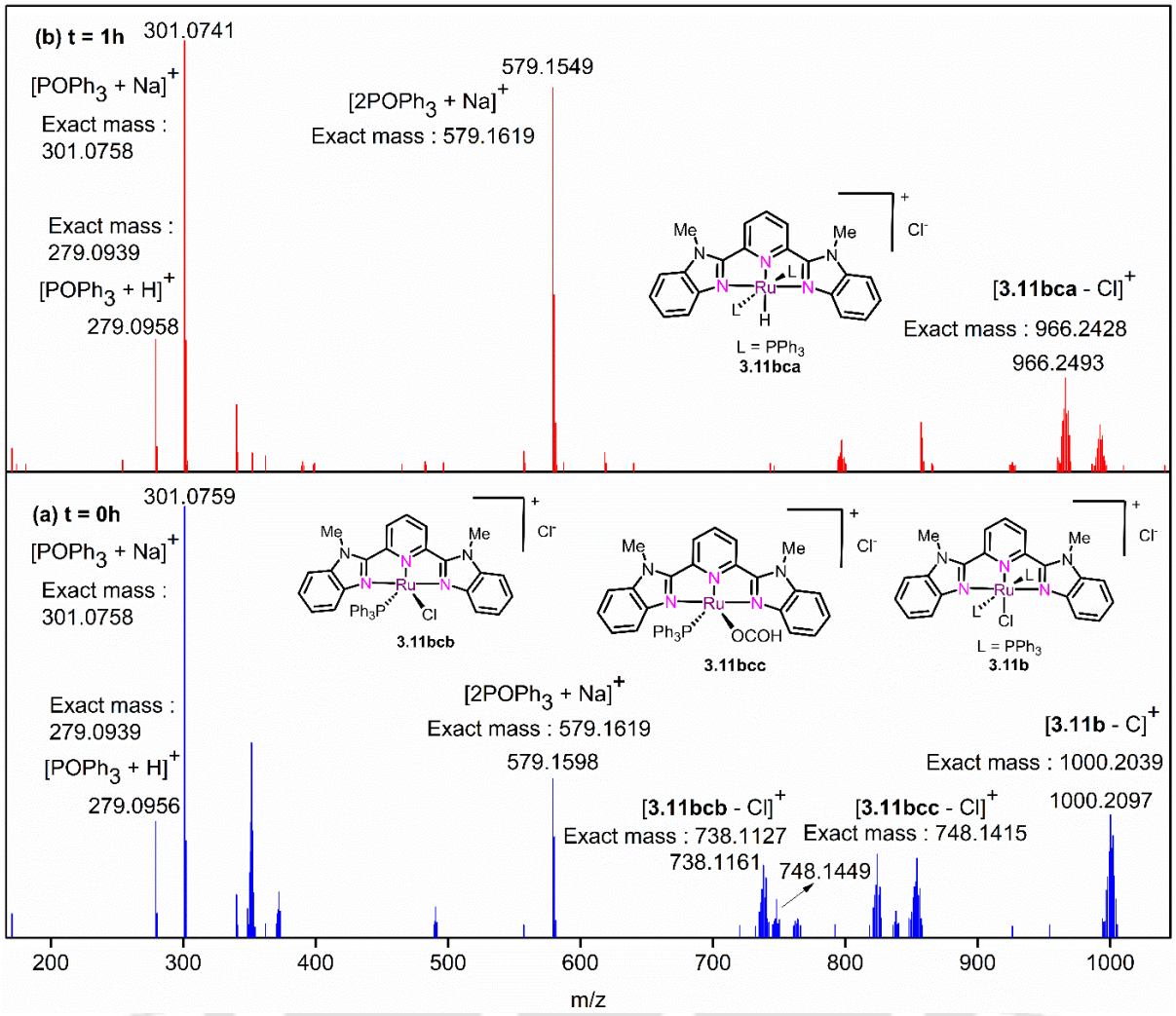

Figure 3.5. HRMS of the reaction mixture containing 2-phenylethanol (**3.1**) (0.6 mL, 0.5 mmol), NaOH (10 mg, 0.25 mmol), toluene (0.5 mL) and **3.11b** (5.2 mg, 5µmol) maintained at (a) room temperature (t = 0 h) and (b) 140 °C for 1 h.

Similarly, the barrier for hydrogenolysis using **3.11b** (**TS- 3.11bg**; $\Delta G_{140}^{\ddagger}$ = 19.75 kcal/mol) is much lower than the corresponding barrier with **3.8a** (**TS-3.8ag**; $\Delta G_{140}^{\ddagger}$ = 27.58 kcal/mol) (Figure 3.4). When one compares the cycle for the transformation **3.2→3.3** the path **3.8ac→TS-3.8ae→3.8af→TS-3.8ah→3.8aa→TS- 3.8ab→3.8ac** *via* the alcoholysis step is more favored than the hydrogenolysis path **3.8ac→TS-3.8ae→3.8af→TS-3.8ag→3.8ac** while using the relatively poor catalyst **3.8a** with the formation of **TS- 3.8ae** ($\Delta G_{140}^{\ddagger}$ = 27.81 kcal/mol) as the RDS (Figure 3.4). Further comparison with the rate-determining barrier (**TS-3.8ad**; $\Delta G_{140}^{\ddagger}$ = 24.49 kcal/mol) of the previous step **3.1→3.1'** (Figure 3.3), reveals that the formation of **TS-3.8ae** ($\Delta G_{140}^{\ddagger}$ = 27.81 kcal/mol, Figure 3.4) during the transformation **3.2→3.3** is the overall RDS for the **3.8b** catalyzed reaction.

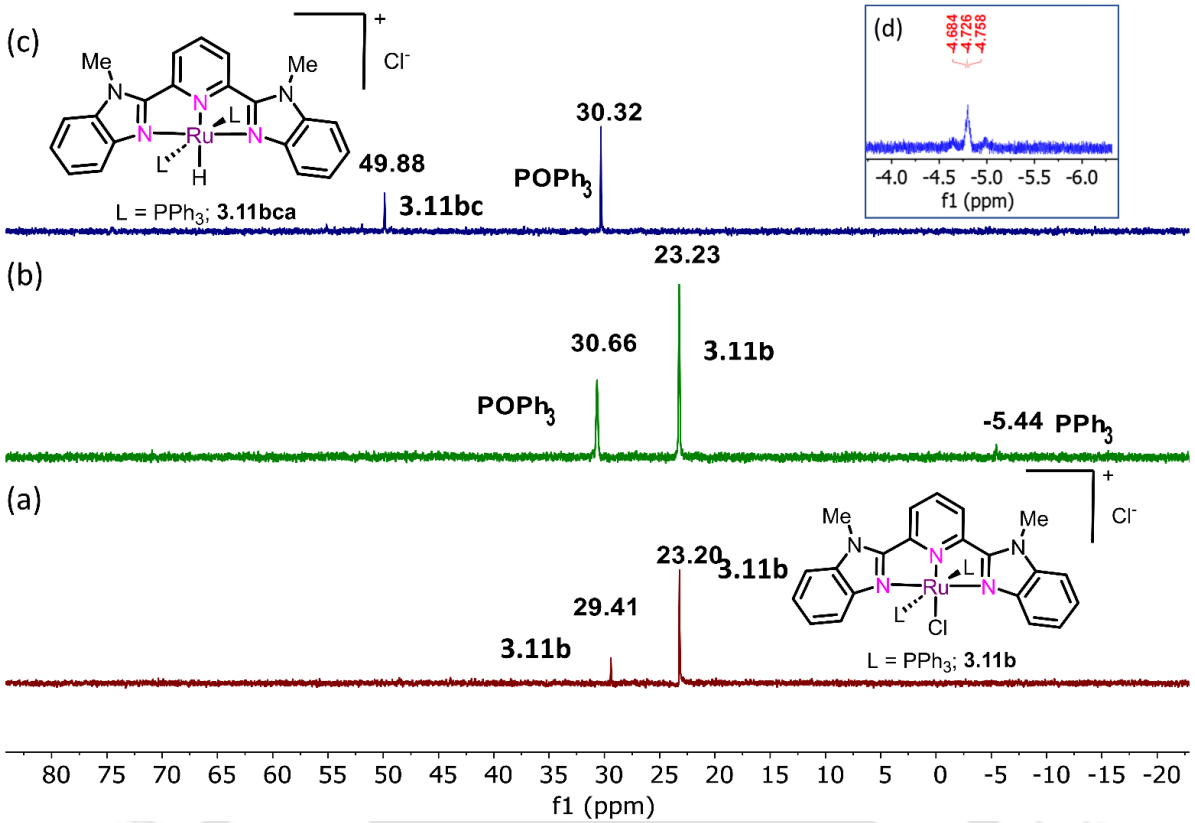

Figure 3.6. (a) The ^{31}P NMR spectrum of **3.11b** in $CDCl_3$. (b) The ^{31}P NMR spectrum of the reaction mixture containing 2-phenylethanol (**3.1**) (0.6 mL, 0.5 mmol), NaOH (10 mg, 0.25 mmol), **3.11b** (10.4 mg, 0.01 mmol) and toluene (0.5 mL) maintained at room temperature (t = 0 h) under air (c) The ^{31}P NMR spectrum of the reaction mixture containing 2-phenylethanol (**3.1**) (0.6 mL, 0.5 mmol), NaOH (10 mg, 0.25 mmol), **3.11b** (10.4 mg, 0.01 mmol) and toluene (0.5 mL) maintained at 140 °C (t = 5 min) under air (d) The hydride region of the ^{1}H NMR spectrum corresponding to reaction conditions provided in Figure 3.6c.

On the other hand, with the most efficient catalyst **3.11b**, the route **3.11bc→TS-3.11be→3.11bf→TS-3.11bg→3.11bc** involving the hydrogenolysis step is energetically more favorable than the alcoholysis path **3.11bc→TS-3.11be→3.11bf→TS-3.11bh→3.11ba→TS-3.11bb→3.11bc**, with the formation of **TS- 3.11bg** ($\Delta G_{140}^{\ddagger}$ = 19.75 kcal/mol) being the RDS (Figure 3.4). In the **3.11b** catalyzed reaction, as the rate-determining barrier for the step **3.2→3.3** (Figure 3.4) is 3.06 kcal/mol lower than the corresponding rate-determining barrier of the step **3.1→3.1'** (Figure 3.3), the formation of **TS-3.11bd** ($\Delta G_{140}^{\ddagger}$ = 22.81 kcal/mol) in the dehydrogenation step is the overall RDS. Gratifyingly, the intermediate **3.11bc** which has the lowest energy among the species involved in the RDS **3.11bc→TS-3.11bd→3.11ba** has been detected as its PPh_3 adduct **3.11bca** in the HRMS analysis (Figure 3.5) and NMR analysis

(Figure 3.6) of the reaction mixture under the optimized conditions (entry 6, Table 3.1 and entry 20, Table 3.2).

Clearly, the sterically more open catalyst **3.11b** has a lower overall rate-determining barrier (**TS-3.11bd**; $\Delta G_{140}^{\ddagger}$ = 22.81 kcal/mol) in comparison with the corresponding overall barrier (**TS-38ae**; $\Delta G_{140}^{\ddagger}$ = 27.81 kcal/mol) of the relatively bulky catalyst **3.8a**. Not surprisingly the **3.11b** outperforms **3.8a** both in terms of selectivity and productivity (entry 1 *vs.* entry 20, Table 3.2 and Table 3.S4) during the catalytic upgradation of lower-molecular weight alcohol **3.1** to higher-molecular weight alkane **3.3**.

3.4. Conclusion

A series of new and known NNN pincer-Ru catalysts of the type (^{R2}NNN)RuCl$_2$L (R = ^{i}Pr, ^{t}Bu, Cy, Ph, *p*-F-C$_6$H$_4$, *p*-OMe- C$_6$H$_4$ and L = PPh$_3$, CO and CH$_3$CN) based on *bis*(imino)pyridine ligands and [(^{RBim2}NNN)RuClL$_2$]Cl (R = H and Me, L = PPh$_3$ and CO) based on 2,6-*bis*(benzimidazole-2-yl)pyridine ligands have been utilized to examine the decarboxylative coupling of lower-molecular weight alcohols to higher-molecular weight alkanes.

While a majority of the considered pincer-Ru complexes including the Ru precursors failed to demonstrate good activity towards the formation of the desired alkane, 1 mol% of (^{MeBim2}NNN)RuCl$_2$(PPh$_3$)$_2$ based on 2,6-*bis*(benzimidazole- 2-yl)pyridine ligand demonstrated excellent activity giving up to 91% yield with 100% selectivity towards the alkane (1,3-diphenyl propane) starting from 2-phenyl ethanol within 5 h of reaction in the presence of 0.5 equivalents of NaOH in toluene at 140 °C.

Detailed mechanistic studies were indicative of the involvement of α, β-unsaturated aldehydes along with the evolution of hydrogen (detected by GC) and formic acid (detected by ^{1}H NMR) during the reaction. A first-order dependence of initial rate on both the catalyst concentration and the concentration of base was observed in the [(^{MeBim2}NNN)RuCl(PPh$_3$)$_2$]Cl catalysed transformation of 2-phenyl ethanol to 1,3-diphenyl propane. This points to the homogeneous and well-defined molecular nature of the catalyst which was also fortified by catalyst poisoning experiments with Hg.

DFT studies nicely complement the experimental findings and indicate that the dehydrogenolysis step leading to the formation of 2-phenyl acetaldehyde and the resting state

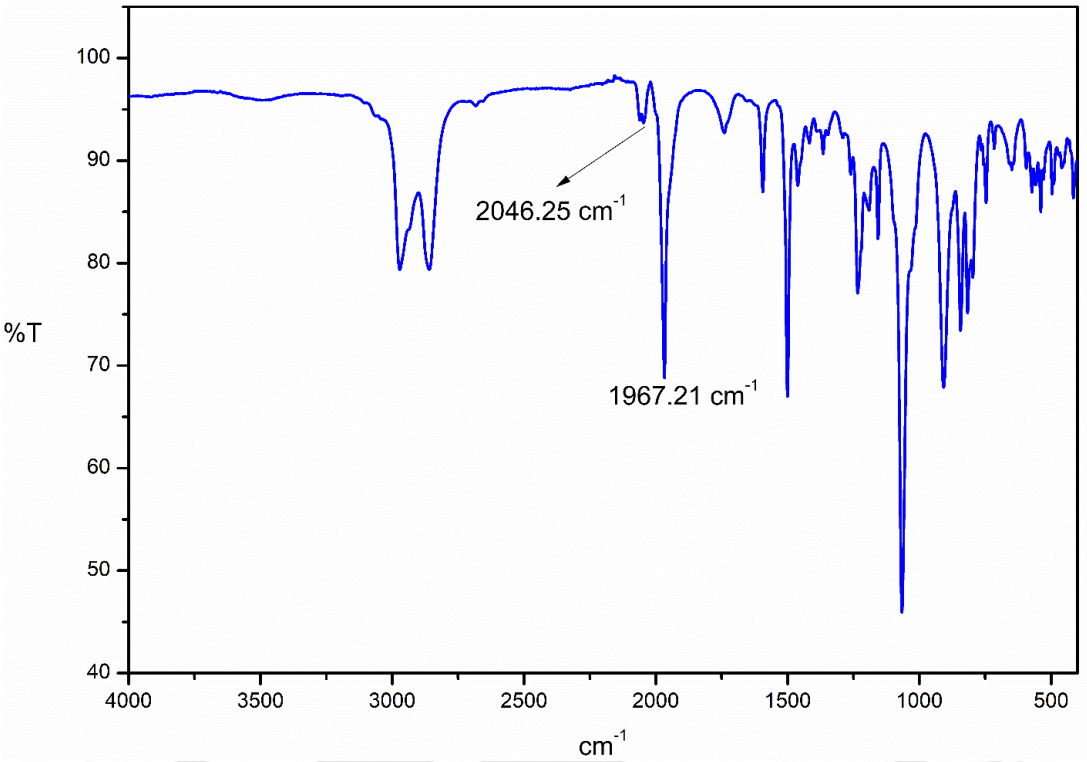

Figure 3.7: IR spectrum of **3.9e**.

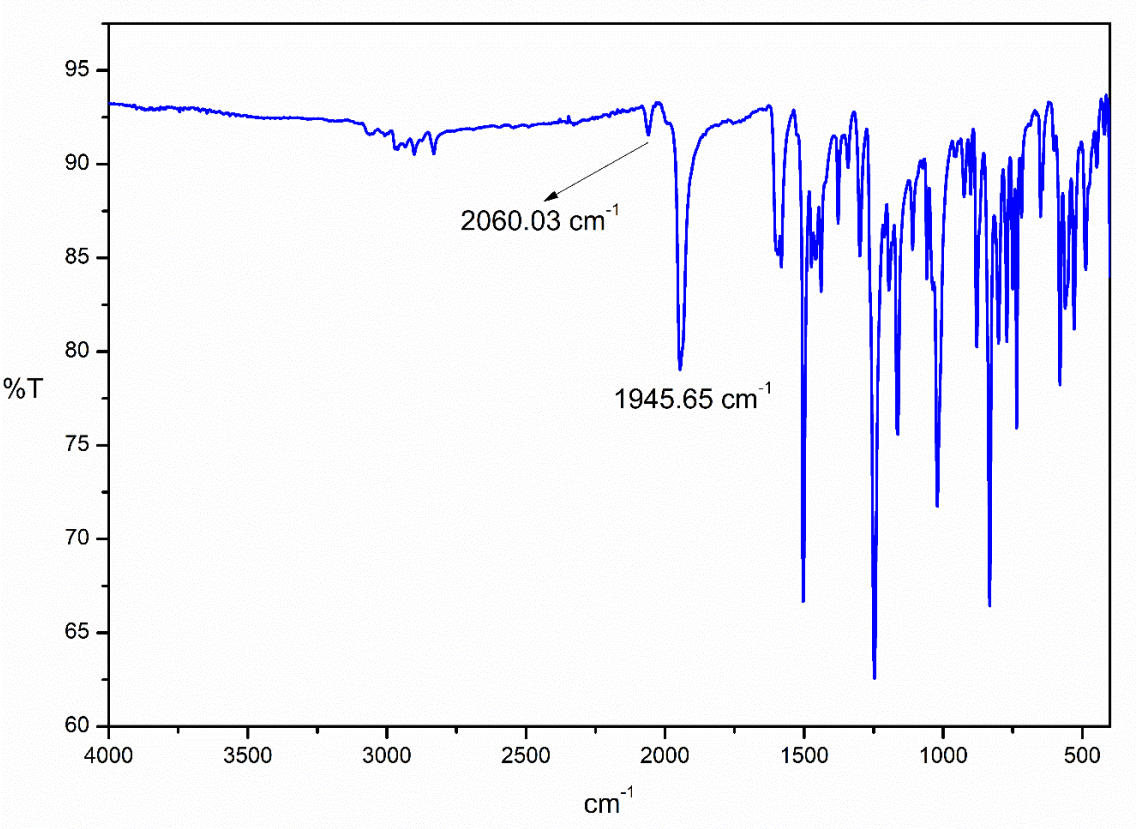

Figure 3.8: IR spectrum of **3.9f**.

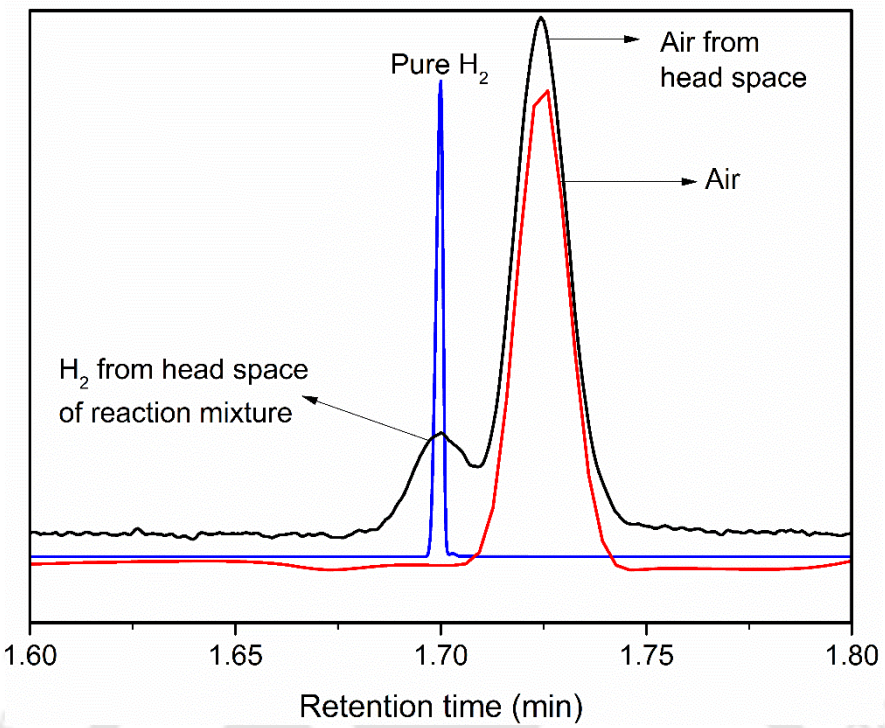

Figure 3.9: Evidence for the evolution of H_2 in dehydrogenation of 2-phenylethanol (**3.1**) catalyzed by **3.11b** (1 mol%) at 140 °C *via* GC analysis.

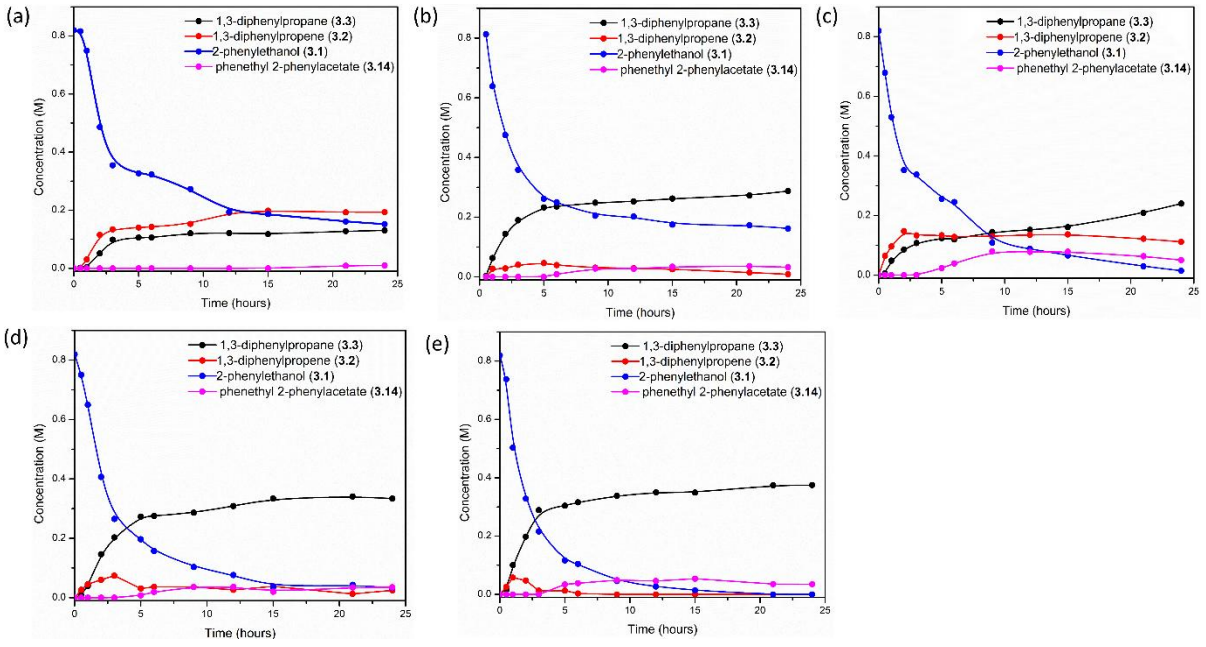

Figure 3.10: Time-profile of the decarboxylative coupling of 2-phenylethanols. Reaction condition: 0.5 mmol of **3.1**, 0.25 mmol (0.5 equivalents, 10 mg) NaOH, 0.5 mL toluene at 140 °C and (a) 1.25 µmol (1.3 mg, 0.25 mol%) **3.11b**, (b) 2.5 µmol (2.6 mg, 0.5 mol%) **3.11b,** (c) 3.75 µmol (3.9 mg, 0.75 mol%) **11b**, (d) 5 µmol (5.2 mg,1 mol%) **3.11b** and (e) 10 µmol (10.4 mg, 2 mol%) **3.11b.**

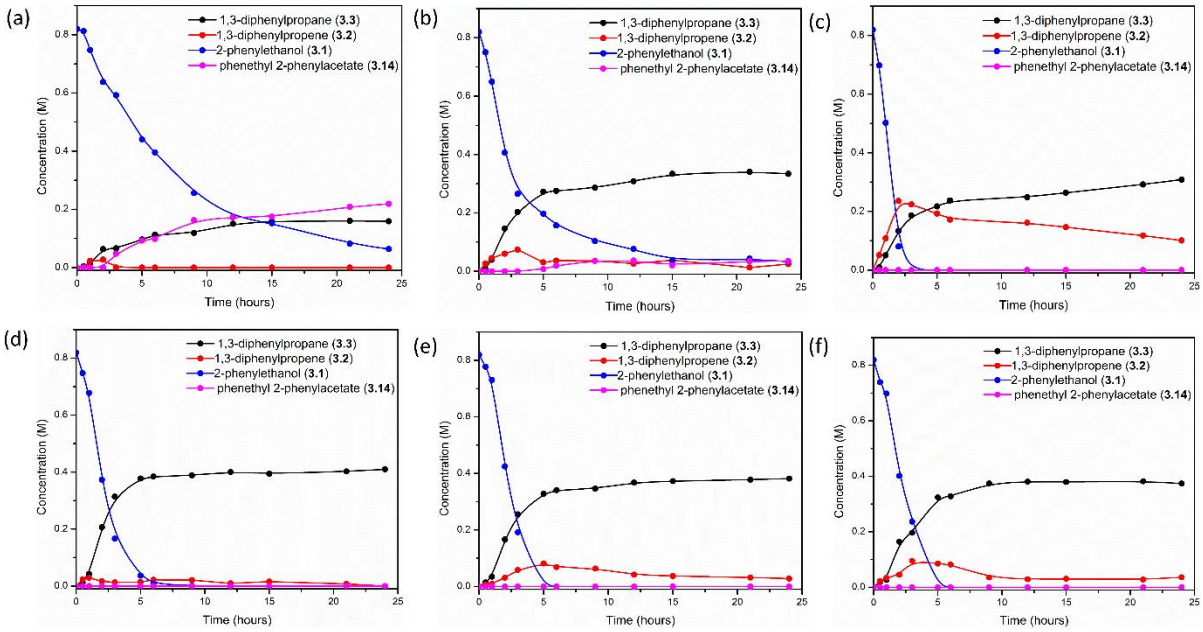

Figure 3.11: Time-profile of the decarboxylative coupling of 2-phenylethanols. Reaction condition: 0.5 mmol of **3.1**, 5 µmol (5.2 mg, 1 mol%) **3.11b**, 0.5 mL toluene at 140 °C and (a) (a) 0.125 mmol (5 mg, 0.25 equivalents) NaOH, (b) 0.25 mmol (10 mg, 0.5 equivalents) NaOH, (c) 0.375 mmol (15 mg, 0.75 equivalents) NaOH, (d) 0.5 mmol (20 mg, 1 equivalents) NaOH, (e) 0.625 mmol (25 mg, 1.25 equivalents) NaOH and (f) 0.75 mmol (30 mg, 1.5 equivalents) NaOH.

(^{MeBim2}NNN)RuHCl is the rate-determining step with a barrier of 22.81 kcal/mole at 140 °C. The resting state [(^{MeBim2}NNN)RuH(PPh_3)$_2$]Cl has been experimentally trapped as the PPh_3 adduct which has been detected by HRMS analysis and NMR studies. In comparison to the rate-determining dehydrogenolysis step of the cycle involving most active catalyst [(^{MeBim2}NNN)RuCl(PPh_3)$_2$]Cl, the corresponding cycle with the least active catalyst (^{iPr2}NNN)RuCl$_2$(PPh_3) involved insertion of 1,3-diphenyl propene into the Ru-H bond as the RDS which is kinetically unfavorable by 5.00 kcal/mol and gives only 14% of 1,3-diphenyl propane at 25% selectivity. To the best of our knowledge, this has been the first example of a Ru based catalyst for the upgradation of alcohols to alkanes directly without the need of an additional hydrogenation step. Selective production of jet-fuel-grade alkanes starting from lower-molecular weight alcohols in a single-step one-pot strategy has been demonstrated here which offers exciting avenues for catalytic production of jet-fuel-grade hydrocarbons.

3.5. Experimental section

3.5.1. General procedure and materials

All manipulations were carriedout under argon conditions. All the additives (NaOH, KOH, NaO^{t}Bu, KO^{t}Bu, Na_2CO_3, $NaHCO_3$, K_2CO_3, $KHCO_3$, Cs_2CO_3 and NaOEt), solvents (tetrahydrofuran, diethyl ether, hexane, toluene, $CDCl_3$ and DMSO-d_6), substrates (2-phenyl ethanol and their derivatives), the ruthenium precursors $[RuCl_2(p\text{-cymene})]_2$ and $RuCl_3.xH_2O$ were purchased either from Sigma−Aldrich or MERCK or Alfa Aeser and used as such. All catalytic reactions were carried out in air using oven-dried glassware. The solvent such as tetrahydrofuran, diethyl ether, toluene and hexane were dried *via* double distillation over Na/ benzophenone prior to the experiment[25]

3.5.2. Physical Measurements

^1H, $^{13}C\{^1H\}$, ^{19}F and ^{31}P NMR spectra were recorded on a Bruker ASCEND 600 operating at 600 MHz for ^1H, 150 MHz for $^{13}C\{1H\}$, 564 MHz for ^{19}F and at 243 MHz for ^{31}P or on a Bruker AVANCE 500 operating at 500 MHz for ^1H, 125 MHz for $^{13}C\{H\}$, 470 MHz for ^{19}F and at 203 MHz for ^{31}P or on a Bruker AVANCE 400 operating at 400 MHz for ^1H, 100 MHz for $^{13}C\{^1H\}$, 377 MHz for ^{19}F and at 162 MHz for ^{31}P. Chemical shifts (δ) are reported here in ppm, spin – spin coupling constant (J) are expressed in Hz and the peak multiplicity is reported as s – singlet, d – doublet, t – triplet, m – multiple and q – quartet. FT-IR spectra were recorded using a PerkinElmer spectrophotometer. X-ray crystallographic data were acquired on a Bruker D8 Venture single-crystal X-ray diffractometer using graphite monochromated Mo Kα radiation. The data refinement and cell reductions were carried out by the Bruker SAINT program.[24] Structures were further solved and refined by the full matrix least squares method using SHELXL-14.25 HRMS measurements were done using an Agilent Accurate-Mass Q-TOF ESI–MS 6520. GC-MS analysis was carried out on an Agilent 5977B GC/MSD. GC analysis were performed on an Agilent 7820 – GC instrument fitted with an Agilent Front SS7 inlet N2 HP – PLOT Q column (30 m × 530 μm × 40 μm) using the following methods. Agilent 7820 – GC back detector, Detector temperature (TCD): 250 °C, Detector temperature (FID): 300 °C, Inlet temperature: 40 °C, Time at starting temp: 0 min, ramp: 40 °C/min upto 250 °C, Hold time = 5 min, Flow rate (carrier): 25 mL/min (N_2), Split ratio: 195. The homo-coupled derivatives of **3.3** were separated using Combi*Flash* NextGen 100 System and hetero-coupled derivatives were separated using column chromatography.

3.5.3. General procedure for pincer-ruthenium catalyzed decarboxylative homo-coupling of 2-phenyl ethanol (3.1)

A 15 mL pressure tube containing **3.11b** (5.2 mg, 5 μmol), NaOH (10 mg, 0.25 mmol), 2-phenyl ethanol (60 μL, 0.5 mmol) and toluene (0.5 mL) under air was sealed and the reaction mixture was heated at 140 °C for 24 h. The reaction mixture was then cooled to room temperature and mesitylene (50 μL) was added with constant stirring. An aliquot (typically 10 mg) was withdrawn from reaction mixture and added to a NMR tube containing $CDCl_3$ (0.5 mL). The yield was determined by ^1H NMR using mesitylene as a standard.[26] The reaction mixture was then diluted with water and washed with dichloromethane. The organic layer was separated and dried over anhydrous Na_2SO_4. The solvent was subsequently removed under reduced pressure. The crude product was then purified using flash chromatography system with a column containing 230-400 mesh silica using hexane as eluent.

3.5.4. General procedure for pincer-ruthenium catalyzed decarboxylative hetero-coupling of 2-phenyl ethanol (3.1)

A 15 mL pressure tube containing **3.11b** (26 mg, 25 μmol), NaOH (50 mg, 0.25 mmol), 2-phenyl ethanol or it's derivative (2 mmol) and another 2-phenyl ethanol derivative (0.5 mmol) in toluene (2 mL) under air was sealed and the reaction mixture was heated at 140 °C for 24 h. The reaction mixture was then cooled to room temperature and mesitylene (50 μL, 0.359 mmol) was added with constant stirring. An aliquot (typically 10 mg) was withdrawn from reaction mixture and added to a NMR tube containing $CDCl_3$ (0.5 mL. The yield was determined by 1H NMR using mesitylene as a standard.[26] The reaction mixture was then diluted with water and washed with dichloromethane. The organic layer was collected and dried over anhydrous Na_2SO_4. The solvent was subsequently removed under reduced pressure. The crude product was then purified by column chromatography using 230-400 mesh silica with hexane as eluent.

3.5.5. General procedure for 3.11b catalyzed decarboxylative coupling of 2-phenyl ethanol (3.1)– kinetic study

(a) Catalyst (3.11b) loading variation

To five 15 mL pressure tubes containing 2-phenyl ethanol (60 μL, 0.5 mmol), NaOH (10 mg, 0.25 mmol), toluene (0.5 mL) and the internal standard mesitylene (50 μL, 0.359 mmol) under air various amounts of catalyst **3.11b** (1.3 – 10.4 mg,1.25 - 10 μmol) were added and sealed.

The reaction mixtures were heated at 140 °C for 24 h. At regular intervals (Figure 3.S38 – Figure 3.S42, Figure 3.10) an aliquot (typically 10 mg) was withdrawn from each of the reaction mixtures and added to a NMR tubes containing $CDCl_3$ (0.5 mL). The yield was determined by ^1H NMR using mesitylene as a standard.[26]

(b) Base loading variation

To six 15 mL pressure tubes containing 2-phenyl ethanol (60 µL, 0.5 mmol), **3.11b** (5.2 mg, 5 µmol), toluene (0.5 mL) and the internal standard mesitylene (50 µL, 0.359 mmol) under air, various amounts of NaOH (5 – 30 mg, 0.125 – 0.75 mmol) were added and sealed. The reaction mixtures were heated at 140 °C for 24 h. At regular intervals (Figure 3.S41 and Fugure 3.S43 – Figure 3.S47, Figure 3.11) an aliquot (typically 10 mg) was withdrawn from each of the reaction mixtures and added to NMR tubes containing $CDCl_3$ (0.5 mL). The yield was determined by ^1H NMR using mesitylene as a standard.[26]

3.5.6. Synthesis of ($(p\text{-F-C6H4})_2$NNN)$RuCl_2$(CO) (3.9e)

In a 10 ml pear shaped flask, [Ru(*p*-cymene)Cl_2]$_2$ (0.060 g, 0.0979 mmol) and the ligand **3.13e** (0.0629 g, 0.1959 mmol) were dissolved in dry and distilled THF (5 mL) and the solution was refluxed for 16 h under a CO atmosphere. The solvent was evaporated under reduced pressure, and the brown-coloured solid was washed with diethyl ether (5 × 4 mL). The resulting residue was dried under vacuum and isolated as a brown solid (0.087 g) in 85% yield. ^1H NMR (600 MHz, $CDCl_3$, 25 °C) δ 8.02 (s, 2H), 7.95 (t, J = 7.8 Hz, 1H), 7.83 (d, J = 7.8 Hz, 2H), 7.57 (dd, J = 8.8, 4.7 Hz, 4H), 7.12 (t, J = 8.5 Hz, 4H). ^{19}F NMR (565 MHz, $CDCl_3$, 25 °C) δ -110.74. $^{13}C\{^1H\}$ NMR (151 MHz, $CDCl_3$, 25 °C) δ 201.15, 164.05, 163.61, 162.39, 156.82, 148.69, 148.66, 138.91, 124.96, 123.69, 123.63, 116.66, 116.51. Molecular weight: 521.3108, HRMS (ESI): m/z calculated for [**3.9e** – Cl]$^+$ = $[C_{20}H_{13}ClF_2N_3ORu]^+$: 485.9759, found 485.9749; m/z calculated for [(**3.9e** – Cl + CH_3CN]$^+$ = $[C_{22}H_{16}ClF_2N_4ORu]^+$: 527.0024, found 527.0020; m/z calculated for [**3.9e1** – Cl]$^+$ = $[C_{38}H_{26}ClF_4N_6Ru]^+$: 779.0887, found 779.0895; m/z calculated for [**3.9f2** – $RuCl_4$]$^{2+}$ = $[C_{38}H_{26}F_4N_6Ru]^{2+}$: 372.0599, found 372.0595.

3.5.7. Synthesis of ($(p\text{-OMe-C6H4})_2$NNN)$RuCl_2$(CO) (3.9f)

In a 10 ml pear shaped flask, [Ru(*p*-cymene)Cl_2]$_2$ (0.060 g, 0.0979 mmol) and the ligand **3.13f** (0.0676 g, 0.1959 mmol) were dissolved in dry and distilled THF (5 mL) and the solution was refluxed for 16 h under a CO atmosphere. The solvent was evaporated under reduced pressure,

and the brown-coloured solid was washed with diethyl ether (5 × 4 mL). The resulting residue was dried under vacuum and isolated as a brown solid (0.085 g) in 80% yield. ^{1}H NMR (600 MHz, DMSO-d_6, 25 °C) δ 8.43 (s, 2H), 8.27– 8.23 (m, 1H), 8.13 (d, J = 7.7 Hz, 2H), 7.56 (d, J = 9.0 Hz, 4H), 7.07 (d, J = 9.0 Hz, 4H), 3.83 (s, 6H). ^{13}C{^{1}H} NMR (151 MHz, DMSO-d_6, 25 °C) δ 204.13, 165.74, 160.00, 156.00, 145.36, 139.99, 126.01, 123.31, 114.23, 55.65. Molecular weight: 545.3820, HRMS (ESI): m/z calculated for [**3.9f** – Cl]$^{+}$ = $[C_{22}H_{19}ClN_3O_3Ru]^{+}$: 510.0158, found 510.0155; m/z calculated for [(**3.9f** – Cl + CH_3CN]$^{+}$ = $[C_{24}H_{22}ClN_4O_3Ru]^{+}$: 551.0424, found 551.0440; m/z calculated for [**3.9f1** – Cl]$^{+}$ = $[C_{42}H_{38}ClN_6O_4Ru]^{+}$: 827.1687, found 827.1733; m/z calculated for [**3.9f2** – $RuCl_4$]$^{2+}$ = $[C_{42}H_{38}N_6O_4Ru]^{2+}$: 396.0999, found 396.1007.

3.5.8. Synthesis of (^{t}Bu^{2}NNN)RuCl$_2$(NCCH$_3$) (3.10b)

In a 10 ml pear shaped flask, [Ru(*p*-cymene)Cl_2]$_2$ (0.060 g, 0.0979 mmol) and the ligand **3.13b** (0.048 g, 0.1959 mmol) were dissolved in dry and distilled acetonitrile (5 mL) and the solution was refluxed for 16 h. The solvent was evaporated under reduced pressure, and the brown-coloured solid was washed with diethyl ether (5 × 4 mL). The resulting residue was dried under vacuum and isolated as a brown solid (0.075 g) in 84% yield. ^{1}H NMR (400 MHz, $CDCl_3$, 25 ^{o}C) δ 8.29 (s, 2H), 7.64 (d, J = 7.8 Hz, 2H), 7.49 (t, J = 7.8 Hz, 1H), 2.86 (s, 3H), 1.65 (s, 18H). ^{13}C{^{1}H} NMR (151 MHz, $CDCl_3$, 25 °C) δ 162.22, 159.14, 129.26, 126.38, 123.79, 66.50, 30.14, 5.08. Molecular weight: 458.3930, HRMS (ESI): m/z calculated for [**3.10b** – Cl]$^{+}$ = $[C_{17}H_{26}ClN_4Ru]^{+}$: 423.0889, found 423.0893.

3.5.9. Synthesis of ((*p*-F-C6H4)^{2}NNN)RuCl$_2$(NCCH$_3$) (3.10e)

In a 10 ml pear shaped flask, [Ru(*p*-cymene)Cl_2]$_2$ (0.060 g, 0.0979 mmol) and the ligand **3.13e** (0.0629 g, 0.1959 mmol) were dissolved in dry and distilled acetonitrile (5 mL) and the solution was refluxed for 16 h. The solvent was evaporated under reduced pressure, and the brown-coloured solid was washed with diethyl ether (5 × 4 mL). The residue was dried under vacuum and isolated as a brown solid (0.084 g) in 80 % yield. NMR analysis shows the presence of two isomers as cis (minor, $NCCH_3$ ligand *trans* to one of the Cl ligands) and *trans* (major, $NCCH_3$ ligand *trans* to pyridyl N) in 1:1.33 ratio. ^{1}H NMR (600 MHz, $CDCl_3$, 25 °C) δ 8.56 (s, 2H), 8.41 (s, 2H), 8.10 (d, J = 7.5 Hz, 2H), 7.80 (s, 1H), 7.79 – 7.72 (m, 5H), 7.70 (dd, J = 8.7, 4.9 Hz, 3H), 7.55 (t, J = 7.8 Hz, 1H), 7.16 (t, J = 8.1 Hz, 4H), 7.11 (t, J = 8.6 Hz, 3H), 2.51 (s, 3H), 2.44 (s, 2H). ^{19}F NMR (565 MHz, $CDCl_3$, 25 °C) δ -111.61, -113.31. ^{13}C{^{1}H} NMR (151 MHz,

$CDCl_3$, 25 °C) δ 166.51, 163.80, 163.45, 162.77, 162.13, 161.81, 161.15, 147.89, 147.87, 146.74, 146.73, 134.13, 129.21, 124.98, 124.92, 124.79, 124.73, 123.83, 116.45, 116.30, 115.97, 115.81, 4.77, 4.50. Molecular weight: 534.3538, HRMS (ESI): m/z calculated for [**3.10e** – Cl]$^+$ = $[C_{21}H_{16}ClF_2N_4Ru]^+$: 499.0075, found 499.0051; m/z calculated for [(**3.10e** – Cl + $CH_3CN]^+$ = $[C_{23}H_{19}ClF_2N_5Ru]^+$: 540.0340, found 540.0270.

3.5.10. Synthesis of ($^{(p\text{-OMe-C6H4})2}$NNN)$RuCl_2(NCCH_3)$ (3.10f)

In a 10 ml pear shaped flask, [Ru(*p*-cymene)$Cl_2]_2$ (0.060 g, 0.0979 mmol) and the ligand **3.13f** (0.0676 g, 0.1959 mmol) were dissolved in dry and distilled acetonitrile (5 mL) and the solution was refluxed for 16 h. The solvent was evaporated under reduced pressure, and the brown-coloured solid was washed with diethyl ether (5 × 4 mL). The residue was dried under vacuum and isolated as a brown solid (0.083 g) in 76% yield. ^{1}H NMR (600 MHz, DMSO-d_6, 25 °C) δ 8.49 (s, 2H), 8.07 (d, J = 7.9 Hz, 2H), 7.92 (t, J = 7.9 Hz, 1H), 7.47 (d, J = 8.9 Hz, 4H), 7.00 (d, J = 8.9 Hz, 4H), 3.80 (s, 6H), 3.34 (s, 4H). ^{13}C{^{1}H} NMR (151 MHz, DMSO-d_6, 25 °C) δ 167.64, 166.43, 159.05, 147.19, 142.89, 126.21, 124.66, 123.01, 114.20, 113.37, 55.48. Molecular weight: 558.4250, HRMS (ESI): m/z calculated for [**3.10f** – Cl]$^+$ = $[C_{23}H_{22}ClN_4O_2Ru]^+$: 523.0475, found 523.0460; m/z calculated for [(**3.10f** – Cl + $CH_3CN]^+$ = $[C_{25}H_{25}ClN_5O_2Ru]^+$: 564.0740, found 564.0724.

3.5.11. Characterization of the products

3.3

1,3-diphenylpropane (3.3).[15,17] Colourless liquid, ^{1}H NMR (600 MHz, $CDCl_3$) δ 7.32 (t, *J* = 8.3 Hz, 4H, Ar), 7.22 (d, *J* = 7.3 Hz, 6H, Ar), 2.69 (t, *J* = 7.7 Hz, 4H, -CH_2Ar), 2.00 (t, *J* = 7.7 Hz, 2H, -CH_2). ^{13}C{^{1}H} NMR (151 MHz, $CDCl_3$) δ 142.43, 128.58, 128.44, 125.87 (Ar), 35.58 (-CH_2Ar), 33.08 (-CH_2). GC-MS [M]$^+$: 196.1.

3.3a

1,3-bis(4-methoxyphenyl)propane (3.3a).[15,17] Colourless liquid, ^{1}H NMR (600 MHz, $CDCl_3$) δ 7.10 (d, *J* = 8.5 Hz, 4H, Ar), 6.83 (d, *J* = 8.6 Hz, 4H, Ar), 3.79 (s, 6H, -OMe), 2.61 – 2.55 (m, 4H, -CH_2Ar), 1.93 – 1.86 (m, 2H, -CH_2). ^{13}C{^{1}H} NMR (151 MHz, $CDCl_3$) δ 157.83, 134.59, 129.44, 113.85 (Ar), 55.39 (-OMe), 34.58 (-CH_2Ar), 33.55 (-CH_2). GC-MS $[M]^+$: 256.1.

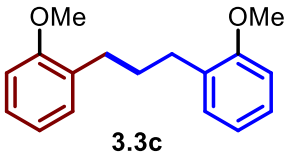

3.3c

1,3-bis(2-methoxyphenyl)propane (3.3c). Colourless liquid, ^{1}H NMR (400 MHz, $CDCl_3$) δ 7.23 – 7.17 (m, 2H, Ar), 6.81 – 6.72 (m, 6H, Ar), 3.80 (s, 6H, -OMe), 2.64 (t, *J* = 7.8 Hz, 4H, -CH_2Ar), 2.02 – 1.91 (m, 2H, -CH_2). ^{13}C{^{1}H} NMR (151 MHz, $CDCl_3$) δ 159.82, 144.08, 129.39, 121.05, 114.41, 111.22 (Ar), 55.29 (-OMe), 35.61 (-CH_2Ar), 32.78 (-CH_2). GC-MS $[M]^+$: 256.1.

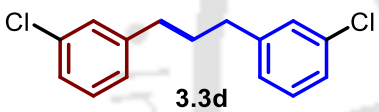

3.3d

1,3-bis(3-chlorophenyl)propane (3.3d).[17] Colourless liquid, ^{1}H NMR (400 MHz, $CDCl_3$) δ 7.24 – 7.13 (m, 6H, Ar), 7.05 (dt, *J* = 7.3, 1.7 Hz, 2H, Ar), 2.62 (t, *J* = 7.7 Hz, 4H, -CH_2Ar), 1.94 (p, *J* = 7.7 Hz, 2H, -CH_2). ^{13}C{^{1}H} NMR (151 MHz, $CDCl_3$) δ 144.10, 134.24, 129.75, 128.67, 126.76, 126.21 (Ar), 35.10 (-CH_2Ar), 32.58 (-CH_2). GC-MS $[M]^+$: 264.0.

3.3f

1,3-bis(4-chlorophenyl)propane(3.3f).[15,17] Colourless liquid, ^{1}H NMR (400 MHz, $CDCl_3$) δ 7.26 – 7.22 (m, 4H, Ar), 7.12 – 7.06 (m, 4H, Ar), 2.62 – 2.57 (m, 4H, -CH_2Ar), 1.90 (p, *J* = 7.6 Hz, 2H, -CH_2). ^{13}C{^{1}H} NMR (151 MHz, $CDCl_3$) δ 140.54, 131.68, 129.89, 128.58 (Ar), 34.71 9-CH_2Ar), 32.87 (-CH_2). GC-MS $[M]^+$: 264.0.

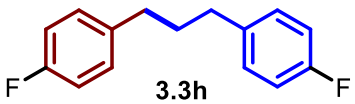

3.3h

1,3-bis(4-fluorophenyl)propane(3.3h).[15,17] Colourless liquid, ^{1}H NMR (600 MHz, $CDCl_3$) δ 7.15 – 7.10 (m, 4H, Ar), 6.97 (t, *J* = 8.7 Hz, 4H, Ar), 2.61 (t, *J* = 7.7 Hz, 4H, -CH_2Ar), 1.94 – 1.88 (m, 2H, -CH_2). ^{19}F NMR (565 MHz, $CDCl_3$) δ -117.81. ^{13}C{^{1}H} NMR (151 MHz, $CDCl_3$) δ 162.18, 160.57, 137.82, 137.80, 129.86, 129.81, 115.26, 115.12 (Ar), 34.59 (-CH_2Ar), 33.36 (-CH_2). GC-MS $[M]^+$: 232.1.

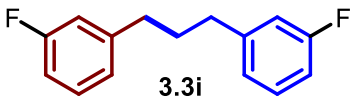

3.3i

1,3-bis(3-fluorophenyl)propane(3.3i). Colourless liquid, ^{1}H NMR (600 MHz, $CDCl_3$) δ 7.11 (dd, *J* = 8.4, 5.6 Hz, 4H, Ar), 6.99 – 6.93 (m, 4H, Ar), 2.60 (t, *J* = 7.7 Hz, 4H, -CH_2Ar), 1.92 – 1.87 (m, 2H, -CH_2). ^{19}F NMR (565 MHz, $CDCl_3$) δ -117.83. ^{13}C{^{1}H} NMR (151 MHz, $CDCl_3$) δ 160.57, 137.79, 129.86, 129.81, 115.26, 115.12 (Ar), 34.59 (-CH_2Ar), 33.36 (-CH_2). GC-MS $[M]^+$: 232.1.

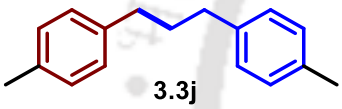

3.3j

1,3-di-*p*-tolylpropane (3.3j). [15,17] Colourless liquid, ^{1}H NMR (600 MHz, $CDCl_3$) δ 7.10 (d, *J* = 9.6 Hz, 8H, Ar), 2.62 (t, *J* = 7.7 Hz, 4H, -CH_2Ar), 2.33 (s, 6H), 1.97 – 1.90 (m, 2H, -CH_3Ar). ^{13}C{^{1}H} NMR (151 MHz, $CDCl_3$) δ 139.41, 135.24, 129.10, 128.46 (Ar), 35.11 (-CH_2Ar), 33.29 (-CH_3Ar), 21.14 (-CH_2). GC-MS $[M]^+$: 224.1.

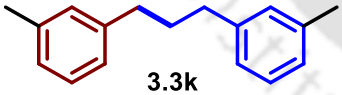

3.3k

1,3-di-*m*-tolylpropane (3.3k).[15] Colourless liquid, ^{1}H NMR (600 MHz, $CDCl_3$) δ 7.20 – 7.15 (m, 2H, Ar), 7.03 – 6.97 (m, 6H, Ar), 2.62 (t, *J* = 7.8 Hz, 4H, -CH_2Ar), 2.34 (s, 6H, -CH_3Ar), 1.98 – 1.91 (m, 2H, -CH_2). ^{13}C{^{1}H} NMR (151 MHz, $CDCl_3$) δ 142.44, 137.95, 129.41, 128.32, 126.58, 125.57 (Ar), 35.58 (-CH_2Ar), 33.14 (-CH_3Ar), 21.56 (-CH_2). GC-MS $[M]^+$: 224.1.

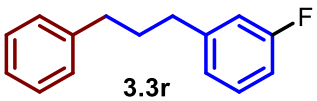

3.3r

1-fluoro-3-(3-phenylpropyl)benzene (3.3r). Colourless liquid (Yield 79%), ^{1}H NMR (600 MHz, $CDCl_3$) δ 7.36 – 7.33 (m, 2H, Ar), 7.30 – 7.22 (m, 5H, Ar), 7.01 (dd, *J* = 7.7, 3.9 Hz, 1H,

Ar), 6.97 – 6.93 (m, 1H, Ar), 2.74 – 2.68 (m, 4H, -CH_2Ar), 2.06 – 1.98 (m, 2H, -CH). ^{19}F NMR (565 MHz, $CDCl_3$) δ -113.90. $^{13}C\{^1H\}$ NMR (151 MHz, $CDCl_3$) δ 163.87, 162.25, 145.02, 142.42, 129.82, 129.77, 128.58, 128.56, 128.49, 128.44, 125.97, 125.87, 124.22, 124.21, 115.42, 115.28, 112.81, 112.67 (Ar), 35.57 (-CH_2Ar), 35.44 (-CH_2Ar), 35.25 (-CH_2Ar), 35.24 (CH_2Ar), 33.09 (-CH_2), 32.79 (-CH_2). GC-MS $[M]^+$: 214.1.

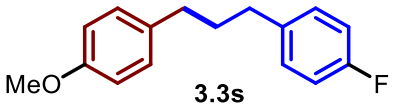

3.3s

1-fluoro-4-(3-(4-methoxyphenyl)propyl)benzene (3.3s).[14,15] Colourless liquid (Yield 75%), ^{1}H NMR (400 MHz, $CDCl_3$) δ 7.15 – 7.06 (m, 4H, Ar), 7.00 – 6.92 (m, 2H, Ar), 6.86 – 6.79 (m, 2H, Ar), 3.79 (s, 3H, -OMe), 2.64 – 2.54 (m, 4H, -CH_2Ar), 1.90 (p, *J* = 7.7 Hz, 2H). ^{19}F NMR (565 MHz, $CDCl_3$) δ -118.00. $^{13}C\{^1H\}$ NMR (151 MHz, $CDCl_3$) δ 162.15, 160.54, 157.90, 138.05, 134.33, 129.87, 129.82, 129.43, 115.19, 115.05, 113.90 (Ar), 55.41 (-OMe), 34.65 (-$CH_{2(}C_6H_4F$)), 34.52 (-$CH_{2(}C_6H_4$OMe)), 33.45 (-CH_2). GC-MS $[M]^+$: 244.1.

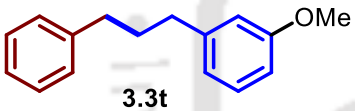

3.3t

1-methoxy-3-(3-phenylpropyl)benzene (3.3t). Colourless liquid (Yield 85%), ^{1}H NMR (400 MHz, $CDCl_3$) δ 7.36 – 7.28 (m, 3H, Ar), 7.23 (dd, *J* = 7.5, 1.4 Hz, 3H), Ar, 6.84 – 6.81 (m, 1H, Ar), 6.80 – 6.75 (m, 2H, Ar), 3.84 (s, 3H, -OMe), 2.68 (q, *J* = 8.2 Hz, 4H, -CH_2Ar), 2.05 – 1.94 (m, 2H, -CH)). $^{13}C\{^1H\}$ NMR (151 MHz, $CDCl_3$) δ 159.76, 144.09, 142.41, 129.39, 128.59, 128.44, 125.88, 121.03, 114.36, 111.15 (Ar), 55.28 (-OMe), 35.61 (-CH_2Ph), 35.56 (-$CH_2C_6H_4$OMe), 32.95 (-CH_2). GC-MS $[M]^+$: 226.1.

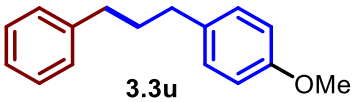

3.3u

1-methoxy-4-(3-phenylpropyl)benzene (3.3u).[15] Colourless liquid (Yield 92%), ^{1}H NMR (600 MHz, $CDCl_3$) δ 7.28 (dd, *J* = 8.6, 6.5 Hz, 2H, Ar), 7.20 – 7.17 (m, 3H, Ar), 7.10 (d, *J* = 8.7 Hz, 2H, Ar), 6.83 (d, *J* = 8.7 Hz, 2H, Ar), 3.79 (s, 3H, -OMe), 2.67 – 2.58 (m, 4H, -CH_2Ar), 1.96 – 1.89 (m, 2H, -CH_2). $^{13}C\{^1H\}$ NMR (151 MHz, $CDCl_3$) δ 157.86, 142.52, 134.52, 129.45, 128.59, 128.43, 125.84, 113.87 (Ar), 55.41 (-OMe), 35.52 (-CH_2Ph), 34.65 (-$CH_2C_6H_4$OMe), 33.32 (-CH_2). GC-MS $[M]^+$: 226.1.

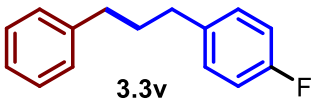

3.3v

1-fluoro-4-(3-phenylpropyl)benzene (3.3v).[15] Colourless liquid (Yield 83%), ^{1}H NMR (600 MHz, $CDCl_3$) δ 7.32 (t, *J* = 7.5 Hz, 3H, Ar), 7.24 – 7.21(m, 4H, Ar), 7.18 – 7.13 (m, 1H, Ar), 7.00 (t, *J* = 8.5 Hz, 1H, Ar), 2.69 (t, *J* = 7.7 Hz, 4H, -CH_2Ar), 2.04 – 1.93 (m, 2H, -CH_2). ^{19}F NMR (565 MHz, $CDCl_3$) δ -117.86. ^{13}C{^{1}H} NMR (151 MHz, $CDCl_3$) δ 160.56, 142.43, 137.98, 129.82, 128.58, 128.44, 125.87, 115.21, 115.07 (Ar), 35.57 (-CH_2Ph), 34.71 (-$CH_2C_6H_4F$), 33.09 (-CH_2). GC-MS $[M]^+$: 214.1.

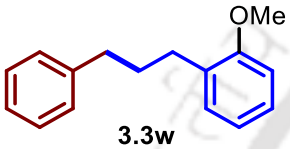

3.3w

1-methoxy-2-(3-phenylpropyl)benzene (3.3w). Colourless liquid (Yield 60%), ^{1}H NMR (600 MHz, $CDCl_3$) δ 7.34 – 7.30 (m, 2H, Ar), 7.27 – 7.20 (m, 4H, Ar), 7.18 (dd, *J* = 7.4, 1.9 Hz, 1H, Ar), 6.93 (t, *J* = 6.8 Hz, 1H, Ar), 6.89 (d, *J* = 8.2 Hz, 1H, Ar), 3.86 (s, 3H, -OMe), 2.75 – 2.69 (m, 4H,-CH_2Ar), 2.01 – 1.95 (m, 2H, -CH_2). ^{13}C{^{1}H} NMR (151 MHz, $CDCl_3$) δ 157.63, 142.79, 130.88, 129.93, 128.57, 128.36, 127.08, 125.74, 120.46, 110.38 (Ar), 55.37 (-OMe), 35.89 (-CH_2Ph), 31.47 (-$CH_2C_6H_4$OMe), 30.08 (-CH_2). GC-MS $[M]^+$: 226.1.

3.5.12. Computational details

The geometries of all the considered complexes were fully optimized using the DFT (PBE)[27] Method on the Gaussian-09 package.[28] The LANL2DZ[29] and 6-311G (d, p) basis set with a polarization function were used, respectively, for the metal (Ru) and non-metal atoms. The method and basis set were selected according to previous reports on pincer ruthenium complexes.[18,20,22] The transition states were located using the synchronous transit-guided quasi Newton (QST2) Genecp (gen keyword with the effective core potential) to define the basis set. The empirical dispersion-GD_3 was used in all molecular geometry optimization and energy computations Frequency calculations characterize the obtained stationary points as minima structures or transition states based on the number of imaginary frequencies. Single point calculations were performed to calculate the relative free energy values at 140 °C.

Supporting information (containing NMR spectra and of various compounds complexes, HRMS data, Kinetics plot, GC plot, Cartesian coordinates of the computed complexes) for chapter III is available as appendix II and can be found at

https://drive.google.com/file/d/1nRhwGf9bdDny5-1W_ZrfScmF2e7tI0ZP/view?usp=sharing

3.6. References

(1) Akhtar, W. M.; Armstrong, R. J.; Frost, J. R.; Stevenson, N. G.; Donohoe, T. J., Stereoselective Synthesis of Cyclohexanes via an Iridium Catalyzed (5 + 1) Annulation Strategy. *J. Am. Chem. Soc.* **2018,** *140* , 11916-11920.

(2) (a) Shi, J.; Tong, X.; Wang, S.; Xue, S. From C5 to C7-11: Selective Carbon-Chain via Copper Mediated Aerobic Oxidative Condensation of Biomass Derived Furfural and Straight Chain Alcohols. *ACS Catal*. **2022**, *12*, 6029−6035. (b) Cai, L.; vom Lehn, F.; Pitsch, H. Higher Alcohol and Ether Biofuels for Compression-Ignition Engine Application: A Review with Emphasis on Combustion Kinetics. *Energy Fuels* **2021**, *35*, 1890− 1917. (c) Kim, Y.; Li, C.-J. Perspectives on green synthesis and catalysis. *Green Synth. Catal.* **2020**, *1*,1−11. (d) Gerardy, R.; Debecker, D. P.; Estager, J.; Luis, P.; Monbaliu, J-C. M. Continuous Flow Upgrading of Selected C2-C6 Platform Chemicals Derived from Biomass. *Chem. Rev.* **2020**, *120*, 7219−7347. (d) Mei, Q.; Shen, X.; Liu, H.; Han, B. Selectively transform lignin into value-added chemicals. *Chin. Chem. Lett.* **2019**, *30*,15−24. (e) Hossain, S. M. Z. Biochemical Conversion of Microalgae Biomass into Biofuel. *Chem. Eng. Technol.* **2019**, *42*, 2594−2607. (f) Liu, W.-J.; Li, W.-W.; Jiang, H.; Yu, H.-Q. Fates of Chemical Elements in Biomass during Its Pyrolysis. *Chem. Rev.* **2017**, *117*, 6367−6398. (g) Shiramizu, M.; Toste, F. D. Deoxygenation of Biomass-Derived Feedstocks: Oxorhenium-Catalyzed Deoxydehydration of Sugars and Sugar Alcohols. *Angew. Chem., Int. Ed.* **2012**, *51*, 8082−8086. (h) Gallezot, P. Conversion of Biomass to Selected Chemical Products. *Chem. Soc. Rev.* **2012**, *41*, 1538−1558. (i) Serrano-Ruiz, J. C.; Luque, R.; Sepulveda-Escribano, A. Transformations of Biomass-Derived Platform Molecules: from High Added-Value Chemicals to Fuels via Aqueous-Phase Processing. *Chem. Soc. Rev.* **2011**, *40*, 5266−5281.

(3) Nandi, P. G.; Kumar, P.; Kumar, A. Ligand-free Guerbet-type reactions in air catalyzed by in situ formed complexes of base metal salt cobaltous chloride. *Catal. Sci. Technol.* **2022**, *12*, 1100−1108.

(4) Das, K.; Kumar, A., Chapter One - Alkane dehydrogenation reactions catalyzed by pincer-metal complexes. In *Advances in Organometallic Chemistry*, Pérez, P. J., Ed. Academic Press: 2019; Vol. 72, pp 1-57.

(5) Kumar, A.; Goldman, A. S., Recent Advances in Alkane Dehydrogenation Catalyzed by Pincer Complexes. In *The Privileged Pincer-Metal Platform: Coordination Chemistry & Applications*, van Koten, G.; Gossage, R. A., Eds. Springer International Publishing: Cham, 2016; pp 307-334.

(6) Kumar, A.; Bhatti, T. M.; Goldman, A. S., Dehydrogenation of Alkanes and Aliphatic Groups by Pincer-Ligated Metal Complexes. *Chem. Rev.* **2017,** *117*, 12357-12384.

(7) Nandi, P. G.; Thombare, P.; Prathapa, S. J.; Kumar, A., Pincer-Cobalt-Catalyzed Guerbet-Type β-Alkylation of Alcohols in Air under Microwave Conditions. *Organometallics* **2022,** *41*, 3387-3398.

(8) Yi, H.; Zhang, G.; Wang, H.; Huang, Z.; Wang, J.; Singh, A. K.; Lei, A., Recent Advances in Radical C–H Activation/Radical Cross-Coupling. *Chem.Rev.* **2017,** *117*, 9016-9085.

(9) Schlagbauer, M.; Kallmeier, F.; Irrgang, T.; Kempe, R., Manganese-Catalyzed β-Methylation of Alcohols by Methanol. *Angew. Chem., Int. Ed* **2020,** *59*, 1485-1490.

(10) Watson, A. J.; Williams, J. M. J., The give and take of alcohol activation. *Science* **2010,** *329*, 635-636.

(11) (a) Davies, M. A.; Li, Y. Z.; Stephenson, R. J. C.; Szymczak, K. N. Valorization of Ethanol: Ruthenium-Catalyzed Guerbet and Sequential Functionalization Processes. *ACS Catal.* **2022**, *12*, 6729−6736. (b) DiBenedetto, T. A.; Jones, W. D. Upgrading of Ethanol to n-Butanol via a Ruthenium Catalyst in Aqueous Solution. *Organometallics* **2021**, *40*, 1884−1888. (c) Dowson, G. R. M.; Haddow, M. F.; Lee, J.; Wingad, R. L.; Wass, D. F. Catalytic Conversion of Ethanol into an Advanced Biofuel: Unprecedented Selectivity form-Butanol. *Angew. Chem., Int. Ed.* **2013**, *52*, 9005−9008. (d) Fu, S.;

Shao, Z.; Wang, Y.; Liu, Q. Manganese-Catalyzed Upgrading of Ethanol into 1Butanol. *J. Am. Chem. Soc.* **2017**, *139*, 11941−11948.
(12) (a) Doménech, P.; Pogrebnyakov, I.; Nielsen, A. T.; Riisager, A. Catalytic production of long-chain hydrocarbons suitable for jet-fuel use from fermentation-derived oxygenates. *Green Chem.* **2022**, *24*, 3461−3474. (b) Dühren, R.; Kucmierczyk, P.; Schneider, C.; Jackstell, R.; Franke, R.; Beller, M. Ruthenium-catalysed domino hydroformylation-hydrogenation-esterification of olefins. *Catal. Sci. Technol.* **2021**, *11*, 5777. (c) Dai, X. J.; Li, C. J. En Route to a Practical Primary Alcohol Deoxygenation. *J. Am. Chem. Soc.* **2016**, *138*, 5433−5440. (d) McLaughlin, M. P.; Adduci, L. L.; Becker, J. J.; Gagné, M. R. Iridium-Catalyzed Hydrosilylative Reduction of Glucose to Hexane(s). *J. Am. Chem. Soc.* **2013**, *135*, 1225−1227.
(13) Obora, Y.; Anno, Y.; Okamoto, R.; Matsu-ura, T.; Ishii, Iridium-Catalyzed Reactions of ω-Arylalkanols to α, ω-Diarylalkanes. *Angew. Chem.* **2011**, *37*, 8777-8781.
(14) Wang, Y.; Shao, Z.; Zhang, K.; Liu, Q. Manganese-Catalyzed Dual-Deoxygenative Coupling of Primary Alcohols with 2-Arylethanols. *Angew. Chem., Int. Ed.* **2018**, *57*, 15143−15147.
(15) Sardar, B.; Biswas, N.; Srimani, D., Ruthenium Pincer-Catalyzed Selective Synthesis of Alkanes and Alkenes via Deoxygenative Coupling of Primary Alcohols. *Organometallics* **2023,** *42*, 55-61.
(16) Manojveer, S.; Forrest, S. J.; Johnson, M. T., Ru-Catalyzed Completely Deoxygenative Coupling of 2-Arylethanols through Base-Induced Net Decarbonylation. *Chem. Eur.J.* **2018,** *24*, 803-807.
(17) Lu, Z.; Zheng, Q.; Yang, S.; Qian, C.; Shen, Y.; Tu, T., NHC-Iridium-Catalyzed Deoxygenative Coupling of Primary Alcohols Producing Alkanes Directly: Synergistic Hydrogenation with Sodium Formate Generated in Situ. *ACS Catal.* **2021,** *11*, 10796-10801
(18) Das, K.; Nandi, P. G.; Islam, K.; Srivastava, H. K.; Kumar, A. N−Alkylation of Amines Catalyzed by a Ruthenium−Pincer Complex in the Presence of in situ Generated Sodium Alkoxide. *Eur. J. Org. Chem.* **2019**, *2019*, 6855−6866.
(19) (a) Arora, V.; Yasmin, E.; Tanwar, N.; Hathwar, V. R.; Wagh, T.; Dhole, S.; Kumar, A. Pincer−Ruthenium-Catalyzed Reforming of Methanol_Selective High-Yield Production of Formic Acid and Hydrogen. *ACS Catal.* **2023**, *13*, 3605−3617. (b) Arora, V.; Dhole, S.; Kumar, A. Reforming of Ethanol to Hydrogen and Acetic Acid Catalyzed by Pincer-Ruthenium Complexes. *Catal. Sci. Technol.*, **2023**,***13***, 6699-6711.
(20) (a) Das, K.; Yasmin, E.; Das, B.; Srivastava, H. K.; Kumar, A. Phosphine-free pincer−ruthenium cat lyzed biofuel production: high rates, yields and turnovers of solventless alcohol alkylation. *Catal. Sci. Technol.* **2020**, *10*, 8347−8358. (b) Narjinari, H.; Bisarya, A.; Arora, V.; Nandi, P. G.; Das, K.; Kumar, A., Current State-of-Art in the Guerbet-Type β-Alkylation of Secondary Alcohols with Primary Alcohols Catalyzed by Complexes Based on 3d Metals. In *Dehydrogenation Reactions with 3d Metals*, Sundararaju, B., Ed. Springer Nature Switzerland: 2024; pp 93-127.
(21) Nandi, P. G.; Jasra, R. V.; Kumar, A. Pincer-Ruthenium Catalyzed *β*-Methylation of Alcohols. *Organometallics* **2023**, *42*, 3138−3152.
(22) Das, K.; Kathuria, L.; Jasra, R. V.; Dhole, S.; Kumar, A. Microwave-assisted pincer−ruthenium catalyzed Guerbet reaction for the upgradation of bio-ethanol to bio-butanol. *Catal. Sci. Technol.* **2023**, *13*, 1763−1776.
(23) Das, K.; Dutta, M.; Das, B.; Srivastava, H. K.; Kumar, A. Efficient Pincer- Ruthenium Catalysts for Kharasch Addition of Carbon Tetrachloride to Styrene. *Adv. Synth. Catal.* **2019**, *361*, 2965−2980.
(24) Dutta, M.; Das, K.; Prathapa, S. J.; Srivastava, H. K.; Kumar, A. Selective and high yield transformation of glycerol to lactic acid using NNN pincer ruthenium catalysts. *Chem. Commun.* **2020**, *56*, 9886− 9889.
(26) Günther, H., *NMR Spectroscopy: Basic Principles, Concepts and Applications in Chemistry*. Wiley: 2013.
(27) Perdew, J. P.; Burke, K.; Ernzerhof, M., *Phys. Rev. Lett.***1996**, 77, 3865–3868.
(28) Frisch, M. J.; Trucks, G. W.; Schlegel, H. B.; Scuseria, G. E.; Robb, M. A.; Cheeseman, J. R.; Scalmani, G.; Barone, V.; Mennucci, B.; Petersson, G. A.; Nakatsuji, H.; Caricato, M.; Li, X.; Hratchian, H. P.; Izmaylov, A. F.; Bloino, J.; Zheng, G.; Sonnenberg, J. L.; Hada, M.; Ehara, M.; Toyota, K.; Fukuda, R.; Hasegawa, J.; Ishida, M.; Nakajima, T.; Honda, Y.; Kitao, O.; Nakai, H.; Vreven, T.; Montgomery, J. A., Jr.; Peralta, J. E.; Ogliaro, F.; Bearpark, M.; Heyd, J. J.; Brothers, E.; Kudin, K. N.; Staroverov, V. N.; Keith, T.; Kobayashi, R.; Normand, J.; Raghavachari, K.; Rendell, A.;

Burant, J. C.; Iyengar, S. S.; Tomasi, J.; Cossi, M.; Rega, N.; Millam, J. M.; Klene, M.; Knox, J. E.; Cross, J. B.; Bakken, V.; Adamo, C.; Jaramillo, J.; Gomperts, R.; Stratmann, R. E.; Yazyev, O.; Austin, A. J.; Cammi, R.; Pomelli, C.; Ochterski, J. W.; Martin, R. L.; Morokuma, K.; Zakrzewski, V. G.; Voth, G. A.; Salvador, P.; Dannenberg, J. J.; Dapprich, S.; Daniels, A. D.; Farkas, O.; Foresman, J. B.; Ortiz, J. V.; Cioslowski, J.; Fox, D. J. *Gaussian 09*, Revision D.01; Gaussian, Inc.: Wallingford, CT, 2013.
(29) (a) Hay, P. J.; Wadt, W. R., Ab initio effective core potentials for molecular calculations. Potentials for the transition metal atoms Sc to Hg. *J. Chem. Phys.*, **1985**, *82*, 270–283. (b) Hay, P. J.; Wadt, W. R., Ab initio effective core potentials for molecular calculations. Potentials for the transition metal atoms Sc to Hg. *J. Chem. Phys.*, **1985**, *82*, 299–310. (c) Hay, P. J.; Wadt, W. R., Ab initio effective core potentials for molecular calculations. Potentials for the transition metal atoms Sc to Hg. *J. Chem. Phys.*, **1985**, *82*, 284–298.

Chapter- IV

Ligand-Free Guerbet-Type Reactions in Air Catalyzed by in-situ Formed Complexes of Base Metal Salt Cobaltous Chloride

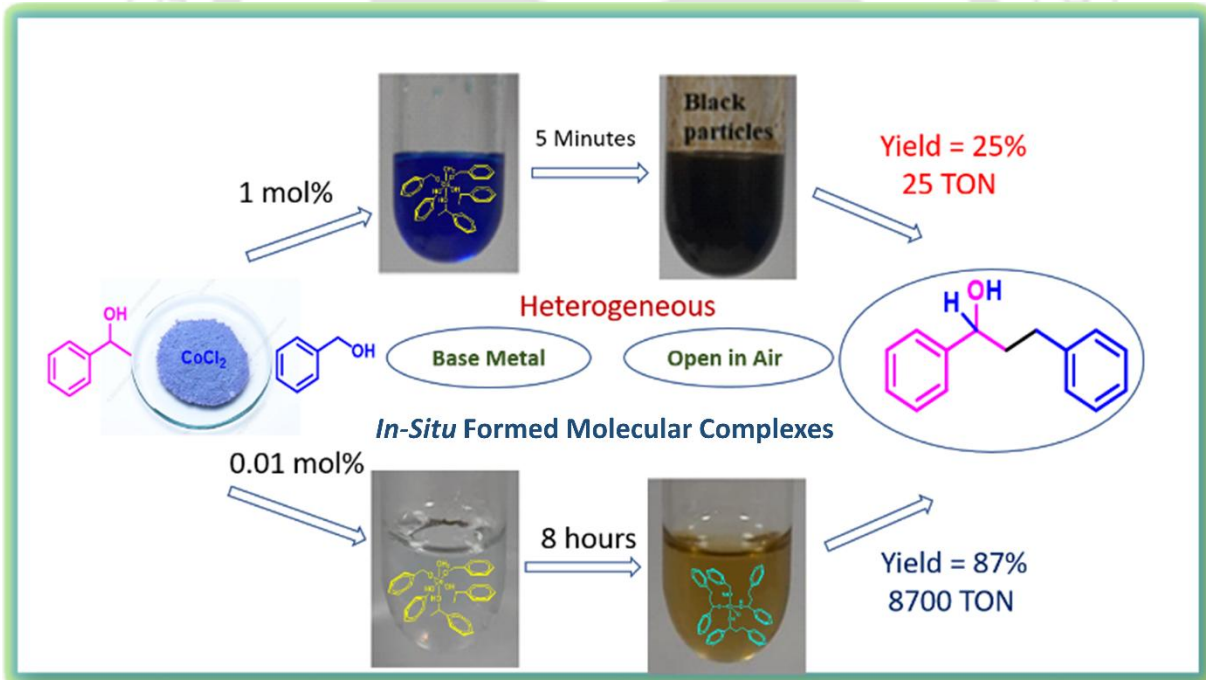

The content of this chapter has been adapted from "*Ligand-Free Guerbet-Type Reactions in Air Catalyzed by in situ Formed Complexes of Base Metal Salt Cobaltous Chloride*" by Nandi, P. G.; Kumar, P.; Kumar, A. *Catal. Sci. Technol*. **2022**, *12*, 1100-1108.

4.1. Introduction

Catalytic methods that bring about the formation of C–C bonds find wide synthetic utility and lead to valuable fuel chemicals, fine chemicals, agrochemicals, pharmaceuticals and natural products.[1] One of the most favourite routes to C–C bond forming reactions include the transition metal catalysed activation of C–X (X = H, Cl, Br and I) bonds *via* radical[2] or organometallic pathways (Scheme 4.1).[3] Of late, there has been a dramatic surge in the exploration of methods that use alcohols as an alkylating agent. Fondly tagged as a "hydrogen borrowing strategy", these C–C bond forming reactions are green and atom-economical as they give water as the sole by-product. While metal-free[4] systems for the *β*-alkylation of alcohols lead to large amounts of waste[4b, c] arising from the use of stoichiometric amounts of base, the use of toxic precious metals such as palladium,[5] iridium,[6] rhodium[7] and ruthenium[6b, d, j, 8] poses challenges in the economic viability of transition metal based homogeneous catalytic systems. In pursuit of earth-abundant, environmentally benign and inexpensive *β*-alkylation systems, researchers have developed catalysts based on cobalt,[9] copper,[10a, b] chromium,[10c] manganese,[11] iron[11k, l] and nickel.[12]

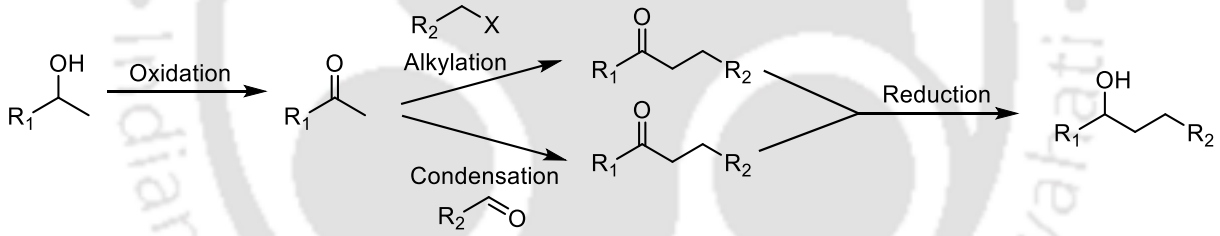

Scheme 4.1: Traditional approach to *C*-alkylation reaction.[2,3]

Transition metal catalysed dehydrogenation of primary and secondary alcohol produces the corresponding aldehyde and ketone which in the presence of a base undergoes aldol-condensation to produce *α*, *β* unsaturated ketone with water as a sole by-product. Hydrogenation of this *α*, *β* unsaturated ketone produces the *β*-alkylated alcohol (Scheme 4.2).

In 2003, Shim and co-workers first demonstrated the *β*-alkylation of secondary alcohols with primary alcohols that is catalyzed by the phosphine based salt dichloro *tris*(triphenylphosphine)ruthenium(II) [$RuCl_2(PPh_3)_3$] in presence of NaOH (3 equivalents) (Scheme 4.3). This methodology afforded a variety of *β*-alkylated alcohol products.[8f]

In 2017, Achard and co-workers reported NPN tridentate pyridine based ruthenium metal complex (**4.Ru1**) for the formation of *α*-alkylated ketones as a major product during the

condensation of primary and secondary alcohols (Scheme 4.4).[8b] A variety of substrates could be α-alkylated using the optimised conditions.

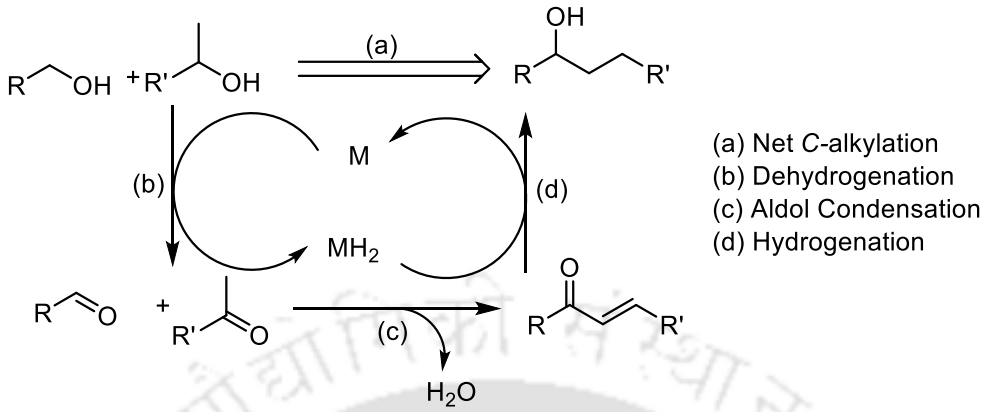

Scheme 4.2: A new strategy towards *C*-alkylation using alcohol as a starting material

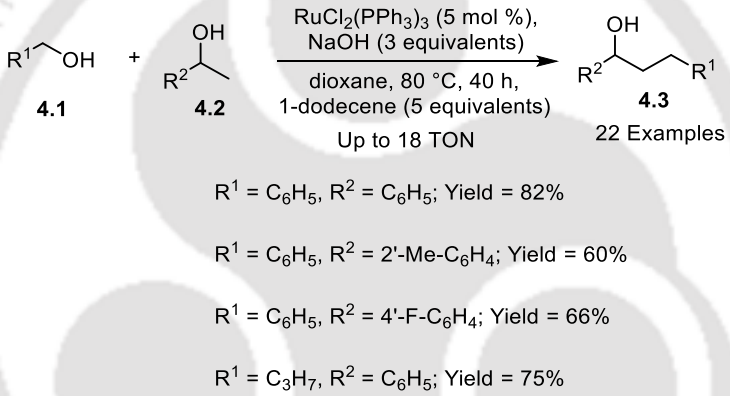

Scheme 4.3: $RuCl_2(PPh_3)_3$ catalyzed β-alkylation of secondary alcohols with primary alcohols.[8f]

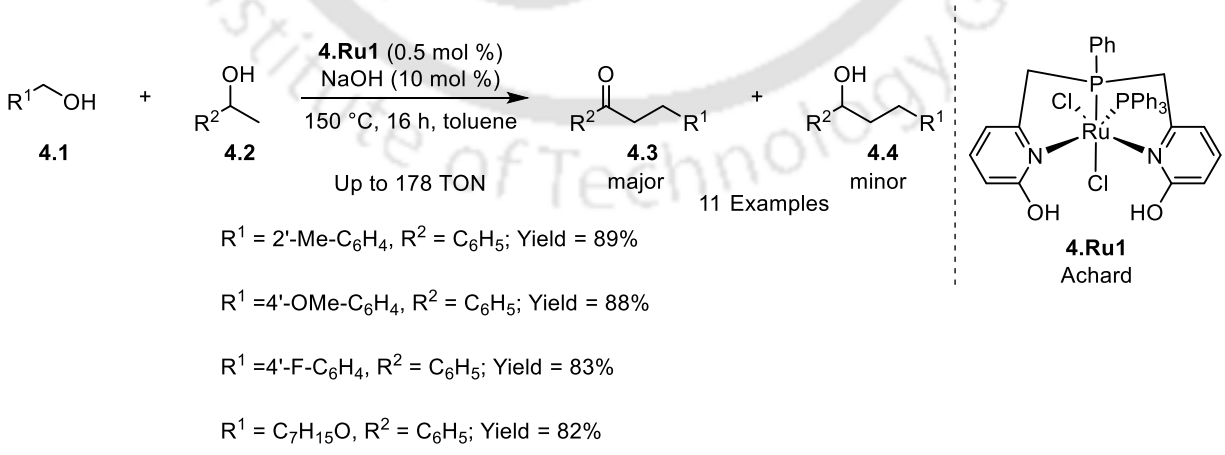

Scheme 4.4: The **4.Ru1** catalyzed formation of α-alkylated ketones starting from primary and secondary alcohols.[8b]

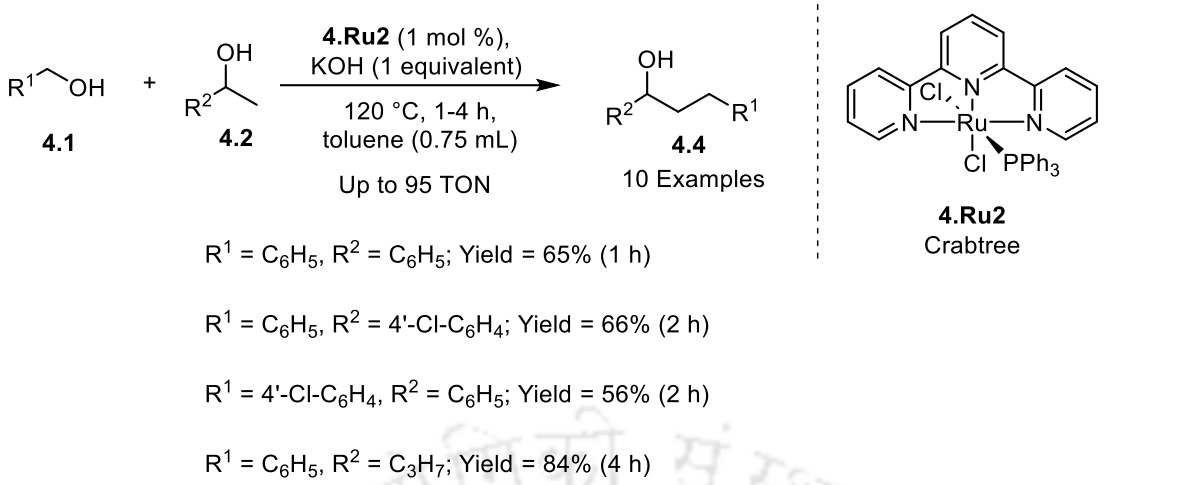

Scheme 4.5: The **4.Ru2** catalyzed formation of *β*-alkylated alcohols starting from primary and secondary alcohols.[6d]

Crabtree carried out the NNN pincer-ruthenium (**4.Ru2**) catalyzed *β*-alkylation of secondary alcohols with primary alcohols (Scheme 4.5).[6d] Using the developed protocol a variety of substrates could be *β*-alkylated and a maximum of 95 TON was obtained.

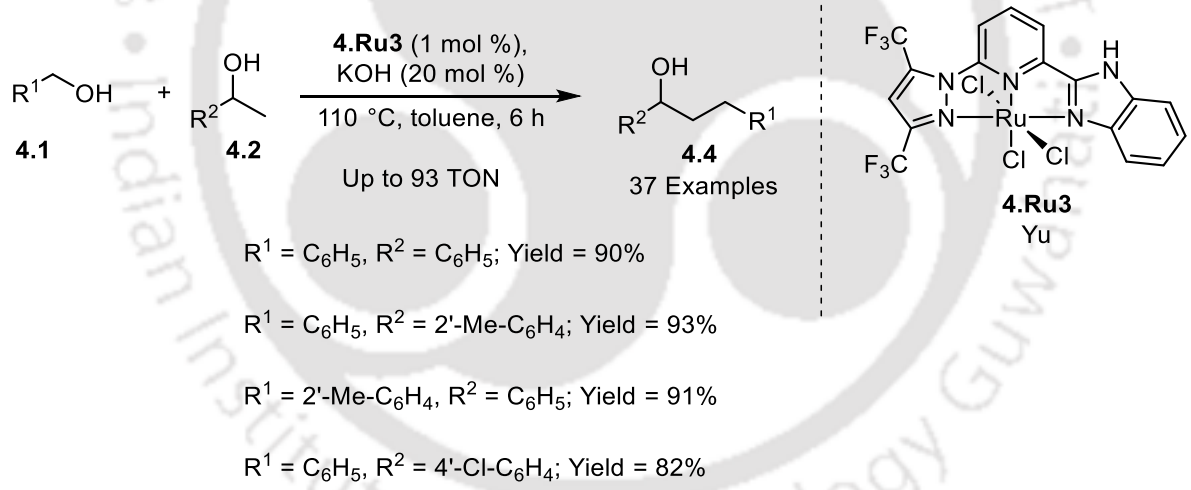

Scheme 4.6: The **4.Ru3** catalyzed *β*-alkylation of secondary alcohols with primary alcohols.[8c]

In 2016, Yu and co-workers introduced a ligand system with trifluoromethylated groups which in presence of a ruthenium salt formed complex **4.Ru3** that is active for the *β*-alkylation of alcohols.[8c] The CF_3 groups present in the metal complex provides the lipophilicity, electronegativity and H-bond formation ability. In presence of **4.Ru3** as catalyst, the *β*-alkylated alcohols were formed from primary and secondary alcohols with excellent yield (Scheme 4.6).[8c] The precursor Ru(III) in presence of KOH transformed to Ru(II) species which

as considered as the active species that give rise to the excellent catalytic activity towards *β*-alkylation.

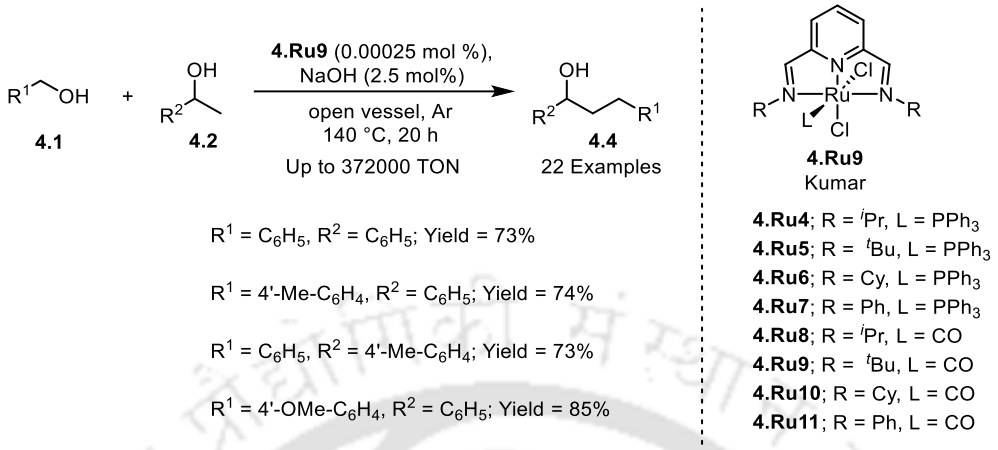

Scheme 4.7: The **4.Ru9** catalyzed *β*-alkylation of secondary alcohols with primary alcohols.[8l]

Recently, Kumar has reported the *β*-alkylation of 1-phenylethanol with benzyl alcohol and it's derivatives catalysed by NNN pincer-Ru complexes based on *bis*(imino)pyridine and 2,6-*bis*(benzimidazole-2-yl) pyridine ligands (Scheme 4.7).[8l] Among all the considered catalysts, **4.Ru9** shows the best activity for the *β*-alkylation. Kumar has achieved highest TON of 372000 at a loading of 0.00025 mol% **4.Ru9** under solvent free conditions.[8l] A detailed analysis of reaction mechanism with the help of several control experiments and DFT studies led to the conclusion that *β*-hydride elimination is the RDS.[8l]

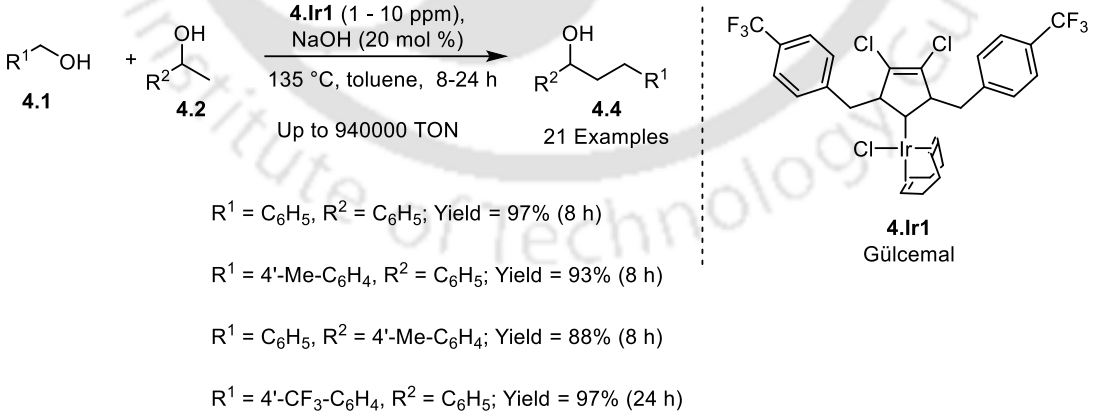

Scheme 4.8: The **4.Ir1** catalyzed *β*-alkylation of secondary alcohols with primary alcohols.[8o]

Gülcemal and co-workers observed excellent activity in the *β*-alkylation of secondary alcohols with primary alcohols in the presence of a imidazol-2-ylidene ligand-based iridium(I) **4.Ir1**

catalyst at very low loadings **(**Scheme 4.8).[8o] Up to 940000 TON was achieved in the presence of 20 mol% NaOH and 0.0001 mol% **4.Ir1** under aerobic conditions.

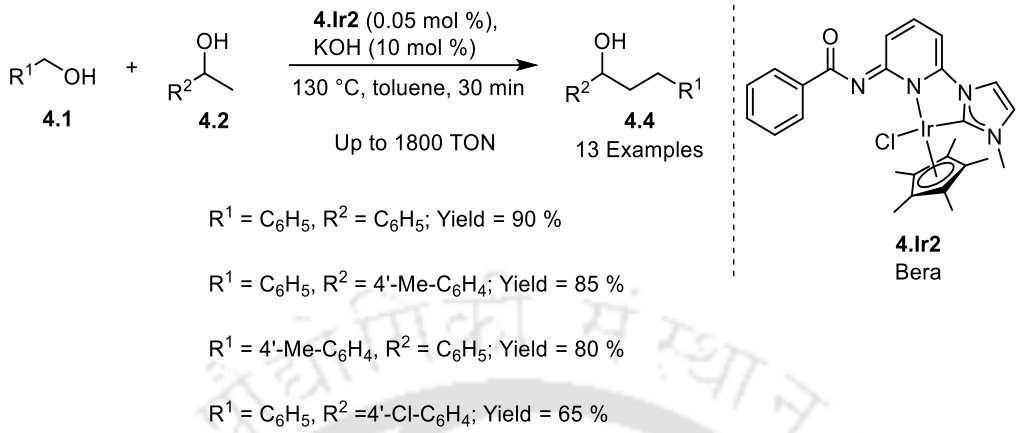

Scheme 4.9: The **4.Ir2** catalyzed *β*-alkylation of secondary alcohols with primary alcohols.[11n]

Bera and co-workers also explored the *β*-alkylation of secondary alcohols with primary alcohols using an *N*-heterocyclic carbene based iridium catalyst **4.Ir2** (Scheme 4.9)**.**[11n] The catalytic system demonstrated very good activity towards the *β*-alkylation owing to the pyridyl(benzamide)-functionalized NHC backbone. The catalyst **4.Ir2** demonstrated good activity over a wide range of substrates using the optimized reaction conditions (Scheme 4.9).[11k]

Kumar has also reported $CrCl_3.6H_2O$ and its NNN-pincer complex **4.Cr1** as efficient catalyst for the *β*-alkylation secondary alcohols with primary alcohols under conventional as well as under microwave heating conditions with high yield (Scheme 4.10).[10c] In particular, pincer-Cr complex **4.Cr1**(0.005 mol%) based on *bis*(iminopyridine) in presence of 5 mol% NaO^tBu at 140 ^oC provide excellent activity for *β*-alkylation under conventional heating (84% yield and 16800 TON at 5600 TOF^{-1}) and microwave condition (90% yield and 18000 TON at 12000 TOh^{-1}) after only 3 hours and 1.5 hours respectively. The precursor salt $CrCl_3.6H_2O$ also exhibited very good reactivity under the same reaction conditions but resulted in comparatively lower yields than its pincer complex under both conventional (79% yield and 15800 TON at 5267 TOh^{-1}) and microwave heating (76% yield and 15200 TON at 10133 TOh^{-1}) (Scheme 4.10).[10c]

In 2012, in a first report, Sun and co-workers carried out the catalytic *β*-alkylation of secondary

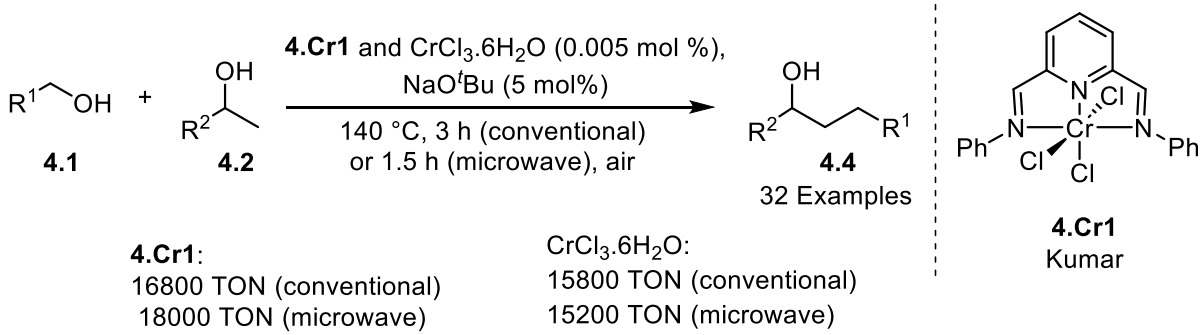

$R^1 = C_6H_5$, $R^2 = C_6H_5$; Yield = 90%

R^1 = 4'-Me-C_6H_4, $R^2 = C_6H_5$; Yield = 83%

R^1 = 4'-OMe-C_6H_4, $R^2 = C_6H_5$; Yield = 84%

$R^1 = C_6H_5$, R^2 = 4'-Cl-C_6H_4; Yield = 91%

Scheme 4.10: The **4.Cr1** catalyzed *β*-alkylation of secondary alcohols with primary alcohols.[10c]

alcohols with primary alcohols using commercially available and inexpensive ferrocenecarboxaldehyde (**4.Fe1**).[10d] In the presence of NaOH (20 mol%) under argon medium at 130 °C in *p*-xylene, **4.Fe1** (5 mol%) catalyzed the *β*-alkylation of 1-phenylethanol with benzyl alcohol to produce *β*-alkylated product in 97% yield (Scheme 4.11).[10d]

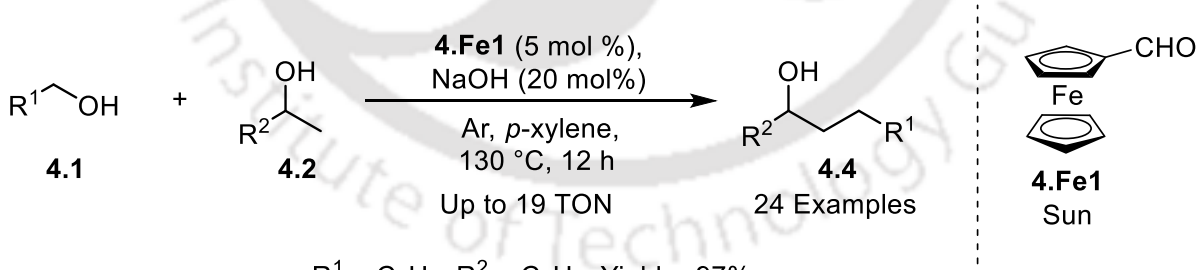

$R^1 = C_6H_5$, $R^2 = C_6H_5$; Yield = 97%

$R^1 = C_6H_5$, R^2 = 4'-Me-C_6H_4; Yield = 80%

R^1 = 4'-Me-C_6H_4, $R^2 = C_6H_5$; Yield = 82%

R^1 = 4'-OMe-C_6H_4, $R^2 = C_6H_5$; Yield = 81%

Scheme 4.11: The **4.Fe1** catalyzed *β*-alkylation of secondary alcohols with primary alcohols.[10d]

Balaraman and co-workers carried out the efficient *β*-alkylation of 1-phenylethanol with benzyl alcohol using $NiBr_2$/TMEDA (1:1) (5 mol%) at 130 °C in *n*-octane in the presence of 1 equivalent KOH and obtained up to 91% yield of the *β*-alkylated product (Scheme 4.12).[12f] This catalytic system is effective for a broad range of substrates and led to the corresponding *β*-alkylated products in good yields.

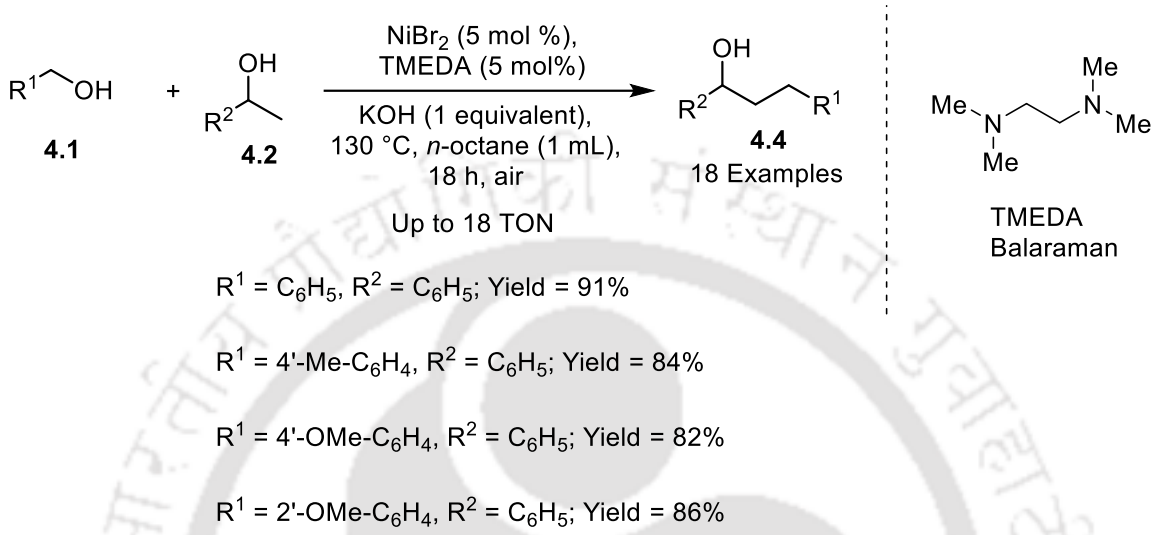

Scheme 4.12: The $NiBr_2$/TMEDA catalyzed *β*-alkylation of secondary alcohols with primary alcohols.[12f]

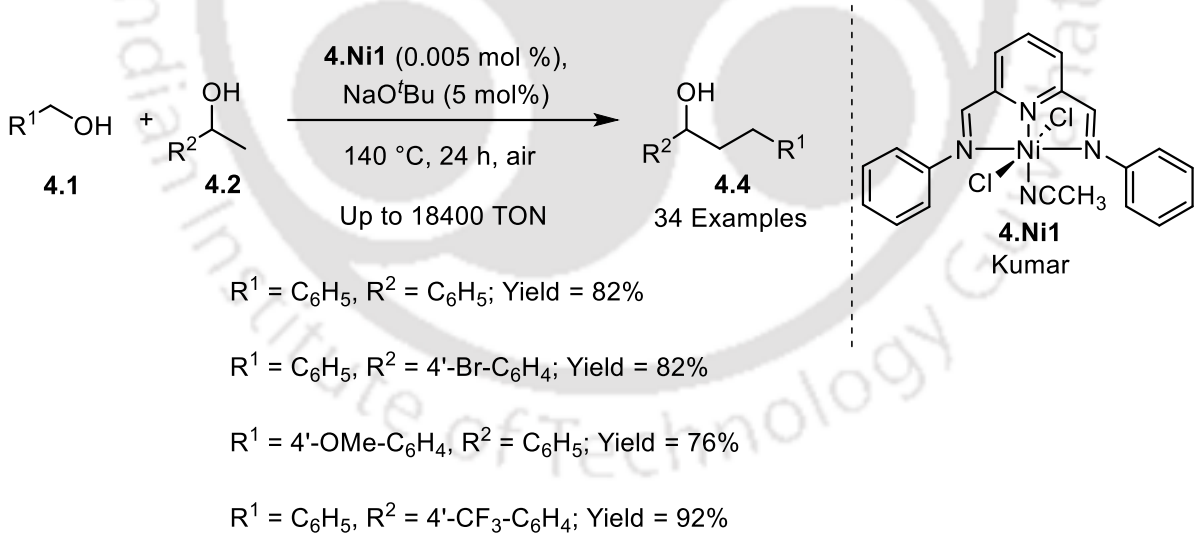

Scheme 4.13: The **4.Ni1** catalyzed *β*-alkylation of secondary alcohols with primary alcohols.[12g]

Kumar has reported a series of pincer-Ni complexes based on *bis*(imino)pyridine ligands.[12g] Among them, **4.Ni1** (0.005 mol%) is most active for the *β*-alkylation of secondary alcohols with primary alcohols which gave very high TONs of upto 18400 in the presence of 5 mol% NaO^{t}Bu at 140 °C under air after 24h (Scheme 4.13).[12g]

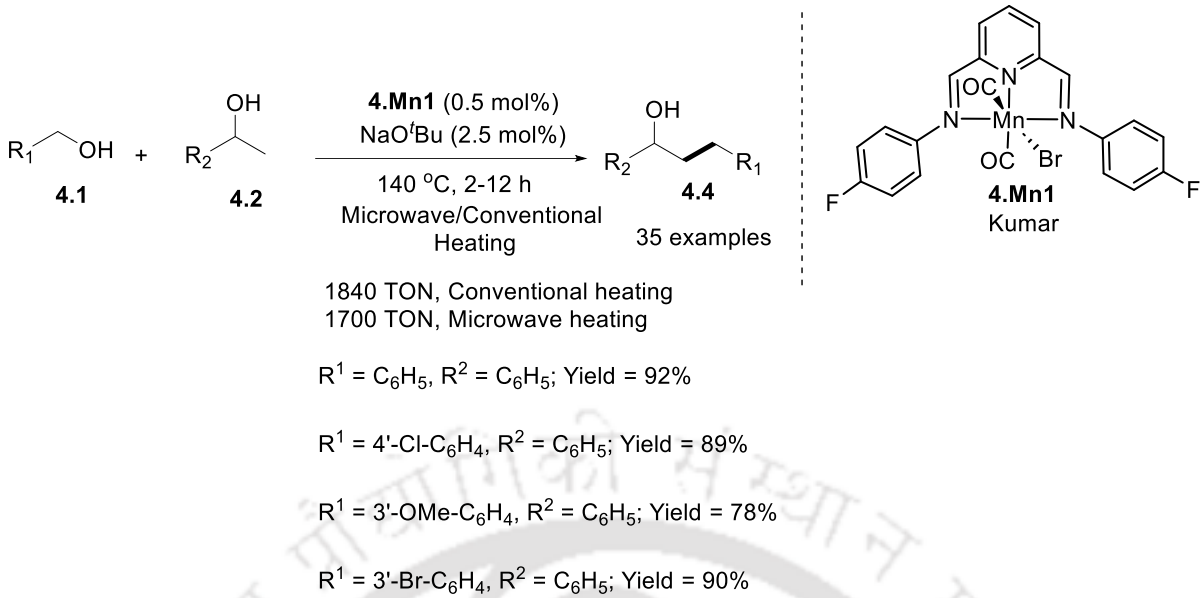

Scheme 4.14: The **4.Mn1** catalyzed *β*-alkylation of secondary alcohols with primary alcohols.[11m]

Recently, Kumar and co-workers have demonstrated the *β*-alkylation of secondary alcohols with primary alcohols by using a series of pincer-Mn complexes based on *bis*(imino)pyridine ligands. Among them, **4.Mn1** (0.5 mol%) proved to be the best while catalyzing the *β*-alkylation in the presence of 2.5 mol% NaOH at 140 °C in neat conditions under both microwave as well as conventional heating to achieve 85% yield (1700 TON, 850 TOs/h) and 92% yield (1840 TON, 153 TOs/h) after 2h and 12 h respectively (Scheme 4.14).[11m] This catalytic system could tolerate a large variety of substrates under both conventional and microwave heating.

The first report on the Co-catalyzed *β*-alkylation of alcohols came from the group of Kempe[9b] using a PN_3P pincer-Co (**4.Co1**) (5 mol%) in the presence of 1.1 equivalents of KHMDS (potassium hexamethyl disilazane) as a base that gave up to 90% yield of the *β*-alkylated product (Scheme 4.15 and 4.18).[9b] The complex **4.Co1** is capable for the alkylation of variety of alcohols starting from aliphatic to aromatic to hetero cyclic alcohols with moderate to good yield though the base loading is very high (1.1 equivalents KHMDS).

In 2021, Ding has reported the use of a cobalt catalyst **4.Co2** (0.7 mol%) supported by a $^{iPr}PPPN^{H}Py^{Me}$ tridentate ligand for the *β*-alkylation of alcohols in up to 80% yield at 110 °C at a very high base loading (110 mol%) (Scheme 4.16).[9c]

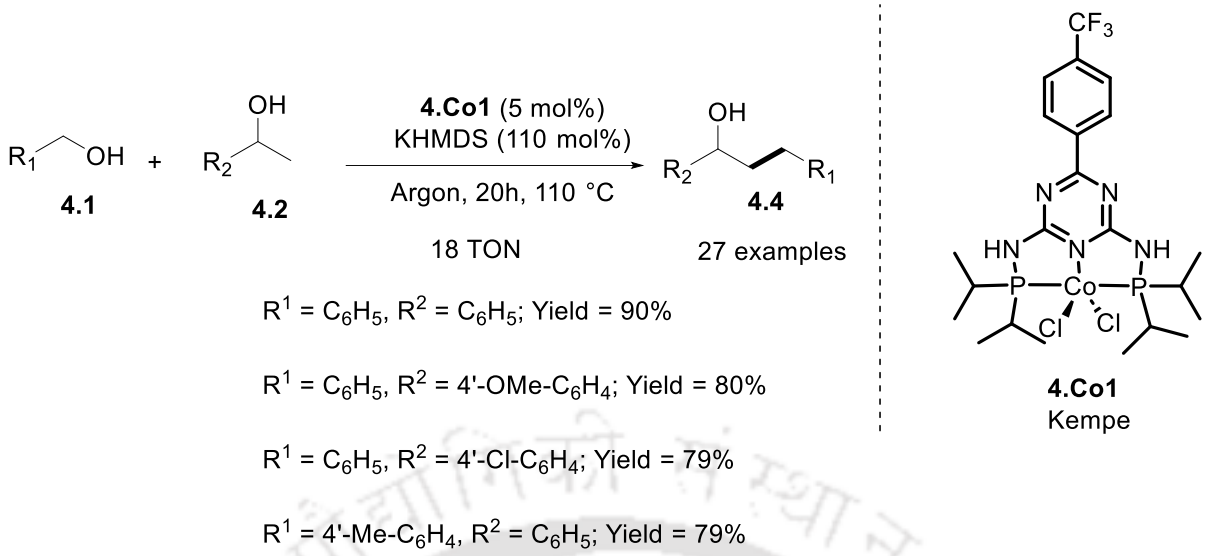

Scheme 4.15: The **4.Co1** catalyzed *β*-alkylation of secondary alcohols with primary alcohols.[9b]

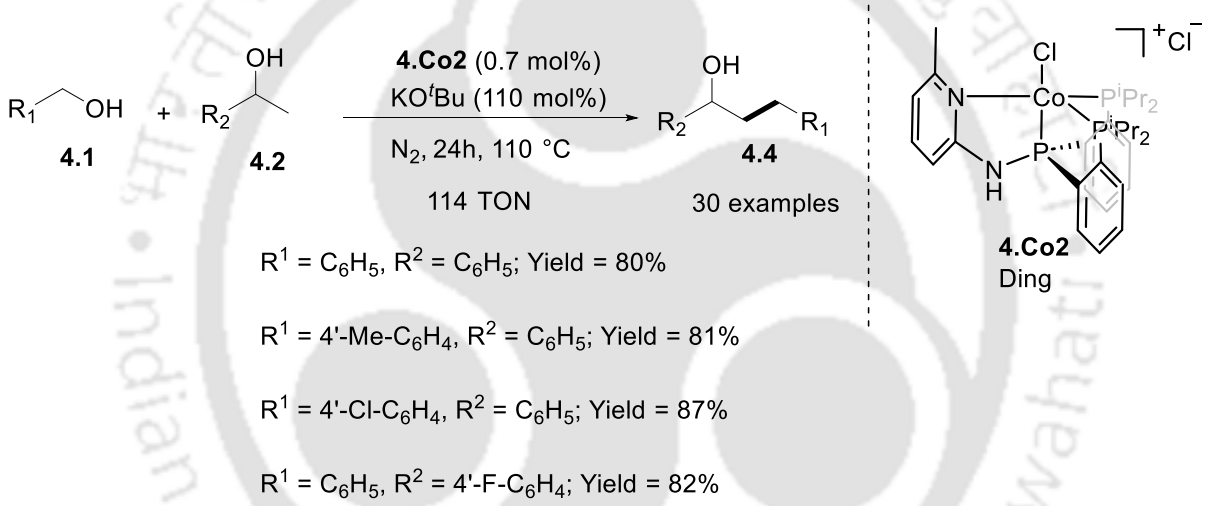

Scheme 4.16: The **4.Co2** catalyzed *β*-alkylation of secondary alcohols with primary alcohols.[9C]

The *β*-alkylation of a large variety of substrates were carried out with **4.Co2** (0.7 mol%) in the presence of KO^{t}Bu(110 mol%) under N_2 atmosphere at 110 °C.[9c]

In 2010, Crabtree demonstrated the *β*-alkylated alcohol formation starting from primary and secondary alcohols using 1 equivalent of NaOH or KOH as base without the need of any metal salt or complex,[10e] where, in very short time duration (4h), good to excellent yields of *β*-alkylated products were achieved (Scheme 4.17).[10e]

Very recently, Gunanathan and co-workers have reported that sub stoichiometric (20 mol%) base mediated *β*-alkylation of secondary alcohols with primary alcohols in toluene (Scheme 4.18).[10f] The *β*-alkylation of 1-phenyl alcohol with benzyl alcohol and it's derivatives were

performed in presence of KOH (20 mol%) in toluene at 135 °C for 36 h to achieve very good yield of *β*-alkylated product.

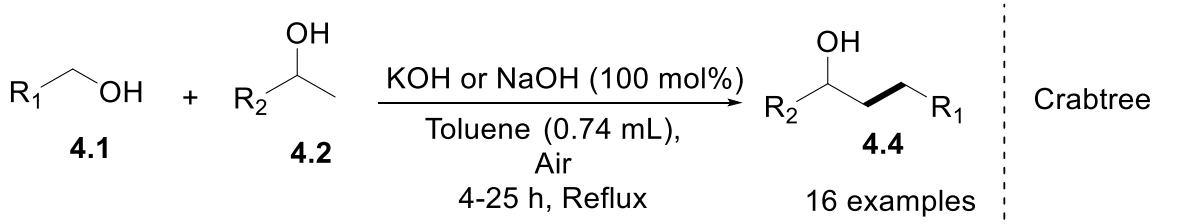

$R^1 = C_6H_5$, $R^2 = C_6H_5$; Yield = 99% (neat, KOH 4h)

$R^1 = 4'\text{-Br-}C_6H_4$, $R^2 = C_6H_5$; Yield = 93% (neat,KOH 4h)

$R^1 = 4'\text{-Cl-}C_6H_4$, $R^2 = C_6H_5$; Yield = 79% (KOH, 4h)

$R^1 = 4'\text{-Cl-}C_6H_4$, $R^2 = C_6H_5$; Yield = 66% (NaOH, 25h)

$R^1 = C_6H_5$, $R^2 = 4'\text{-Cl-}C_6H_4$; Yield = 68% (KOH, 4h)

Scheme 4.17: KOH or NaOH (1 equivalent) mediated *β*-alkylated alcohol formation starting from primary and secondary alcohols.[4b]

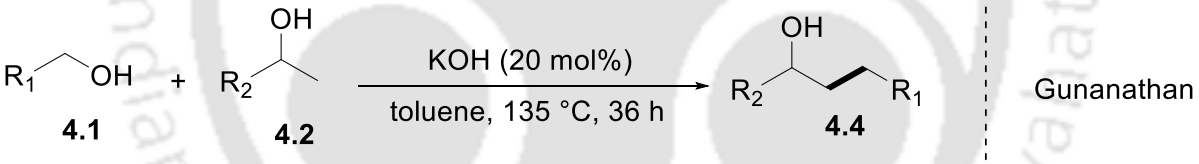

$R^1 = C_6H_5$, $R^2 = C_6H_5$; Yield = 80%

$R^1 = 4'\text{-Br-}C_6H_4$, $R^2 = C_6H_5$; Yield = 76%

$R^1 = 4'\text{-Me-}C_6H_4$, $R^2 = C_6H_5$; Yield = 780%

$R^1 = 4'\text{-Me-}C_6H_4$, $R^2 = C_6H_5$; Yield = 80%

$R^1 = 4'\text{-OMe-}C_6H_4$, $R^2 = C_6H_5$; Yield = 80%

Scheme 4.18: KOH (20%) mediated *β*-alkylation secondary alcohols with primary alcohols.[10e]

4.2. Objectives of the current work

A comprehensive literature survey reveals that the pincer complexes and also other metal complexes are very active for the *β*-alkylation of alcohols with very high base loading.

Crabtree,[4b] Gunanathan,[10e] Jhonson and Wendit[10f] independently reported *β*-alkylation of secondary alcohols with primary alcohols mediated only by a base albeit at high loadings.

On the basis of these facts, the current work attempts to address the following questions:

- Can we attempt the *β*-alkylation of alcohols with catalytic amount of base loading?
- Can we utilize the base metal salt instead of precious metal salt or metal complexes for the *β*-alkylation of alcohols?
- If yes, can we design a very good catalytic system based on base metal salts that can tolerate various functional group on alcohol molecules for *β*-alkylation of alcohols?
- Can we carry out the reaction in air which is easy to perform?

To the best of our knowledge there are no other reports on Co catalyzed *β*-alkylation of alcohols with catalytic amount of base loading. The current study reports high yields (up to 89% yield, *ca.* 8900 TON) in *β*-alkylation of alcohols using readily available $CoCl_2$ at loading as low as 0.01 mol% in the presence of relatively small amounts of NaO^tBu (2.5 mol%) (Scheme 4.19).

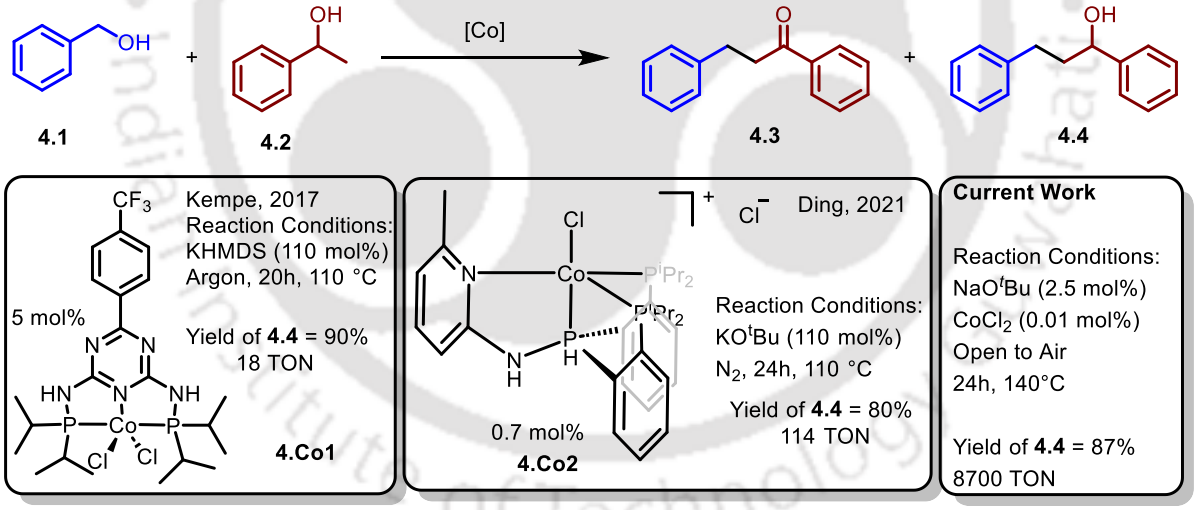

Scheme 4.19. Efficient cobalt-based catalysts reported for *β*-alkylation of 1-phenyl ethanol and benzyl alcohol.

4.3. Results and discussion

4.3.1. Studies on the cobaltous chloride catalyzed *β*-alkylation of 1-phenyl ethanol with benzyl alcohol

The *β*-alkylation studies were initiated using benzyl alcohol and 1-phenyl ethanol as a model primary and secondary alcohol, respectively (Table 4.1). The reaction carried out in the presence of cobaltous chloride (1.0 mol%) and NaO^{t}Bu (2.5 mol%) (entry 1, Table 4.1) yielded 25% of the *β*-alkylated product **4.4** (*ca.* 25 TON) in 86% selectivity (entry 1, Table 4.1 and 4.S1). However, the yield of **4.4** dropped to 8% in the presence of mercury (entry 2, Table 4.1). Similar to the very recent report by Wang[14b] on $CoCl_2$ catalyzed borylation, we found black heterogeneous Co nanoparticles (NPs) within 5 minutes of reaction (Figure 4.S91). However, in contrast to Wang's conditions, as the current reaction was performed in air, these particles were inactive and gave poor yields. Not surprisingly, repeating the reaction in an argon atmosphere under otherwise identical conditions gave better yields (*ca.* 44%) of **4.4** (entry 3, Table 4.1).

The rate of formation of Co NPs could be slowed down by a systematic decrease in the $CoCl_2$ loading while maintaining the amount of NaO^{t}Bu at 2.5 mol% (entries 4–7, Table 4.1). One may note that as the catalyst loading was varied from 1 mol% to 0.01 mol%, the concentration of the catalyst changed from 89.4 mM to 0.894 mM. This led to identification of the best (87% yield of **4.4** at 8700 TON with 91% selectivity) catalytic system (entry 7, Table 4.1). In contrast to the results obtained with 1 mol% $CoCl_2$ (entries 1, 2 and 3, Table 4.1), at lower loadings (0.01 mol%) of cobaltous chloride, the yield of **4.4** was comparable (entries 7, 8 and 9, Table 4.1) when the reaction was carried out in air, Ar and also in the presence of mercury which is indicative of the absence of highly sensitive Co NPs under these conditions. The exceptional activity could actually be attributed to molecular Co catalysts that are formed *in situ* (*vide infra*).

FETEM images were recorded by drop-casting the reaction mixture solution of **4.1** (5 mmol), **4.2** (5 mmol) and NaO^{t}Bu (2.5 mol%)) containing 1 mol%, 0.5 mol% and 0.01 mol% $CoCl_2$ on a TEM grid (Figure 4.1). It is evident that the density of nanoparticles was higher in the reaction mixture containing 1 mol% $CoCl_2$ (Figures 4.1a and b) in comparison to the one containing 0.5 mol% $CoCl_2$ (Figures 4.1c and d). While the NPs formed with 1 mol% $CoCl_2$ were of larger dimensions (*ca.* 5– 6 nm), the size of the Co NPs formed upon use of 0.5 mol% $CoCl_2$ was relatively smaller (*ca.* 2–3 nm).

Notably there was hardly any NP formation when 0.01 mol% $CoCl_2$ was used as demonstrated by the TEM images (Figures 4.1e and f). It is thus evident that the molecular Co species are

Table 4.1. The catalytic *β*-alkylation of **4.2** with **4.1** under varying conditions[a]

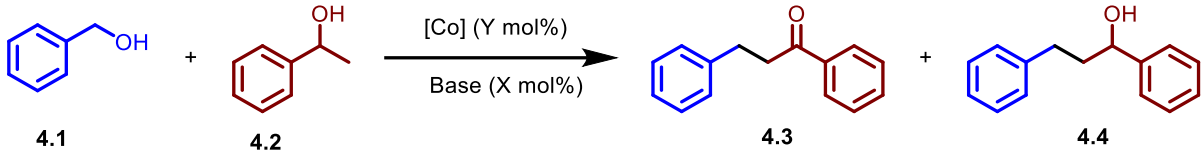

4.1 4.2 4.3 4.4

Entry	Catalyst (Y mol %)[b]	Base (X mol%)[b]	Yield[c] %		Selectivity[g] of **4.4**
			4.3	**4.4**	
1	$CoCl_2$ (1.0)	NaO^{t}Bu (2.5)	4	25	86
2[d]	$CoCl_2$ (1.0)	NaO^{t}Bu (2.5)	4	8	67
3[e]	$CoCl_2$ (1.0)	NaO^{t}Bu (2.5)	7	44	86
4	$CoCl_2$ (0.5)	NaO^{t}Bu (2.5)	4	49	92
5	$CoCl_2$ (0.1)	NaO^{t}Bu (2.5)	4	74	95
6	$CoCl_2$ (0.05)	NaO^{t}Bu (2.5)	4	81	95
7	$CoCl_2$ (0.01)	NaO^{t}Bu (2.5)	9	87	91
8[d]	$CoCl_2$ (0.01)	NaO^{t}Bu (2.5)	9	88	91
9[e]	$CoCl_2$ (0.01)	NaO^{t}Bu (2.5)	2	88	98
10	$CoCl_2$ (0.005)	NaO^{t}Bu (2.5)	4	78	95
11	$CoCl_2$ (0.01)	NaO^{t}Bu (1.25)	4	58	94
12	$CoCl_2.6H_2O$ (0.01)	NaO^{t}Bu (2.5)	3	63	95
13	$CoCl_2$ (0.01)	KO^{t}Bu (2.5)	4	41	91
14	$CoCl_2$ (0.01)	Na_2CO_3 (2.5)	0	0	0
15	$CoCl_2$ (0.01)	K_2CO_3 (2.5)	0	0	0
16	$CoCl_2$ (0.01)	KOH (2.5)	3	40	93
17	$CoCl_2$ (0.01)	NaOH (2.5)	6	82	93
18	$Co(OAc)_2$ (0.01)	NaO^{t}Bu (2.5)	4	84	95
19	$Co(acac)_2$ (0.01)	NaO^{t}Bu (2.5)	4	68	94
20	-	NaO^{t}Bu (2.5)	2	8	80
21	$CoCl_2$ (0.01)	NaO^{t}Bu (1)	6	19	76
22	$CoCl_2$ (0.01)	NaO^{t}Bu (5)	10	88	90
23	$CoCl_2$ (0.01)	NaO^{t}Bu (10)	8	86	91
24[f]	$CoCl_2$ (0.01)	NaO^{t}Bu (5)	2	70	97

[a]Reaction conditions: 5 mmol of **4.1**, 5 mmol of **4.2**, X mol% of base and Y mol% of Co catalyst at 140 °C. [b]mol % of base and catalyst is with respect to total alcohol content (**4.1**+**4.2**). [c]Yield is determined from ^{1}H NMR using toluene as standard. [d]Performed in the presence of excess Hg. [e]Performed under argon atmosphere. [f]Performed at 120 °C. [g]Selectivity of **4.4** = **((**Yield of **4.4***/ Total yield (**4.3** + **4.4**)) *100).

the major contributor towards catalysis when the *β*-alkylation is performed with 0.01 mol%

$CoCl_2$. Interestingly, with 0.01 mol% $CoCl_2$, the formation of Co NPs is observed only after stirring for prolonged times (*ca.* 8 h, Figure 4.S89). However, by this time, the *β*-alkylation had almost levelled off.

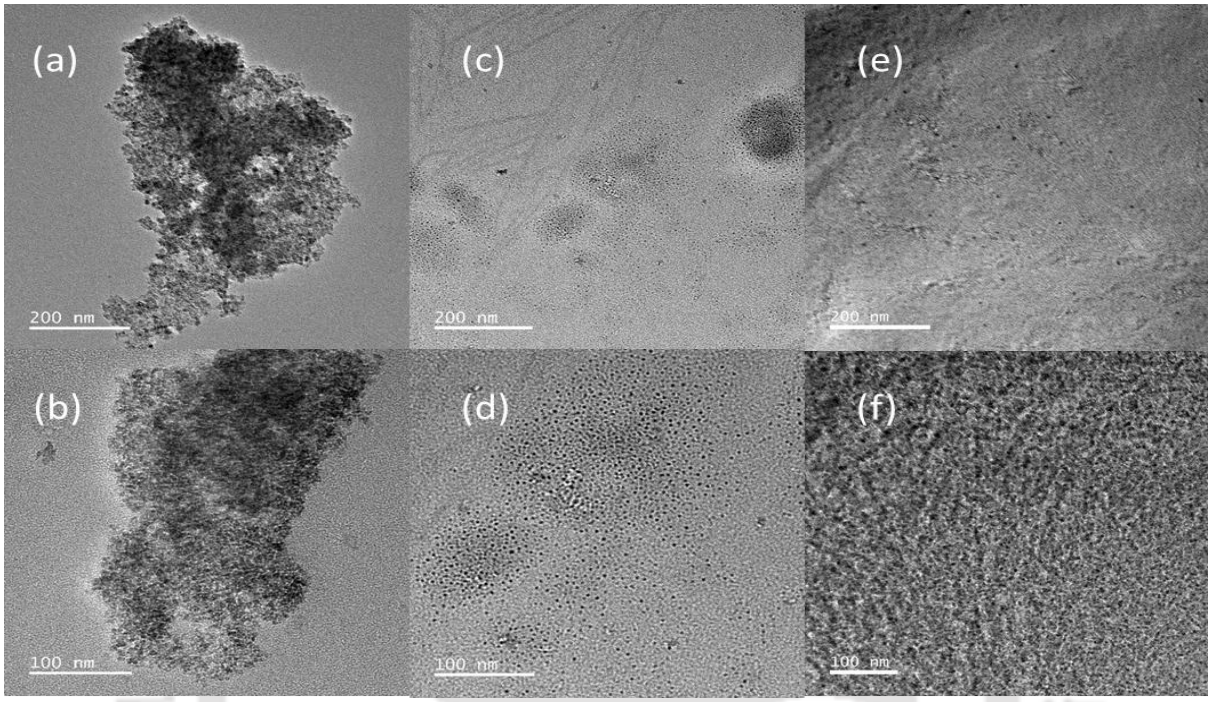

Figure 4.1. FETEM images obtained by drop-casting a solution of **4.1** (5 mmol), **4.2** (5 mmol) and NaO^{t}Bu (2.5 mol%) in the presence of (a and b) $CoCl_2$ (1.0 mol%), (c and d) $CoCl_2$ (0.5 mol%) and (e and f) $CoCl_2$ (0.01 mol%) immediately after mixing.

Utilization of KO^{t}Bu, Na_2CO_3, K_2CO_3 and KOH in combination with 0.01 mol% $CoCl_2$ was found to yield inferior results (entries 13–16, Table 4.1). The yield of the *β*-alkylated alcohol **4.4** in reactions catalyzed by other Co(II) catalysts (that are typically derived from $CoCl_2$) was either poorer (entries 12 and 19, Table 4.1) or comparable (entry 18, Table 4.1). Using $CoCl_2$ as a catalyst, under the best conditions (entry 7, Table 4.1), the alkylation of several 1-phenyl ethanol derivatives with a variety of benzyl alcohols was carried out (Tables 4.2 and 4.3). Notably, the yield of the *β*-alkylation decreased upon the use of benzyl alcohols with electron withdrawing groups in the *para*-position (**4.4a** and **4.4g**, Table 4.2), with primary/secondary alcohols based on heterocyclic rings (**4.4d**, **4.4e**, **4.4f** and **4.4l**, Table 4.2; **4.4y**, **4.4.za** and **4.4zb**, Table 4.3), primary aliphatic alcohols (**4.4n–p** and **4.4zi** Table 4.2) and secondary aliphatic alcohols (**4.4s**, Table 4.3).

Table 4.2. The $CoCl_2$ catalyzed *β*-alkylation of 1-phenyl ethanol with various derivatives of benzyl alcohol[a]

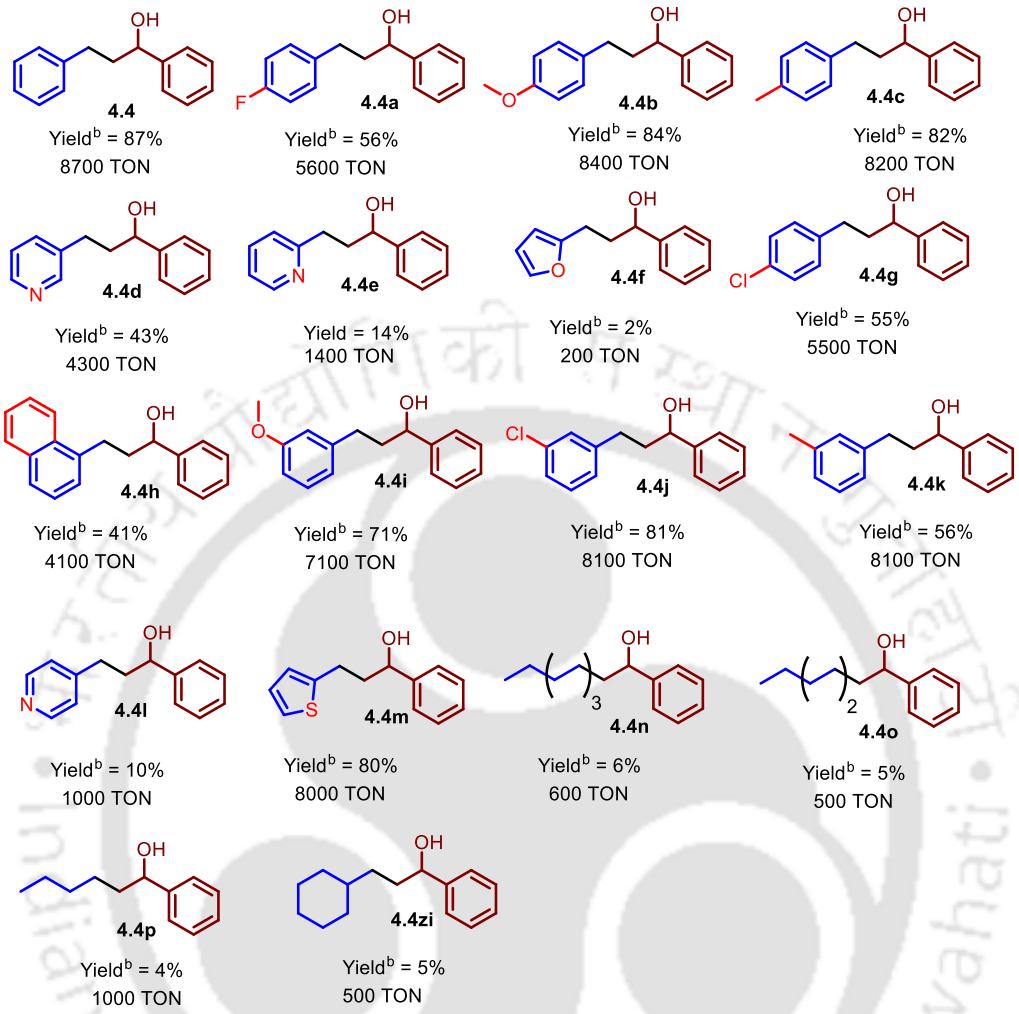

[a]Reaction conditions: 5 mmol of **4.1**, 5 mmol of **4.2**, 2.5 mol% of NaO^{t}Bu and 0.01 mol% of $CoCl_2$. [b]Yield is determined from ^{1}H NMR using toluene as a standard.

4.3.2. Control experiments

The following points form the basis of the proposed mechanism of the $CoCl_2$ catalyzed *β*-alkylation of alcohols:

(i) Higher loadings (1 mol%) of $CoCl_2$ lead to instant particle formation (Figure 4.S91) which are rendered inactive (entry 1, Table 4.1) by air.

(ii) At lower (0.01 mol%) loading of $CoCl_2$, the similar product profiles observed for consumption of **4.2** and formation of **4.4** as a function of time for the reactions with (blue Figure 4.2a) and without (purple legends, Figure 4.2a) hot filtration[13b,c] suggest the involvement of molecular Co species (Figures 4.S86 and 4.S88) rather than the heterogeneous

species.

(iii) Interestingly, in both cases, the catalyst heterogenized (see SEM images, Figures 4.2c and 4.S89) when the reaction levelled off after 8 h. The onset of particle formation requires about 8 h after which the reactivity is lost.

Table 4.3. The $CoCl_2$ catalyzed β-alkylation of various 1-phenyl ethanol derivatives with benzyl alcohol[a]

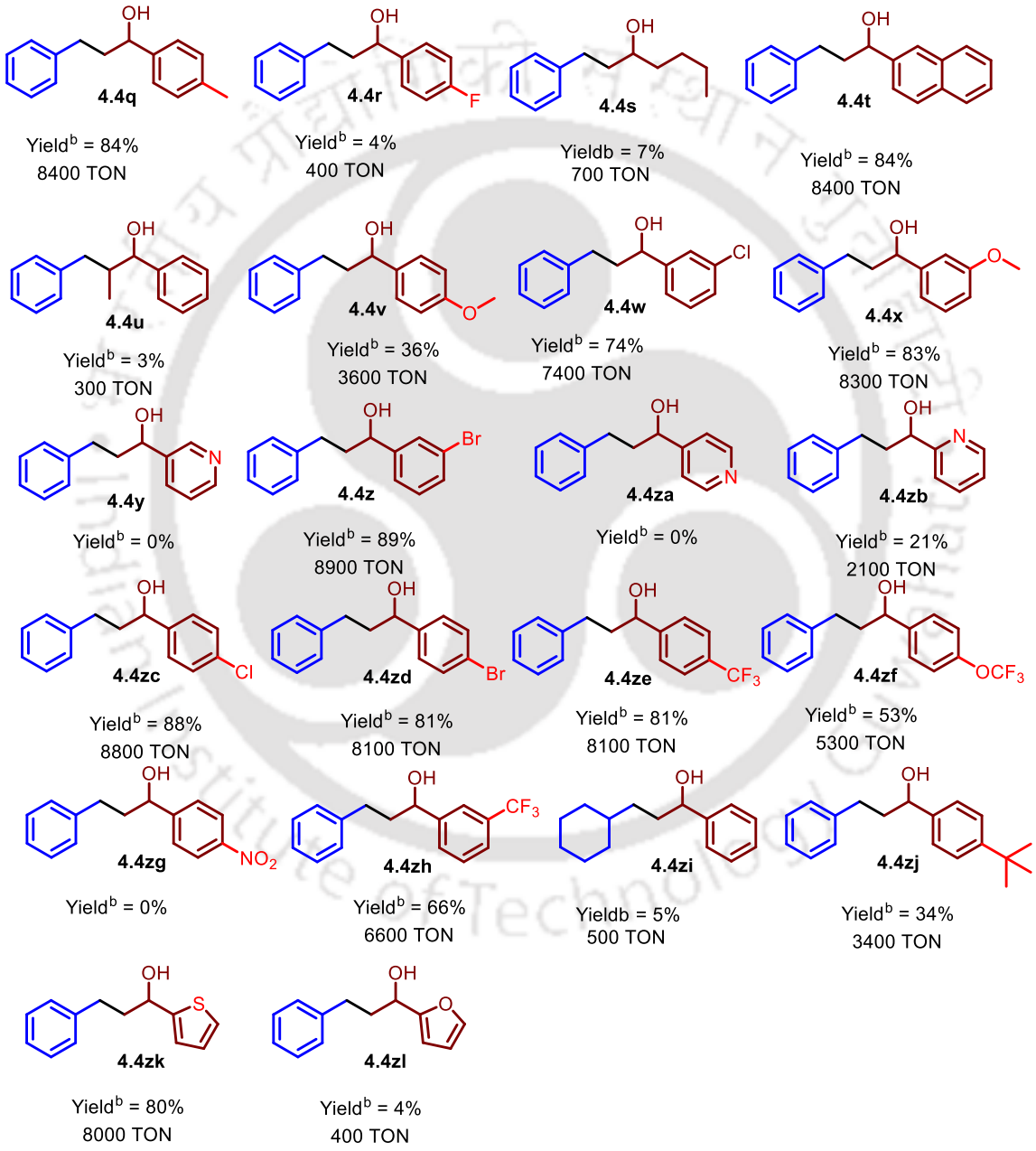

[a]Reaction conditions: 5 mmol of **4.1**, 5 mmol of **4.2**, 2.5 mol% of NaO^{t}Bu and 0.01 mol% of $CoCl_2$. [b]Yield is determined from ^{1}H NMR using toluene as a standard.

(iv) The decrease in productivity as we move from an interval-free reaction (Figure 4.2a, purple legend) to reactions with a three-hour break after 3 h of reaction (Figure 4.2a, brown legends) further fortifies the contribution of molecular species rather than the heterogeneous species. A three-hour break after 3 h of reaction would mean a residence time of six hours for the catalyst in the solution. By this time the reaction mixture would be ready to witness the onset of formation of Co NPs. Hence further make-up for the lost heating time does not lead to the same productivity as interval-free heating owing to the fact that the majority of the active molecular Co species are lost as Co NPs.

With an objective of elucidating the mechanism of the reaction, **4.1** (5 mmol) and **4.2** (5 mmol) were independently heated at 140 °C with $CoCl_2$ (0.01 mol%) and NaO^tBu (2.5 mol%) under non-inert conditions for 1 h. While analysis of the head-space indicated the formation of hydrogen (Figures 4.7 and 4.S69), the corresponding analysis of the reaction mixture indicated the formation of trace amounts of benzaldehyde and acetophenone respectively (Figures 4.S40 and 4.S41). In another experiment, a mixture of **4.1** (5 mmol) and **4.2** (5 mmol) was heated at 140 °C in the presence of $CoCl_2$ (0.1 mol%) and NaO^tBu (2.5 mol%) in air. The brown reaction mixture was followed with time by ESR (Figure 4.S63) and HRMS (Figure 4.3) analysis. The HRMS analysis at t = 0 h (prior to heating) showed a peak at m/z = 351.2727 and m/z = 679.5467 that corresponds to molecular complexes **4.5a** and **4.5b**, respectively, arising from the *in-situ* complex formation of **4.1** and/or **4.2** with $CoCl_2$.

Upon heating, the reaction mixture had a statistical mixture of various Co(II) complexes (**4.19a**–**4.c**) (Figures 4.3b and 4.S45**)** that could be attributed to coordination of starting materials and products (**4.1**–**4.4**) from the reaction mixture with $CoCl_2$. These observations clearly indicate the involvement of molecular Co(II) species during catalysis with 0.01 mol% $CoCl_2$ in line with the observations made in Figure 4.2. All throughout, the reaction mixture was ESR silent (Figures 4.S64–4.S68) indicative of the fact that these Co(II) species **4.5** and **4.19** are in an octahedral environment.[14] One could envisage that while species **4.5a** could complete its octahedral environment by incorporation of a Cl^- ligand, species **4.19a** and **4.19b** can include neutral alcohol/solvent molecules to satisfy their coordination.

On the other hand, in the HRMS analysis of the reaction mixture at a higher loading of $CoCl_2$ (1 mol%), the only molecular species that was discernible was the one observed at m/z = 679.5034 which corresponds to **4.5b** (Figures 4.4a and 4.S55). The rest of the species could

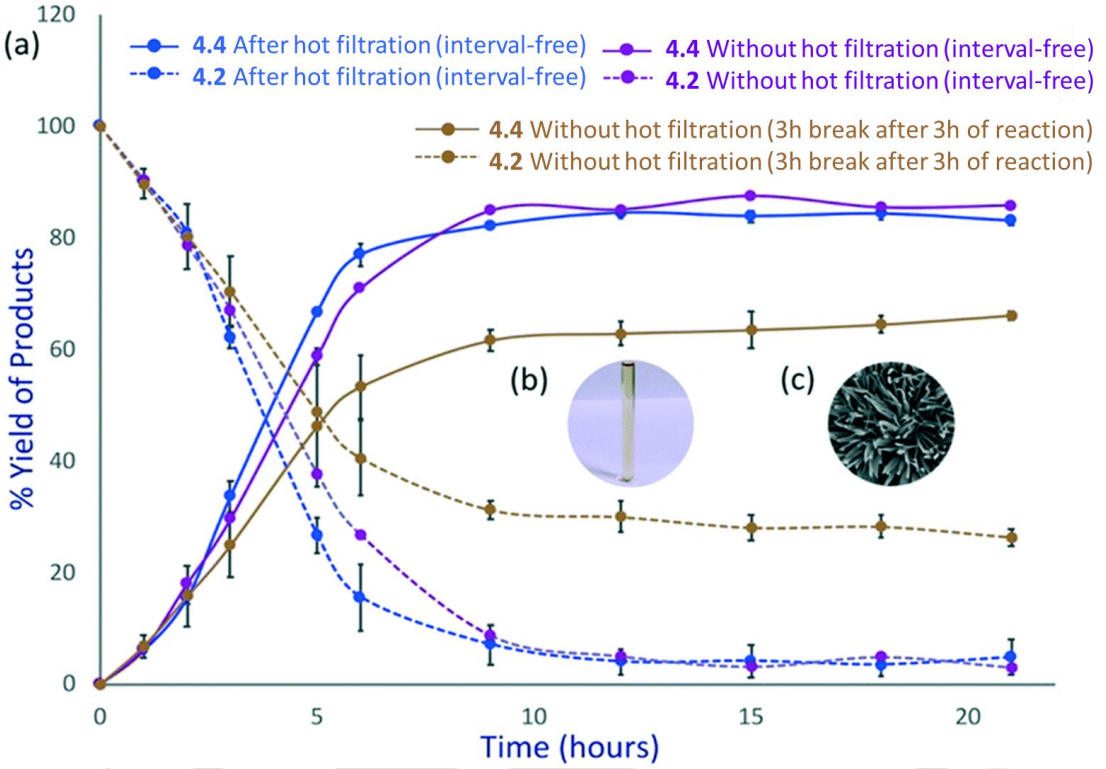

Figure 4.2. (a) Effect of hot-filtration on the $CoCl_2$ (0.01 mol%) catalysed *β*-alkylation of **4.2** with **4.1**. (b) Typical reddish-brown clear solution observed during initial times (0–8 h) of the $CoCl_2$ (0.01 mol%) catalysed *β*-alkylation of **4.2** with **4.1**. (c) SEM image of the black Co NPs formed in the $CoCl_2$ (0.01 mol%) catalyzed *β*-alkylation of **4.2** with **4.1**.

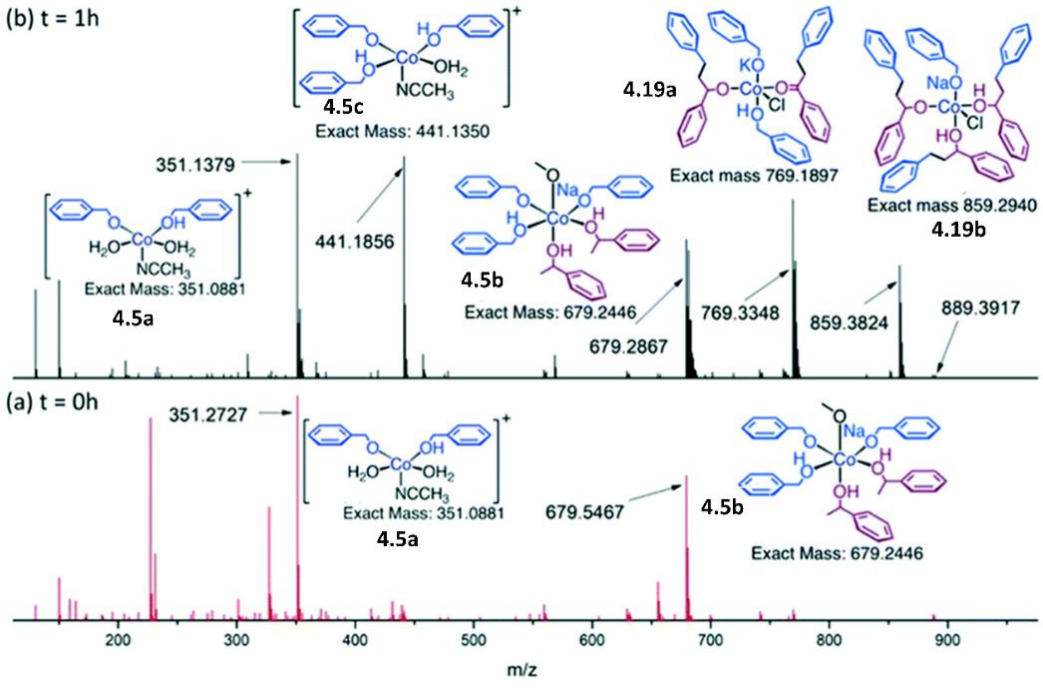

Figure.4.3. HRMS analysis of a mixture of **4.1** (5 mmol) and **4.2** (5 mmol) in the presence of $CoCl_2$ (0.1 mol%) and NaO^tBu (2.5 mol%) after (a) 0 h and (b) 1 h.

be mapped to Co NPs (**4.5g**, Figures 4.4a and 4.S55–4.S62) or their precursors (**4.5d**, **4.5e**, 5h and **4.5i**, Figures 4.4 and 4.S55-4.S62). Notably, NPs **4.5g**–**4.5i** are not detected by HRMS after 1 h (Figure 4.4b) of reaction owing to the fact that these species grow with time and are effectively removed by the pre-filtration (through 0.2 μm filter paper) process during mass sampling. These observations fortify our argument of rapid formation of Co NPs at a higher loading of $CoCl_2$. Furthermore, one must note that species **4.5g**–**4.5i** are not observed during the time frame (up to 8 h) when good reactivity is observed in the $CoCl_2$ (0.1 mol%) catalysed *β*-alkylation of **4.2** with **4.1**. This is indicative of the fact that NPs that were capable of escaping the pre-filtration were not present and have not contributed to the reactivity observed in entry 7, Table 4.1.

Valuable information was obtained from deuterium labelling experiments. Heating a mixture of **4.2** (5 mmol) and **4.1a** (5 mmol) at 140 °C with $CoCl_2$ (0.01 mol%) and NaO^tBu (2.5 mol%) in open air provided **4.4a** in 43% yield (Figure 4.5). In comparison, the corresponding yield obtained from **4.1** under similar conditions is 87%.

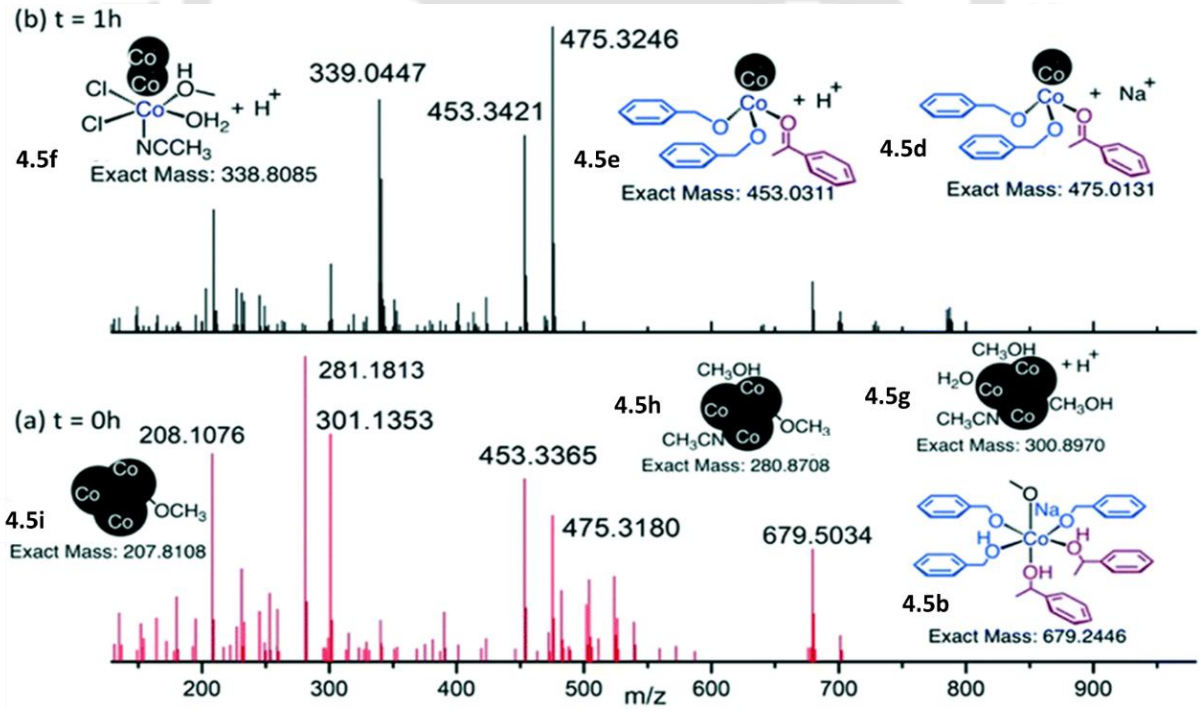

Figure 4.4. HRMS analysis of a mixture of **4.1** (5 mmol) and **4.2** (5 mmol) in the presence of $CoCl_2$ (1.0 mol%) and NaO^tBu (2.5 mol%) after (a) 0 h and (b) 1 h.

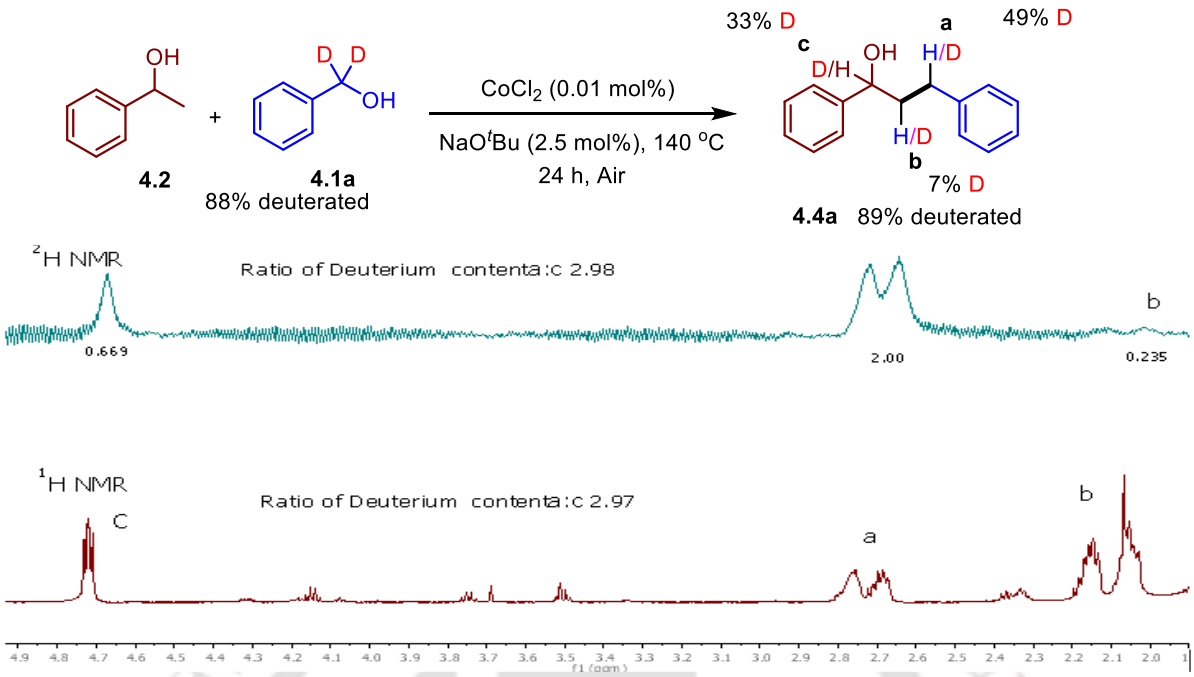

Figure 4.5. NMR (^{1}H and ^{2}H) analysis of a mixture of **4.1** (5 mmol) and **4.2a** (5 mmol) in the presence of $CoCl_2$ (0.01 mol%) and NaO^{t}Bu (2.5 mol%).

Analysis of the ^{1}H and ^{2}H NMR of the reaction mixture containing **4.4a** indicated C_a, C_b and C_c to be 49%, 7% and 33% deuterated, respectively. The deuterium content (88%) of **4.1a** was comparable to the net deuterium incorporated (89%) in the product **4.4a**. The ratio of deuterium incorporation at position "a" to the corresponding incorporation at position "c" was found to be 2.97 and 2.98 by ^{1}H and ^{2}H NMR, respectively. On the other hand, the reaction of a mixture of **4.2** (5 mmol), **4.1** (2.5 mmol) and **4.1a** (2.5 mmol) at 140 °C with $CoCl_2$ (0.01 mol%) and NaO^{t}Bu (2.5 mol%) in open air provided **4.4a** in 63% yield (Scheme 4.20) with a KIE of 1.61.[11k,15] These studies provide key evidence for the involvement of C–H activation (*vide infra*) in the *β*-alkylation of 1-phenyl ethanol with benzyl alcohol.[11i]

4.3.3. Plausible mechanism

The results obtained from filtration experiments, GC analysis of intermediates, ESR and HRMS studies form the basis of the proposed mechanism (Schemes 4.21–4.23). When $CoCl_2$ is dissolved in a mixture of **4.1** and **4.2**, it spontaneously forms an octahedral complex **4.5**/**5.6** (Scheme 4.21). A *β*-hydride elimination *via* transition state (TS) **4.7**/**4.8** gives the corresponding carbonyl compounds **1′**/**2′** and the hydride complex **4.12** (Scheme 4.21). While **4.1′** and **4.2′** are detected by NMR in the independent dehydrogenation of **4.1** and **4.2**

respectively **(**Figures 4.S40 and 4.S41), only **4.2′** is detected by NMR in the Guerbet reaction mixture (Figures 4.S70–4.S87). Subsequent σ-bond metathesis of the O–H bond in **4.1**/**4.2** with Co–H of **4.12** regenerates **4.5**/**4.6** (Scheme 4.21) with the evolution of H_2 (detected by GC, Figure 4.7 and 4.S69).

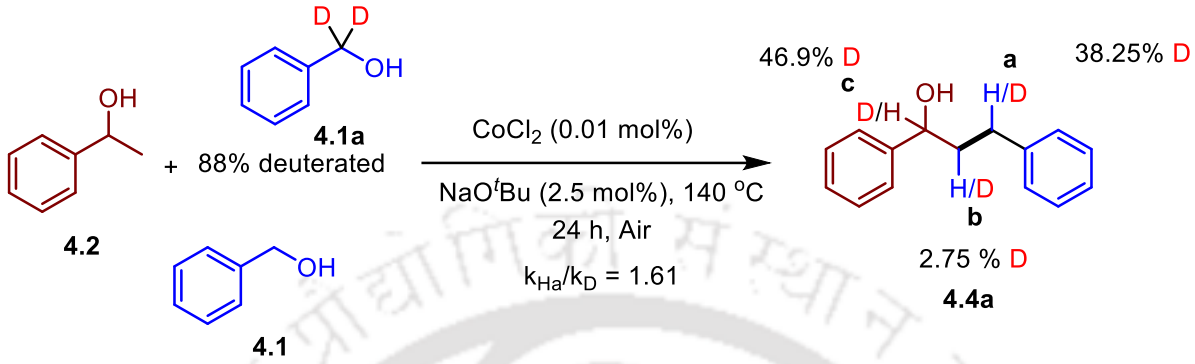

Scheme 4.20. KIE determination via competitive labelling.

The base mediated reaction of benzaldehyde (**4.1′**) with acetophenone (**4.2′**) results in the formation of the *α*, *β*-unsaturated ketone **4.3′** (not observed in ^{1}H NMR but detected in a few HRMS analyses, Figure 4.S49, 4.S52 and 4.S54). The next step (Scheme 4.22) involves the insertion of the double bond of **4.3′** into the Co–H bond in **4.12** to yield **4.14** *via* **TS 4.13**. The cycle is completed by the σ-bond metathesis of the Co–C bond in **4.14** with the H_2 or the O–H bond of **4.1**/**4.2** to yield the corresponding ketone **4.3** with the regeneration of catalytically active **4.12**/**4.5**/**4.6** (Scheme 4.22). One could envisage a similar cycle for the transformation of **4.3** to **4.4** (Scheme 4.5). The loss of deuterium (*ca.* 39%) at C_a and the very low deuterium content on C_b (Figure 4.5) indicate the involvement of the dehydrogenation step **4.5** → **4.12** and a rapid equilibrium of the σ-bond metathesis step **4.12** ↔ **4.5**/**4.6** (Scheme 4.21). For instance, dehydrogenation of **4.1a** would result in formation of Co–D species **4.12a**. The HD that is released *via* σ-bond metathesis step **4.12a** → **4.5**/**4.6** can result in D scrambling while reacting back in the reverse direction to give a Co–H species **4.12** and the corresponding alcohol that is deuterated at O. This O–D upon σ-bond metathesis with **4.14** would transfer the deuterium back to C_a. Insertion of **4.3′** into **4.12** would lead to no deuterium incorporation at C_b.

Similar to earlier reports with Ru[8l] and Ir[6h] catalysts, there is no initial build-up of **4.3** at very low loadings of $CoCl_2$ (Figures 4.S70 and 4.S71). This indicates rapid formation of **4.3** and **4.4** with a rate-determining dehydrogenation of either **4.1** or **4.2**. While we do not observe benzaldehyde **4.1′**, trace amounts (1–2%) of acetophenone **4.2′** are observed in the ^{1}H NMR of

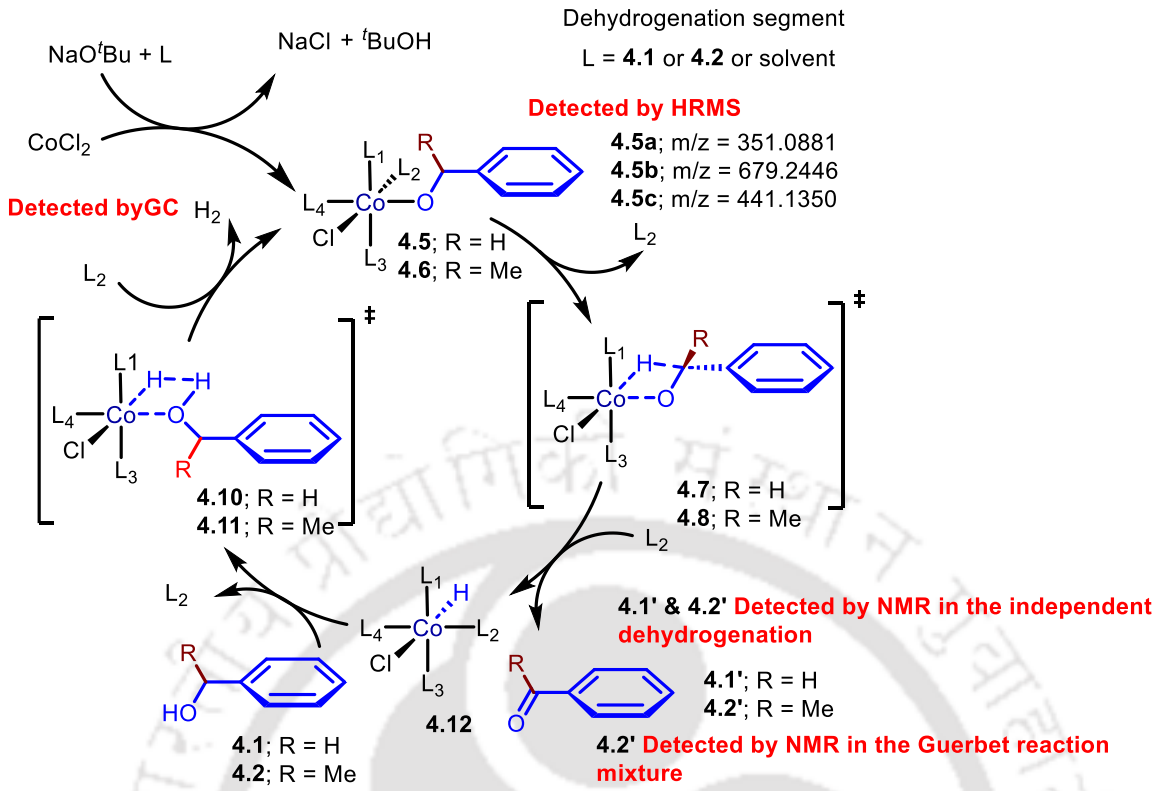

Scheme 4.21. Dehydrogenation segment of the proposed catalytic cycle for the cobaltous chloride catalyzed *β*-alkylation of **4.2** with **4.1**.

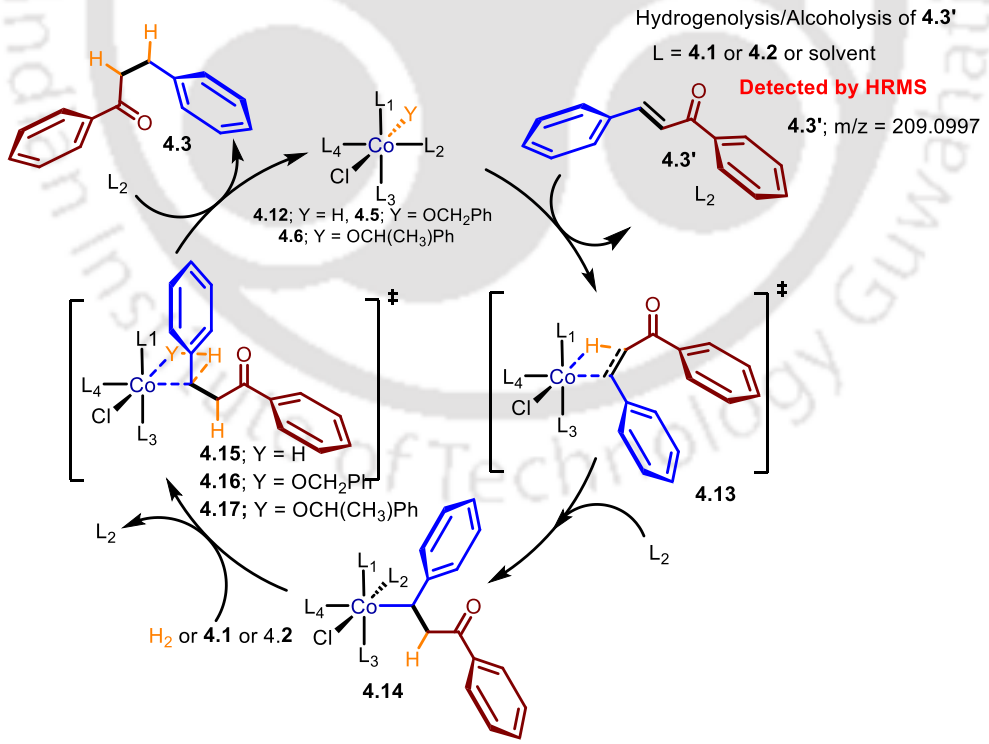

Scheme 4.22. Hydrogenolysis/alcoholysis of **4.3′** in the proposed catalytic cycle for the cobaltous chloride catalyzed *β*-alkylation of **4.2** with **4.1**.

the *β*-alkylation reaction mixture (Figures 4.S70–4.S87). Hence, it is likely that, very similar to our previous report,[8l] the step **4.6** → **4.12** is rate-determining.

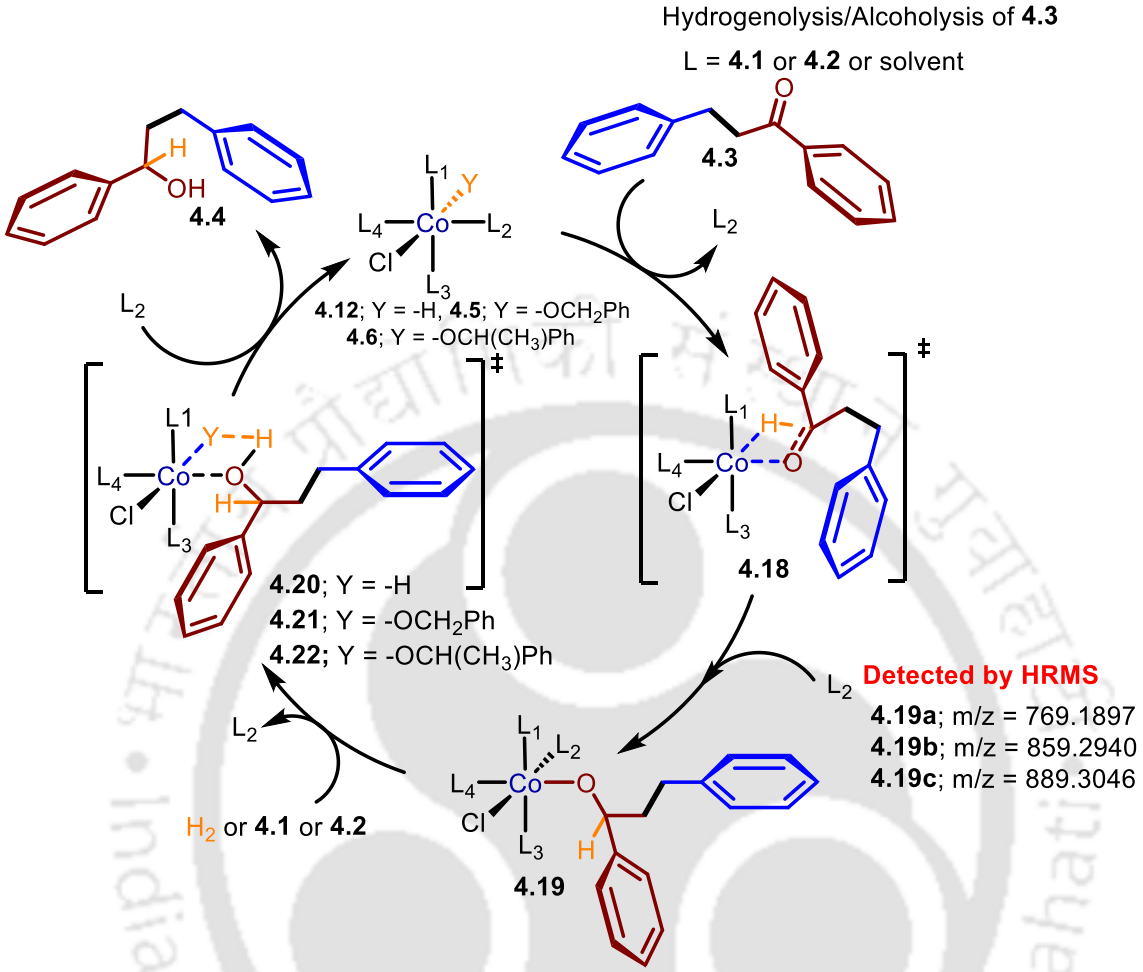

Scheme 4.23. Hydrogenolysis/alcoholysis of **4.3** in the proposed catalytic cycle for the cobaltous chloride catalyzed *β*-alkylation of **4.2** with **4.1.**

The observed KIE of 1.61 is also consistent with this argument. This means that **4.2′** has enough time to react back with Co–D species **4.12a** in a reversible fashion which eventually would reflect in the deuterium content at Cc. Hence, the deuterium distribution clearly indicates that the Co–D **4.12a** species formed in the first step is mostly transformed to a Co–H **4.12** species *via* a facile reverse reaction with HD and **4.2′**. Alternatively, the insertion of **4.3** into the Co–D species **4.12a** can also conveniently explain the deuterium incorporation at C*c*. Further in such a case, the deuterium distribution at C_a and C_b can also be rationalized if one invokes the possibility of Co–D species **4.12a** doing a D− transfer to the *β*-carbon of **4.3′**. through the step **14.2a** → **4.14a** (rather than the *α*-carbon as shown in the step **4.12** → **4.14**, Scheme 4.22) and

a subsequent σ-bond metathesis with O–H of the alcohol (Scheme 4.24). However, this possibility can be ruled out owing to steric reasons.

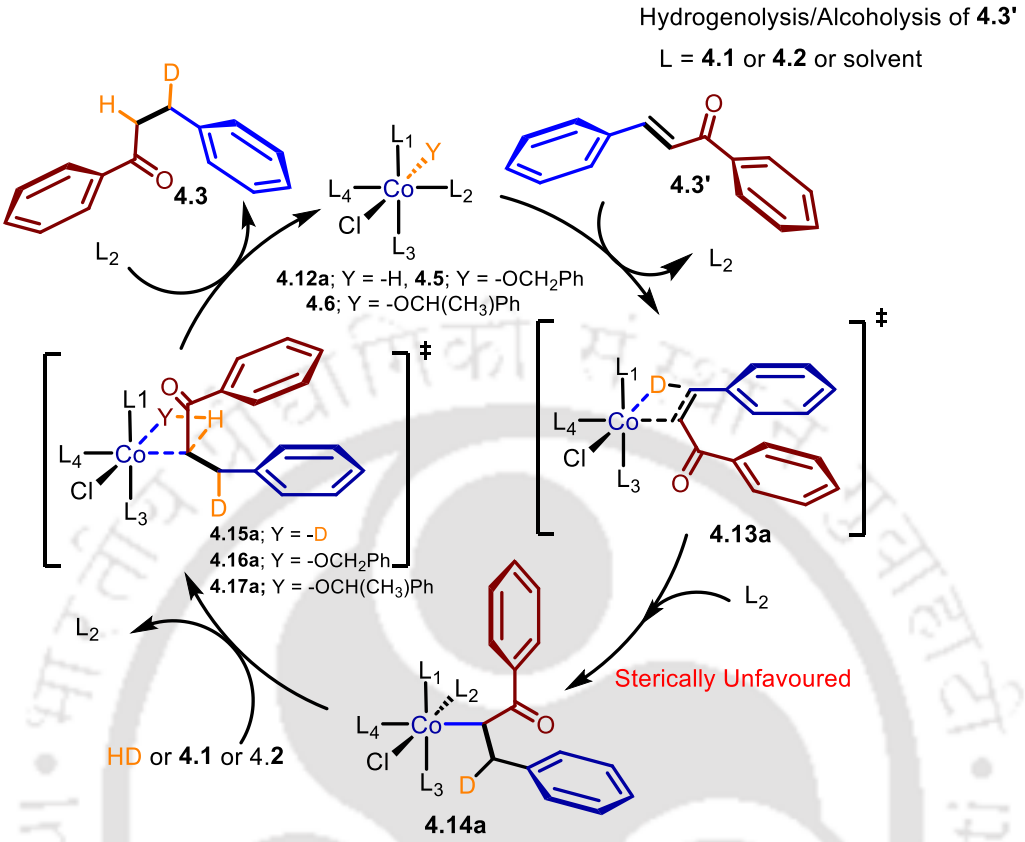

Scheme 4.24. An alternate path for hydrogenolysis/alcoholysis of **4.3′**.

4.3.4. Kinetic studies

The time course profiles of the cobaltous chloride catalysed *β*-alkylation of **4.2** with **4.1** at various concentrations of catalyst, base and alcohol are shown in Figures 4.S70–4.S82c. For each reaction, the concentration of a given compound was varied while keeping all other concentrations unchanged. For kinetic reactions involving alcohol (**4.1** or **4.2**) variations, mesitylene was used as a make-up solvent. It is evident from Table 4.1 (entries 7, 8 and 9), Figures 4.2 and 4.3 that the cobaltous chloride catalyzed *β*-alkylation of **4.2** with **4.1** is mostly homogeneous at low catalyst loadings. Accordingly, for a range of low catalyst concentrations (<0.025 mol% $CoCl_2$ equivalent to <2.24 mM), we have compiled the kinetic data using the initial rate method. The plots of initial rate vs. [$CoCl_2$] and initial rate vs. [NaO^tBu] were linear with a negligible intercept (Figure 4.6a and b). This points to a first order dependence of the rate on the concentration of both $CoCl_2$ and NaO^tBu. On the other hand, the dependence on concentration of both **4.1** and **4.2** was nonlinear (Figure 4.6c and d).

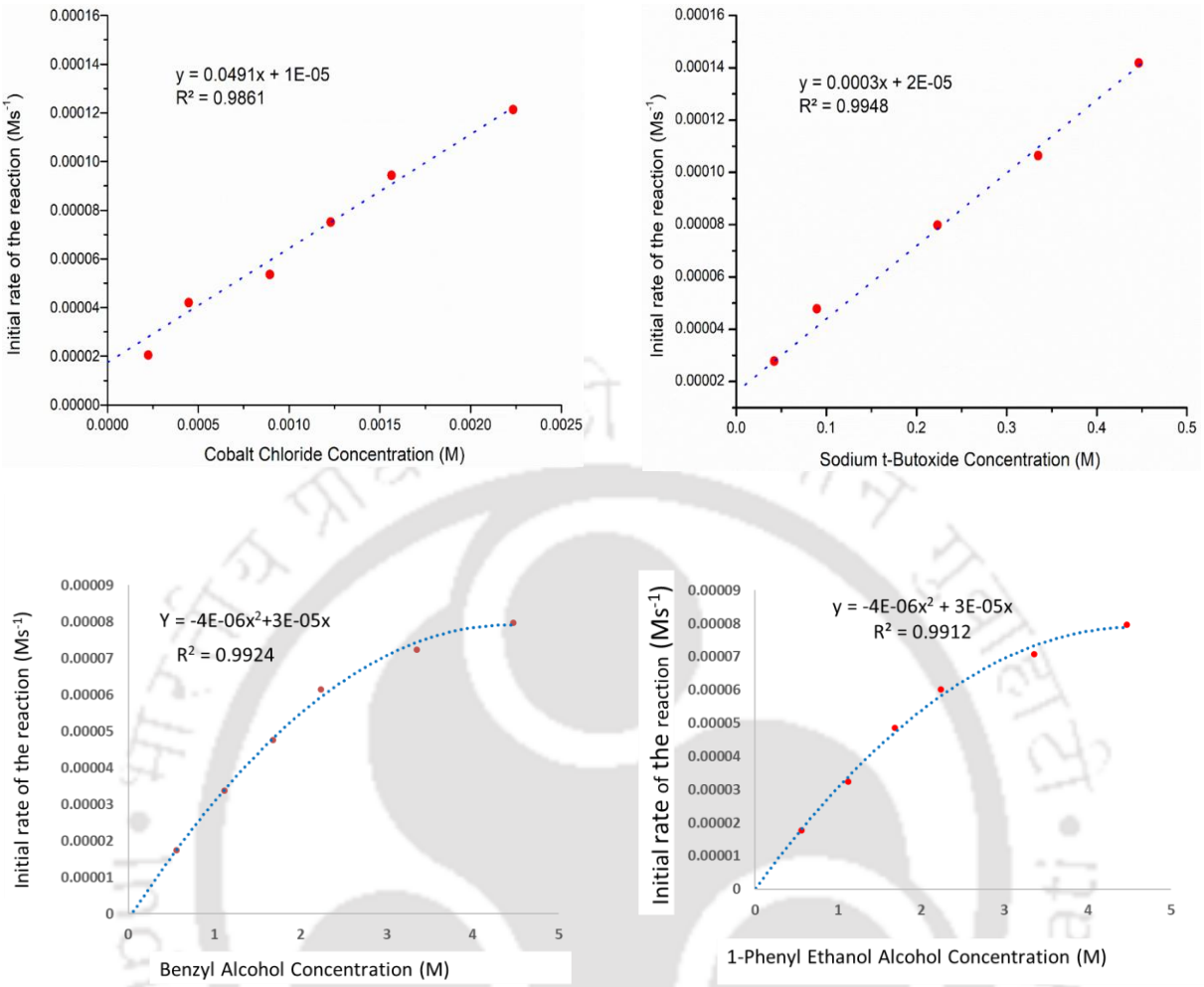

Figure 4.6. Dependence of the initial rate of the Guerbet reaction on the concentration of (a) cobaltous chloride (extracted from 30 minutes data of Figures 4.S70, 4.S71, 4.S72, 4.S75a, 4.S75b and 4.S75c), (b) Sodium *t*-butoxide (extracted from 60 minutes data of Figure 4.S70, 4.S76, 4.S77, 4.S78a and 4.S78b), (c) Benzyl alcohol (extracted from 60 minutes data of Figures 4.S70, 4.S79, 4.S80, 4.S80a, 4.S80b and 4.S80c) and (d) 1-Phenyl ethanol (extracted from 60 minutes data of Figures 4.S70, 4.S81, 4.S82, 4.S82a, 4.S82b and 4.S82c) (see Figure 4.11).

4.4. Conclusion

For the first time, we report the use of readily available $CoCl_2$ that forms complexes with alcohols *in-situ* which efficiently catalyzes the *β*-alkylation of alcohols in air. Higher loading of $CoCl_2$ (1 mol%) is accompanied with rapid formation of heterogeneous cobalt NPs which being sensitive to air result in poor yields (25%) of *β*-alkylated products. A better control over

reactivity (87% yield, *ca.* 8700 TON) could be obtained by delaying the heterogenization upon operating at very small amounts of $CoCl_2$ (0.01 mol%). Deuterium labelling studies are indicative of the involvement of C–H activation in the cobaltous chloride catalyzed *β*-alkylation with a k_H/k_D value of 1.61. The reaction exhibits a first-order dependence of the initial rate on the concentration of both cobaltous chloride and sodium *t*-butoxide. On the other hand, a non-linear dependence of the rate on the concentration of 1-phenyl ethanol and benzyl alcohol was observed. Molecular Co catalysts rather than heterogeneous Co NPs thus lead to superior reactivity owing to the reaction conditions. These studies could open up several related reactivity with substrates that are capable of forming *in-situ* complexes with $CoCl_2$.

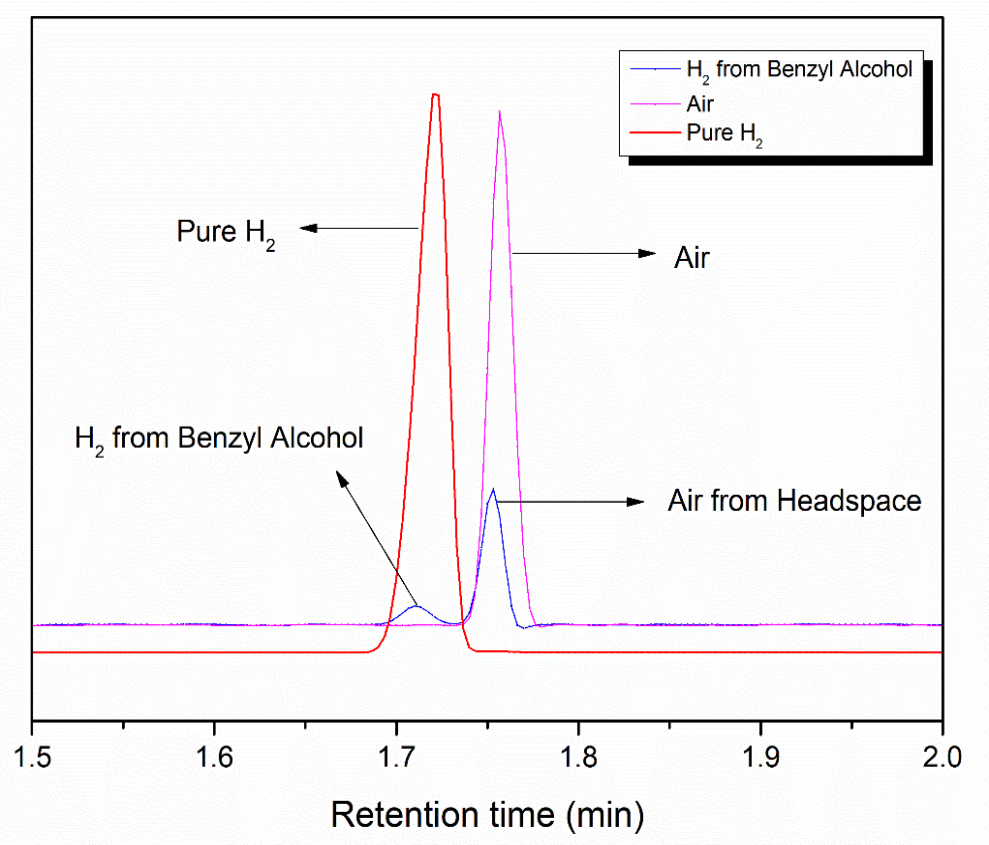

Figure 4.7. Evidence for H_2 evolution in the dehydrogenation of benzyl alcohol (**4.1**) catalyzed by $CoCl_2$ (0.01 mol %) at 140 °C *via* GC analysis.

4.5. Experimental section

4.5.1. General procedure and materials

All manipulations were carried out in air. The Co metal salts, NaO^{t}Bu, KO^{t}Bu, NaOH, KOH, Na_2CO_3, K_2CO_3, $CDCl_3$, benzyl alcohol, 1-phenyl ethanol and their derivatives were purchased

either from MERCK or Sigma−Aldrich and used as such. To prepare the stock solution, $CoCl_2$ was dissolved either in benzyl alcohol or 1-phenyl ethanol. All catalytic reactions were carried out in air using oven-dried glassware. The 1-phenyl ethanol derivatives which were commercially not available were prepared according to literature procedure.

4.5.2. Physical measurements

^{1}H, $^{13}C\{H\}$ and ^{19}F NMR were recorded on a Bruker ASCEND 600 operating at 600 MHz for ^{1}H, 150 MHz for $^{13}C\{H\}$ or on a Bruker AVANCE 400 operating at 400 MHz for ^{1}H, 100 MHz for $^{13}C\{H\}$ or on a Bruker AVANCE 500 operating at 500 MHz for ^{1}H, 125 MHz for $^{13}C\{H\}$. Chemical shifts (δ) are reported in ppm. HRMS measurements were done using an Agilent Accurate-Mass Q-TOF ESI–MS 6520. The X-band EPR spectra were recorded on a JES-FA200 ESR spectrometer. The field-emission scanning electon microscopy (FESEM) were performed using JSM-7610F instrument. Transmission electron microscopy (TEM) analysis were carried out using a JEOL JEM-2100F FETEM instrument. GC analysis (TCD detection) was performed on a Agilent 7820-GC instrument fitted with Agilent Front SSZ Inlet N_2 HP-PLOT Q column (30 m length x 530 μm x 40 μm) using the following method: Agilent 7820-GC back detector TCD, Oven temperature: 50 °C, Inlet temperature: 100 °C, Detector temperature (TCD): 250 °C, Detector, temperature (FID): 300 °C, Time at starting temp: 0 min , Hold time = 10 min , Flow rate (carrier): 25 mL/min (N_2) , Split flow: 50 mL/min, Split ratio: 10.

4.5.3. General procedure for $CoCl_2$ catalyzed *β*-alkylation of alcohols

In a 10 mL pear-shaped flask, 1-phenyl ethanol or benzyl alcohol were taken in air. This was followed by addition of 2.5 mol % of NaO^tBu and 0.01 mol % of $CoCl_2$ (from a stock solution either in 1-phenyl ethanol or benzyl alcohol). After the addition, the reaction mixture contained 0.61 mL (5.00 mmol) of 1-phenyl ethanol, 0.52 mL (5.00 mmol) of benzyl alcohol, 24 mg (0.25 mmol) of NaO^tBu and 0.13 mg (1 μmol) of $CoCl_2$. The mixture was heated at 140 °C for 24 h in air. The reaction mixture was then cooled to room temperature. An aliquot (Typically 10 mg) was withdrawn from reaction mixture and the yield was determined by ^{1}H NMR using $CDCl_3$ as solvent and toluene (Typically 10 μL) as a standard.

4.5.4. Preparation of FESEM sample

An aliquot (approximately 10 mg) was withdrawn from reaction mixture and drop casted on a

glass slide. The drop casted sample was submitted for FESEM analysis. A JSM-7610F instrument was used for the field-emission scanning electron microscopy (FESEM) analysis.

4.5.5. Preparation of TEM sample

An aliquot (approximately 10 mg) was withdrawn from reaction mixture and drop casted on a TEM grid. The dropcasted sample was submitted for TEM analysis. Transmission electron microscopy (TEM) analysis were carried out using a JEOL JEM-2100F FETEM instrument.

4.5.6. General procedure for $CoCl_2$ catalyzed *β*-alkylation of alcohols-kinetic study

In a 10 mL pear-shaped flask, 1-phenyl ethanol or benzyl alcohol were taken in air. This was followed by addition of 2.5 mol % of NaO^tBu and 0.01 mol % of $CoCl_2$ (from a stock solution either in 1-phenyl ethanol or benzyl alcohol). After the addition, the reaction mixture contained 0.61 mL (5.00 mmol) of 1-phenyl ethanol, 0.52 mL (5.00 mmol) of benzyl alcohol, 24 mg (0.25 mmol) of NaO^tBu and 0.13 mg (1 μmol) of $CoCl_2$. The mixture was heated at 140 °C and aliquots were withdrawn at periodic intervals of 0.5h, 1h, 2h, 3h, 5h, 6h, 9h, 12h, 15h, 18h, 21h and 24 h. Yield of the desried product was determined by ^1H NMR using $CDCl_3$ as solvent and toluene as standard.

4.5.7. Procedure for $CoCl_2$ catalyzed *β*-alkylation of alcohols with hot filtration

In a 10 mL pear-shaped flask, 1-phenyl ethanol or benzyl alcohol were taken in air. This was followed by addition of 5 mol % of NaO^tBu and 0.02 mol % of $CoCl_2$ (from a stock solution either in 1-phenyl ethanol or benzyl alcohol). After the addition, the reaction mixture contained 0.61 mL (5.00 mmol) of 1-phenyl ethanol, 0.52 mL (5.00 mmol) of benzyl alcohol, 24 mg (0.25 mmol) of NaO^tBu and 0.13 mg (1 μmol) of $CoCl_2$. The mixture was heated at 140 °C and an aliquot was withdrawn after 1h and the yield of the desried product was determined by ^1H NMR using $CDCl_3$ as solvent and toluene as standard. The hot reaction mixture was subsequently filtered using 0.2 μm Nylon Membrane Filter. The filterate was then heated at 140 °C and aliquots were withdrawn at periodic intervals of 0.5h, 1h, 2h, 3h, 5h, 6h, 9h, 12h, 15h, 18h, 21h and 24 h. Yield of the desried product was determined by ^1H NMR using $CDCl_3$ as solvent and toluene as standard.

4.5.8. Procedure for $CoCl_2$ catalyzed *β*-alkylation of alcohols with 3h interval after 3h of reaction

In a 10 mL pear-shaped flask, 1-phenyl ethanol or benzyl alcohol were taken in air. This was followed by addition of 5 mol % of NaO^{t}Bu and 0.02 mol % of $CoCl_2$ (from a stock solution either in 1-phenyl ethanol or benzyl alcohol). After the addition, the reaction mixture contained 0.61 mL (5.00 mmol) of 1-phenyl ethanol, 0.52 mL (5.00 mmol) of benzyl alcohol, 24 mg (0.25 mmol) of NaO^{t}Bu and 0.13 mg (1 μmol) of $CoCl_2$. The mixture was heated at 140 °C and aliquots were withdrawn after 1h, 2h and 3h. The reaction mixture was then allowed to stand for 3h. After this 3h break, heating was then resumed and aliquots were withdrawn at periodic intervals of 5h, 6h, 9h, 12h, 15h, 18h, 21h and 24 h of reaction at 140 °C. Yield of the desried product was determined by ^{1}H NMR using $CDCl_3$ as solvent and toluene as standard.

Supporting information (containing NMR spectra and of reaction mixtures, HRMS data, Kinetics plot, GC plot, EPR data, TEM image, SEM image) for chapter IV is available as appendix III and can be found at
https://drive.google.com/file/d/1nRhwGf9bdDny5-1W_ZrfScmF2e7tI0ZP/view?usp=sharing

4.6. References

(1) Akhtar, W. M.; Armstrong, R. J.; Frost, J. R.; Stevenson, N. G.; Donohoe, T. J. Stereoselective Synthesis of Cyclohexanes via an Iridium Catalyzed (5 + 1) Annulation Strategy. *J. Am. Chem. Soc.* **2018**, *140*, 11916-11920.
(2) Yi, H.; Zhang, G.; Wang, H.; Huang, Z.; Wang, J.; Singh, A. K.; Lei, A. Recent Advances in Radical C–H Activation/Radical Cross-Coupling. *Chem. Rev.* **2017**, *117*, 9016-9085.
(3) (a) Zhang, Y.-F.; Shi, Z.-J. Upgrading Cross-Coupling Reactions for Biaryl Syntheses. Acc. *Chem. Res.* **2019**, *52*, 161-169. (b) Das, K.; Kumar, A. Chapter One - Alkane dehydrogenation reactions catalyzed by pincer-metal complexes. In *Advances in Organometallic Chemistry*, Pérez, P. J., Ed. Academic Press: 2019; Vol. 72, pp 1-57. (c) Kumar, A.; Bhatti, T. M.; Goldman, A. S. Dehydrogenation of Alkanes and Aliphatic Groups by Pincer-Ligated Metal Complexes. *Chem. Rev.* **2017**, *117*, 12357-12384. (d) A. Kumar and A. Goldman, in The Privileged Pincer-Metal Platform: Coordination Chemistry & Applications, eds. G. van Koten and R. A. Gossage, Springer International Publishing, 2016, vol. 54, ch. 113, pp. 307-334.
(4) (a) Xu, Q.; Chen, J.; Liu, Q. Aldehyde-Catalyzed Transition Metal-Free Dehydrative β-Alkylation of Methyl Carbinols with Alcohols. *Adv. Synth. Catal.* **2013**, *355*, 697-704. (b) Allen, L. J.; Crabtree, R. H. Green alcohol couplings without transition metal catalysts: base-mediated β-alkylation of alcohols in aerobic conditions. *Green Chem.* **2010**, *12*, 1362-1364. (c) Xu, Q.; Chen, J.; Tian, H.; Yuan, X.; Li, S.; Zhou, C.; Liu, J. Catalyst-Free Dehydrative α-Alkylation of Ketones with Alcohols: Green and Selective Autocatalyzed Synthesis of Alcohols and Ketones. *Angew. Chem. Int. Ed.* **2014**, *53*, 225-229.
(5) (a)Kose, O.; Saito, S. Cross-coupling reaction of alcohols for carbon–carbon bond formation using pincer-type NHC/palladium catalysts. *Org. Biomol. Chem.* **2010**, *8*, 896-900. (b) Mamidala, R.; Biswal, P.; Subramani, M. S.; Samser, S.; Venkatasubbaiah, K., Palladacycle-Phosphine Catalyzed Methylation of Amines and Ketones Using Methanol. The *J. Org. Chem.* **2019**, *84*, 10472-10480.
(6) (a) Fujita, K.-i.; Asai, C.; Yamaguchi, T.; Hanasaka, F. Yamaguchi, R., Direct β-Alkylation of Secondary Alcohols with Primary Alcohols Catalyzed by a Cp*Ir Complex. *Org. Lett.* **2005**, *7*, 4017-4019. (b) Cheung, H. W.; Lee, T. Y.; Lui, H. Y.; Yeung, C. H.; Lau, C. P. Ruthenium-Catalyzed β-

Alkylation of Secondary Alcohols with Primary Alcohols. *Adv. Synth. Catal.* **2008**, *350*, 2975-2983. (c) Pontes da Costa, A.; Viciano, M.; Sanaú, M.; Merino, S.; Tejeda, J.; Peris, E.; Royo, B. First Cp*-Functionalized N-Heterocyclic Carbene and Its Coordination to Iridium. Study of the Catalytic Properties. *Organometallics* **2008,** *27*, 1305-1309. (d) Gnanamgari, D.; Sauer, E. L. O.; Schley, N. D.; Butler, C.; Incarvito, C. D.; Crabtree, R. H. Iridium and Ruthenium Complexes with Chelating N-Heterocyclic Carbenes: Efficient Catalysts for Transfer Hydrogenation, β-Alkylation of Alcohols, and N-Alkylation of Amines. *Organometallics*, **2009**, *28*, 321-325. (e) Gong, X.; Zhang, H.; Li, X. J. T. l. Iridium phosphine abnormal N-heterocyclic carbene complexes in catalytic hydrogen transfer reactions. *Tetrahedron Lett.* **2011**, *52*, 5596-5600. (f) Xu, C.; Goh, L. Y.; Pullarkat, S. A. J. O. Efficient iridium-thioether-dithiolate catalyst for β-alkylation of alcohols and selective imine formation via N-alkylation reactions. *Organometallics*, **2011**, *30*, 6499-6502. (g) Jiménez, M. V.; Fernández-Tornos, J.; Modrego, F. J.; Pérez-Torrente, J. J.; Oro, L. A. Oxidation and β-Alkylation of Alcohols Catalysed by Iridium(I) Complexes with Functionalised N-Heterocyclic Carbene Ligands. *Chem. Eur. J.* **2015**, *21*, 17877-17889. (h Genç, S.; Arslan, B.; Gülcemal, S.; Günnaz, S.; Çetinkaya, B.; Gülcemal, D. Iridium(I)-Catalyzed C–C and C–N Bond Formation Reactions via the Borrowing Hydrogen Strategy. *J. Org. Chem.* **2019**, *84*, 6286-6297. (i) Wang, D.; McBurney, R. T.; Pernik, I.; Messerle, B. A. Controlling the selectivity and efficiency of the hydrogen borrowing reaction by switching between rhodium and iridium catalysts. *Dalton Trans.* **2019**, *48*, 13989-13999. (j) Musa, S.; Ackermann, L.; Gelman, D. Dehydrogenative Cross-Coupling of Primary and Secondary Alcohols. *Adv. Synth. Catal.* **2013**, *355*, 3077-3080. (k) Ruiz-Botella, S.; Peris, E. Unveiling the Importance of π-Stacking in Borrowing-Hydrogen Processes Catalysed by Iridium Complexes with Pyrene Tags. *Chem. Eur. J.* **2015**, *21*, 15263-15271. (l) Genç, S.; Günnaz, S.; Çetinkaya, B.; Gülcemal, S. l.; Gülcemal, D. Iridium (I)-Catalyzed Alkylation Reactions To Form α-Alkylated Ketones. *J. Org. Chem.* **2018**, *83*, 2875-2881. (m) Koda, K.; Matsu-ura, T.; Obora, Y.; Ishii, Y. Guerbet reaction of ethanol to n-butanol catalyzed by iridium complexes. *Chem. Lett.* **2009**, *38*, 838-839.

(7) Satyanarayana, P.; Reddy, G. M.; Maheswaran, H.; Kantam, M. L. Catalysis, Tris (acetylacetonato) rhodium (III)-Catalyzed α-Alkylation of Ketones, β-Alkylation of Secondary Alcohols and Alkylation of Amines with Primary Alcohols. *Adv. Synth. Catal.* **2013**, *355*, 1859-1867.

(8) (a) Zhang, C.; Zhao, J.-P.; Hu, B.; Shi, J.; Chen, D. Ruthenium-Catalyzed β-Alkylation of Secondary Alcohols and α-Alkylation of Ketones via Borrowing Hydrogen: Dramatic Influence of the Pendant N-Heterocycle. *Organometallics* **2019**, *38*, 654-664. (b) Sahoo, A. R.; Lalitha, G.; Murugesh, V.; Bruneau, C.; Sharma, G. V.; Suresh, S.; Achard, M. Ruthenium Phosphine–Pyridone Catalyzed Cross-Coupling of Alcohols To form α-Alkylated Ketones. *J. Org. Chem.* **2017**, *82*, 10727-10731. (c) Wang, Q.; Wu, K.; Yu, Z. Ruthenium (III)-catalyzed β-alkylation of secondary alcohols with primary alcohols. *Organometallics* **2016**, 35, 1251- 1256. (d) Roy, B. C.; Chakrabarti, K.; Shee, S.; Paul, S.; Kundu, S. Bifunctional RuII-Complex-Catalysed Tandem C− C Bond Formation: Efficient and Atom Economical Strategy for the Utilisation of Alcohols as Alkylating Agents. *Chem. Eur. J.* **2016**, *22*, 18147-18155. (e) Chakrabarti, K.; Paul, B.; Maji, M.; Roy, B. C.; Shee, S.; Kundu, S. Bifunctional Ru (ii) complex catalysed carbon–carbon bond formation: an eco-friendly hydrogen borrowing strategy. *Org. Biomol. Chem.* **2016**, *14*, 10988-10997. (f) Cho, C. S.; Kim, B. T.; Kim, H.-S.; Kim, T.-J.; Shim, S. C. Ruthenium-catalyzed one-pot β-alkylation of secondary alcohols with primary alcohols. *Organometallics* **2003**, *22*, 3608-3610. (g) Shi, J.; Hu, B.; Ren, P.; Shang, S.; Yang, X.; Chen, D. Synthesis and Reactivity of Metal–Ligand Cooperative Bifunctional Ruthenium Hydride Complexes: Active Catalysts for β-Alkylation of Secondary Alcohols with Primary Alcohols. *Organometallics* **2018**, *37*, 2795-2806. (h) Dowson, G. R.; Haddow, M. F.; Lee, J.; Wingad, R. L.; Wass, D. F. Catalytic conversion of ethanol into an advanced biofuel: unprecedented selectivity for n-butanol. *Angew. Chem. Int. Ed.* **2013**, *52*, 9005- 9008. (i) Wingad, R. L.; Gates, P. J.; Street, S. T.; Wass, D. F. Catalytic conversion of ethanol to n-butanol using ruthenium P–N ligand complexes. *ACS Catal.* **2015**, *5*, 5822-5826. (j) Tseng, K.-N. T.; Lin, S.; Kampf, J. W.; Szymczak, N. K. Upgrading ethanol to 1-butanol with a homogeneous air-stable ruthenium catalyst. *Chem. Commun.* **2016**, *52*, 2901- 2904. (k) Xie, Y.; Ben-David, Y.; Shimon, L. J.; Milstein, D. Highly efficient process for production of biofuel from ethanol catalyzed by ruthenium pincer complexes. *J. Am. Chem. Soc.* **2016**, *138*, 9077-9080. (l) Das, K.; Yasmin, E.; Das, B.; Srivastava, H. K.; Kumar, A. Technology, Phosphine-free pincer-ruthenium catalyzed biofuel production: high rates, yields and turnovers of solventless alcohol alkylation. *Catal.*

Sci. Technol. **2020**, *10*, 8347-8358. (m) Bhattacharyya, D.; Sarmah, B. K.; Nandi, S.; Srivastava, H. K.; Das, A. Selective Catalytic Synthesis of α-Alkylated Ketones and β-Disubstituted Ketones via Acceptorless Dehydrogenative Cross-Coupling of Alcohols. *Org. Lett.* **2021**, *23*, 869-875. (n) Liu, T.-T.; Tang, S.-Y.; Hu, B.; Liu, P.; Bi, S.; Jiang, Y.-Y. Mechanism and Origin of Chemoselectivity of Ru-Catalyzed Cross-Coupling of Secondary Alcohols to β-Disubstituted Ketones. *J. Org. Chem.* **2020**, *85*, 12444-12455. (o) Genç, S.; Arslan, B.; Gülcemal, S.; Günnaz, S.; Çetinkaya, B.; Gülcemal, D., Iridium(I)-Catalyzed C–C and C–N Bond Formation Reactions via the Borrowing Hydrogen Strategy. *J. Org. Chem.* **2019,** *84*, 6286-6297.

(9) (a) Pandey, B.; Xu, S.; Ding, K. Selective Ketone Formations via Cobalt-Catalyzed β-Alkylation of Secondary Alcohols with Primary Alcohols. *Org. Lett.* **2019**, *21*, 7420-7423. (b) Freitag, F.; Irrgang, T.; Kempe, R. Cobalt-Catalyzed Alkylation of Secondary Alcohols with Primary Alcohols via Borrowing Hydrogen/Hydrogen Autotransfer. *Chem. Eur. J.* **2017**, *23*, 12110-12113. (c) Pandey, B.; Xu, S.; Ding, K. Switchable *β*-alkylation of Secondary Alcohols with Primary Alcohols by a Well-Defined Cobalt Catalyst. *Organometallics* **2021,** *40*, 1207-1212. (d) Zhang, S.-Q.; Guo, B.; Xu, Z.; Li, H.-X.; Li, H.- Y.; Lang, J.-P. J. T., Ligand-controlled phosphine-free Co (II)- catalysed cross-coupling of secondary and primary alcohols. *Tetrahedron* **2019,** *75*, 130640. (e) Zhang, L.; Wang, A.; Wang, W.; Huang, Y.; Liu, X.; Miao, S.; Liu, J.; Zhang, T., Co–N–C Catalyst for C–C Coupling Reactions: On the Catalytic Performance and Active Sites. *ACS Catal*. **2015**, *5*, 6563-6572.

(10) (a) Liao, S.; Yu, K.; Li, Q.; Tian, H.; Zhang, Z.; Yu, X.; Xu, Q. Copper-catalyzed C-alkylation of secondary alcohols and methyl ketones with alcohols employing the aerobic relay race methodology. *Org. Biomol. Chem.* **2012**, *10*, 2973-2978. (b) Tan, D.-W.; Li, H.-X.; Zhu, D.-L.; Li, H.-Y.; Young, D. J.; Yao, J.-L.; Lang, J.-P. Ligand-Controlled Copper (I)-Catalyzed Cross-Coupling of Secondary and Primary Alcohols to α-Alkylated Ketones, Pyridines, and Quinolines. *Org. Lett.* **2018**, *20*, 608-611. (c) Narjinari, H.; Tanwar, N.; Kathuria, L.; Jasra, R. V.; Kumar, A. Guerbet-type *β*-alkylation of secondary alcohols catalyzed by chromium chloride and its corresponding NNN pincer complex. *Catal. Sci. Technol.* **2022**, *12*, 4753-4762. (d) Yang, J.; Liu, X.; Meng, D.-L.; Chen, H.-Y.; Zong, Z.-H.; Feng, T.-T.; Sun, K. Efficient Iron-Catalyzed Direct b-Alkylation of Secondary Alcohols with Primary Alcohols. *Adv. Synth. Catal*. **2012**, *354*, 328-334. (e) Nayak, A. S.; Jaiswal, S.; Sahu, M. K.; Gunanathan. KOH-catalyzed cross-coupling of primary and secondary alcohols: evidence for radical pathways C. *J. Chem. Sci.* **2024,** *136*, 5. (f) Garg, N. K.; Tan, M.; Johnson, M. T.; Wendt, O. F. Highly Efficient Base Catalyzed N-alkylation of Amines with Alcohols and β-Alkylation of Secondary Alcohols with Primary Alcohols. *ChemCatChem* **2023,** *15*, e202300741.

(11) (a) Barman, M. K.; Jana, A.; Maji, B. Catalysis, Phosphine-Free NNN-Manganese Complex Catalyzed α-Alkylation of Ketones with Primary Alcohols and Friedländer Quinoline Synthesis. *Adv. Synth. Catal.* **2018**, *360*, 3233-3238. (b) Chakraborty, S.; Daw, P.; Ben David, Y.; Milstein, D. Manganese-Catalyzed α-Alkylation of Ketones, Esters, and Amides Using Alcohols. *ACS Catal.*, **2018**, *8*, 10300-10305. (c) Jana, A.; Reddy, C. B.; Maji, B. Manganese Catalyzed α-Alkylation of Nitriles with Primary Alcohols. *ACS Catal.* **2018**, *8*, 9226-9231. (d) Liu, T.; Wang, L.; Wu, K.; Yu, Z. Manganese-Catalyzed β-Alkylation of Secondary Alcohols with Primary Alcohols under Phosphine-Free Conditions. *ACS Catal.* **2018**, *8*, 7201-7207. (e) Schlagbauer, M.; Kallmeier, F.; Irrgang, T.; Kempe, R. Manganese-Catalyzed β-Methylation of Alcohols by Methanol. *Chem., Intl. Ed.* **2020,** *59*, 1485-1490. (f) Kaithal, A.; Gracia, L.-L.; Camp, C.; Quadrelli, E. A.; Leitner, W. Direct synthesis of cycloalkanes from diols and secondary alcohols or ketones using a homogeneous manganese catalyst. *J. Am. Chem. Soc.* **2019**, *141*, 17487-17492. (g) Fu, S.; Shao, Z.; Wang, Y.; Liu, Q. Manganese-catalyzed upgrading of ethanol into 1-butanol. *J. Am. Chem. Soc.* **2017**, *139*, 11941-11948. (h) Waiba, S.; Jana, S. K.; Jati, A.; Jana, A.; Maji, B. Manganese complex-catalysed α-alkylation of ketones with secondary alcohols enables the synthesis of β-branched carbonyl compounds. *Chem. Commun.* **2020**, *56*, 8376-8379. (i) El-Sepelgy, O.; Matador, E.; Brzozowska, A.; Rueping, M. C-Alkylation of Secondary Alcohols by Primary Alcohols through Manganese-Catalyzed Double Hydrogen Autotransfer. *ChemSusChem* **2019,** *12*, 3099-3102. (j) Sklyaruk, J.; Borghs, J. C.; El-Sepelgy, O.; Rueping, M., Catalytic C1 Alkylation with Methanol and Isotope-Labeled Methanol. *Angew. Chem. Int. Ed*. **2019**, *58*, 775-779. (k) Alanthadka, A.; Bera, S.; Banerjee, D., Iron-Catalyzed Ligand Free α-Alkylation of Methylene Ketones and β-Alkylation of Secondary Alcohols Using Primary Alcohols. *J. Org. Chem.* **2019**, *84*, 11676-11686. (l) Sarki, N.; Goyal, V.; Natte, K.; Jagadeesh, R. V., Base Metal-

Catalyzed C-Methylation Reactions Using Methanol. *Adv. Synth. Catal.* **2021**, *363*, 1-20. (m) Bisarya, A.; Jasra, R. V.; Kumar, A. NNN Pincer-Manganese- Catalyzed Guerbet-Type *β*-Alkylation of Alcohols under Microwave Irradiation. *Organometallics* **2023**, *42*, 1818-1831. (n) Kaur, M.; U Din Reshi, N.; Patra, K.; Bhattacherya, A.; Kunnikuruvan, S.; Bera, J. K., A Proton-Responsive Pyridyl(benzamide)-Functionalized NHC Ligand on Ir Complex for Alkylation of Ketones and Secondary Alcohols. *Chem. Eur. J.* **2021,** *27* , 10737-10748.

(12) (a) Zhang, M.-J.; Li, H.-X.; Young, D. J.; Li, H.-Y.; Lang, J.-P. Reaction condition controlled nickel (ii)-catalyzed C–C cross-coupling of alcohols. *Org. Biomol. Chem.* **2019**, *17*, 3567-3574. (b) Alonso, F.; Riente, P.; Yus, M. The α-Alkylation of Methyl Ketones with Primary Alcohols Promoted by Nickel Nanoparticles under Mild and Ligandless Conditions. *Synlett* **2007**, *2007*, 1877-1880. (c) Alonso, F.; Riente, P.; Yus, M. Alcohols for the α-Alkylation of Methyl Ketones and Indirect Aza-Wittig Reaction Promoted by Nickel Nanoparticles. *Eur. J. Org. Chem.* **2008,** *2008*, 4908-4914. (d) Das, J.; Vellakkaran, M.; Banerjee, D. Nickel-Catalyzed Alkylation of Ketone Enolates: Synthesis of Monoselective Linear Ketones. *J. Org. Chem.* **2019**, *84*, 769-779. (e) Das, J.; Singh, K.; Vellakkaran, M.; Banerjee, D. Nickel-Catalyzed Hydrogen-Borrowing Strategy for α-Alkylation of Ketones with Alcohols: A New Route to Branched gem-Bis(alkyl) Ketones. *Org. Lett.* **2018**, *20*, 5587-5591. (f) Babu, R.; Subaramanian, M.; Midya, S. P.; Balaraman, E., Nickel-Catalyzed Guerbet Type Reaction: C-Alkylation of Secondary Alcohols via Double (de)Hydrogenation. *Org.let.* **2021,** *23*, 3320-3325. (g) Arora, V.; Narjinari, H.; Kumar, A. Pincer-Nickel Catalyzed Selective Guerbet-Type Reactions. *Organometallics* **2021**, *40*, 2870− 2880.

(13) (a) Widegren, J. A.; Finke, R. G. A review of the problem of distinguishing true homogeneous catalysis from soluble or other metal-particle heterogeneous catalysis under reducing conditions. *J. Mol. Cat. A* **2003**, *198*, 317-341. (b) Crabtree, R. H. Resolving Heterogeneity Problems and Impurity Artifacts in Operationally Homogeneous Transition Metal Catalysts. *Chem. Rev.* **2012**, *112*, 1536-1554.

(14) (a) Hoffmann, S. K.; Goslar, J.; Lijewski, S. Electron paramagnetic resonance and electron spin echo studies of Co 2+ coordination by nicotinamide adenine dinucleotide (NAD+) in water solution. *Appl. Magn. Reson.* **2013**, *44*, 817-826. (b) Li, C.; Song, S.; Li, Y.; Xu, C.; Luo, Q.; Guo, Y.; Wang, X. Selective hydroboration of unsaturated bonds by an easily accessible heterotopic cobalt catalyst. *Nat. Commun.* **2021**, *12*, 3813.

(15) Simmons, E. M.; Hartwig, J. F. On the Interpretation of Deuterium Kinetic IsotopeEffects in C-H Bond Functionalizations by Transition-Metal Complexes. *Angew. Chem., Int. Ed.*, **2012**, *51*, 3066–3072.

Chapter- V

Pincer-Cobalt Catalyzed Guerbet-Type β-alkylation of Alcohols in Air under Microwave Conditions

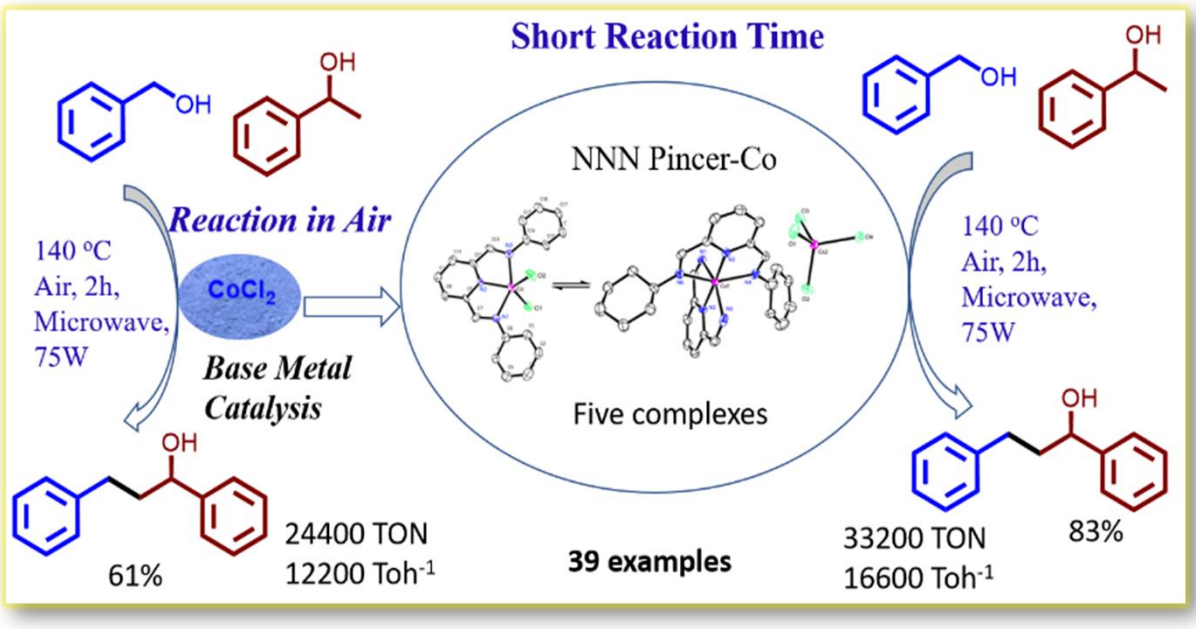

The contents of this chapter have been adapted from "*Pincer-Cobalt Catalyzed Guerbet-Type β-alkylation of Alcohols in Air under Microwave Conditions*" by Nandi, P. G.; Thombare, P.; Prathapa, S. J; Kumar, A. *Organometallics* **2022**, *41*, 22, 3387–3398.

5.1. Introduction

Methods that create C−C bonds provide convenient and versatile routes to agrochemicals, pharmaceuticals, natural products, fuels, and fine chemicals.[1] Radical[2] and organometallic[3] pathways have largely contributed to C−C bond-forming reactions mainly via the transition-metal-catalyzed activation of C−X (X = H, Cl, Br, I) bonds. Recent years have witnessed the rise of several methods that use alcohols as an alkylating agent. These "hydrogen borrowing strategies" have continued to garner greater research interest due to their green and atom-economical nature with water as the only by-product. The use of stoichiometric amounts of base leads to large amounts of waste[4b,c] and renders the metal-free[4] systems inappropriate for the *β*-alkylation of alcohols. In a similar vein, several challenges are associated with the use of homogeneous catalytic systems based on toxic precious metals such as palladium,[5] iridium,[6] rhodium,[7] and ruthenium.[6b,d,j,8] Earth-abundant, environmentally benign, and inexpensive *β*-alkylation catalytic systems have been an area of intense research lately, which have rightly led to catalysts based on cobalt,[9] copper,[10] manganese,[11] iron,[11k,l] nickel,[12] and chromium.[13]

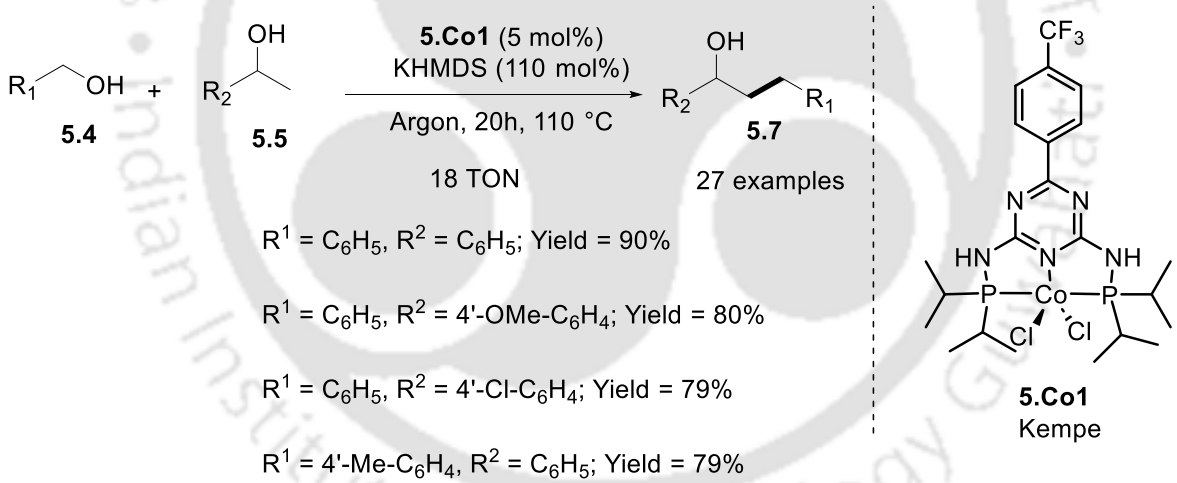

Scheme 5.1: The **5.Co1** catalyzed *β*-alkylation of secondary alcohols with primary alcohols.[9b]

The first report on Co-catalyzed *β*-alkylation of alcohols came from the group of Kempe[9b] using a PN_3P pincer-Co (**5.Co1**) (5 mol%) in the presence of 1.1 equivalents of KHMDS (potassium hexamethyl disilazane) as a base with up to 90% yield of the *β*-alkylated product (Scheme 5.1).[9b] The complex **5.Co1** is capable for the alkylation of variety of alcohols starting from aliphatic to aromatic to hetero cyclic alcohols with moderate to good yields however, at a very high base loading (1.1 equivalents of KHMDS).

In 2021, Ding has reported the use of a Co catalyst (0.7 mol%) supported by a ^{iPr}PPPN^{H}Py^{Me} tridentate ligand for the *β*-alkylation of alcohols in up to 80% yield at 110 °C at a very high base loading (110 mol%) (Scheme 5.2).[9c] A large variety of substrates could be *β*-alkylated with **5.Co2** (0.7 mol%) in the presence of KO^{t}Bu(110 mol%) under N_2 atmosphere at 110 °C.[9c]

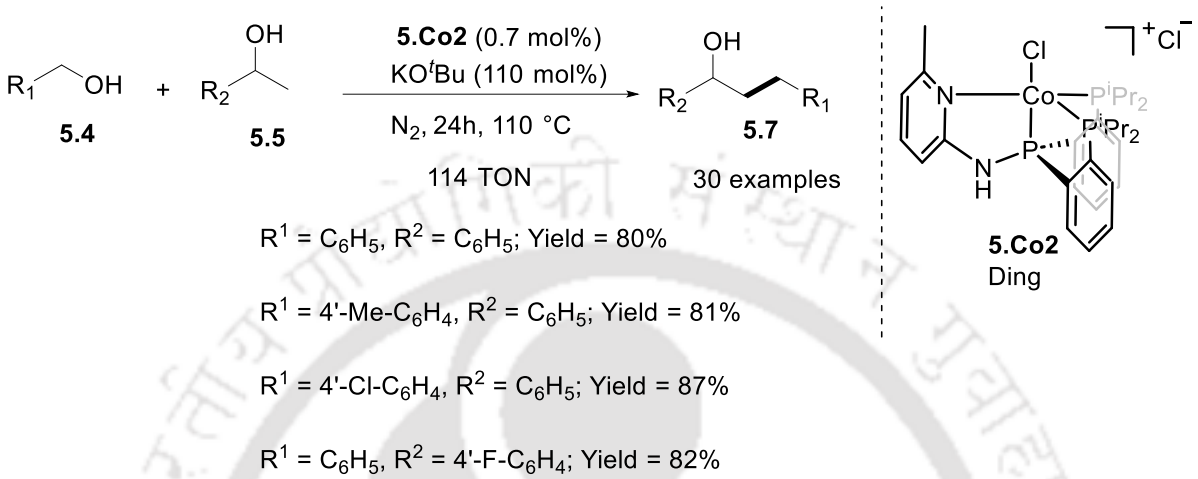

Scheme 5.2: The **5.Co2** catalyzed *β*-alkylation of secondary alcohols with primary alcohols.[9C]

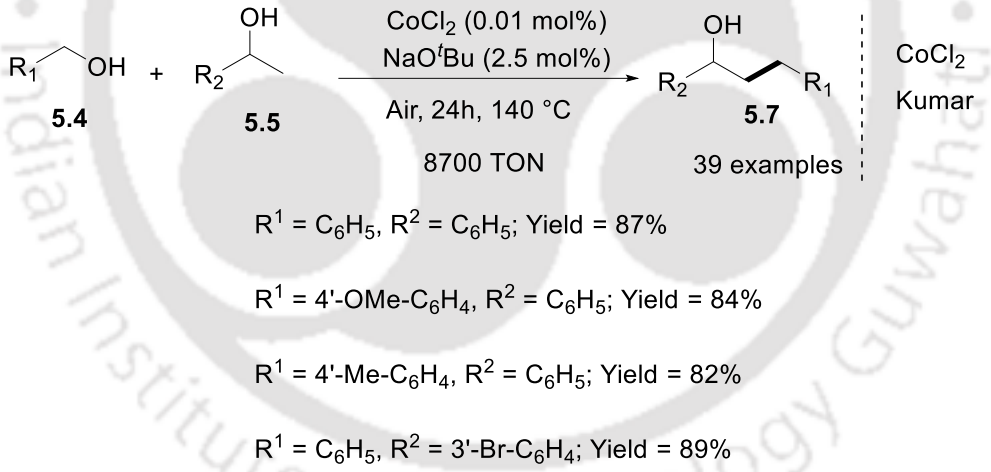

Scheme 5.3: $CoCl_2$ catalyzed *β*-alkylation of secondary alcohols with primary alcohols.[9C]

We recently reported that cobaltous chloride (0.01 mol %) efficiently accomplishes the catalytic *β*-alkylation of alcohols with high yields (up to 87%) and unprecedented turnovers (ca. 8700) in the presence of only 2.5 mol % of NaO^{t}Bu (Scheme 5.3).[9f] This reaction has been discussed in detail in the previous chapter.

5.2. Objectives of the current work

A comprehensive literature survey reveals that the pincer complexes and also other metal complexes are very active for *β*-alkylation of alcohols at a very high base loading. Crabtree,[10e] Gunanathan,[10f] Jhonson and Wendit[10g] have independently reported that only base can mediate the *β*-alkylation of secondary alcohols with primary alcohols albeit at very high loadings. In the Chapter-IV, we have demonstrated that base metal salt $CoCl_2$ itself acts as a very active catalyst for the *β*-alkylation of various secondary alcohols with primary alcohols (also see Scheme 5.3) in the presence of NaO^tBu at loadings as low as 2.5 mol% in air at 140 °C. A comprehensive literature survey reveals that the pincer complexes are very much active for the activation of alcohols molecules. Following the success in the synthesis of a series of NNN pincer-ruthenium complexes (**2.6a**–**d**, Figure 5.2**, Chapter-II**) based on *bis*(imino)pyridine ligands and their application as efficient catalysts for the *β*-alkylation of alcohols,[8l] the current work attempts to address the following questions:

- Using the same *bis*(imino)pyridine ligand system, can we utilize pincer-cobalt complexes rather than pincer-ruthenium complexes as catalysts for the very important *β*-alkylation reactions?

- How does the *β*-alkylation activity of pincer-cobalt complexes compare with corresponding activity of the precursor $CoCl_2$?

- What will be the functional group tolerance of the resulting *β*-alkylation catalytic system based on pincer-cobalt?

- Can we carry out the reaction in air which facilitates the ease of operation without compromise on the overall performance?

Apart from the studies by Kempe,[9b] Ding[9c] and Kumar[9f] (Scheme 5.4), there have been no other reports on Co-based *β*-alkylation systems, to the best of our knowledge. In the current study, we report the synthesis of a series of NNN pincer-Co complexes based on *bis*(imino)pyridine ligands to yield complexes of the type (^{R2}NNN)$CoCl_2$ (**5.1a**, R = ^{i}Pr; **5.1b**, R = ^{t}Bu; **5.1c**, R = Cy; **5.1d**, R = Ph; **5.1e**, R = *p*-F-C_6H_4) (Figure 5.1). While cobaltous chloride at a 0.0025 mol % loading in the presence of 2.5 mol % of NaO^tBu at 140 °C gives about a 66% yield in the *β*-alkylation of 1-phenylethanol with benzyl alcohol, its corresponding pincer complex

(^{iPr2}NNN)$CoCl_2$ (0.0025 mol %) is highly productive (ca. 1.3-fold vs $CoCl_2$) and results in up to 85% yield (ca. 34000 TON) of the *β*-alkylation product under otherwise identical conditions (Scheme 5.4).

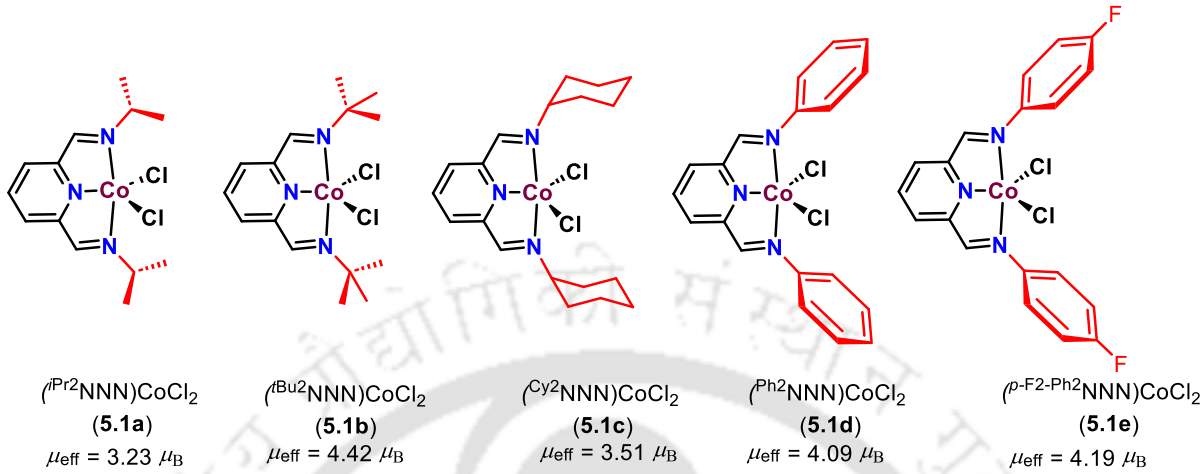

Figure 5.1. Magnetic moment of pincer-cobalt complexes investigated in the current study for the *β*-alkylation of 1-phenylethanol with benzyl alcohol

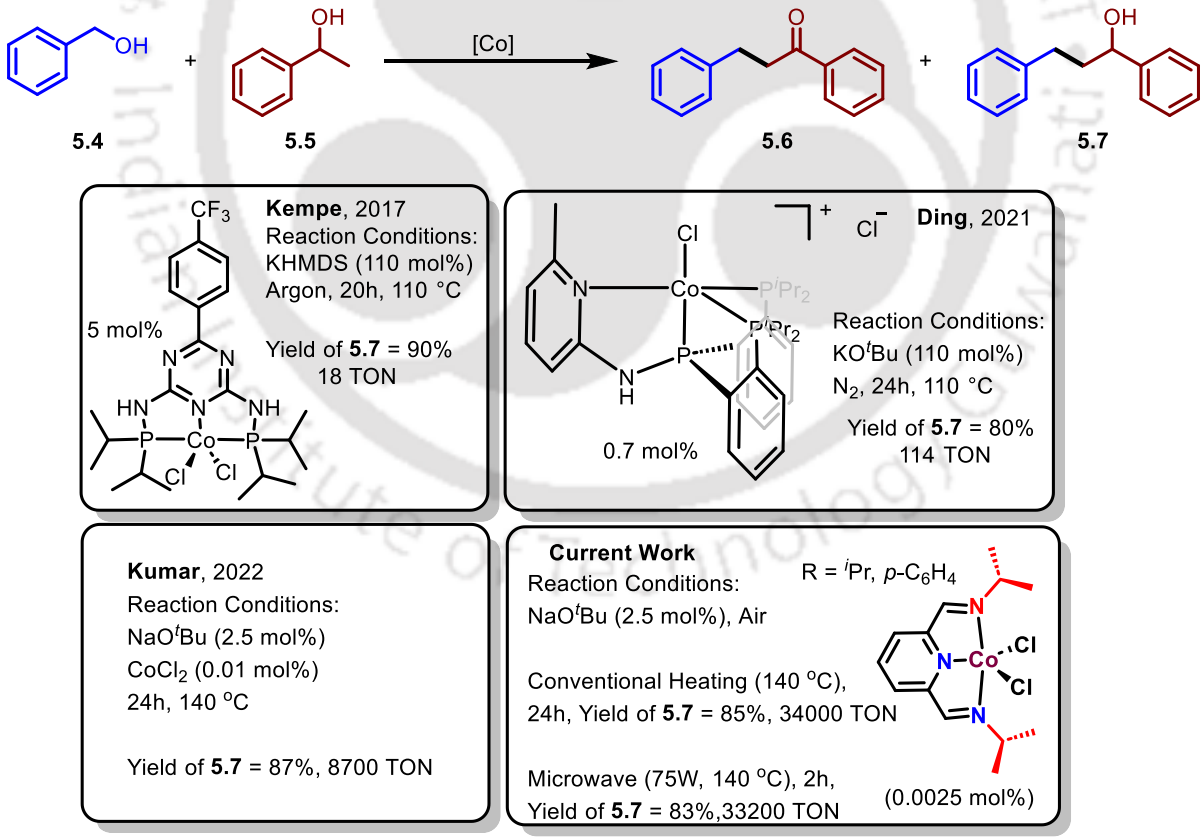

Scheme 5.4. Efficient cobalt-based catalysts reported for the *β*-alkylation of alcohols.

5.3. Results and discussions

5.3.1. Synthesis and characterization of pincer-cobalt complexes based on *bis*(imino)pyridine ligands

The NNN pincer-Co complexes **5.1a−e** were synthesized in good yields by the treatment of the corresponding ligands[14] with $CoCl_2$ in THF at room temperature for 20 h, followed by washing with diethyl ether (Scheme 5.5). The NNN pincer-Co complexes **5.1a−e** were paramagnetic in nature, as indicated by their magnetic susceptibility measurements (**5.1a**, μ_{eff} = 3.23 μ_B; **5.1b**, μ_{eff} = 4.42 μ_B; **5.1c**, μ_{eff} = 3.51 μ_B; **5.1d**, μ_{eff} = 4.09 μ_B; **5.1e**, μ_{eff} = 4.19 μ_B;).[15] The paramagnetic behavior of the considered complexes was further confirmed by an EPR analysis (Figure 5.2).[16]

All of the considered complexes other than **5.1d**[14c] are new and have not been reported. In contrast to Jiang's report[14c] on the structure of **5.1d**, which contained two molecules per asymmetric unit, the single-crystal X-ray analysis of **5.1d** in the current study shows only one molecule in the asymmetric unit with Co in a trigonal-bipyramidal environment having the pincer ligand bound in a meridional fashion with the two chlorides *cis* to each other. Very similar to our studies with pincer-Ni complexes[12g] and pincer-Fe complexes,[12h] the dicationic octahedral complex $[(^{R2}NNN)_2Co]^{2+}$ in **5.3c** whose charge is balanced by a dianionic tetrahedral cobalt tetrachloride is obtained during crystallization upon layering a solution of **5.1c** in methanol with hexane (Scheme 5.2). This presumably arises due to the equilibration of **5.1c** with **5.3c** in the mother liquor (Scheme 5.5). In **5.3c**, which has two molecules per asymmetric unit, the two pincer ligands are attached in a meridional fashion to the Co, which is in an octahedral environment (Scheme 5.5). While the complex (^{Ph2}NNN)$CoCl_2$ (**5.1d**) crystallized in P21/n space group, the complex $[(^{Cy2}NNN)_2Co][CoCl_4]$ (**5.3c**) crystallized in the $I\bar{4}$ space group (Table 5.1 and Table 5.S1). The Co−N(pyridyl) bond distance is slightly elongated in the case of neutral complex **5.1d**, 2.011(10) Å; **5.3c**, 1.972(8) and 1.968(7) Å). In **5.1d**, one of the Co-N(imine) bonds was longer (2.287(11) Å) than the other (2.260(10) Å) with (pyridyl)N-Co-N(imine) bond angles of 74.7(4) and 76.20(4)° respectively (Table 5.2 and Table 5.S2).

Similarly, each of the pincer fragments in **5.3c** had one long Co-N(imine) bond (2.190(9) and 2.194(10) Å) and one short Co-N(imine) bond (2.149(8) and 2.163(8) Å). The corresponding (pyridyl)N-Co-N(imine) bond angles were also larger (77.40(4) and 76.40(3)°) and smaller (75.30(4) and 76.10(4)°), respectively. The N(imine)−(pyridyl)N− N(imine) bond angle in the

case of **5.1d** (113.83°) is slightly larger than the corresponding angles in **5.3c** (110.88 and 110.91°).

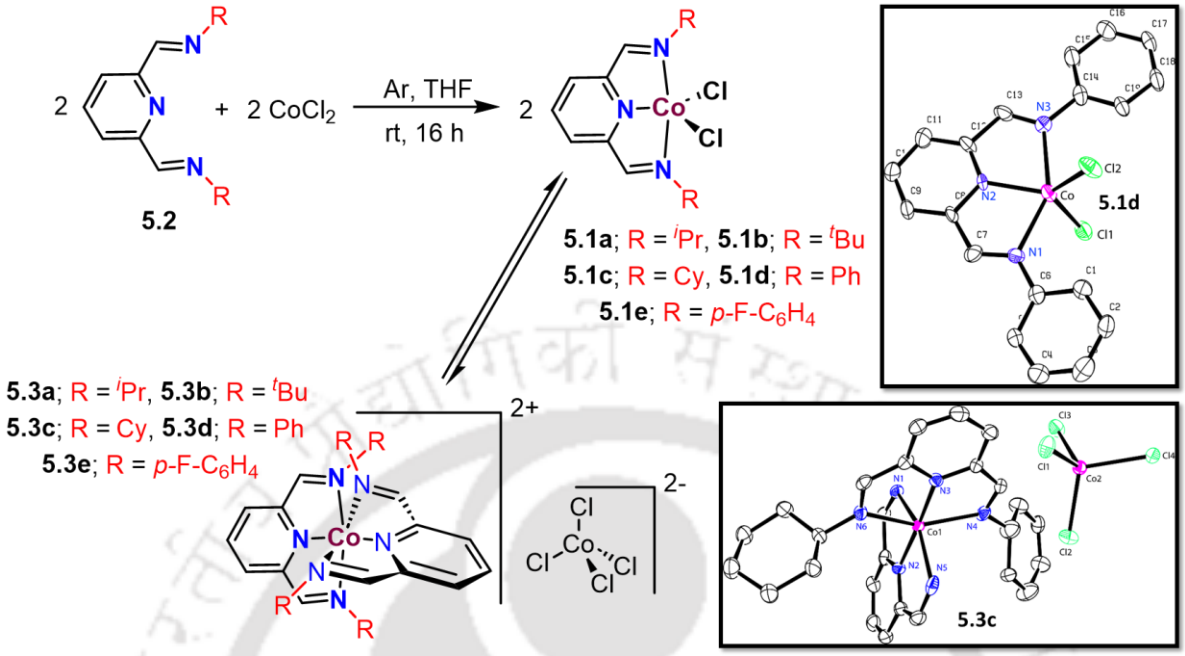

Scheme 5.5. General synthetic pathway towards (^{R2}NNN)$CoCl_2$ (**5.1a-e**)[a]

[a]The molecular structures of **5.1d** and **5.3c** are provided as ORTEP figures drawn at 40% probability. The cyclohexyl groups on two N atoms of one of the pincer fragments in **5.3c** and all of the hydrogen atoms on both **5.1d** and **5.3c** are omitted for the sake of clarity.

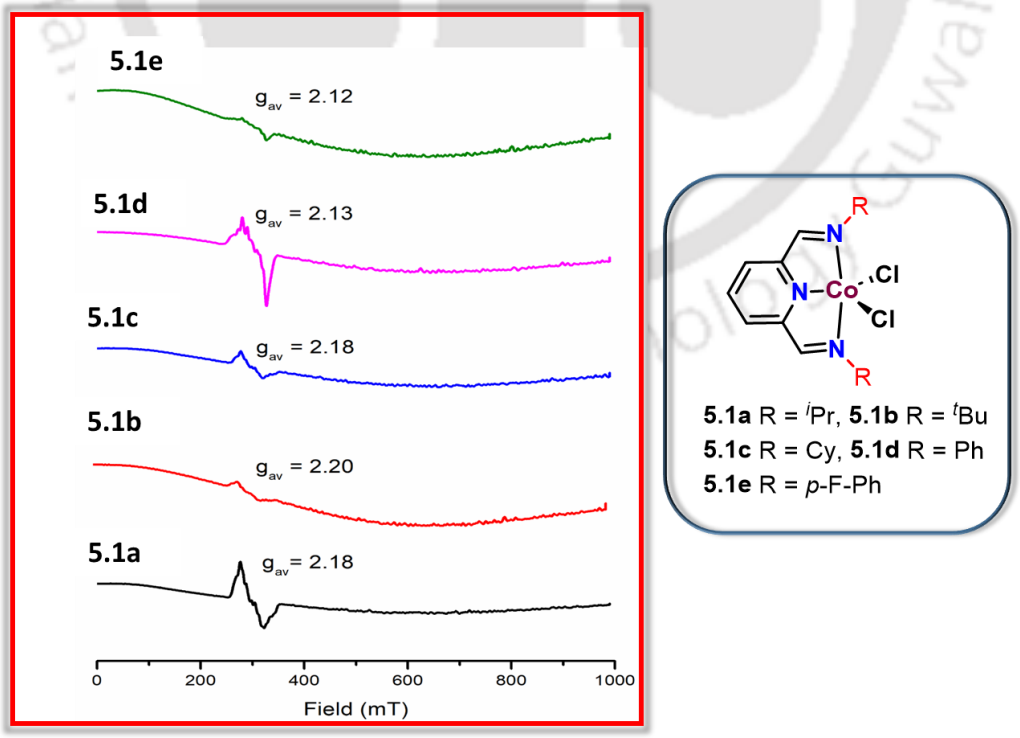

Figure 5.2. EPR spectra of pincer-Co complexes **5.1a-e** in methanol at 77 K.

Table 5.1. Crystal structure and refinement parameters of 5.1d and 5.3c

Complex	**5.1d**	**5.3c**
Empirical formula	$C_{13}H_{15}Cl_2CoN_3$	$C_{38}H_{54}Cl_4Co_2N_6$
Formula weight	415.17	854.53
Temperature/K	296.15	296.15
Crystal system	monoclinic	tetragonal
Space group	$P2_1/n$	I-4
a/Å	7.716(6)	25.1147(13)
b/Å	13.681(14)	25.1147(13)
c/Å	17.066(13)	16.3935(9)
α/°	90.00	90
β/°	91.95(2)	90
γ/°	90.00	90
Volume/Å^3	1800(3)	10340.2(12)
Z	4	10
ρ_{calc}g/cm^3	1.531	1.372
μ/mm^{-1}	1.241	1.095
F(000)	700.0	4460.0
Crystal size/mm^3	0.31 × 0.25 × 0.21	0.32 × 0.24 × 0.21
Radiation	MoKα (λ = 0.71073)	MoKα (λ = 0.71073)
2Θ range for data collection/°	5.62 to 50	3.24 to 50.14
Index ranges	$-9 \le h \le 9$, $-16 \le k \le 16$, $-20 \le l \le 20$	$-19 \le h \le 19$, $-29 \le k \le 29$, $-19 \le l \le 17$
Reflections collected	12567	8228
Independent reflections	3121 [R_{int} = 0.1201, R_{sigma} = 0.1150]	8221 [R_{int} = 0.0101, R_{sigma} = 0.0237]
Data/restraints/parameters	3121/0/226	8221/390/566
Goodness-of-fit on F^2	1.046	1.346
Final R indexes [I>=2σ (I)]	R_1 = 0.1362, wR_2 = 0.2719	R_1 = 0.0723, wR_2 = 0.2296
Final R indexes [all data]	R_1 = 0.2096, wR_2 = 0.2929	R_1 = 0.0992, wR_2 = 0.2489
Largest diff. peak/hole / e Å^{-3}	0.74/-0.95	0.61/-0.42
Flack parameter		0.48(7)

However, the N(imine)−Co−N(imine) bond angle in **5.1d** (150.80(4)°) is smaller than the corresponding angles in **5.3c** (152.40(4) and 152.60(4)°). In line with the single-crystal

Table 5.2. Selected bond lengths and bond angles around the Co centre

	5.1d	**5.3c**
Co-N (Å) (Pyridyl)	2.011(10)	1.972(8), 1,968 (4)
Co –N (imine) (Å)	2.260(10), 2.287 (11)	2.194(10), 2.163 (8)
		2.190(9), 2.149(8)
(Imine)N-Co-N(Imine) (°)	150.8(4)	152.4(4), 152.6(4)
(Pyridyl)N-Co-N(Imine) (°)	74.7(4),76.2(4)	76.1(4),76.4(3), 75.3(4), 77.4(4)
(Pyridyl)N-Co-(Pyridyl)N (°)	NA	177.2(3)

X-ray diffraction studies, HRMS analysis provided key evidence for the presence of fragments originating from both **5.1** and **5.3** (Figure 5.3). For example, the HRMS analysis of **5.1a** showed peaks at m/z values of 246.6250, 311.0593. 406.1107 and 469.1891 that correspond to [**5.3a** − $CoCl_4$]$^{2+}$, [**5.1a** − Cl]$^+$, [**5.1a** − Cl + CH_3CN + $3H_2O$]$^+$, and [**5.1a′** + $2CH_3CN$ + $3H_2O$ + Na]$^+$, respectively. HRMS analyses were thus complementary to single-crystal X- ray diffraction studies, clearly indicating that in solution complex **5.1** exists in equilibrium with **5.3** (Scheme 5.5), the position of which is dictated by the nature of the R group (R = ^{i}Pr, ^{t}Bu, Cy, Ph, *p*-F-C_6H_4).

The TGA analysis demonstrated the excellent thermal stability of the synthesized NNN pincer-Co complexes **5.1a−e/5.3a−e** (Figure 5.4). Due to the lack of labile ancillary ligands, hardly any mass loss was observed at lower temperatures and a sudden decomposition was observed at elevated temperatures (Figure 5.4). However, prior to decomposition, **5.1a** and **5.1c** demonstrated gradual mass losses of about 11% and 10%, respectively, that correspond to the loss of one chloride.[12g]

5.3.2. Studies on the 5.1-catalyzed *β*-alkylation of 1-phenyl-ethanol with benzyl alcohol

Employing benzyl alcohol and 1-phenylethanol as model primary and secondary alcohol, respectively, the studies on *β*-alkylation at 140 °C were initiated using **5.1a** as the catalyst (Table 5.3). In the presence of **5.1a** (0.01 mol %) and NaO^{t}Bu (5 mol %) (entry 1, Table 5.3) about 87% of the *β*-alkylated product **5.7** (ca. 8700 TON) was obtained in 96% selectivity (Table 5.3). The yield of **5.7** was comparable when the reaction was carried out at a lower loading of NaO^{t}Bu (2.5 mol %) (entry 2, Table 5.3).

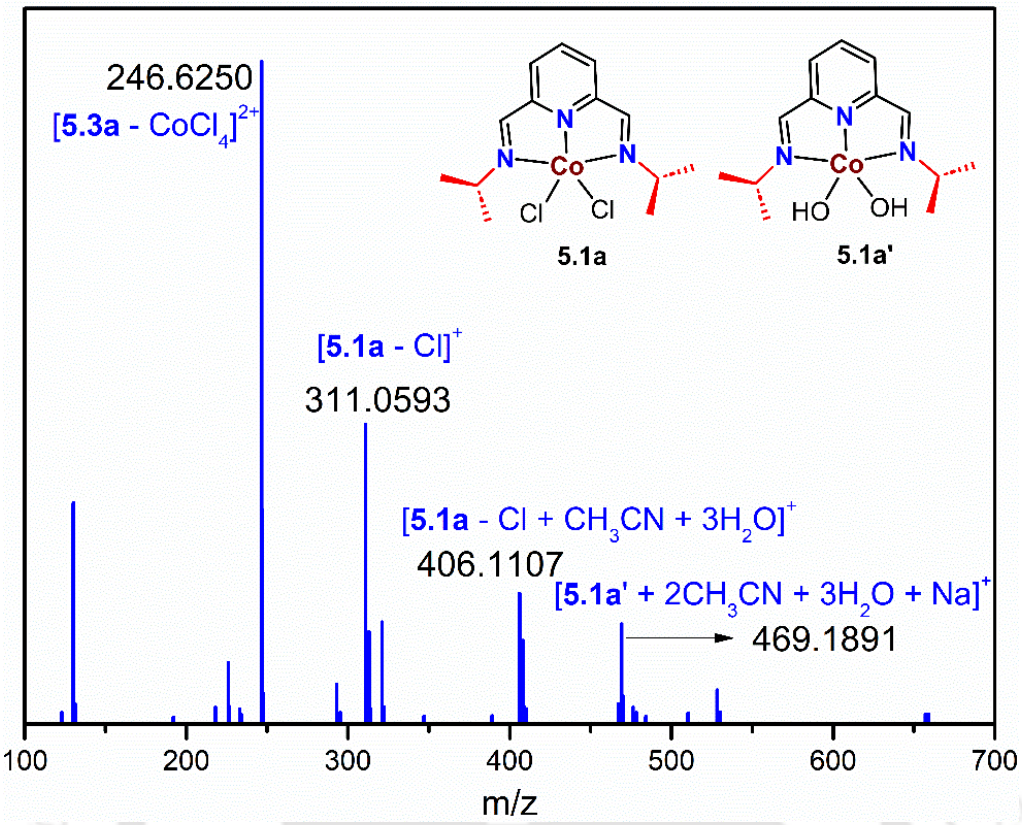

Figure 5.3. HRMS analysis of **5.1a** in acetonitrile and methanol.

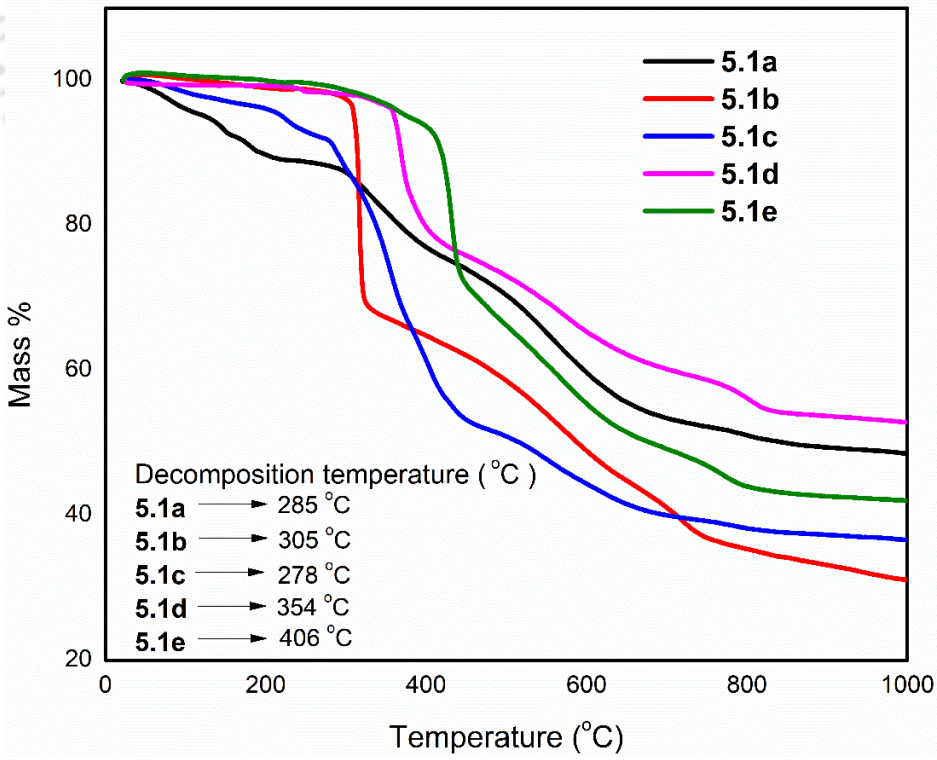

Figure 5.4. TGA analysis of pincer-Co complexes **5.1a**–**e** under argon with a heating rate of 10 °C min^{-1}.

Though this reactivity is seemingly comparable with the results obtained by us recently with $CoCl_2$ as catalyst (0.01 mol %) (entry 2 vs entry 3, Table 5.3),[9f] one can appreciate the value of **5.1a** as a more efficient catalyst, as is evident from further optimizations. Lowering of the base loading (1.25 mol % NaO^{t}Bu) resulted in poorer yields (entry 4, Table 5.3). Hence, further studies were carried out at a catalyst and base loadings of 0.01 and 2.5 mol %, respectively. The *β*-alkylation did not occur upon use of Na_2CO_3 and K_2CO_3 (entries 5 and 6, Table 5.3). While KOH demonstrated poor reactivity (entry 7, Table 5.3) in the **5.1a**-catalyzed *β*-alkylation, good yields were obtained in the corresponding reaction with NaOH (entry 8, Table 5.3). In the **5.1a**-catalyzed reaction, among NaO^{t}Bu (2.5 mol %) (entry 2, Table 5.3) and KO^{t}Bu (entry 9, Table 5.3), the yield of **5.7** in the case of the former was better than that of the latter. Among the catalysts considered (entry 2 and entries 10-13, Table 5.3), the yield of *β*-alkylated product was very good with **5.1a** (88% yield at 8800 TON, entry 2, Table 5.3) and **5.1e** (83% yield at 8300 TON, entry 13, Table 5.3). The yields of **5.7** hardly changed (84%, ca. 16800 TON) when the loading of both **5.1a** and **5.1e** was decreased to 0.005 mol % (entries 14 and 15, Table 5.3). However, since **5.1e** had poor solubility, further optimization was carried out only with **5.1a**. Upon a further decrease in the amount of **5.1a** to 0.0025 mol %, the *β*-alkylation in the presence of NaO^{t}Bu (2.5 mol %) resulted in an 85% yield (34000 TON) of **5.7** (entry 16, Table 5.3). These are the highest turnovers reported for a *β*-alkylation system based on Co and are far superior to the best ones reported, also by us very recently.[9f] In contrast, the corresponding reaction catalyzed by $CoCl_2$ (0.0025 mol %) resulted in only a 66% yield (ca. 26400 TON) (entry 17, Table 5.3). Subsequent lowering of the catalyst loading of **5.1a** (0.00125 mol %) gave inferior yields (52%, ca. 41600 TON) (entry 18, Table 5.3). Similarly, the *β*-alkylation carried out at higher loadings of **5.1a** resulted in moderate yields (entries 19 and 20, Table 5.3).

These reactions were associated with formation of black particles that are very similar to the observations reported by us recently and can be attributed to the formation of cobalt nanoparticles (Co NPs) that are inactive due to the fact that the reaction is carried out in air.[9f] Repeating the *β*-alkylation with the best composition of **5.1a** (0.0025 mol %) and NaO^{t}Bu (2.5 mol %) at a lower temperature (120 °C) under otherwise identical conditions resulted in reduced yields (35%, ca. 14000 TON) (entry 21, Table 5.3). Negligible reactivity was observed either in the absence of catalyst or in the absence of NaO^{t}Bu (entries 22 and 23, Table 5.3). The total yield of products (**5.6** + **5.7**) was comparable when the reaction was performed in a closed vessel (entry 16 vs entry 24, Table 5.3), which points to alcoholysis as the major

contributor toward product formation (see Plausible Mechanism; *vide infra*). Furthermore, the yields were similar under atmospheres of argon and air (entry 25 vs entry 16, Table 5.3).

Table 5.3. The 5.1-Catalyzed *β*-alkylation of 5.5 with 5.4 under varying conditions[a]

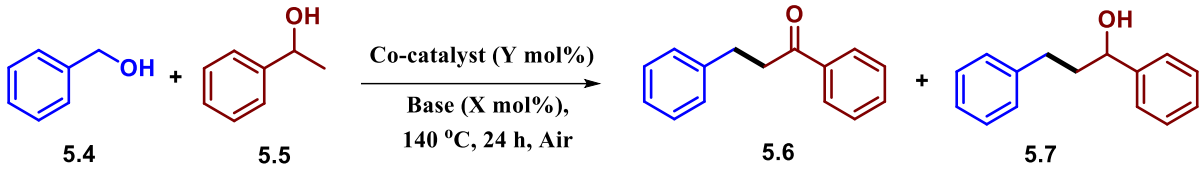

5.4 5.5 5.6 5.7

Entry	Catalyst (Y mol %)[b]	Base (X mol%)[b]	% Yield[c]		**5.7** Selectivity[d]
			5.6	**5.7**	
1	**5.1a** (0.01)	NaO^{t}Bu (5)	4	87	96
2	**5.1a** (0.01)	NaO^{t}Bu (2.5)	3	88	97
3	$CoCl_2$(0.01)	NaO^{t}Bu (2.5)	9	87	91
4	**5.1a** (0.01)	NaO^{t}Bu (1.25)	2	58	97
5	**5.1a** (0.01)	Na_2CO_3 (2.5)	0	0	0
6	**5.1a** (0.01)	K_2CO_3 (2.5)	trace	0	0
7	**5.1a** (0.01)	KOH (2.5)	3	40	93
8	**5.1a** (0.01)	NaOH (2.5)	2	76	97
9	**5.1a** (0.01)	KO^{t}Bu (2.5)	2	65	97
10	**5.1b** (0.01)	NaO^{t}Bu (2.5)	4	63	94
11	**5.1d** (0.01)	NaO^{t}Bu (2.5)	5	70	93
12	**5.1c** (0.01)	NaO^{t}Bu (2.5)	4	66	94
13	**5.1e** (0.01)	NaO^{t}Bu (2.5)	6	83	93
14	**5.1a** (0.005)	NaO^{t}Bu (2.5)	5	84	94
15	**5.1e** (0.005)	NaO^{t}Bu (2.5)	5	84	94
16	**5.1a** (0.0025)	NaO^{t}Bu (2.5)	5	85	94
17	$CoCl_2$(0.0025)	NaO^{t}Bu (2.5)	4	66	94
18	**5.1a** (0.00125)	NaO^{t}Bu (2.5)	2	52	96
19	**5.1a** (0.05)	NaO^{t}Bu (2.5)	5	78	94
20	**5.1a** (0.25)	NaO^{t}Bu (2.5)	7	52	88
21[e]	**5.1a** (0.0025)	NaO^{t}Bu (2.5)	3	35	92
22	-	NaO^{t}Bu (2.5)	2	8	80
23	**5.1a** (0.0025)	-	0	0	0
24[f]	**5.1a** (0.0025)	NaO^{t}Bu (2.5)	2	90	98
25[g]	**5.1a** (0.0025)	NaO^{t}Bu (2.5)	10	84	89

[a] Reaction conditions unless specified otherwise: 2 mmol of **5.4**, 2 mmol of **5.5**, X mol % of base, and Y mol % of Co catalyst at 140 °C (conventional heating) for 24 h in an open vessel. [b] The mol % values of base and catalyst are with respect to the total alcohol content (**5.4** + **5.5**). [c] The yield is determined from ^{1}H NMR using toluene as a standard. [d] Selectivity = (Yield of **5.7**/ Total yield (**5.6** + **5.7**)) *100 [e] Performed at 120 °C. [f] Performed in a closed vessel. [g] Performed under an argon atmosphere.

Table 5.4. The 5.1a-Catalyzed *β*-alkylation of 5.5 with 5.4 under microwave heating

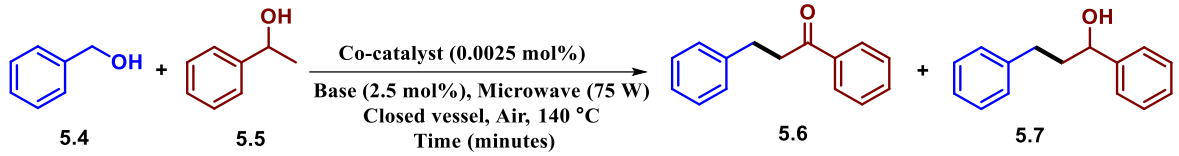

5.4 5.5 5.6 5.7

Entry	Catalyst (0.0025 mol%)[b]	Time (minutes)	% Yield[c]		Selectivity[d] of **5.7**
			5.6	**5.7**	
1	**5.1a**	30	3	23	88
2	**5.1a**	60	4	55	93
3	**5.1a**	90	6	75	93
4	**5.1a**	120	7	83	92
5[e]	**5.1a**	120	1	16	94
6	$CoCl_2$	120	2	61	97
7[f]	$CoCl_2$	120	10	85	89

[a]Reaction conditions: 2 mmol of **5.4**, 2 mmol of **5.5**, 2.5 mol% (0.0048 g, 0.05 mmol) of NaO^{t}Bu and 0.0025 mol% of Co catalyst at 140 °C (microwave heating at 75 W) in a closed vessel. [b]The mol % of base and catalyst is with respect to total alcohol content (**5.4** + **5.5**). [c]Yield is determined from ^{1}H NMR using toluene as a standard. [d]Selectivity = (Yield of **5.7**/ Total yield (**5.6** + **5.7**)) *100 [e] Reaction Performed under 120 °C. [f]Performed in an open vessel.

Apart from the conventional heating method, under the optimized reaction conditions (entry 16, Table 5.3), the reactions were carried out under the influence of microwave heating (140 °C, 75 W, and 20 psi, Table 5.4). Very similar to our recent observation with Cr-based catalysts,[13] microwave conditions led to better yields of **5.7** (ca. 83%, 33200 TON at 16600 TO/h) after only 2 h of the reaction (entry 4, Table 5.4). The productivity was poor at lower temperatures (entry 5, Table 5.4) in the **5.1a**-catalyzed reaction under microwave conditions. In comparison to the yields obtained with conventional heating, the yield of *β*-alkylation with $CoCl_2$ (0.0025 mol %) under microwave conditions was similar (ca. 61%, 24400 TON) at a much-reduced reaction time (2 h). However, even under microwave conditions, **5.1a** was more efficient than $CoCl_2$ (entries 4 and 6, Table 5.4).

Using **5.1a** as catalyst, under the best conditions (entry 16, Table 5.3, and entry 4, Table 5.4), the alkylations of several 1- phenylethanol derivatives with variety of benzyl alcohols were carried out under both conventional and microwave heating (Tables 5.5 and 5.6).

Electron-withdrawing and electron-donating groups on benzyl alcohols hardly affected the

Table 5.5. The 5.1a-catalyzed *β*-alkylation of 1-phenylethanol with various derivatives of benzyl alcohol[a]

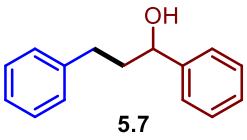

85%,[b] 34000 TON
83%,[b,c] 33200 TON

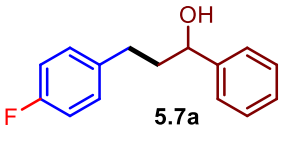

79%,[b] 31600 TON
55%,[b,c] 22000 TON

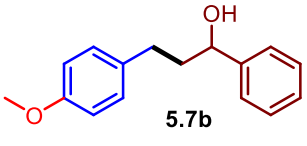

83%,[b] 33200 TON
85%,[b,c] 34000 TON

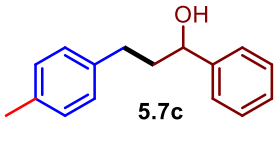

81±0.5%,[b] 32400 TON
89%,[b,c] 35600 TON

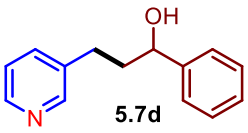

73%,[b] 29200 TON
48%,[b,c] 19200 TON

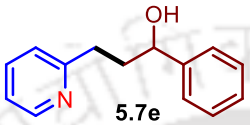

25%,[b] 10000 TON

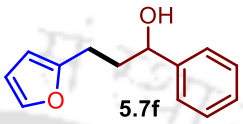

0%,[b] 0 TON
0%,[b,c]0 TON

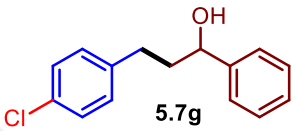

81±0.5%,[b] 32400 TON
89%,[b,c] 35600 TON

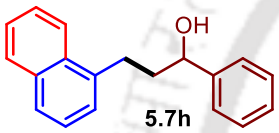

75%,[b] 30000 TON
53%,[b,c] 21200 TON

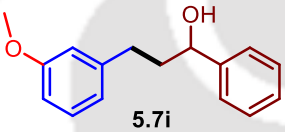

82±1.5%,[b] 32800 TON
70±0.5%,[b,c] 28000 TON

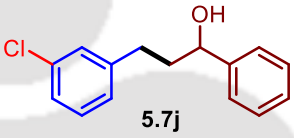

26%,[b] 10400 TON
31%,[b,c] 12400 TON

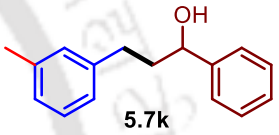

82%,[b] 32800 TON
89%,[b,c] 35600 TON

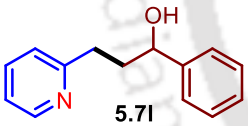

11%,[b] 4400 TON

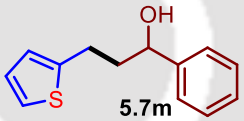

82%,[b] 32800 TON
89%,[b,c] 35600 TON

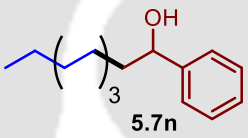

9%,[b] 3600 TON
7%,[b,c] 2800 TON

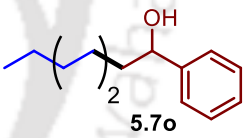

7%,[b] 2800 TON
8%,[b,c] 3200 TON

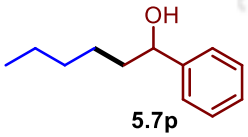

7%,[b]2800 TON

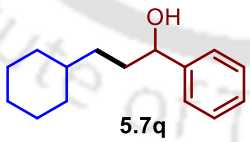

2%,[b] 800 TON

[a] Reaction conditions unless specified otherwise: 2 mmol of **5.4**, 2 mmol of **5.5**, 2.5 mol% (0.0048 g, 0.05 mmol) of NaO^{t}Bu and 0.0025 mol% (0.00001735 g, 0.00005 mmol) of **5.1a** at 140 °C (conventional heating) for 24 h in an open vessel. [b]The yield is determined from ^{1}H NMR using toluene as a standard. [c]At 140 °C under microwave heating at 75 W for 2 h in a closed vessel.

yield of *β*-alkylation of 1-phenylethanol (**5.7**, **5.7a–c, 5.7g, 5.7i** and **5.7k,** Table 5.3). While the yield of *β*-alkylated product **5.7d** was good with pyridine-3-ylmethanol- as the starting

Table 5.6. The 5.1a-catalyzed *β*-alkylation of various 1- phenylethanol derivatives with benzyl alcohol[a]

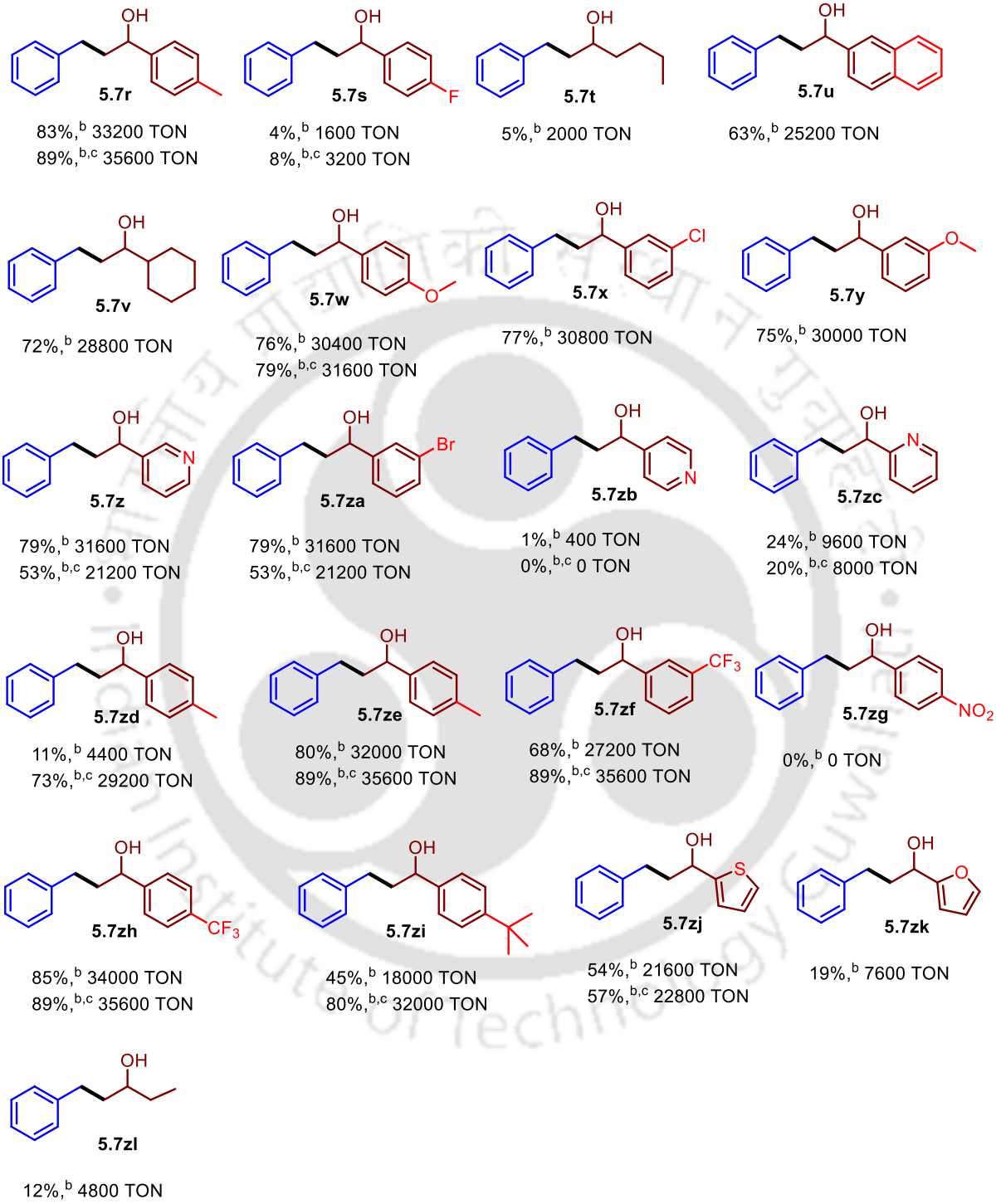

[a] Reaction conditions unless specified otherwise: 2 mmol of **5.4**, 2 mmol of **5.5**, 2.5 mol% (0.0048 g, 0.05 mmol) of NaO^{t}Bu and 0.0025 mol% (0.00001735 g, 0.00005 mmol) of **5.1a** at 140 °C (conventional heating) for 24 h in an open vessel. [b]The yield is determined from ^{1}H NMR using toluene as a standard. [c]At 140 °C under microwave heating at 75 W for 2 h in a closed vessel.

material, the corresponding yields with pyridin-4-ylmethanol and pyridine-2-ylmethanol (**5.7l** and **5.7e**, Table 5.5) were low.

Very similar to our earlier observations,[9f,12g] the yield of **5.1a**-catalyzed *β*-alkylation of 1-phenylethanol with thiophen-2-ylmethanol was better than that of the corresponding reaction with furan-2- ylmethanol (**5.7m** Vs **5.7f**, Table 5.3**).** Furthermore, **5.1a**-catalyzed *β*-alkylation of 1-phenylethanol with primary aliphatic alcohols resulted in poor yields (**5.7n−q**, Table 5.3). In stark contrast to the observation with primary alcohols, the presence of electron-withdrawing groups in the *para* position of 1-phenyl ethanol (−F, −Cl, and $-NO_2$ in **5.7s**, **5.7zd**, **5.7zg** respectively, Table 5.6) leads to lower yields of products. This observation is significant and likely points to the involvement of a methine C−H bond in the RDS (Scheme 5.7 and discussion in Plausible Mechanism, *vide infra*).

With the exception of heteroaromatic secondary alcohols (**5.7z**, **5.7zb**, **5.7zc** and **5.7zk**, Table 5.6) and acyclic aliphatic secondary alcohols (**5.7t**, **5.7zl**, Table 5.6), reasonably good yields were observed for the **5.1a**-catalyzed *β*-alkylation of most of the 1-phenylethanol derivatives using benzyl alcohol as the alkylating agent (Table 5.6).

5.3.3. Control experiments

We have recently demonstrated that hot-filtration experiments are complementary to a mercury-drop test and that the former could be used as an effective alternate to the hazardous latter.[9f,13] In the current study it was observed that, heating a mixture of 2 mmol of **5.4**, 2 mmol of **5.5**, 2.5 mol % of NaO^{t}Bu, and 0.0025 mol % of **5.1a** at 140 °C for 24 h under conventional heating conditions resulted in an 85% yield of **5.7** (entry 16, Table 5.3 and equation 1, Scheme 5.6).

In a repeat experiment, the reaction mixture was heated for 1 h and hot-filtered and the filtrate was heated for another 23 h. An analysis of the resulting mixture indicated the formation of **5.7** in 80% yield. The comparable yields of *β*-alkylation of reactions with (equation 2**,** Scheme 5.6) and without (equation 1, Scheme 5.6) hot-filtration[13,17] fortifies the involvement of a well-defined molecular Co catalyst rather than heterogeneous Co.

Furthermore, when **5.4** (2 mmol) and **5.5** (2 mmol) were independently heated at 140 °C with**5.1a** (0.0025 mol %) and NaO^{t}Bu (2.5 mol %) in air for 1 h, the formation of hydrogen

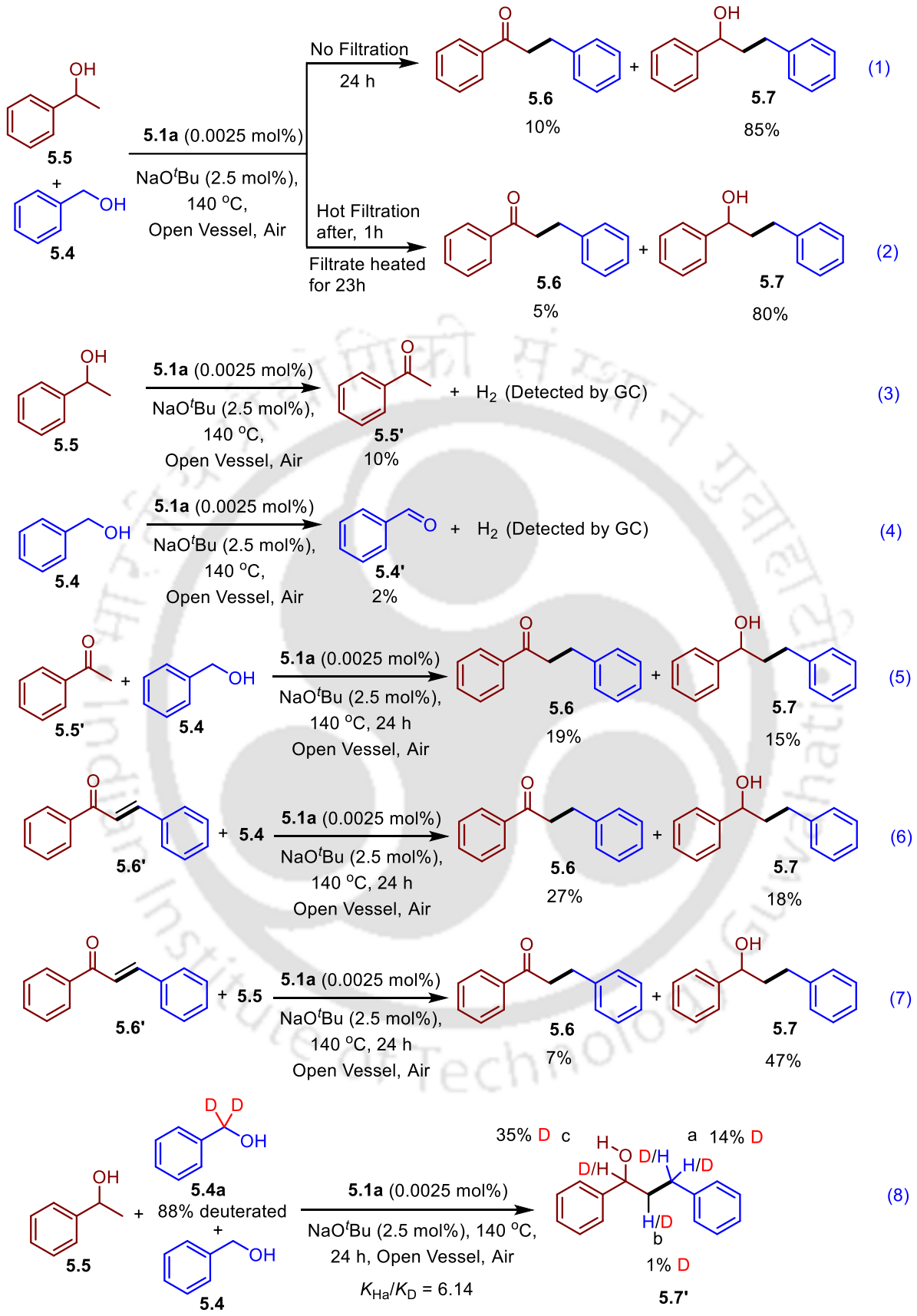

Scheme 5.6. Control Experiments

(Figures 5.8 and 5.9) was detected by GC analysis of the headspace. Trace amounts of benzaldehyde and acetophenone, respectively, were also observed in the ^{1}H NMR of the reaction mixture. As a trace amount of acetophenone **5.5′** is observed in all of the **5.1a**-catalyzed *β*-alkylations (Figures 5.S1−5.S66), a control experiment was performed in which **5.5′** was heated with **5.4** under the optimized *β*-alkylation conditions (equation **5,** Scheme 5.6). This led to the formation of **5.6** and **5.7** in 19% and 15% yields, respectively.

The observation of the *α,β*-unsaturated ketone **5.6′** and hence its possible intermediacy in the reaction was confirmed by heating it with either **5.4** or **5.5**, which served as a sacrificial hydrogen donor under the optimized *β*-alkylation conditions to yield **5.6** and **5.7**, respectively (equations 6 and 7, Scheme 5.6). More mechanistic insights were obtained from labelling studies by the use of deuterated benzyl alcohol **5.4a**. When a mixture of **5.5** (2 mmol), **5.4** (1 mmol), and **5.4a** (1 mmol) was heated to 140 °C with **5.1a** (0.0025 mol %) and NaO^{t}Bu (2.5 mol %) in an open vessel under air, the *β*-alkylated product **5.7′** was obtained in 49% yield (equation 8, Scheme 5.6). On the basis of the amount of deuterium incorporation at Ca, the KIE was found to be 6.14.[9f,11k,12g,13,18]

Valuable information was obtained from following a reaction of **5.4** (2 mmol) and **5.5** (2 mmol) catalyzed by **5.1a** (0.25 mol %) in the presence of NaO^{t}Bu (2.5 mol %) at 140 °C in air by ESR (Figure 5.5) and HRMS (Figure 5.7). Complex **5.1a** is paramagnetic (μ_{eff} = 3.23 μ_B in the solid state and μ_{eff} = 4.29 μ_B in solution), which indicates it to be either octahedral or trigonal bipyramidal.[15] On the basis of an HRMS analysis (Figure 5.3) it is clear that there is actually a mixture of **5.1a** (trigonal bipyramidal) and **5.3a** (octahedral). However, it should be noted that the well-defined ESR signal (Figure 5.5a) arises from only **5.1a** with a trigonal-bipyramidal geometry, as Co(II) in an octahedral geometry is reported to be ESR inactive.[9f,16] The reaction mixture was ESR silent (Figure 5.5) throughout the reaction, which points to Co(II) species in an octahedral environment.[9f,16] The paramagnetic nature of these ESR-silent octahedral Co(II) species was confirmed by magnetic moment measurements (Figure 5.6b) by the Evans method. The observed magnetic moment value of 3.04 μB [15] (Figure 5.6b) and the ESR-silent nature[9f,16] (Figure 5.5b−i) points to the involvement of octahedral Co(II) species[8−12] **5.8**-**5.12** (Scheme 5.7). Notably under the reaction conditions both the TBP precursor **5.1** and the O_h/T_h ion pair precursor **5.3** is likely to transform irreversibly to O_h species **5.8**-**5.12.**

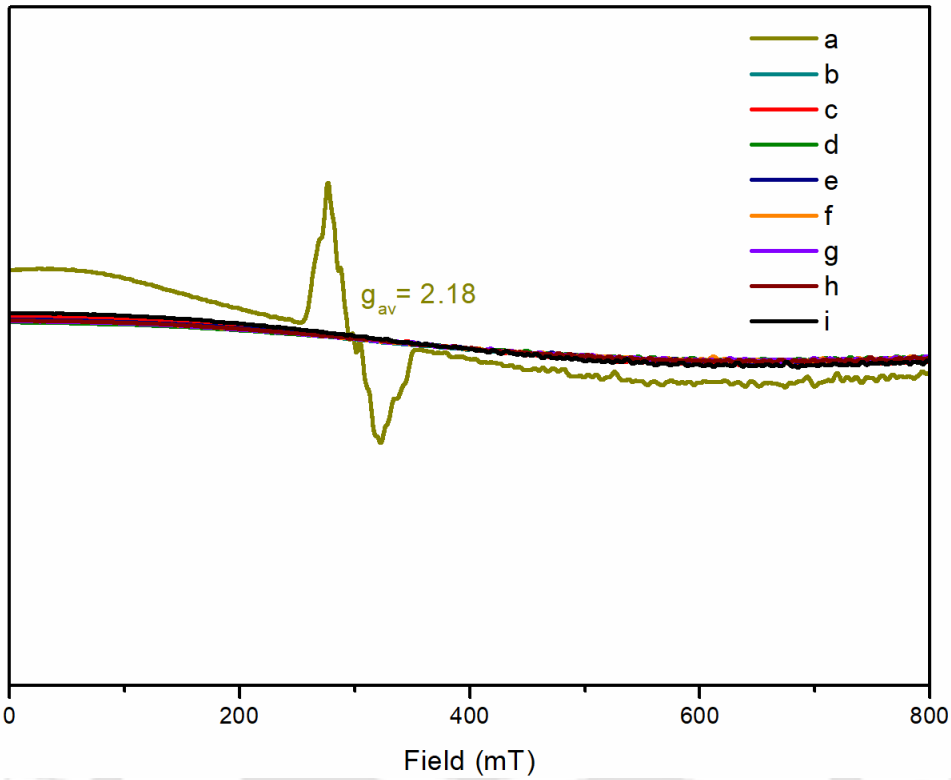

Figure 5.5. ESR spectra of (a) **5.1a** in methanol, (b) reaction mixture containing **5.1a** (0.25 mol %) in a solution of **5.4** and **5.5** immediately after mixing, (c) reaction mixture containing **5.1a** (0.25 mol %) and NaO^{t}Bu (2.5 mol %) in a solution of **5.4** and **5.5** immediately after mixing, (d) reaction mixture containing **5.1a** (0.25 mol %) and NaO^{t}Bu (2.5 mol %) in a solution of **5.4** and **5.5** after heating at 140 °C for 30 min, (e) reaction mixture containing **5.1a** (0.25 mol %) and NaO^{t}Bu (2.5 mol %) in a solution of **5.4** and **5.5** after heating at 140 °C for 1 h, (f) reaction mixture containing **5.1a** (0.25 mol %) and NaO Bu (2.5 mol %) in a solution of **5.4** and **5.5** after heating at 140 °C for 3 h, (g) reaction mixture containing **5.1a** (0.25 mol %) and NaO^{t}Bu (2.5 mol %) in a solution of **5.4** and **5.5** after heating at 140 °C for 5 h, (h) reaction mixture containing **5.1a** (0.25 mol %) and NaO^{t}Bu (2.5 mol %) in a solution of **5.4** and **5.5** after heating at 140 °C for 14 h, (i) reaction mixture containing **5.1a** (0.25 mol %) and NaO^{t}Bu (2.5 mol %) in a solution of **5.4** and **5.5** after heating at 140 °C for 24 h.

At t = 0 h (prior to heating), a HRMS analysis (Figure 5.7) of the reaction mixture showed peaks at m/z 338.3429 and 675.6765 that correspond to **5.8a′** and [**5.9a′** + H_2O + $2CH_3CN$ + K]$^+$, respectively, with the former presumably arising from the methoxide for benzyl oxide/1-phenyl ethoxide substitution of **5.8a/5.9a** (when X = OCH_2Ph, $OCH(CH_3)Ph$, Scheme 5.7) in the methanol solvent used for analysis. When the system is heated for 1 h, apart from the peaks

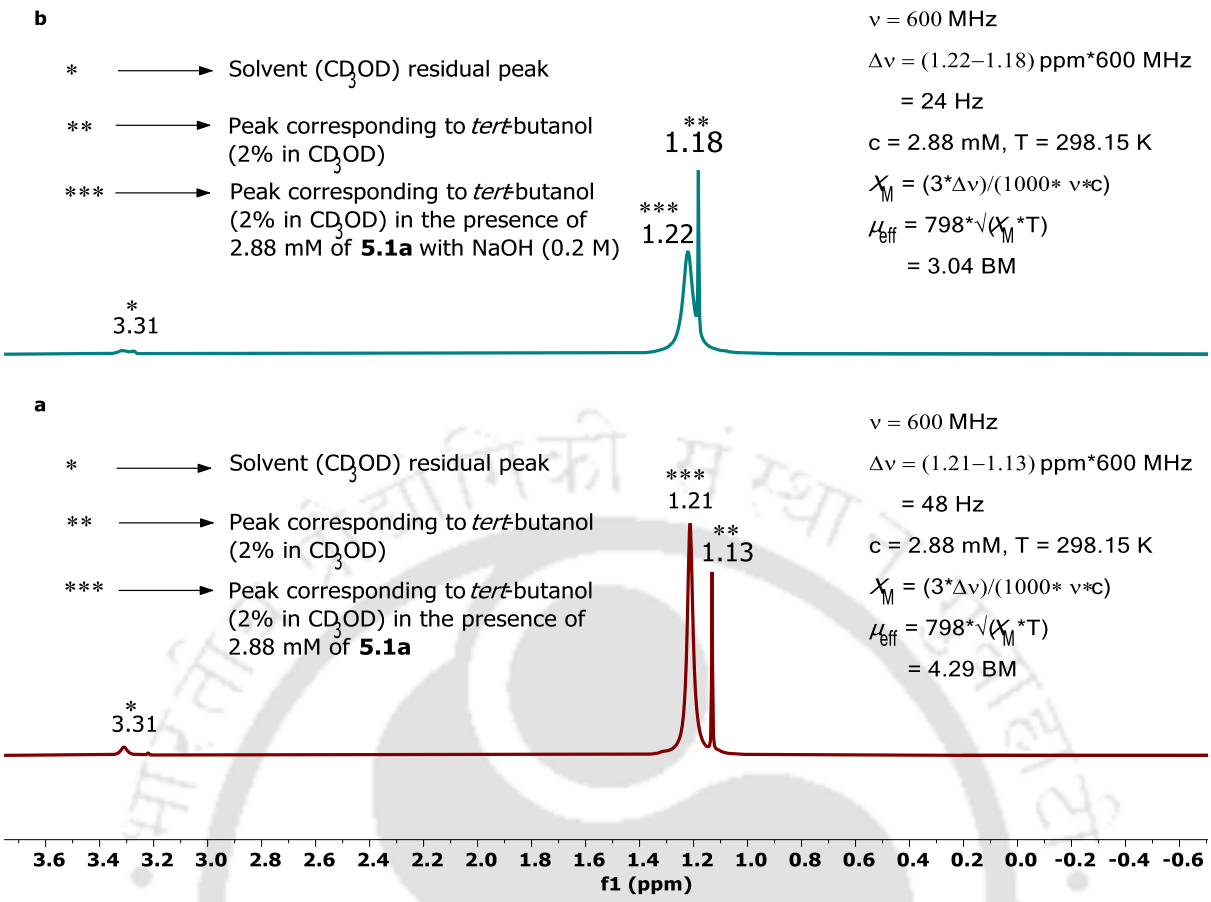

Figure 5.6. Determination of the magnetic moment of the Co species present in the solution containing **5.1a** (a) before the addition of base and (b) after the addition of base.

observed at 0 h, an additional peak at m/z 419.2005 corresponding to [**5.8a″** + H]$^+$ was observed in the HRMS analysis. The HRMS analyses at later times (Figures 5.S82−5.S85) were similar to those observed at 1 h . These observations indicate the involvement of well-defined molecular Co(II) species during catalysis, in line with the observations made in equations 1 and 2 (Scheme 5.6). The HRMS analyses are also indicative of the integrity of the pincer fragment and show that the imino groups are intact during catalysis. Furthermore, the similar yields obtained under atmospheres of air and argon (entry 16 vs entry 25, Table 5.3) are indicative of the absence of any redox species (Co(II)/ Co(0) or Co(II)/Co(III)) in the catalytic cycle. One should also not ignore the fact that pincer-Co adducts containing the products **5.6** and **5.7** are not observed. This points to their absence in the RDS.

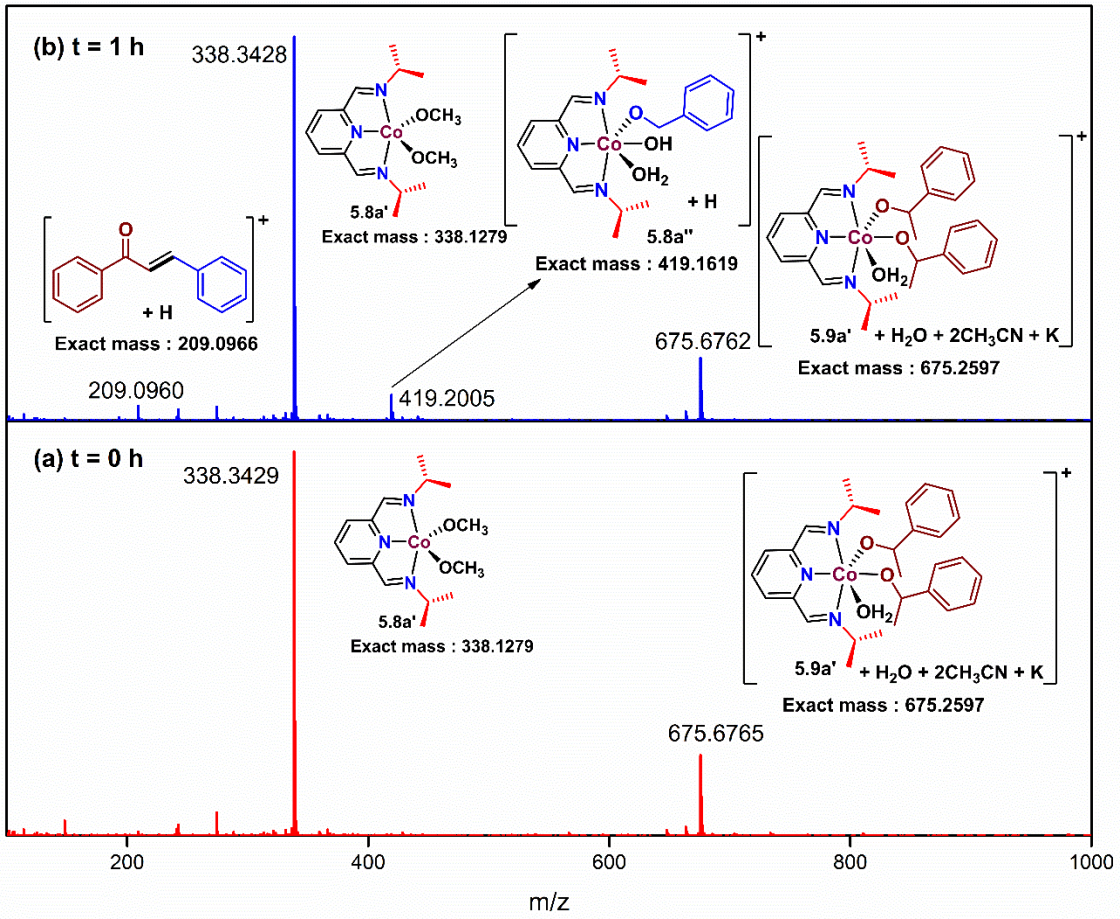

Figure 5.7. HRMS analysis of a mixture of **5.4** (2 mmol) and **5.5** (2 mmol) in the presence of **5.1a** (0.001735 g, 0.005 mmol 0.25 mol %) and NaO^{t}Bu (0.0048 g, 0.05 mmol, 2.5 mol %) after (a) 0 h and (b) 1h.

5.3.4. Plausible Mechanism

The inferences drawn from control experiments (Scheme 5.6 and Figures 5.5−5.7) have been instrumental in arriving at a plausible mechanism (Scheme 5.7). The NNN pincer-Co complex **5.1/5.3** upon treatment with NaO^{t}Bu in the presence of **5.4/5.5** yields octahedral Co(II) species **5.8/5.9** along with the formation of NaCl (Scheme 5.7). The detection of **5.8a′** and **5.9a′** in the HRMS of the reaction mixture at room temperature suggests that the salt metathesis of **5.1/5.3** with NaO^{t}Bu occurs at room temperature. Subsequent β-hydride elimination from **5.8/5.9** gives the corresponding carbonyl compounds **5.4′/5.5′** and the hydride complex **5.10**. Notably **5.4′** and **5.5′** are detected by NMR in the independent dehydrogenations of **5.4** and **5.5**, respectively (equations 3 and 4, Scheme 5.6). On the other hand, in the Guerbet reaction mixture, only **5.5′** is detected by NMR. The absence of Co adducts with either **5.6** or **5.7** in the HRMS analysis (Figure 5.7) suggests that the rate-determining step (RDS) lies in the alcohol dehydrogenation

fragment (Scheme 5.7) and more so in the *β*-hydride elimination from **5.9**, which is in good agreement with the KIE of 6.14, lower yields in the presence of electron-withdrawing groups in the - *para* position of 1- phenyl ethanol, and the observation of **5.5′** in trace amounts in the reaction mixture.

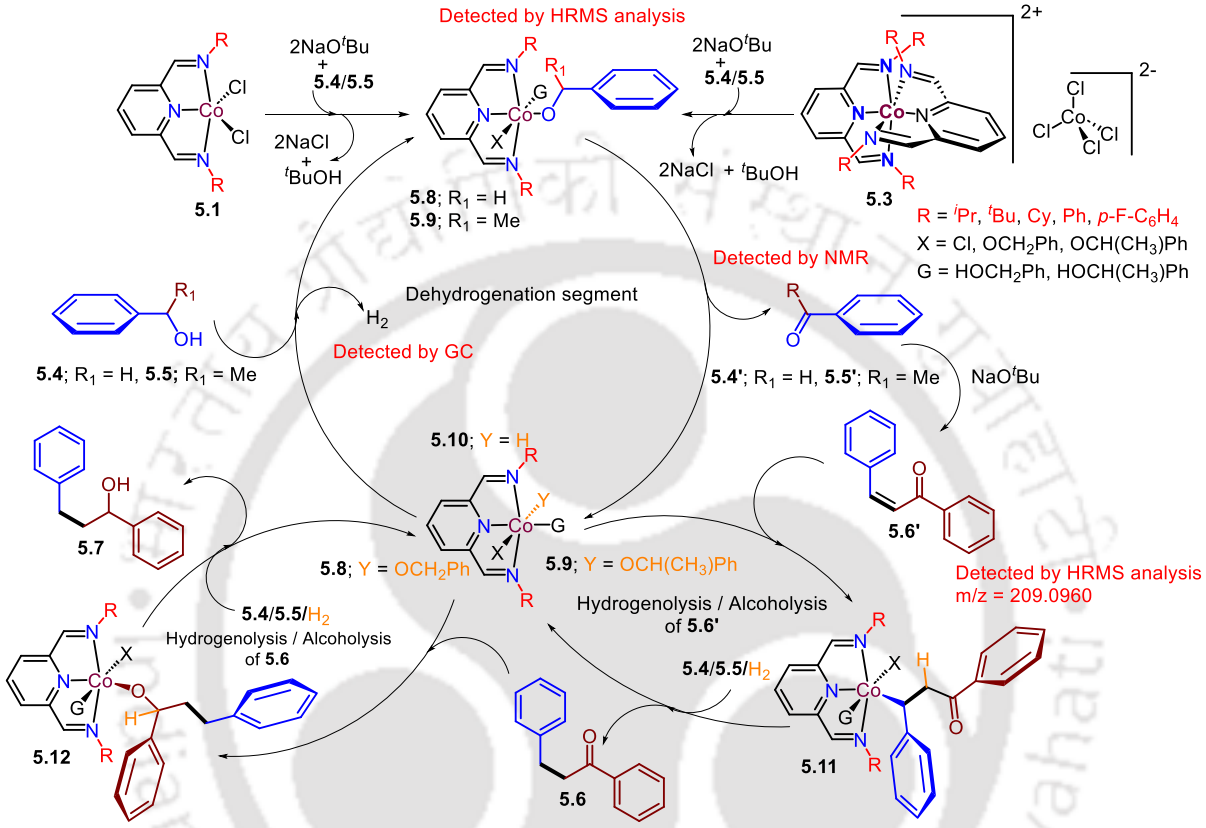

Scheme 5.7. Plausible mechanism involved in the **5.1/5.3**-catalyzed *β*-alkylation of 1-phenylethanol with benzyl Alcohol.

A follow-up σ-bond metathesis of the O−H bond of **5.4/5.5** with Co−H of **5.10** regenerates **5.8/5.9** along with the liberation of H_2 (detected by GC, Figures 5.8 and 5.9). Further, the formation of the *α, β*-unsaturated ketone **5.6′** from the aldol condensation of benzaldehyde (**5.4′**) and acetophenone (**5.5′**) is uncatalyzed and is mediated by the base (NaO^{t}Bu). Though **5.6′** is not observed in ^{1}H NMR, it is detected in a few HRMS analyses (m/z 209.0960, Figure 5.7). The insertion of the double bond of **5.6′** into the Co−H bond in **5.10** yields **5.11**. A further σ-bond metathesis of the Co−C bond in **5.11** either with the O−H bond of **5.4/5.5** or with H_2 completes the cycle to yield the corresponding ketone **5.6** along with the regeneration of catalytically active **5.8/5.9/5.10** (Scheme 5.7). A similar cycle involving insertion and

alcoholysis/ hydrogenolysis via **5.10** → **5.12** → **5.8/5.9/5.10** can be envisaged for the transformation of **5.6** to **5.7**. If hydrogenolysis is involved, it requires closed-vessel conditions. On the other hand, the reaction is unaffected by either a closed-vessel or open-vessel condition if alcoholysis is involved. In our current studies, apparently, alcoholysis is a major contributor to product (entries 16 and 24, Table 5.3 and entries 4 and 7, Table 5.4) formation and hence not surprisingly the reaction yields are similar under either open-vessel or closed-vessel conditions. Though hydrogen is involved, it is likely to be in a low steady-state concentration and could be rapidly consumed back in a reverse reaction apart from leading to a minor amount of product formation via hydrogenolysis. This is very similar to our recent reports on *β*-alkylation with $CoCl_2$,[9f] pincer-Ni,[12g] and pincer-Cr-based catalysts.[13]

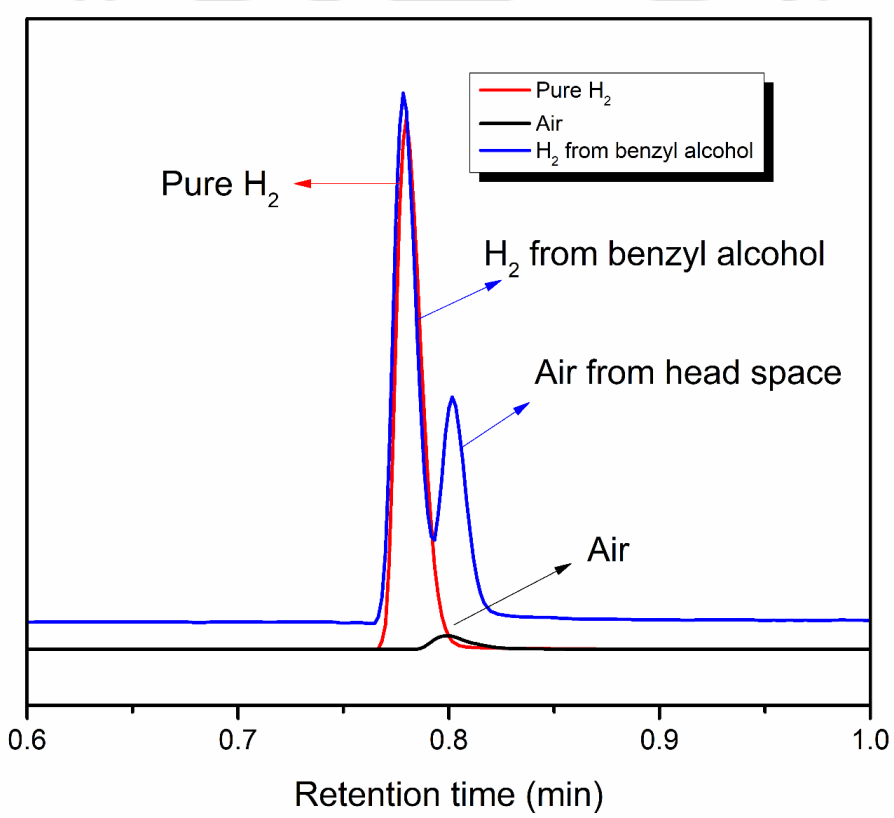

Figure 5.8. Evidence for the evolution of H_2 in dehydrogenation of benzyl alcohol (**5.4**) catalyzed by **5.1a** (0.005 mol %) at 140 °C via GC analysis.

5.4. Conclusion

The environmentally benign, earth-abundant, and inexpensive base metal cobaltous chloride has been used to synthesize pincer-Co complexes of the type (^{R2}NNN)$CoCl_2$ (R = ^{i}Pr, ^{t}Bu, Cy, Ph, *p*-F-C_6H_4). On the basis of the nature of the R group, these complexes are found to exist

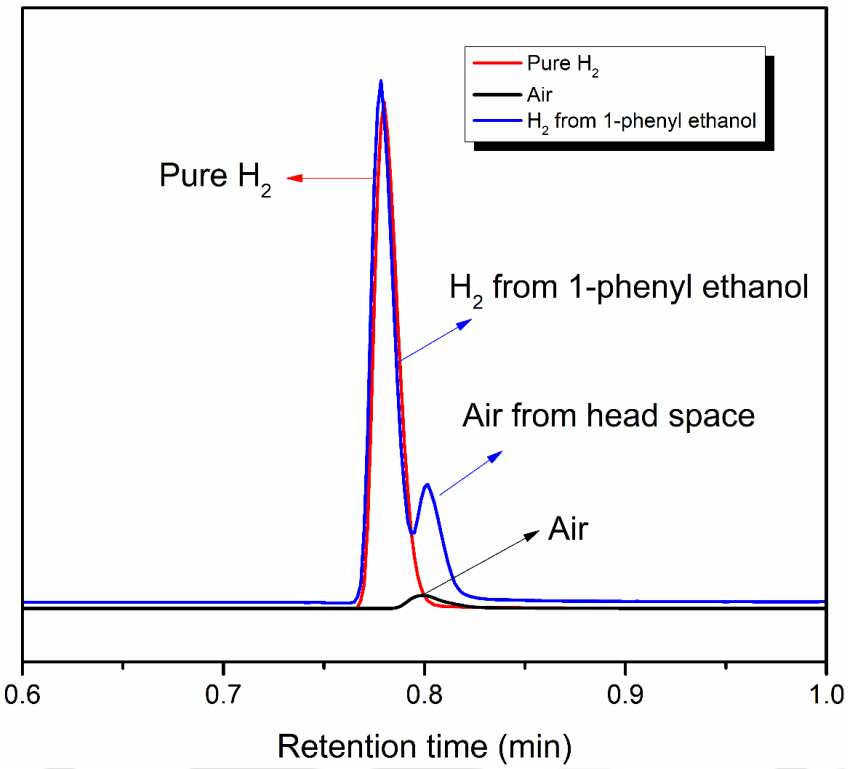

Figure 5.9. Evidence for the evolution of H_2 in dehydrogenation of 1-phenyl ethanol (**5.5**) catalyzed by **5.1a** (0.005 mol %) at 140 °C via GC analysis.

in equilibrium with the corresponding ion-pair $[(^{R2}NNN)_2Co]CoCl_4$. The TGA analysis indicates that the considered pincer-Co complexes demonstrate very good thermal stability. All of the considered pincer-Co complexes have been found to efficiently catalyze *β*-alkylation of 1-phenylethanol with benzyl alcohol. In particular, $(^{iPr2}NNN)CoCl_2$ has demonstrated the best activity in air at 140 °C. Under conventional heating, $(^{iPr2}NNN)CoCl_2$ (0.0025 mol %) catalyzed the *β*-alkylation in the presence of NaO^tBu (2.5 mol %) in 24 h to yield 85% (34000 TON at 1417 TO/h) of the *β*-alkylated product. On the other hand, the corresponding reaction under microwave conditions (140 °C at 75 W) was complete in only 2 h with a comparable yield (83%, 33200 TON) and far better TOF (16600 TOs/h). Under similar conditions, the precursor $CoCl_2$ (0.0025 mol %) gave relatively poor results under both conventional (ca. 66%, 26400 TON at 1100 TOs/h) and microwave heating (ca. 61%, 24400 TON at 12200 TOs/h). The *β*-alkylations (ca. 39 examples) of a range of secondary alcohols with several primary alcohols have been successfully accomplished using $(^{iPr2}NNN)CoCl_2$ as a catalyst under both conventional and microwave heating.

Hot-filtration experiments and HRMS analyses suggest the existence of well-defined molecular Co(II) species during the catalytic *β*-alkylation. During the reaction Co remains in its +2 state,

as inferred from EPR studies and magnetic moment measurements using the Evans method. In good agreement with HRMS analyses that show pincer-Co adducts only with reactant alcohols and in line with the observation of trace amounts of acetophenone during the *β*-alkylation, key evidence for the involvement of C−H activation (*β*-hydride elimination of acetophenone in particular) in the RDS of the pincer-Co-catalyzed reaction is obtained from competitive deuterium labelling experiments that result in a KIE of 6.14. This also explains the low yields of *β*-alkylation of 1-phenylethanol derivatives with electron-withdrawing groups. To the best of our knowledge, these unprecedented turnovers (33200 TON at 16600 TO/h) in such a short time (2 h) are the best reported hitherto with base-metal catalysis for *β*-alkylation. These pincer-Co catalytic systems that operate in air under microwave conditions offer exciting possibilities for related tandem (de)hydrogenation reactions.

5.5. Experimental section

5.5.1. General Procedure and Materials

All manipulations were carried out in air. The chemicals NaO^{t}Bu, KO^{t}Bu, NaOH, KOH, Na_2CO_3, K_2CO_3, $CDCl_3$, benzyl alcohol, 1-phenylethanol, and their derivatives were purchased either from Sigma-Aldrich or MERCK and used as such. All catalytic reactions were carried out in air using oven dried glassware. The 1-phenyl ethanol derivatives that were not commercially available were prepared according to a literature procedure.[19a] Tetrahydrofuran (THF) was dried via double distillation over Na/benzophenone.

5.5.2. Physical Measurements

The ^{1}H and ^{13}C{^{1}H} NMR spectra were recorded on a Bruker ASCEND 600 instrument operating at 600 MHz for ^{1}H and 150 MHz for ^{13}C{^{1}H}, a Bruker AVANCE 500 instrument operating at 500 MHz for ^{1}H and 125 MHz for ^{13}C{^{1}H}, or a Bruker AVANCE 400 instrument operating at 400 MHz for ^{1}H and 100 MHz for ^{13}C{^{1}H}. Chemical shifts (*δ*) are reported in ppm. HRMS measurements were carried out using an Agilent Accurate- Mass Q-TOF ESI-MS 6520 instrument. The X-band EPR spectra were recorded on a JES-FA200 ESR spectrometer. X-ray crystallographic data were acquired on a Bruker D8 Venture single-crystal Xray diffractometer using graphite-monochromated Mo K*α* radiation. The data refinement and cell reductions were carried out with the Bruker SAINT program.[20] Structures were further solved and refined by the full-matrix least-squares method using SHELXS-14.[21] Thermogravimetric analyses were performed using a thermal analyser (SDTQ600) with a simultaneous DTA/TGA

system, under argon with a heating rate of 10 °C min^{-1}. Solid-state magnetic susceptibilities of the complexes were recorded using a Sherwood Scientific MSB-1 magnetic balance at room temperature. Microwave reactions were carried out with a CEM Discover apparatus operating at a voltage of 110 V and microwave irradiation of 2.45 GHz with a maximum microwave output of 300 W.

5.5.3. Synthesis of (^{iPr2}NNN)$CoCl_2$ (5.1a)

The metal salt $CoCl_2$ (0.045 g, 0.346 mmol) was stirred with the ligand **5.2a** (0.075 g, 0.346 mmol) in dry and distilled THF (3 mL) for 16 h at room temperature. The solvent was evaporated under reduced pressure, and the light green solid was washed with diethyl ether (3 × 3 mL). The residue was dried under vacuum and isolated as a light green solid (0.103 g) in 86% yield. HRMS (ESI): *m*/*z* calculated for [**5.3a** − $CoCl_4$]$^{2+}$ = [$C_{26}H_{38}CoN_6$],$^{2+}$ 246.6245, found 246.6250; *m*/*z* calculated for [**5.1a** − Cl]$^+$ = [$C_{13}H_{19}ClCoN_3$]$^+$, 311.0600, found 311.0593; *m*/*z* calculated for [**5.1a** − Cl + CH_3CN + 3H_2O]$^+$ = [$C_{15}H_{28}ClCoN_4O_3$],$^+$ 406.1182, found 406.1107; *m*/*z* calculated for [**5.1a′** + 2CH_3CN + 3H_2O + Na]$^+$ = [$C_{17}H_{33}CoN_5NaO_5$]$^+$, 469.1891, found 469.1711. Magnetic susceptibility: μ_{eff} = 3.23 μ_B.

5.5.4. Synthesis of (^{tBu2}NNN)$CoCl_2$ (5.1b)

The metal salt $CoCl_2$ (0.065 g, 0.5 mmol) was stirred with the ligand **5.2b** (0.129 g, 0.5 mmol) in dry and distilled THF (3 mL) for 16 h at room temperature. The solvent was evaporated under reduced pressure, and the green solid was washed with diethyl ether (3 × 3 mL). The residue was dried under vacuum and isolated as a green solid (0.146 g) in 78% yield. HRMS (ESI): *m*/*z* calculated for [**5.1b** − Cl]$^+$ = [$C_{15}H_{23}ClCoN_3$]$^+$, 339.0913, found 339.0907; *m*/*z* calculated for [(^{tBu2}NNN)Co(OH)(OCH_3) + 2CH_3CN + H]$^+$ = [$C_{20}H_{34}CoN_5O_2$]$^+$ 435.2045, found 435.3767. Magnetic susceptibility: μ_{eff} = 4.42 μ_B.

5.5.5. Synthesis of (^{Cy2}NNN)$CoCl_2$ (5.1c)

The metal salt $CoCl_2$ (0.045 g, 0.346 mmol) was stirred with the ligand **5.2c** (0.103 g, 0.346 mmol) in dry and distilled THF (3 mL) for 16 h at room temperature. The solvent was evaporated under reduced pressure, and the blackish green solid was washed with diethyl ether (3 × 3 mL). The residue was dried under vacuum and isolated as a blackish green solid (0.126 g) in 43% yield. HRMS (ESI): *m*/*z* calculated for [**5.3c** − $CoCl_4$]$^{2+}$ = [$C_{38}H_{54}CoN_6$]$^{2+}$, 326.6871,

found 326.6866; *m*/*z* calculated for [**5.1c** − Cl]$^+$ = [$C_{19}H_{27}ClCoN_3$]$^+$, 391.1226, found 391.1221. Magnetic susceptibility: μ_{eff} = 3.51 μ_B.

5.5.6. Synthesis of (^{Ph2}NNN)$CoCl_2$ (5.1d)

The metal salt $CoCl_2$ (0.045 g, 0.346 mmol) was stirred with the ligand **5.2d** (0.099 g, 0.346 mmol) in dry and distilled THF (3 mL) for 16 h at room temperature. The solvent was evaporated under reduced pressure, and the yellow solid was washed with diethyl ether (3 × 3 mL). The residue was dried under vacuum and isolated as a yellow solid (0.129 g) in 90% yield. HRMS (ESI): *m*/*z* calculated for [**5.3d** − $CoCl_4$]$^{2+}$ = [$C_{38}H_{30}CoN_6$]$^{2+}$ 314.5932, found 314.5943; *m*/*z* calculated for [**5.1d** − Cl]$^+$ = [$C_{19}H_{15}ClCoN_3$]$^+$, 379.0287, found 379.0281. Magnetic susceptibility: μ_{eff} = 4.09 μ_B.

5.5.7. Synthesis of ($^{(p\text{-}F\text{-}C6H4)2}$NNN)$CoCl_2$ (5.1e)

The metal salt $CoCl_2$ (0.045 g, 0.346 mmol) was stirred with the ligand **5.2e** (0.111 g, 0.346 mmol) in dry and distilled THF (3 mL) for 16 h at room temperature. The solvent was evaporated under reduced pressure, and the yellow solid was washed with diethyl ether (3 × 3 mL). The residue was dried under vacuum and isolated as a yellow solid (0.144 g) in 93% yield. HRMS (ESI): *m*/*z* calculated for [**5.1e** – Cl + 3CH_3OH + CH_3CN]$^+$ = [$C_{24}H_{28}ClCoF_2N_4O_3$]$^+$, 552.1150, found 552.3152. Magnetic susceptibility: μ_{eff} = 4.19 μ_B.

5.5.8. General Procedure for 5.1a-Catalyzed *β*-Alkylation of Alcohols

In a 10 mL pear-shaped flask containing 1-phenylethanol and benzyl alcohol were added 2.5 mol % of NaO^{t}Bu and 0.0025 mol % of (^{iPr2}NNN)$CoCl_2$ (from a stock solution in either 1-phenylethanol or benzyl alcohol). Ultimately, the reaction mixture contained 0.0347 mg (0.1 μmol) of (^{iPr2}NNN)$CoCl_2$, 9.6 mg (0.1 mmol) of NaO^{t}Bu, 0.241 mL (2.00 mmol) of 1-phenylethanol, and 0.206 mL (2.00 mmol) of benzyl alcohol. The contents were heated at 140 °C (either under conventional heating for 24 h or under microwave (75 W) for 2 h) in air and subsequently cooled to room temperature. A known amount of toluene was then added to the reaction mixture. From the reaction mixture, an aliquot (10 mg) was withdrawn and the ^{1}H NMR recorded in $CDCl_3$. The yield (in mmol) of product formed was calculated from ^{1}H NMR using a known amount of toluene as a standard.[19b] The percentage yield was obtained by multiplying the ratio of calculated yield to theoretical yield by 100.

Supporting information (containing NMR spectra and of reaction mixtures, HRMS data, GC plot, TGA data, EPRS data) for chapter V is available as appendix IV and can be found at https://drive.google.com/file/d/1nRhwGf9bdDny5-1W_ZrfScmF2e7tI0ZP/view?usp=sharing

5.6. References

(1) Akhtar, W. M.; Armstrong, R. J.; Frost, J. R.; Stevenson, N. G.; Donohoe, T. J. Stereoselective Synthesis of Cyclohexanes via an Iridium Catalyzed (5 + 1) Annulation Strategy. *J. Am. Chem. Soc.* **2018**, *140*, 11916−11920.
(2) Yi, H.; Zhang, G.; Wang, H.; Huang, Z.; Wang, J.; Singh, A. K.; Lei, A. Recent Advances in Radical C−H Activation/Radical CrossCoupling. *Chem. Rev.* **2017**, *117*, 9016−9085.
(3) (a) Zhang, Y.-F.; Shi, Z.-J. Upgrading Cross-Coupling Reactions for Biaryl Syntheses. *Acc. Chem. Res.* **2019**, *52*, 161−169. (b) Das, K.; Kumar, A. Alkane dehydrogenation reactions catalyzed by pincer metal complexes. In *Advances in Organometallic Chemistry*, Pérez, P. J., Ed. Academic Press, 2019; Vol. *72*, Chapter 1, pp 1−57. DOI: 10.1016/bs.adomc.2019.02.004. (c) Kumar, A.; Bhatti, T. M.; Goldman, A. S. Dehydrogenation of Alkanes and Aliphatic Groups by Pincer-Ligated Metal Complexes. *Chem. Rev.* **2017**, *117*, 12357− 12384. (d) Kumar, A.; Goldman, A. S. Recent Advances in Alkane Dehydrogenation Catalyzed by Pincer Complexes. In *The Privileged Pincer-Metal Platform: Coordination Chemistry & Applications*, van Koten, G., Gossage, R. A., Eds.; Springer International Publishing: Cham, 2016; pp 307−334. (e) Hess, W.; Treutwein, J.; Hilt, G. Cobalt-catalysed carbon-carbon bond-formation reactions. *Synthesis* **2008**, *22*, 3537−3562. (f) Irrgang, T.; Kempe, R. 3d-Metal Catalyzed N- and C-Alkylation Reactions via Borrowing Hydrogen or Hydrogen Autotransfer. *Chem. Rev.* **2019**, *119*, 2524−2549. (g) Borthakur, I.; Sau, A.; Kundu, S. Cobalt-catalyzed dehydrogenative functionalization of alcohols: Progress and future prospect. *Coord. Chem. Rev.* **2022**, *451*, 214257. (h) Subaramanian, M.; Sivakumar, G.; Balaraman, E. Recent advances in nickel catalysed C−C and C−N bond formation via HA and ADC reactions. *Org. Biomol. Chem.* **2021**, *19*, 4213−4227.
(4) (a) Xu, Q.; Chen, J.; Liu, Q. Aldehyde-Catalyzed Transition Metal-Free Dehydrative β-Alkylation of Methyl Carbinols with Alcohols. *Adv. Synth. Catal.* **2013**, *355*, 697−704. (b) Allen, L. J.; Crabtree, R. H. Green alcohol couplings without transition metal catalysts: base-mediated β-alkylation of alcohols in aerobic conditions. *Green Chem.* **2010**, *12*, 1362−1364. (c) Xu, Q.; Chen, J.; Tian, H.; Yuan, X.; Li, S.; Zhou, C.; Liu, J. Catalyst-Free Dehydrative αAlkylation of Ketones with Alcohols: Green and Selective A utocatalyzed Synthesis of Alcohols and Ketones. *Angew. Chem., Int. Ed.* **2014**, *53*, 225−229.
(5) (a) Kose, O.; Saito, S. Cross-coupling reaction of alcohols for carbon−carbon bond formation using pincer-type NHC/palladium catalysts. *Org. Biomol. Chem.* **2010**, *8*, 896−900. (b) Mamidala, R.; Biswal, P.; Subramani, M. S.; Samser, S.; Venkatasubbaiah, K. Palladacycle-Phosphine Catalyzed Methylation of Amines and Ketones Using Methanol. *J. Org. Chem.* **2019**, *84*, 10472−10480.
(6) (a) Fujita, K.-i.; Asai, C.; Yamaguchi, T.; Hanasaka, F.; Yamaguchi, R. Direct β-Alkylation of Secondary Alcohols with Primary Alcohols Catalyzed by a Cp*Ir Complex. *Org. Lett.* **2005**, *7*, 4017−4019. (b) Cheung, H. W.; Lee, T. Y.; Lui, H. Y.; Yeung, C. H.; Lau, C. P. Ruthenium-Catalyzed β-Alkylation of Secondary Alcohols with Primary Alcohols. *Adv. Synth. Catal.* **2008**, *350*, 2975− 2983. (c) Pontes da Costa, A.; Viciano, M.; Sanau, M.; Merino, S.; Tejeda, J.; Peris, E.; Royo, B. First Cp*-Functionalized NH eterocyclic Carbene and Its Coordination to Iridium. Study of the Catalytic Properties. *Organometallics* **2008**, *27*, 1305−1309. (d) Gnanamgari, D.; Sauer, E. L. O.; Schley, N. D.; Butler, C.; Incarvito, C. D.; Crabtree, R. H. Iridium and Ruthenium Complexes with Chelating N-Heterocyclic Carbenes: Efficient Catalysts for Transfer Hydrogenation, β-Alkylation of Alcohols, and N-Alkylation of Amines. *Organometallics* **2009**, *28*, 321−325. (e) Gong, X.; Zhang, H.; Li, X. J. T. l. Iridium phosphine abnormal N-heterocyclic carbene complexes in catalytic hydrogen transfer reactions. *Tetrahedron Lett.* **2011**, *52*, 5596−5600. (f) Xu, C.; Goh, L. Y.; Pullarkat, S. A. J. O. Efficient iridium-thioether-dithiolate catalyst for β-alkylation of alcohols and selective imine formation via N-alkylation

reactions. *Organometallics* **2011**, *30*, 6499−6502. (g) Jiménez, M. V.; Fernández-Tornos, J.; Modrego, F. J.; Pérez-Torrente, J. J.; Oro, L. A. Oxidation and β-Alkylation of Alcohols Catalysed by Iridium(I) Complexes with Functionalised N-Heterocyclic Carbene Ligands. *Chem. - Eur. J.* **2015**, *21*, 17877−17889. (h) Genç, S.; Arslan, B.; Gülcemal, S.; Günnaz, S.; Çetinkaya, B.; Gülcemal, D. Iridium(I)- Catalyzed C−C and C−N Bond Formation Reactions via the Borrowing Hydrogen Strategy. *J. Org. Chem.* **2019**, *84*, 6286−6297. (i) Wang, D.; McBurney, R. T.; Pernik, I.; Messerle, B. A. Controlling the selectivity and efficiency of the hydrogen borrowing reaction by switching between rhodium and iridium catalysts. *Dalton Trans.* **2019**, *48*, 13989−13999. (j) Musa, S.; Ackermann, L.; Gelman, D. Dehydrogenative Cross-Coupling of Primary and Secondary Alcohols. *Adv. Synth. Catal.* **2013**, *355*, 3077−3080. (k) Ruiz-Botella, S.; Peris, E. Unveiling the Importance of π-Stacking in Borrowing-Hydrogen Processes Catalysed by Iridium Complexes with Pyrene Tags. *Chem. - Eur. J.* **2015**, *21*, 15263−15271. (l) Genç, S.; Günnaz, S.; Çetinkaya, B.; Gülcemal, S. l.; Gülcemal, D. Iridium (I)-Catalyzed Alkylation Reactions To Form α-Alkylated Ketones. *J. Org. Chem.* **2018**, *83*, 2875−2881. (m) Koda, K.; Matsu-ura, T.; Obora, Y.; Ishii, Y. Guerbet reaction of ethanol to n-butanol catalyzed by iridium complexes. *Chem. Lett.* **2009**, *38*, 838−839. (n) Kaur, M.; U Din Reshi, N.; Patra, K.; Bhattacherya, A.; Kunnikuruvan, S.; Bera, J. K. A ProtonResponsive Pyridyl (benzamide)-Functionalized NHC Ligand on Ir Complex for Alkylation of Ketones and Secondary Alcohols. *Chem. - Eur. J.* **2021**, *27*, 10737−10748.
(7) Satyanarayana, P.; Reddy, G. M.; Maheswaran, H.; Kantam, M. L. Catalysis, Tris (acetylacetonato) rhodium (III)-Catalyzed αAlkylation of Ketones, β-Alkylation of Secondary Alcohols and Alkylation of Amines with Primary Alcohols. *Adv. Synth. Catal.* **2013**, *355*, 1859−1867.
(8) (a) Zhang, C.; Zhao, J.-P.; Hu, B.; Shi, J.; Chen, D. Ruthenium Catalyzed β-Alkylation of Secondary Alcohols and α-Alkylation of Ketones via Borrowing Hydrogen: Dramatic Influence of the Pendant N-Heterocycle. *Organometallics* **2019**, *38*, 654−664. (b) Sahoo, A. R.; Lalitha, G.; Murugesh, V.; Bruneau, C.; Sharma, G. V.; Suresh, S.; Achard, M. Ruthenium Phosphine−Pyridone Catalyzed Cross Coupling of Alcohols To form α-Alkylated Ketones. *J. Org. Chem.* **2017**, *82*, 10727−10731. (c) Wang, Q.; Wu, K.; Yu, Z. Ruthenium (III)-catalyzed β-alkylation of secondary alcohols with primary alcohols. *Organometallics* **2016**, *35*, 1251−1256. (d) Roy, B. C.; Chakrabarti, K.; Shee, S.; Paul, S.; Kundu, S. Bifunctional RuIIComplex-Catalysed Tandem C− C Bond Formation: Efficient and Atom Economical Strategy for the Utilisation of Alcohols as Alkylating Agents. *Chem. - Eur. J.* **2016**, *22*, 18147−18155. (e) Chakrabarti, K.; Paul, B.; Maji, M.; Roy, B. C.; Shee, S.; Kundu, S. Bifunctional Ru (ii) complex catalysed carbon−carbon bond formation: an eco-friendly hydrogen borrowing strategy. *Org. Biomol. Chem.* **2016**, *14*, 10988−10997. (f) Cho, C. S.; Kim, B. T.; Kim, H.-S.; Kim, T.-J.; Shim, S. C. Ruthenium-catalyzed one-pot β-alkylation of secondary alcohols with primary alcohols. *Organometallics* **2003**, *22*, 3608−3610. (g) Shi, J.; Hu, B.; Ren, P.; Shang, S.; Yang, X.; Chen, D. Synthesis and Reactivity of Metal−Ligand Cooperative Bifunctional Ruthenium Hydride Complexes: Active Catalysts for β-Alkylation of Secondary Alcohols with Primary Alcohols. *Organometallics* **2018**, *37*, 2795−2806. (h) Dowson, G. R.; Haddow, M. F.; Lee, J.; Wingad, R. L.; Wass, D. F. Catalytic conversion of ethanol into an advanced biofuel: unprecedented selectivity for n-butanol. *Angew. Chem., Int. Ed.* **2013**, *52*, 9005−9008. (i) Wingad, R. L.; Gates, P. J.; Street, S. T.; Wass, D. F. Catalytic conversion of ethanol to n-butanol using ruthenium P−N ligand complexes. *ACS Catal.* **2015**, *5*, 5822−5826. (j) Tseng, K.-N. T.; Lin, S.; Kampf, J. W.; Szymczak, N. K. Upgrading ethanol to 1-butanol with a homogeneous air-stable ruthenium catalyst. *Chem. Commun.* **2016**, 52, 2901−2904. (k) Xie, Y.; Ben-David, Y.; Shimon, L. J.; Milstein, D. Highly efficient process for production of biofuel from ethanol catalyzed by ruthenium pincer complexes. *J. Am. Chem. Soc.* **2016**, *138*, 9077−9080. (l) Das, K.; Yasmin, E.; Das, B.; Srivastava, H. K.; Kumar, A. Phosphine-free pincer-ruthenium catalyzed biofuel production: high rates, yields and turnovers of solventless alcohol alkylation. *Catal. Sci. Technol.* **2020**, *10*, 8347−8358. (m) Bhattacharyya, D.; Sarmah, B. K.; Nandi, S.; Srivastava, H. K.; Das, A. Selective Catalytic Synthesis of α-Alkylated Ketones and β-Disubstituted Ketones via Acceptorless Dehydrogenative Cross-Coupling of Alcohols. *Org. Lett.* **2021**, *23*, 869−875. (n) Liu, T.-T.; Tang, S.-Y.; Hu, B.; Liu, P.; Bi, S.; Jiang, Y.-Y. Mechanism and Origin of Chemoselectivity of Ru-Catalyzed Cross-Coupling of Secondary Alcohols to β-Disubstituted Ketones. *J. Org. Chem.* **2020**, *85*, 12444−12455. (o) Kaithal, A.; Schmitz, M.; Hölscher, M.; Leitner, W. Ruthenium(II)-Catalyzed β-Methylation of Alcohols using Methanol as C1 Source. *ChemCatChem.* **2019**, *11*, 5287−5291. (p)

Prakasham, A. P.; Ta, S.; Dey, S.; Ghosh, P. One pot tandem dual C-C and C-O bond reductions in the β-alkylation of secondary alcohols with primary alcohols by ruthenium complexes of amido and picolyl functionalized N-heterocyclic carbenes. *Dalton Trans.* **2021**, *50*, 15640−15654.
(9) (a) Pandey, B.; Xu, S.; Ding, K. Selective Ketone Formations via Cobalt-Catalyzed β-Alkylation of Secondary Alcohols with Primary Alcohols. *Org. Lett.* **2019**, *21*, 7420−7423. (b) Freitag, F.; Irrgang, T.; Kempe, R. Cobalt-Catalyzed Alkylation of Secondary Alcohols with Primary Alcohols via Borrowing Hydrogen/Hydrogen Autotransfer. *Chem. - Eur. J.* **2017**, *23*, 12110−12113. (c) Pandey, B.; Xu, S.; Ding, K. Switchable β-alkylation of Secondary Alcohols with Primary Alcohols by a Well-Defined Cobalt Catalyst. *Organometallics* **2021**, *40*, 1207−1212. (d) Zhang, S.-Q.; Guo, B.; Xu, Z.; Li, H.-X.; Li, H.-Y.; Lang, J.-P. J. T. Ligand-controlled phosphine-free Co (II)-catalysed cross-coupling of secondary and primary alcohols. *Tetrahedron* **2019**, *75*, 130640. (e) Zhang, L.; Wang, A.; Wang, W.; Huang, Y.; Liu, X.; Miao, S.; Liu, J.; Zhang, T. Co−N−C Catalyst for C−C Coupling Reactions: On the Catalytic Performance and Active Sites. *ACS Catal.* **2015**, *5*, 6563−6572. (f) Nandi, P. G.; Kumar, P.; Kumar, A. Ligand-free Guerbet-type reactions in air catalyzed by *in situ* formed complexes of base metal salt cobaltous chloride *Catal. Sci. Technol.* **2022**, *12*, 1100−1108.
(10) (a) Liao, S.; Yu, K.; Li, Q.; Tian, H.; Zhang, Z.; Yu, X.; Xu, Q. Copper-catalyzed C-alkylation of secondary alcohols and methyl ketones with alcohols employing the aerobic relay race methodology. *Org. Biomol. Chem.* **2012**, *10*, 2973−2978. (b) Tan, D.-W.; Li, H.-X.; Zhu, D.-L.; Li, H.-Y.; Young, D. J.; Yao, J.-L.; Lang, J.-P. Ligand Controlled Copper (I)-Catalyzed Cross-Coupling of Secondary and Primary Alcohols to α-Alkylated Ketones, Pyridines, and Quinolines. *Org. Lett.* **2018**, *20*, 608−611.
(11) (a) Barman, M. K.; Jana, A.; Maji, B. Phosphine-Free NNN Manganese Complex Catalyzed α-Alkylation of Ketones with Primary Alcohols and Friedlander¨Quinoline Synthesis. *Adv. Synth. Catal.* **2018**, *360*, 3233−3238. (b) Chakraborty, S.; Daw, P.; Ben David, Y.; Milstein, D. Manganese-Catalyzed α-Alkylation of Ketones, Esters, and Amides Using Alcohols. *ACS Catal.* **2018**, *8*, 10300−10305. (c) Jana, A.; Reddy, C. B.; Maji, B. Manganese Catalyzed α-Alkylation of Nitriles with Primary Alcohols. *ACS Catal.* **2018**, *8*, 9226−9231. (d) Liu, T.; Wang, L.; Wu, K.; Yu, Z. Manganese-Catalyzed β Alkylation of Secondary Alcohols with Primary Alcohols under Phosphine-Free Conditions. *ACS Catal.* **2018**, *8*, 7201−7207. (e) Schlagbauer, M.; Kallmeier, F.; Irrgang, T.; Kempe, R. Manganese-Catalyzed β-Methylation of Alcohols by Methanol. *Chem., Int. Ed.* **2020**, *59*, 1485−1490. (f) Kaithal, A.; Gracia, L.-L.; Camp, C.; Quadrelli, E. A.; Leitner, W. Direct synthesis of cycloalkanes from diols and secondary alcohols or ketones using a homogeneous manganese catalyst. *J. Am. Chem. Soc.* **2019**, *141*, 17487−17492. (g) Fu, S.; Shao, Z.; Wang, Y.; Liu, Q. Manganese catalyzed upgrading of ethanol into 1-butanol. *J. Am. Chem. Soc.* **2017**, *139*, 11941−11948. (h) Waiba, S.; Jana, S. K.; Jati, A.; Jana, A.; Maji, B. Manganese complex-catalysed α-alkylation of ketones with secondary alcohols enables the synthesis of β-branched carbonyl compounds. *Chem. Commun.* **2020**, *56*, 8376−8379. (i) El-Sepelgy, O.; Matador, E.; Brzozowska, A.; Rueping, M. C-Alkylation of Secondary Alcohols by Primary Alcohols through Manganese Catalyzed Double Hydrogen Autotransfer. *ChemSusChem* **2019**, *12*, 3099−3102. (j) Liu, Y.; Shao, Z.; Wang, Y.; Xu, L.; Yu, Z.; Liu, Q. Manganese-Catalyzed Selective Upgrading of Ethanol with Methanol into Isobutanol. *ChemSusChem* **2019**, *12*, 3069−3072. (k) Alanthadka, A.; Bera, S.; Banerjee, D. Iron-Catalyzed Ligand Free α-Alkylation of Methylene Ketones and β-Alkylation of Secondary Alcohols Using Primary Alcohols. *J. Org. Chem.* **2019**, *84*, 11676−11686. (l) Polidano, K.; Williams, J. M. J.; Morrill, L. C. Iron-Catalyzed Borrowing Hydrogen β-C(sp3)-Methylation of Alcohols. *ACS Catal.* **2019**, *9*, 8575−8580. (m) Sklyaruk, J.; Borghs, J. C.; El-Sepelgy, O.; Rueping, M. Catalytic C1 Alkylation with Methanol and Isotope-Labeled Methanol. *Angew. Chem., Int. Ed.* **2019**, *58*, 775−779. (n) Sarki, N.; Goyal, V.; Natte, K.; Jagadeesh, R. V. Base Metal-Catalyzed C Methylation Reactions Using Methanol. *Adv. Synth. Catal.* **2021**, *363*, 5028−5046.
(12) (a) Zhang, M.-J.; Li, H.-X.; Young, D. J.; Li, H.-Y.; Lang, J.-P. Reaction condition controlled nickel (ii)-catalyzed C−C cross coupling of alcohols. *Org. Biomol. Chem.* **2019**, *17*, 3567−3574. (b) Alonso, F.; Riente, P.; Yus, M. The α-Alkylation of Methyl Ketones with Primary Alcohols Promoted by Nickel Nanoparticles under Mild and Ligand less Conditions. *Synlett* **2007**, *2007*, 1877− 1880. (c) Alonso, F.; Riente, P.; Yus, M. Alcohols for the α-Alkylation of Methyl Ketones and Indirect Aza-Wittig Reaction Promoted by Nickel Nanoparticles. *Eur. J. Org. Chem.* **2008**, *2008*, 4908−4914. (d) Das, J.; Vellakkaran, M.; Banerjee, D. Nickel-Catalyzed Alkylation of Ketone Enolates: Synthesis of Mono selective Linear Ketones. *J. Org. Chem.* **2019**, *84*, 769−779. (e) Das, J.; Singh, K.; Vellakkaran,

M.; Banerjee, D. Nickel-Catalyzed Hydrogen-Borrowing Strategy for α-Alkylation of Ketones with Alcohols: A New Route to Branched gem-Bis(alkyl) Ketones. *Org. Lett.* **2018**, *20*, 5587−5591. (f) Babu, R.; Subaramanian, M.; Midya, S. P.; Balaraman, E. Nickel-Catalyzed Guerbet Type Reaction: C-Alkylation of Secondary Alcohols via Double (de)Hydrogenation. *Org. Lett.* **2021**, *23*, 3320−3325. (g) Arora, V.; Narjinari, H.; Kumar, A. Pincer-Nickel Catalyzed Selective Guerbet-Type Reactions. *Organometallics* **2021**, *40*, 2870− 2880. (h) Venkateshappa, B.; Bisarya, A.; Nandi, P. G.; Dhole, S.; Kumar, A., Production of Lactic Acid via Catalytic Transfer Dehydrogenation of Glycerol Catalyzed by Base Metal Salt Ferrous Chloride and Its NNN Pincer-Iron Complexes. *Inorg. Chem.* **2024,** *63*, 15294-15310.
(13) Narjinari, H.; Tanwar, N.; Kathuria, L.; Jasra, R. V.; Kumar, A. Guerbet-Type β-alkylation of Secondary Alcohols Catalyzed by Chromium Chloride and its Corresponding NNN Pincer Complex. *Catal. Sci. Technol.* **2022**, *12*, 4753−4762.
(14) (a) Das, K.; Dutta, M.; Das, B.; Srivastava, H. K.; Kumar, A. Efficient Pincer-Ruthenium Catalysts for Kharasch Addition of Carbon Tetrachloride to Styrene. *Adv. Synth. Catal*. **2019**, *361*, 2965−2980. (b) Nandi, P. G.; Jadi, P. K.; Das, K.; Prathapa, S. J.; Mandal, B. B.; Kumar, A. Synthesis of NNN Chiral Ruthenium Complexes and Their Cytotoxicity Studies. *Inorg. Chem. 2021*, 60, 7422−7432. (c) Gong, D.; Wang, B.; Cai, H.; Zhang, X.; Jiang, L. Synthesis, characterization and butadiene polymerization studies of cobalt(II) complexes bearing bisiminopyridine ligand. *J. Organomet. Chem*. **2011**, *696*, 1584−1590.
(15) Huheey, J. E.; Keiter, E. A.; Keiter, R. L.; Medhi, O. K. Inorganic Chemistry: Principles of Structure and Reactivity; Pearson Education: 2006;.
(16) Hoffmann, S. K.; Goslar, J.; Lijewski, S. Electron paramagnetic resonance and electron spin echo studies of Co 2+ coordination by nicotinamide adenine dinucleotide (NAD+) in water solution. *Appl. Magn. Reson.* **2013**, *44*, 817−826.
(17) (a) Widegren, J. A.; Finke, R. G. A review of the problem of distinguishing true homogeneous catalysis from soluble or other metal-particle heterogeneous catalysis under reducing conditions. *J. Mol. Catal. A* **2003**, *198*, 317−341. (b) Crabtree, R. H. Resolving Heterogeneity Problems and Impurity Artifacts in Operationally Homogeneous Transition Metal Catalysts. *Chem. Rev.* **2012**, *112*, 1536−1554. (c) Li, C.; Song, S.; Li, Y.; Xu, C.; Luo, Q.; Guo, Y.; Wang, X. Selective hydroboration of unsaturated bonds by an easily accessible heterotopic cobalt catalyst. *Nat. Commun.* **2021**, *12*, 3813.
(18) Simmons, E. M.; Hartwig, J. F. On the Interpretation of Deuterium Kinetic Isotope Effects in C-H Bond Functionalizations by Transition-Metal Complexes. *Angew. Chem., Int. Ed.* **2012**, *51*, 3066−3072.
(19) (a) Chaikin, S. W.; Brown, W. G. Reduction of aldehydes, ketones and acid chlorides by sodium borohydride. *J. Am. Chem. Soc.* **1949**, *71*, 122−125. (b) Armarego, W. L. F.; Chai, C., Chapter 5 - Purification of Inorganic and Metal-Organic Chemicals. In *Purification of Laboratory Chemicals*, 7th ed.; Armarego, W. L. F., Chai, C., Eds.; Butterworth-Heinemann: 2013; pp 555−661. (c) Günther, H. NMR *Spectroscopy: Basic Principles, Concepts and Applications in Chemistry*; Wiley: 1995; pp 22.
(20) APEX2, SAINT and SADABS; Bruker AXS Inc.: Madison, WI, USA, 2013.
(21) Sheldrick, G. M. Crystal structure refinement with SHELXL. Acta Crystallogr., Sect. C: *Struct. Chem*. **2015**, *71*, 3−8.

Summary and outlook

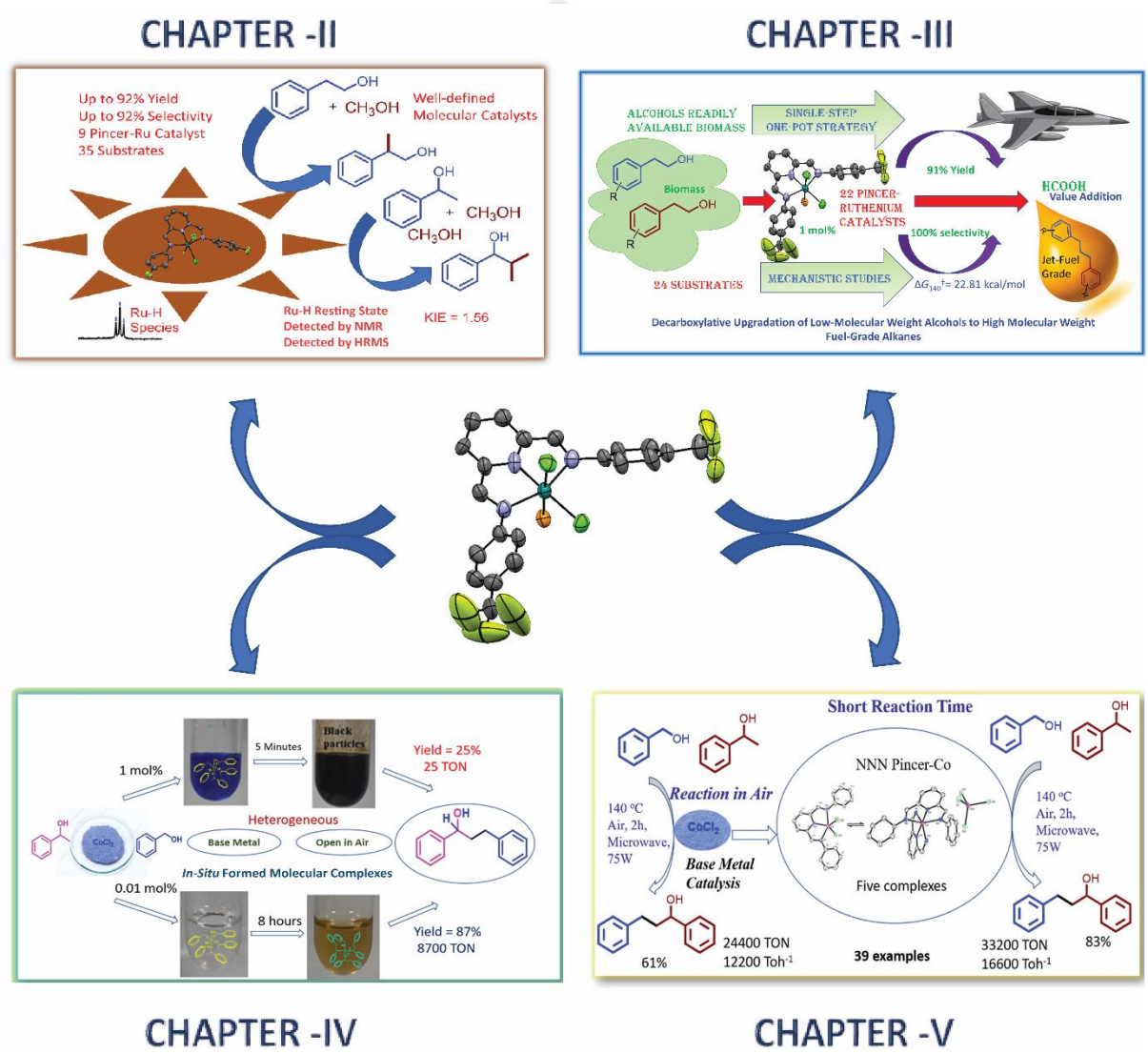

Chapter-I discusses the use of pincer complexes as efficient catalysts for various transformations. Pincer-metal complexes, due to their robust nature and high thermal stability, have been at the forefront in the dehydrogenation of alkanes and alcohols. Further, the use of alcohols as alkylating agent with various substrates using these complexes has been reviewed. The chapter ends with the discussion of the scope of the current thesis.

Chapter-II deals with the synthesis and characterization of three new NNN pincer-ruthenium complexes based on *bis*(imino)-pyridine ligands. These complexes in addition to their 2,6-*bis*(benzimidazol-2-yl)pyridine counterparts have been further applied towards the *β*-methylation of 2-phenylethanol and selective *β*-dimethylation of 1-phenylethanol using methanol as an alkylating agent. Among all the considered complexes, the pincer-ruthenium complex [(^{MeBim2}NNN)RuCl(PPh_3)$_2$]Cl exhibited the best catalytic activity. The complex [(^{MeBim2}NNN)RuCl(PPh_3)$_2$]Cl (0.5 mol %) catalyzed the *β*-methylation of 2- phenylethanol in presence of 0.75 equivalents of KOH and 7.5 equivalents of methanol, resulting in 92% yield of *β*-methylated alcohol at 140 °C after 24h. Further, the selective *β*-dimethylation of 1-phenylethanol was achieved in presence of [(^{MeBim2}NNN)RuCl(PPh_3)$_2$]Cl (0.5 mol %) with 2 equivalents of Na using 24.8 equivalents of methanol at 140 °C to obtain *β*-dimethylated alcohol with 92% yield and 92% selectivity. The kinetic experiments showed the linear dependence of rate of product formation on the concentrations of both 2-phenylethanol and the pincer-ruthenium catalyst. The reaction was catalyzed by well-defined molecular catalysts as inferred from the mercury-drop test and kinetic studies. The kinetic isotope effect studies were performed, where a secondary KIE of 1.56 was obtained. The *σ*-bond metathesis of methanol with the Ru−H species with concomitant evolution of hydrogen is the RDS with a barrier of 24.06 kcal/mol as inferred from the DFT calculations.

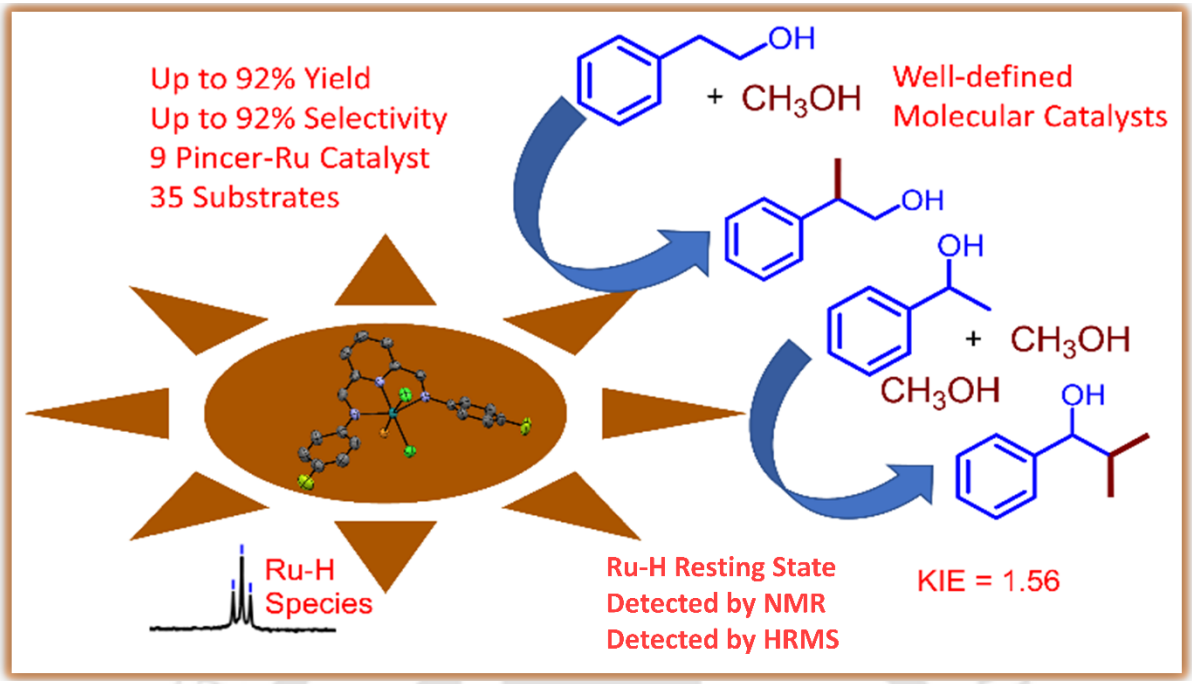

Figure 1: [(^{MeBim2}NNN)RuCl(PPh$_3$)$_2$]Cl catalyzed *β*-methylation of 2-phenylethanol and 1-phenylethanol.

Chapter-III discusses a series of new and previously known NNN pincer-Ru catalysts of the type (^{R2}NNN)RuCl$_2$L (R = ^{i}Pr, ^{t}Bu, Cy, Ph, *p*-F-C$_6$H$_4$, *p*-OMe- C$_6$H$_4$ and L = PPh$_3$, CO and CH$_3$CN) based on *bis*(imino)pyridine ligands and [(^{RBim2}NNN)RuClL$_2$]Cl (R = H and Me, L = PPh$_3$ and CO) based on 2,6-*bis*(benzimidazole-2-yl)pyridine ligands. All complexes were tested for the decarboxylative coupling of lower-molecular weight alcohols to higher-molecular weight alkanes. The (^{MeBim2}NNN)RuCl$_2$(PPh$_3$)$_2$ (1 mol%) based on 2,6-*bis*(benzimidazole-2-yl)pyridine ligand catalyzed the decarboxylation of 2-phenylethanol in presence of 0.5 equivalents of NaOH to produce 91% of 1,3-diphenyl propane with 100% selectivity at 140 °C within 5 hours. The first-order dependence of initial rate on both the concentration of base and catalyst concentration was inferred from the kinetic studies. The DFT calculations were in accordance with the experimental findings and indicate that the dehydrogenolysis step leading to the formation of 2-phenyl acetaldehyde and the resting state (^{MeBim2}NNN)RuHCl is the rate-determining step with a barrier of 22.81 kcal/mole at 140 °C.
In comparison to the rate-determining dehydrogenolysis step of the cycle involving most active catalyst [(^{MeBim2}NNN)RuCl(PPh$_3$)$_2$]Cl, the corresponding cycle with the least active catalyst (^{iPr2}NNN)RuCl$_2$(PPh$_3$) involved insertion of 1,3-diphenyl propene into the Ru-H bond as the RDS which is kinetically unfavorable by 5.00 kcal/mol and gives only 14% of 1,3-diphenyl propane at 25% selectivity. To the best of our knowledge, this is the first example of a Ru based

catalyst for the upgradation of alcohols to alkanes directly without the need of an additional hydrogenation step.

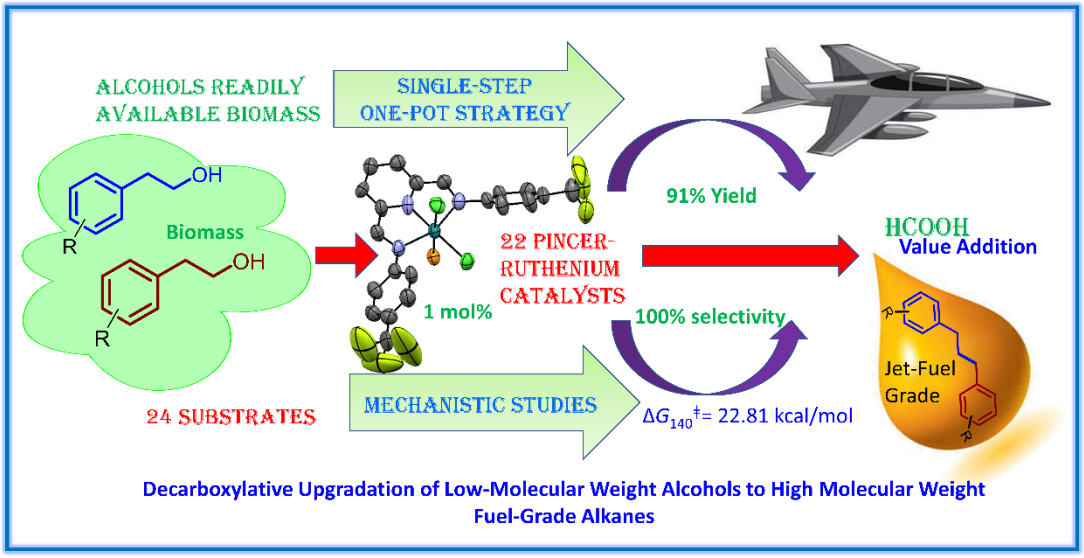

Figure 2: [(^{MeBim2}NNN)RuCl(PPh$_3$)$_2$]Cl catalyzed deoxygenative coupling of alcohols to alkane.

Chapter-IV describes the use of readily available $CoCl_2$ that forms complexes with alcohols *in-situ* and efficiently catalyzes the *β*-alkylation of alcohols under air. The rapid formation of heterogeneous cobalt NPs was observed in the presence of 1 mol% of $CoCl_2$, which were sensitive to air, resulting in poor yields (25%) of *β*-alkylated products. When the reaction was carried out with 0.01 mol% of $CoCl_2$, a better control over reactivity (87% yield, *ca.* 8700 TON) was observed with the delay in the heterogenization. The kinetic experiments exhibited the linear dependence of rate of the product formation on the concentrations of both, cobaltous chloride (in the regime of homogenity) and sodium *tert*-butoxide. Further, the concentration of 1-phenyl ethanol and benzyl alcohol showed a non-linear dependence on the rate of the product formation. The superior reactivity for the *β*-alkylation of alcohols was observed with molecular Co catalysts rather than heterogeneous Co NPs. The possible involvement of C–H activation in the cobaltous chloride catalyzed *β*-alkylation was inferred from the deuterium labelling experiments with a k_H/k_D value of 1.61.

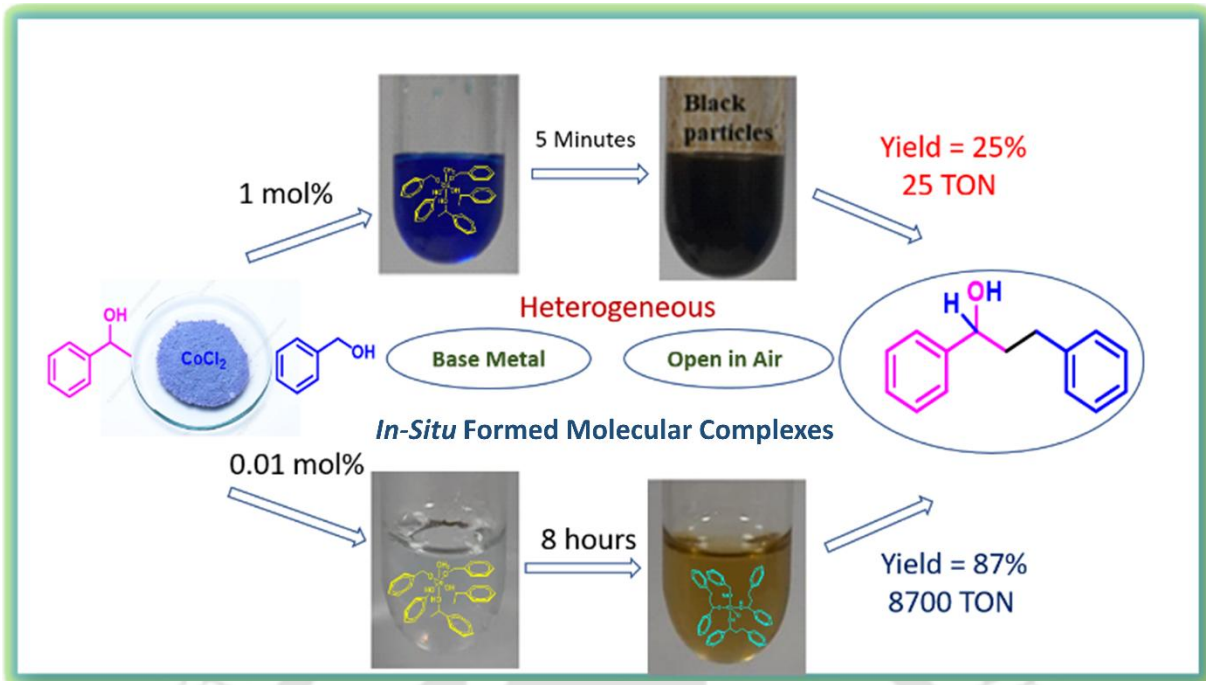

Figure 3: $CoCl_2$ catalyzed β-alkylation of secondary alcohols with primary alcohols.

Chapter-V discuss the use of earth-abundant, inexpensive, environmentally benign base metal cobaltous chloride to synthesize pincer-Co complexes of the type (^{R2}NNN)$CoCl_2$ (R = ^{i}Pr, ^{t}Bu, Cy, Ph, *p*-F-C_6H_4). These complexes are found to exist in equilibrium with the corresponding ion-pair [(^{R2}NNN)$_2$Co]$CoCl_4$ depending on the nature of the R group. The high thermal stability of considered pincer-Co complexes was tested using TGA analysis. Among the considered complexes, (^{iPr2}NNN)$CoCl_2$ demonstrated the best activity in air under both thermal and microwave heating at 140 °C for the β-alkylation of secondary alcohols with primary alcohols. The (^{iPr2}NNN)$CoCl_2$ (0.0025 mol %) complex in the presence of 2.5 mol% of NaO^{t}Bu gave 85% (34000 TON at 1417 TO/h) of the β-alkylated product in 24 h under conventional heating. On the other hand, the same reaction under microwave conditions (140 °C at 75 W) was accomplished within 2 h with a comparable yield of 83% (33200 TON) with a better TOF of 16600 TOs/h. Upon using $CoCl_2$ with similar reaction conditions, poor results under both conventional (ca. 66%, 26400 TON at 1100 TOs/h) and microwave heating (ca. 61%, 24400 TON at 12200 TOs/h) were observed. The existence of well-defined molecular Co(II) species formed during the catalytic β-alkylation was proved by HRMS analysis and hot-filtration experiments. The EPR studies and magnetic moment measurements using the Evans method, pointed towards the presence of octehadral cobalt in +2 oxidation state. The C-H activation (β-hydride elimination of acetophenone in particular) is the RDS, which was

confirmed from HRMS analysis and competitive deuterium labelling experiments that result in a KIE of 6.14.

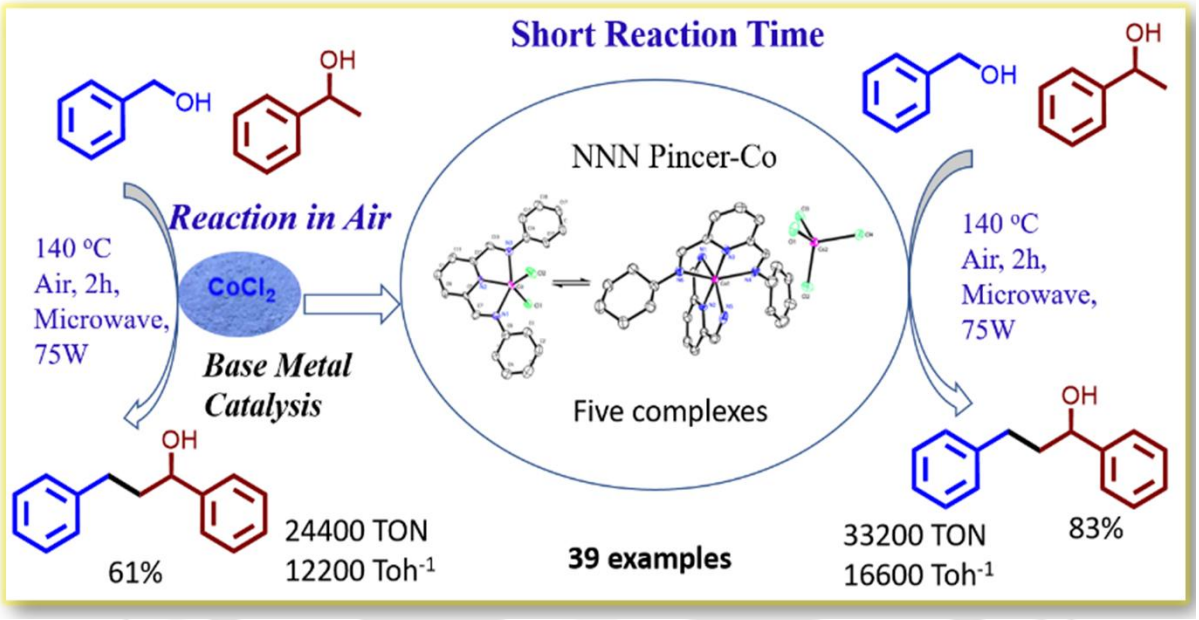

Figure 4: (^{iPr2}NNN)$CoCl_2$ catalyzed *β*-alkylation of secondary alcohols with primary alcohols.

The current thesis has explored the synthetic methodologies to arrive at new pincer-Ru and pincer-Co complexes based on *bis*(imino)pyridine and 2,6-*bis*(benzimidazol-2-yl)pyridine ligands. These pincer complexes have been utilized for various organic transformations with a special emphasis towards the transformation of alcohols to value-added chemicals. Attempts have been made to attain systematic understanding of reaction mechanism wherever possible.

The finding of the thesis could open new route for the synthesis of fuels, organic reaction intermediates, fine chemicals and value-added chemicals from readily available alcohols.

Due to high selectivity, high efficiency and increased reaction rate, the catalytic reactions are of utmost importance in the industrial sectors. They enable the transformation of several raw materials into various value-added commodities, by lowering the activation energy while simultaneously cutting down on the costs. Studying their catalytic activity and understanding the underlying mechanism of various consider pincer-metal systems throughout the chapters of this thesis, it is obvious that several challenges remains and need to be addressed, such as

1. Can one activate the small molecules like N_2, CO_2 using the most effective and efficient pincer-ruthenium catalyst based on *bis*(imino)pyridine or *bis*(benzimidazole-2-yl)pyridine ligand system?
2. Is it possible to heterogenize these pincer-ruthenium and pincer-cobalt complexes for catalytic recyclability?
3. Is it possible to design better catalyst and perform the reactions which have been studied throughout the thesis under milder reaction conditions for safe and efficient catalytic process?
4. Can one design catalytic system based on *bis*(benzimidazole-2-yl)pyridine ligands that employ Co(I) or Co(II) that can show high efficiency for such challenging organic transformations?

Overall there is a need of designing a catalytic system consisting of earth abundant metals which is less sensitive, air stable, environmentally benign and which is highly efficient towards catalytic value-addition of alcohols under mild reaction conditions.

Curriculum Vitae Pran Gobinda Nandi, IIT Guwahati

Phd student
Department of Chemistry
Indian Institute of Technology, Guwahati,
Guwahati-781039, Assam, India
Date of birth: 12/12/1994
Mobile: 9564772396, 7003321187
Sex: Male
Nationality: Indian
Language: Bengali, Hindi, English
Address: T-220, Brahmaputra Hostel, IIT Guwahati, Guwahati-781039, Assam, India
Email: prangobinda94@gmail.com, pran@iitg.ac.in
Google Scholar ID:
https://scholar.google.com/citations?hl=en&user=6yFMVi0AAAAJ&view_op=list_works&sortby=pubdate

Academic Background

Doctor of Philosophy (PhD) in Chemistry from Indian Institute of Technology, Guwahati, (2018-2024), Assam, India under the supervision of Dr. Akshai Kumar A.S.

Thesis title: *Pincer-Ruthenium and Pincer-Cobalt Catalyzed Value-Addition of Alcohols.*

MSc Chemistry in Inorganic Specialization from Jadavpur University, West Bengal, India. (2015-2017).

BSc (H) Chemistry from Kandi Raj College, University of Kalyani, West Bengal, India. (2012-2015).

Research Interest

1. Catalysis
2. Organometallics chemistry
3. Inorganic synthesis
4. DFT calculation

Conferences Attended

- **Nandi, P. G.;** Kumar, A. Poster presentation during 30th International Conference on Organometallic Chemistry, ICOMC, Agra, India, July **2024**. "Pincer-Ruthenium-Catalyzed β-Methylation of Alcohols".
- **Nandi, P. G.;** Jasra, R.V.; Kumar, A. Poster presentation during 3rd International Conference on Main-group Molecules to Materials MMM III, IIT Hyderabad,University of Hyderabad, Telangana, December **2023**."Pincer-Ruthenium-Catalyzed β-Methylation of Alcohols".
- **Nandi. P. G.;** Kumar, A. Poster presentation during Modern Trends in Inorganic Chemistry MTIC-XIX, Banaras Hindu University, Varanasi. December **2022**. "Pincer-Cobalt-CatalyzedGuerbet-Type *β*-Alkylation of Alcohols in Air under Microwave Conditions".
- **Nandi. P. G.;** Kumar, A. Oral presentation during ACS National Meeting & Exposition, ACS Fall 2022, Aug 21-25, **2022**. " Ligand-free Guerbet-type reactions in air catalyzed by *in situ* formed complexes of base metal salt cobaltous chloride".
- **Nandi, P. G.;** Kumar, A. Poster presentation during 28th CRSI National Symposium in Chemistry, IIT Guwahati. March **2022**. "Ligand-free Guerbet-type reactions in air catalyzed by in situ formed complexes of base metal salt cobaltous chloride".
- Das, K.; **Nandi, P. G.**; Islam, K.; Srivastava, H. K.; Kumar. Poster presentation during 2021#Catalysis Science & Technology 10th anniversary symposium **2021**, Nov 2021."Solvent Free and Efficient Pincer−Ruthenium Catalytic Systems for *N*−Alkylation of Amines Promoted by a Base Generated *In−Situ* from Alcohol".

Publications

- **Nandi, P. G.**; Maity, P.; Kumar, A., Pincer-Ruthenium-Catalyzed Direct Formation of Fuel-Grade Alkanes via a Net-Decarboxylative Coupling of Alcohols. *ACS Catal* **2025,** *15*, 543-556.
- **Nandi, P. G.;** Kumar, P.; Kumar, A., Ligand-free Guerbet-type reactions in air catalyzed by in situ formed complexes of base metal salt cobaltous chloride. *Catal. Sci. Technol.* **2022,** *12*, 1100-1108.

- **Nandi, P. G.;** Thombare, P.; Prathapa, S. J.; Kumar, A., Pincer-Cobalt-Catalyzed Guerbet-Type β-Alkylation of Alcohols in Air under Microwave Conditions. *Organometallics* **2022,** *41*, 3387-3398.
- **Nandi, P. G**.; Jasra, R. V.; Kumar, A., Pincer–Ruthenium-Catalyzed β-Methylation of Alcohols. *Organometallics* **2023,** *42*, 3138-3152.
- **Nandi, P. G.;** Jadi, P. K.; Das, K.; Prathapa, S. J.; Mandal, B. B.; Kumar, A., Synthesis of NNN Chiral Ruthenium Complexes and Their Cytotoxicity Studies. *Inorg. Chem.* **2021,** *60*, 7422-7432.
- Tanwar, N.; **Nandi, P. G.**; Dhole, S.; Jasra, R. V.; Kumar, A., 3d-Metal Based Anodic Pincer Electro-Catalysts Dispersed in Solution for the Electro-Catalytic Oxidation of (M)ethanol. *Catal. Sci. Technol*. **2025,** *15*, 2493-2509.
- Das, K.; **Nandi, P. G**.; Islam, K.; Srivastava, H. K.; Kumar, A., N–Alkylation of Amines Catalyzed by a Ruthenium–Pincer Complex in the Presence of in situ Generated Sodium Alkoxide. *Eur. J. Org. Chem.* **2019,** *2019*, 6855-6866.
- Venkateshappa, B.; Bisarya, A.; **Nandi, P. G**.; Dhole, S.; Kumar, A., Production of Lactic Acid via Catalytic Transfer Dehydrogenation of Glycerol Catalyzed by Base Metal Salt Ferrous Chloride and Its NNN Pincer-Iron Complexes. *Inorg. Chem.* **2024,** *63*, 15294-15310.

Book Chapters and Review Articles

- Narjinari, H.; Bisarya, A.; Arora, V.; **Nandi, P. G**.; Das, K.; Kumar, A., Current State of-Art in the Guerbet-Type β-Alkylation of Secondary Alcohols with Primary Alcohols Catalyzed by Complexes Based on 3d Metals. In *Dehydrogenation Reactions with 3d Metals*, Sundararaju, B., Ed. Springer Nature Switzerland: Cham, 2024; pp 93-127.
- **Nandi, P. G.;** Arora, V.; Yasmin, E.; Kumar, A., Chapter 2 - Pincer-group(8) and pincer-group(9) metal complexes for catalytic alkane dehydrogenation reactions. In *Pincer-Metal Complexes*, Kumar, A., Ed. Elsevier: 2022; pp 69-122.
- Arora, V.; Narjinari, H.; **Nandi, P. G.**; Kumar, A., Recent advances in pincer–nickel catalyzed reactions. *Dalton Trans.* **2021,** *50*, 3394-3428.